

UCL

**Prostate cancer detection and
characterisation using innovative
medical imaging**

Miss Lucy Simmons MBBS MRCS (Eng)

MD (Res) Clinical Research Thesis

Division of Surgery and Interventional Science

University College London

July 2011- April 2016

Declaration

I, Lucy Alexandra Marie Simmons confirm that the work presented in this thesis is my own. Where information has been derived from other sources, I confirm that this has been indicated in the thesis

This work has not previously been accepted in substance for any degree and is not being concurrently submitted in candidature for any degree.

This thesis is the result of my own investigations, except where otherwise stated.

I hereby give consent for my thesis, if accepted, to be available for photocopying and for inter-library loan, and for the title and summary to be made available to outside organisations.

Signed:



Miss Lucy Alexandra Marie Simmons MBBS MRCS

Date: April 2016

Acknowledgement and Dedication

I dedicate this thesis to my dear friend Ross Bolton, who sadly died of prostate cancer, to all men affected by prostate cancer and their families: I hope that this work may contribute to the improvement of the prostate cancer pathway for them in the future.

I would like also to thank all of the men who participated in the studies within this thesis: without their willingness to take part none of this research would have been possible.

My acknowledgement and thanks to my supervisors Professor Mark Emberton and Mr Hashim Uddin Ahmed - without their support and encouragement I would not have been able to complete this work.

There is also a number of other people to whom I owe a debt of gratitude as without their input this thesis would not have been possible:- firstly, I would like to thank my colleagues at University College London and University College London Hospitals whom if I named individually would run to several pages; secondly, I would like to thank Dr Shonit Punwani and Dr Alex Freeman for their valuable input into the PICTURE study and support; thirdly, I would also like to thank Miss Abi Kanthabalan, without whom the PICTURE Study would have been impossible to finish; fourthly, my colleagues in the Centre for Medical Imaging and Computing, Professor Dean Barret and a special mention to Dr Yipeng Hu - my appreciation will never be able to repay all your hours of work. Dr Hu helped with the MRI/US registration within PICTURE and the computer simulation studies. My sincere thanks and gratitude also to Mrs Susan C Charman for the many hours staring at STATA that were necessary to make this thesis possible. Susan was the lead statistician in the PHS02 blind phase and for the PICTURE study.

I owe also a debt of thanks to Dror Nir and the Advanced Medical Diagnostics team for their support during my research and for allowing me to investigate the technology they developed.

Lastly, and most importantly, I would like to thank my supportive husband Neil Thompson and my family for the many sacrifices they have made to help me complete this work.

Abstract

Prostate cancer is the second most common cancer affecting men worldwide. All prostate cancer however, is not equal: some forms of the disease are inert and do not require intervention; other, more aggressive forms benefit from early detection and treatment.

Thus, accurate risk stratification is paramount. Inadequacies in the current diagnostic pathway for prostate cancer lead to incorrect risk assignment. Ways of enhancing the diagnostic pathway and improving risk stratification using novel bio-markers are being actively researched worldwide.

This thesis focuses on work carried out at University College London (UCL)/University College London Hospitals (UCLH), investigating imaging as a biomarker in prostate cancer.

The development of an enhanced form of ultrasound imaging - Prostate HistoScanning (PHS), and the use of multi-parametric magnetic resonance imaging (mpMRI) for prostate cancer detection and risk stratification are investigated.

The main body of work: Prostate Imaging Compared to Transperineal Ultrasound guided biopsy for significant prostate cancer Risk Evaluation; the acronym for this is the PICTURE Study, was designed and carried out at UCLH between 2012 and 2014.

This research aimed to establish if imaging has a role in improving prostate cancer detection and, if by utilizing imaging in the form of either multi-parametric MRI (mpMRI) or prostate HistoScanning (PHS), men with a negative test may be spared further prostate biopsy.

Additionally, for men with a lesion detected on imaging, could a targeted sampling strategy afford accurate disease detection and risk stratification.

Despite initial promising results, prostate HistoScanning was found to have no role in prostate cancer detection.

Multiparametric MRI however, demonstrated high performance characteristics for the detection of disease. It shows potential as a useful tool for men in whom diagnostic uncertainty remains following primary biopsy; it is asserted that it should therefore be used to help risk stratify these men. Moreover, mpMRI targeted biopsy provides accurate risk stratification; and is an approach that should be adopted.

Abbreviations

ADC- Apparent diffusion coefficient

AFMS- Anterior fibromuscular stroma

ANNA- Artificial neural network analysis

B-mode- Brightness mode

BPH- Benign prostatic hypertrophy

CED- Contrast enhanced doppler

CEUS- Contrast enhanced Ultrasound

CFD- Colour flow doppler

C-TRUS- Computerised Transrectal Ultrasound

CZ- Central zone

DCE- Dynamic contrast enhanced

DRE- Digital rectal examination

DWI- Diffusion weighted imaging

EN-2- Engrailed 2

EPE- Extra prostatic extension

GSU- Grey scale ultrasound

MCCL- Maximum cancer core length

MRI - Magnetic resonance imaging

mpMRI- Multi-parametric magnetic resonance imaging

mpUS- Multi-parametric ultrasound

MRSI- Magnetic resonance spectroscopic imaging

NICE- National Institute for Health and Care Excellence

PDI- Power doppler imaging

PHS- Prostate HistoScanning

PIN- Prostatic intraepithelial neoplasia

PSA – Prostate specific antigen

PZ- Peripheral zone

RBIE- Real time balloon inflation elastography

RF- Radio frequency

ROI- Region of interest

RTE- Real time elastography

SE- Strain/static elastography

SEER- Surveillance, epidemiology and end results

SI- Signal intensity

SNR- Signal-to-noise ratio

SWE- Shear wave elastography

TPM – Transperineal template mapping biopsies

TRUS – Transrectal Ultrasound

TTI- Tissue type imaging

TZ- Transition zone

UCL- University College London

UCLH- University College London Hospitals

UK- United Kingdom

List of Figures

Figure 1.	Schematic of prostate anatomy.....	18
Figure 2.	The Gleason grading system.....	20
Figure 3.	The 20 most common cancers in the UK in 2011	21
Figure 4.	Prostate Cancer (C61), European Age-Standardised Incidence Rates, Males, UK, 1993-2011	22
Figure 5.	TRUS image A, with colour doppler B	30
Figure 6.	Power doppler	31
Figure 7.	Grey scale and contrast enhanced image of prostate lesion.....	32
Figure 8.	Elastography	34
Figure 9.	Forest plots of sensitivity (a) and specificity (b) for real-time elastography in the diagnosis of prostate cancer.	38
Figure 10.	Summary receiver operating characteristic (SROC) curve for prostate cancer detection.....	39
Figure 11.	RTE images and corresponding CEUS and RP histology.....	44
Figure 12.	T2 weighted image	47
Figure 13.	Dynamic contrast enhanced image signal intensity	49
Figure 14.	Semi-quantitative post processing of DCE	50
Figure 15.	Diffusion weighted images and ADC map.....	52
Figure 16.	MRSI images.....	55
Figure 17.	Predictive value of each MRI sequence	57
Figure 18.	B mode Ultrasound image of the prostate –transverse and sagittal view.....	60
Figure 19.	HistoScanning algorithms.....	61
Figure 20.	Photograph of gland.....	68
Figure 21.	3D Tumour map	69
Figure 22.	5 x 5mm Histopathology grid analysis	69
Figure 23.	PHS02 open phase patient study flow	72
Figure 24.	Relationship of total cancer volume at HistoScanning (embedded software) and Histopathology.....	74
Figure 25.	Relationship of total cancer volume at HistoScanning manual volume estimation method and Histopathology.....	75
Figure 26.	Relationship of total cancer volume correlation with respect to probe gland difference.....	76
Figure 27.	Recruitment flow diagram for the blind verification phase of PHS-02 study.....	81

Figure 28. Box plot of total cancer volumes at Prostate HistoScanning and Radical Prostatectomy.....84

Figure 29. Bland Altman plot indicating the agreement between RP and Prostate HistoScanning in assessing total cancer volume85

Figure 30. Scatter graph of correlation between HistoScanning total cancer volume (TCV) and RP TCV –blind phase.....86

Figure 31. Graph demonstrating Prostate gland size correlation95

Figure 32. Graph demonstrating HistoScanning signal correlation.....95

Figure 33. Least squared regression for unrefined HistoScanning volumes.....97

Figure 34. Least squared regression for refined HistoScanning volumes.....98

Figure 35. Prostate HistoScanning image with Gleason detection overlay and corresponding histopathology grid.100

Figure 36. Graph of Prostate HistoScanning Gleason tool frequency analysis102

Figure 37. PICTURE trial study flow.....105

Figure 38. SEER 9 Incidence & U.S. Mortality 1975-2012, All Races, Males. Rates are Age-Adjusted110

Figure 39. UCL definitions of clinically significant disease111

Figure 40. PICTURE mp-MRI reporting form.....113

Figure 41. HistoScanning Reporting form.....115

Figure 42. Transperinaltemplate biopsy set up116

Figure 43. Modified Barzell Zones.....117

Figure 44. ROC curves for TPM and TRUS biopsy strategies118

Figure 45. ROC curve for Biopsy strategies for TPM in Cystoprostatectomy series (definition one disease).....123

Figure 46. Sensitivity curves for Biopsy strategies for TPM in Cystoprostatectomy series (definition one disease).....124

Figure 47. Specificity Curve for Biopsy strategies for TPM in Cystoprostatectomy series (definition one disease).....124

Figure 48. ROC curve for Biopsy strategies for TPM in Cystoprostatectomy series (definition two disease)125

Figure 49. Sensitivity curves for Biopsy strategies for TPM in Cystoprostatectomy series (definition two disease).....126

Figure 50. Specificity Curve for Biopsy strategies for TPM in Cystoprostatectomy series (definition two disease).....126

Figure 51. ROC curve for Biopsy strategies for TPM in Radical Prostatectomy series (definition one disease)127

Figure 52. Sensitivity curves for biopsy strategies for TPM in Radical prostatectomy series (definition one disease)..... 128

Figure 53. Specificity curves for biopsy strategies for TPM in Radical prostatectomy series (definition one disease)..... 128

Figure 54. ROC curve for Biopsy strategies for TPM in Radical Prostatectomy series (definition two disease) 129

Figure 55. Sensitivity curves for biopsy strategies for TPM in Radical prostatectomy series (definition two disease)..... 130

Figure 56. Specificity curves for biopsy strategies for TPM in Radical prostatectomy series (definition two disease)..... 130

Figure 57. PICTURE recruitment STARD flow diagram..... 146

Figure 58. ROC curve analysis for mpMRI detection of disease 152

Figure 59. PICTURE Prostate HistoScanning flow diagram 161

Figure 60. Bland Altman plot of 8818 gland volume at consent and prior to TPM..... 169

Figure 61. Bland Altman plot of 8818 total predicted cancer (totvol) volume and lesion (l1vol) volume at consent and prior to TPM 170

Figure 62. Comparing probes 8818 & 8848 at baseline- Gland Volume 171

Figure 63. Comparing probes 8818 & 8848 at baseline- 171

Figure 64. EN2 vs. Definition one cancer..... 173

Figure 65. EN2 vs. Definition two cancer..... 174

List of Tables

Table 1.	Colour and Power doppler imaging studies	30
Table 2.	Contrast enhanced doppler	33
Table 3.	Elastography performance characteristics	37
Table 4.	T2 weighted imaging performance characteristics	48
Table 5.	DCE imaging performance characteristics.....	51
Table 6.	Diffusion weighted imaging.....	53
Table 7.	MRSI performance characteristics	56
Table 8.	PHS02 exclusion criteria	66
Table 9.	Eligible patients according to recruiting centre	71
Table 10.	PHS02 open phase data.....	73
Table 11.	Multiple linear regression of volumes predicted by HistoScanning on volumes found at pathology	77
Table 12.	Sextant analysis for all 27 men.....	79
Table 13.	Sextant analysis of the 23 men with index foci ≥ 0.5 cc at histopathology.	79
Table 14.	Sextant analysis sensitivity/specificity results for HistoScanning™ at differing volume thresholds	80
Table 15.	Blind phase patient disease characteristics	82
Table 16.	Total cancer volume and lesion volume at histopathology and HistoScanning	83
Table 17.	Sextant analysis for detection of 0.5cc and 0.2cc lesions using Boot Strapping correction as a result of non-independence of the sectors of analysis.....	87
Table 18.	Inter-observer variability.....	97
Table 19.	Histological vs HistoScanning attribution of Gleason grade (GIG)	101
Table 20.	Demographic data for Cystoprostatectomy series for 96 men.....	120
Table 21.	Demographic data for Radical Prostatectomy series	121
Table 22.	Detection rates of significant disease for different biopsy strategies	131
Table 23.	Numbers for precision based estimates with 95% Confidence level with varying confidence widths	138
Table 24.	Sample size calculation- calculated for 95% CI around NPV- assuming sensitivity and specificity of 70%.....	138
Table 25.	Sample size calculation- Calculated for 95% CI around NPV- assuming sensitivity and specificity of 80%.....	139
Table 26.	Sample size calculation-calculated for 95% CI around NPV- assuming sensitivity and specificity of 70%.....	139
Table 27.	Sample size calculation -Calculated for 95% CI around NPV- assuming sensitivity and specificity of 80%.....	140

Table 28. 2 by 2 tables to demonstrate accuracy of MRI with respect to TPM 141

Table 29. 2 by 2 tables to demonstrate accuracy of HistoScanning with respect to TPM 143

Table 30. PICTURE Patient demographics 147

Table 31. Study entry TRUS biopsy Gleason grading 148

Table 32. Template biopsy disease distribution for eligible men n=249 149

Table 33. MRI characteristics 150

Table 34. mpMRI performance characteristics for Definition 1 disease 151

Table 35. MRI Cognitive vs TPM biopsies by UCL risk criteria 153

Table 36. MRI/US registration targeted biopsy 154

Table 37. MRI pooled targeted biopsy demographics n=200 155

Table 38. Pooled MRI Targeted results 155

Table 39. MRI Targeted performance characteristics for detection of UCL Definition 1 disease for MRI score ≥ 3 . (Including men not targeted and assuming non targeted are benign) 157

Table 40. MRI Targeted performance characteristics for detection of UCL Definition 1 disease, excluding non-targeted men, for MRI score ≥ 3 157

Table 41. MRI Cognitive (MRI score ≥ 4) vs TPM biopsies by UCL risk criteria 158

Table 42. MRI/US registration targeted biopsy- MRI score ≥ 4 158

Table 43. Pooled MRI Targeted results- MRI score ≥ 4 159

Table 44. MRI Targeted performance characteristics for detection of UCL Definition 1 disease excluding non-targeted men, for MRI score ≥ 4 159

Table 45. Comparison of performance characteristics between targeting for MRI lesion ≥ 3 and MRI lesion ≥ 4 160

Table 46. Template biopsy disease distribution for all study eligible men n=249, and men eligible for PHS analysis n=220 162

Table 47. PHS Performance Characteristics for Definition 1 Disease 163

Table 48. PHS Targeted performance characteristics for detection of UCL Definition 1 disease (excluding non-targeted men) 163

Table 49. PHS Targeted results for definition one disease 164

Table 50. Kappa Values 165

Table 51. MRI Comparison for Any Disease 166

Table 52. MRI comparison for Definition 2 Disease 166

Table 53. MRI reporter comparison for Definition 1 Disease 167

Table 54. AUROC curve analysis for each reporter 167

Table 55. Engrailed 2, Citrate and Zinc Performance AUROC analysis 173

Table 56. EN2, Citrate and Zinc levels at varying disease thresholds 174

Table of Contents

Declaration	2
Acknowledgement and Dedication	3
Abstract	4
Abbreviations	5
List of Figures	7
List of Tables	10
Table of Contents	12
1 Introduction and Background	17
1.1 Introduction	17
1.1.1 Prostate Anatomy and Physiology	17
1.2 Prostate Gland Function	18
1.3 Prostate Disease.....	19
1.3.1 Prostate Cancer.....	19
1.4 Current Prostate Cancer Diagnostic Pathway.....	23
1.4.1 Problems with TRUS Biopsy	24
1.4.2 Prostate Cancer Significance.....	25
1.5 Imaging as a Diagnostic Test for Prostate Cancer	26
1.6 Thesis Aims and Hypothesis.....	27
2 Imaging in Prostate Cancer.....	28
2.1 Current Role of Imaging in Prostate Cancer	28
2.2 Review of Transrectal Ultrasound and Enhanced Ultrasound Imaging	29
2.2.1 Enhanced TRUS - Colour Flow Doppler/Power Doppler Imaging	29
2.2.2 Contrast Enhanced Doppler- Microbubble	31
2.2.3 Elastography.....	34
2.2.4 Artificial Neural Network Analysis/Computerised-TRUS	41
2.2.5 Prostate HistoScanning	42
2.2.6 Multiparametric Ultrasound	43
2.2.7 Ultrasound Summary	45
2.3 Review of Magnetic Resonance Imaging.....	46
2.2.1 T2 Weighted Imaging	46

2.2.2	T1 Weighted and Dynamic Contrast Enhanced (DCE).....	48
2.3.1	Diffusion Weighted Imaging (DWI)	52
2.2.3	MR Spectroscopy Imaging (MRSI)	54
2.2.4	Multi-Parametric MRI Summary	56
2.4	Imaging Review Summary.....	59
3	Prostate HistoScanning	60
3.1	HistoScanning Background and Development.....	60
3.2	Algorithm Development	62
3.3	PHS02 Study.....	65
3.3.1	Methodology of PHS02 Study	65
3.3.2	The Index test- Prostate HistoScanning	66
3.3.3	The Reference Test – Radical Prostatectomy step sectioned Histopathology	67
3.3.4	Data Matching and Statistics	70
3.4	Results of PHS02 Open Phase.....	70
3.4.1	Open Phase Analysis Plan	70
3.4.2	Open Phase Results.....	71
3.4.3	Whole Gland Analysis	74
3.4.4	Lesional Analysis	77
3.4.5	Sextant Analysis	78
3.5	Results of the Blind Phase of PHS02	80
3.5.1	Recruitment	80
3.5.1	Results of Blind Phase	81
3.5.2	Total Cancer Volume Comparison	84
3.5.3	Whole Gland Analysis	86
3.5.4	Sextant Analysis	87
3.5.5	Lesional Analysis	87
3.6	PHS02 Study Design Challenges.....	88
3.6.1	Target Patient Selection and the Ideal Reference Test.....	88
3.6.2	Problems with the Reference Test.....	90
3.6.3	Problems with the Index test	90
3.6.4	Problems with Matching between the Index and Reference Test	91
3.6.5	Defining Prostate Cancer Significance/Determining Volume Thresholds	92
3.7	Discussion of PHS02.....	92

3.8	HistoScanning Reliability Work	94
3.8.1	Intra-operator Pilot Data.....	94
3.8.2	Inter-observer Reporting Work.....	96
3.8.3	Pilot Study Prostate HistoScanning Gleason Grade Discrimination.....	98
4	Prostate Imaging Compared to Transperineal Ultrasound guided biopsy for significant prostate cancer Risk Evaluation (PICTURE).....	103
4.1	PICTURE Study Design and Objectives	103
4.1.1	Study Objectives.....	103
4.1.2	Trial Design.....	104
4.1.3	Inclusion/Exclusion criteria	106
4.1.4	Ethics and Registration.....	106
4.2	Rationale and Methodological Discussion	107
4.2.1	Choice of Patient Population	107
4.2.2	Choice of Reference Test	108
4.2.3	Definitions of Clinically Significant Disease.....	109
4.3	Index Tests	111
4.3.1	Multiparametric-MRI	111
4.3.2	Prostate HistoScanning	114
4.4	The Reference Test- Transperineal Template Mapping Biopsy	116
4.4.1	Template Mapping Biopsy Sampling Density.....	117
4.4.2	Cystoprostatectomy Series Simulation	122
4.4.3	Radical Prostatectomy series:.....	127
4.5	Targeted Biopsies	132
4.5.1	Rationale for Targeted biopsy.....	132
4.6	PICTURE Additional Procedures	135
4.6.1	Urine Engrailed 2 (EN2).....	135
4.6.2	Seminal Fluid Analysis for Citrate and Zinc (FScan)	136
4.7	PICTURE Study Size Calculation	137
4.7.1	Sample Size Calculation.....	137
4.8	Statistical Analysis	140
4.8.1	Analysis of Multi-parametric MRI and Prostate Mapping Biopsy Results ...	140
4.8.2	Varying the Definitions of Clinical Significance at TPM	141
4.8.3	MRI Targeted Biopsy Analysis	142
4.8.4	Secondary Analysis.....	142

4.9	Analysis of Prostate HistoScanning™ and Transperineal Template Prostate Mapping Biopsy Results.....	142
4.9.1	Varying the Definitions of Clinical Significance at TPM	143
4.9.2	PHS Targeted Biopsy Analysis	143
4.9.3	HistoScanning Test Re-Test Reproducibility	144
4.9.4	Biomarker Analysis.....	144
5	PICTURE Results.....	145
5.1	Recruitment	145
5.2	Baseline Demographic Data	146
5.3	Template Mapping Biopsy (TPM) Results	148
5.4	Whole Gland MRI Results	150
5.4.1	Report Demographics	150
5.4.2	Primary Outcome 1	151
5.5	MRI Targeting Results.....	153
5.5.1	MRI ‘Cognitive’ Targeted Results - MRI Score ≥ 3	153
5.5.2	MRI/US Registration Targeted Results - MRI Score ≥ 3	154
5.5.3	Pooled MRI Targeted Results - MRI Score ≥ 3	154
5.5.4	Summary MRI Targeting Results - MRI Score ≥ 3	156
5.5.5	MRI Cognitive Targeted Results - MRI Score ≥ 4	157
5.5.6	MRI/US Registration Targeted Results - MRI Score ≥ 4	158
5.5.7	Pooled MRI Targeted Results - MRI Score ≥ 4	159
5.5.8	Summary MRI Targeting Results MRI score ≥ 4	159
5.5.9	Altering the MRI Threshold for Biopsy.....	160
5.6	Whole Gland Prostate HistoScanning Results	161
5.6.1	Report Demographics	161
5.6.2	Primary Outcome 1	162
5.7	Prostate HistoScanning Targeting Results.....	163
5.8	Discussion of Prostate HistoScanning Results	164
6	Secondary PICTURE Results	165
6.1	MRI Inter-Reporter Reproducibility Results	165
6.1.1	Discussion of Multiparametric MRI Reliability Results	168
6.2	Prostate HistoScanning Reproducibility Results	169
6.2.1	Test re-test Reliability - 8818 to 8818 Comparison	169

6.2.2	8818 vs. 8848 Probe Comparison	170
6.2.3	Discussion of HistoScanning Reliability Results	172
6.3	Biomarker Analysis.....	172
6.3.1	Engrailed 2 Urine Biomarker	172
6.3.2	FScan	175
7	PICTURE Discussion.....	176
7.1	PICTURE Study Limitations.....	176
7.2	Summary of PICTURE Study Results	178
7.3	PICTURE Study Conclusions.....	179
8	Critical Analysis of Work and Thesis Discussion.....	180
8.1	Main Limitations	180
8.2	Novel Contributions	180
8.3	Impact and Future Directions.....	183
8.4	Summary.....	185
9	Bibliography	187
10	Appendix- Papers/Protocols.....	200
10.1	Papers in Peer Reviewed Journals	200
10.1.1	PHS02 Open Phase Paper.....	200
10.1.2	PHS02 Blind Phase Paper (submitted pending publication)	208
10.1.3	Prostate HistoScanning Editorial.....	228
10.1.4	PICTURE Methodology Paper.....	229
10.2	PHS02 Study Protocol	244
10.3	PICTURE Study Protocol	269
10.4	PICTURE MRI Sequences	363

1 Introduction and Background

1.1 Introduction

1.1.1 Prostate Anatomy and Physiology

The prostate is a small walnut sized exocrine gland that sits beneath the bladder and in front of the rectum in males; the prostatic urethra passes through the prostate en-route from the bladder base to the urogenital diaphragm.

The seminal vesicles sit adjacent to the prostate and the ejaculatory ducts join the prostatic urethra at the verumontanum.

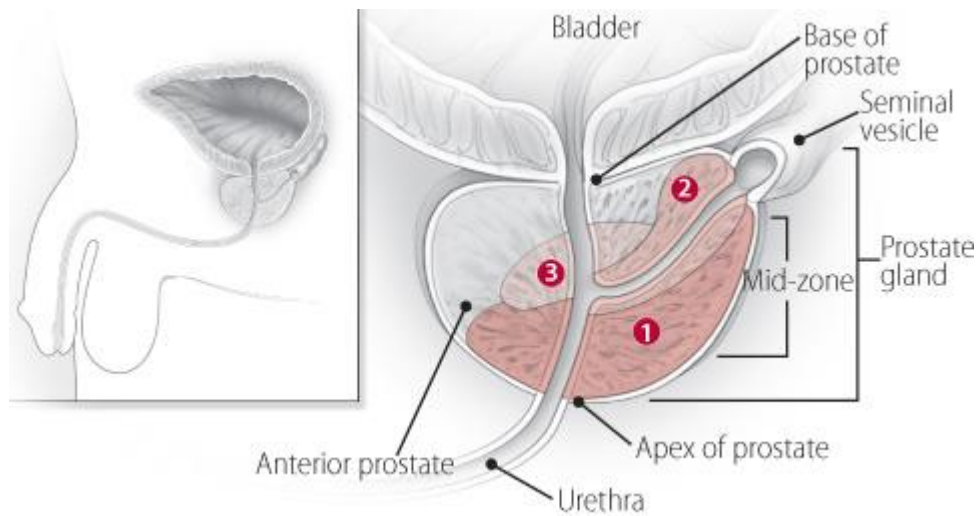
The prostate is divided into four zones, comprising the three glandular zones - the peripheral zone (PZ), the central zone (CZ), the transition zone (TZ) and the non-glandular anterior fibromuscular stroma (AFMS) (Figure 1) (McNeal, 1981).

The peripheral zone surrounds the distal urethra and is the most postero-lateral aspect of the prostate and makes up around 75% of the prostate. Historically most cancers have been found to be located in the peripheral zone.

The central zone makes up approximately 20% of the prostate. It extends from the transition zone to encapsulate the ejaculatory ducts and peri-urethral glandular tissue.

The transition zone surrounds the proximal urethra occupying around 5% of the prostate gland at puberty. However, it is the area of the prostate responsible for benign prostatic hypertrophy (BPH) and continues to grow throughout male adult life.

Figure 1. Schematic of prostate anatomy¹



1= Peripheral Zone; 2= Central zone; 3= Transition zone

1.2 Prostate Gland Function

The prostate gland secretes alkaline prostatic fluid that makes up about a third of the proportion of semen. This alkaline fluid is responsible for helping protect spermatozoa in the acidic environment of the vagina.

Prostatic fluid is composed of a number of electrolytes including very high levels of the anion citrate and lower concentrations of chloride. Other ions are mainly sodium, potassium, calcium, magnesium and zinc (Kavanagh, 1985).

There has been some suggestion that observation of the change of composition of prostatic fluid may be a useful biomarker for prostate cancer (Costello and Franklin, 2009).

Prostate specific antigen (PSA), a glycoprotein enzyme secreted by prostate epithelial cells, is also found in the prostatic fluid. Very small quantities of PSA are found in blood serum and at present PSA testing is one of the gold standard diagnostic tests for identifying men at risk of prostate cancer. However PSA rises are non-specific and can be associated with any of the major prostatic diseases, or urinary tract infections.

¹ Image kindly reproduced with permission from <http://www.harvardprostateknowledge.org/choosing-and-sticking-with-active-surveillance-a-patients-story> accessed 3/6/13

1.3 Prostate Disease

There exist three major prostatic diseases: - benign prostatic hypertrophy (BPH); prostatitis; and prostate cancer. All are predominantly found in men over 50 years of age.

Benign prostatic hyperplasia is a non-cancerous enlargement of the prostate gland that arises from the glandular element of the transition zone. On account of the prostate's anatomical connection with the urethra, this enlargement can cause a decrease in urinary flow and may require treatment if symptomatic.

Prostatitis is an inflammatory condition of the prostate gland that is characterised by pelvic pain; it can be either acute or chronic, and in most cases the aetiology is unknown.

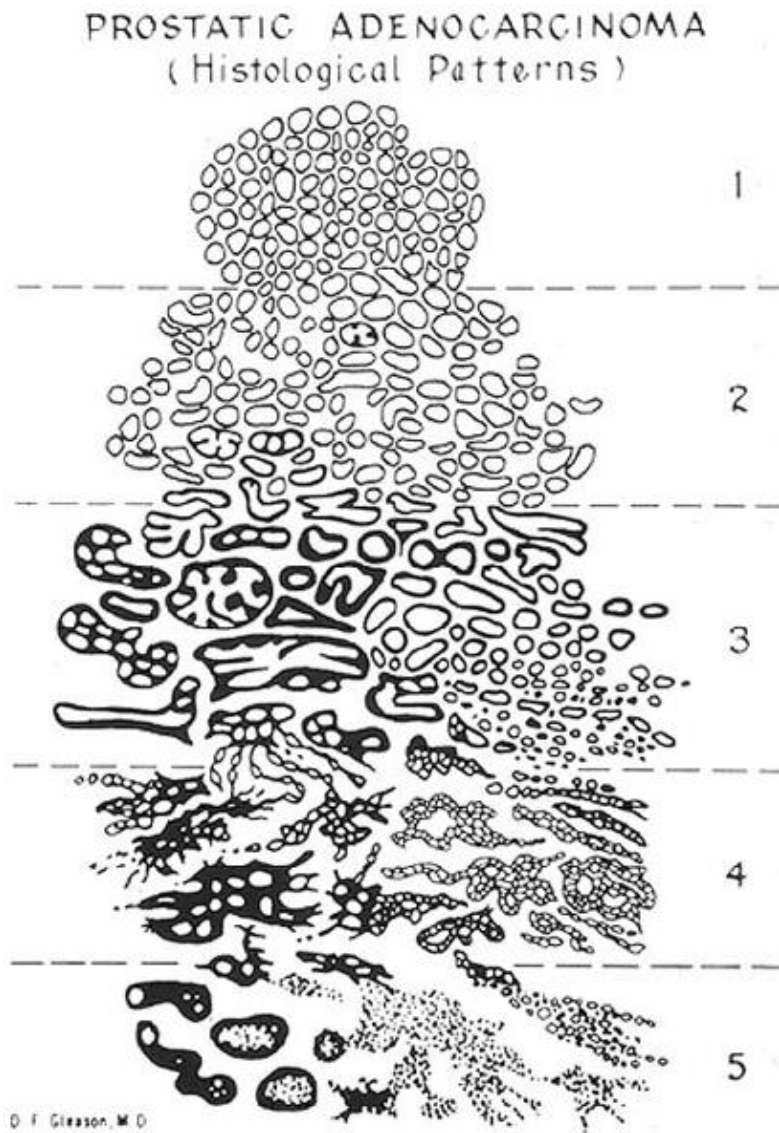
The third and most worrying prostatic disease is prostate cancer. The main aetiological factors for prostate cancer are: - age; race; and positive family history.

1.3.1 Prostate Cancer

The majority of prostate cancers are adenocarcinoma's that arise from the acini of the prostatic ducts. On a microscopic level the features that differentiate prostate cancer from benign tissue are the loss of the glandular architecture, increased neo-vascularity and micro vessel density, and increased cellular density. Gleason grading devised in the late 1960's (Figure 2) is still used to histologically quantify and grade prostate cancers.

Gleason grading is represented by two numbers which identify the most prevalent pattern and the second most prevalent pattern of disease seen by the histopathologist when assessing prostate cancer tissue under a microscope.

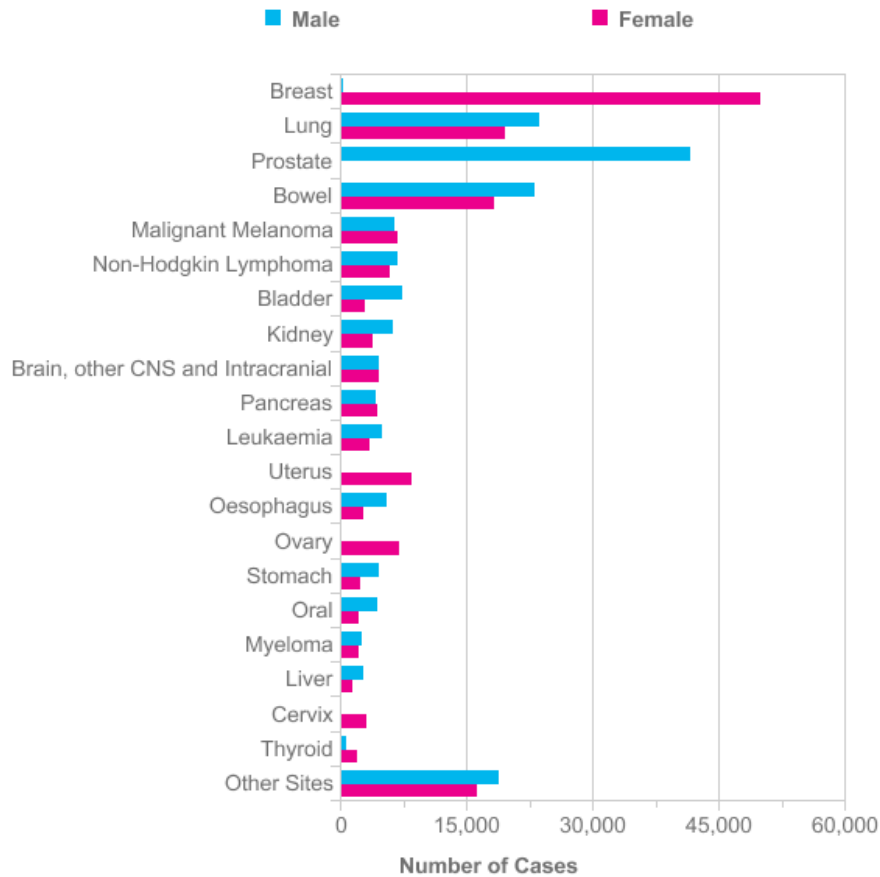
Figure 2. The Gleason grading system



Prostate cancer is a significant public health issue in the United Kingdom (UK) and worldwide. In 1998 prostate cancer became the most commonly diagnosed solid organ cancer in the UK overtaking both bowel and lung cancer.

Figure 3 shows the 20 most common cancers in the UK in 2011 (Cancer Research UK, 2011).

Figure 3. The 20 most common cancers in the UK in 2011²



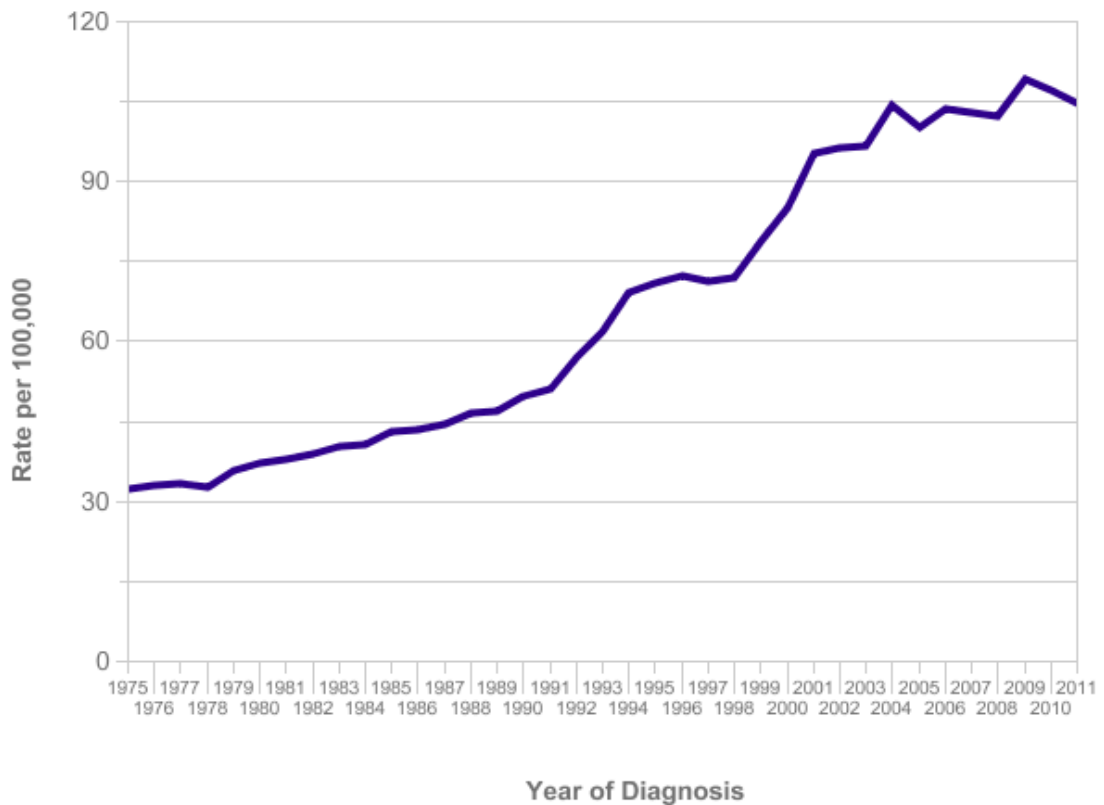
Between 2008 - 2010 there was an average of 40,460 newly diagnosed cases of prostate cancer each year in the UK. (Office for National Statistics, 2010). Their report states that 'the age standardised incidence over the same period was 105 new cases per 100,000 men, with the average number of men dying from prostate cancer each year being 10,427, a mortality rate of 24 deaths per 100,000 men' (Office for National Statistics, 2010).

In the United States, the SEER (Surveillance, Epidemiology and End Results) database age-adjusted incidence rates between 2005 - 2009 were 154.8 per 100,000 men, with almost 250,000 men per year in the United States receiving a new diagnosis of prostate cancer (Siegel et al., 2011). Mortality rates in the US during the same time period were 23.6 per 100,000 men per year.

² CANCER RESEARCH UK. 2011. <http://www.cancerresearchuk.org/>. Available: <http://www.cancerresearchuk.org/cancer-info/cancerstats/incidence/commoncancers/#Twenty> [Accessed 19/04/2014 2014].

There have been significant increases in the reported incidence of prostate cancer in many countries including the UK over recent years. Figure 4 demonstrates the Prostate Cancer (C61), European Age-Standardised Incidence Rates, Males, UK, 1976-2011 (Cancer Research UK, 2014).

Figure 4. Prostate Cancer (C61), European Age-Standardised Incidence Rates, Males, UK, 1993-2011³



The rise in incidence is in part due to the use of the serum blood test Prostate Specific Antigen (PSA) (Thompson et al., 2008) as a screening test both formally in the USA and informally in Europe. However, PSA is false positive-prone - 7 out of 10 men (Thompson et al., 2004) with a raised PSA will not have prostate cancer.

In addition, it is accepted that not all men with localised prostate cancer need treatment and a significant proportion with low to intermediate risk disease could be kept under surveillance (Bill-Axelsson et al., 2005). Indeed, many men over the age of 50 have indolent or insignificant prostate cancer that does not impact upon their life expectancy (Haas et al., 2008).

³ CANCER RESEARCH UK 2014. *CancerStats*. Available: <http://www.cancerresearchuk.org/health-professional/cancer-statistics/statistics-by-cancer-type/prostate-cancer/incidence#heading-Zero> [Accessed 21/06/2015]

The results of a recent large randomised trial the PIVOT study (Wilt et al., 2012) have shown that in men with low to intermediate risk prostate cancer there appears to be little if any survival benefit from radical treatment, and if anything morbidity increased amongst those men with low to intermediate risk prostate cancer with radical treatment. The incidence of low volume, low risk prostate cancer that in all likelihood does not need treatment is also increasing (Cooperberg et al., 2005).

The increasing use of PSA screening and the inability of the current diagnostic pathway (PSA and then prostate biopsy) to differentiate between significant and indolent cancer is contributing to the over-diagnosis and over-treatment of low risk prostate cancer. The healthcare and economic implications of detecting and treating this group of men are significant.

1.4 Current Prostate Cancer Diagnostic Pathway

In most countries in the developed world, when men present with a raised PSA or abnormal DRE they are advised to undergo a trans-rectal ultrasound guided prostate biopsy (TRUS biopsy). Between 65 - 80 000 men have a prostate biopsy in the UK annually (Cross and McPhail, 2008) and over one million biopsies are carried out in the USA.

National Institute for Health and Care Excellence (NICE) guidelines state: "To help men decide whether to have a prostate biopsy, discuss with them their prostate specific antigen (PSA) level, digital rectal examination (DRE) findings (including an estimate of prostate size) and co-morbidities, together with their risk factors (including increasing age and black African-Caribbean family origin) and any history of a previous negative prostate biopsy" (National Institute for Health and Care Excellence, 2014a).

The initial diagnostic test performed for most men at risk of prostate cancer is a standard 6 to 12 core transrectal ultrasound (TRUS) guided biopsy. There is a significant healthcare burden resulting from TRUS biopsy in terms of over-diagnosis, over-treatment and test-related side effects (Bangma et al., 2007).

1.4.1 Problems with TRUS Biopsy

Many men have a negative initial biopsy

Overall, men undergoing trans-rectal ultrasound (TRUS) guided biopsy of 6-12 cores of prostatic tissue have approximately a 1 in 3 probability of being diagnosed with prostate cancer. Of these, about half are diagnosed with low risk disease (Singh et al., 2004).

It therefore follows that the majority of men presenting with an abnormal PSA do not have prostate cancer or have insignificant disease that need not be treated. If this group of men could be identified by a test that could reliably reassure them that they were free of clinically significant cancer, they could avoid biopsy.

Men with low risk disease on trans-rectal biopsy

Around two thirds of men diagnosed with low risk prostate cancer will have this status confirmed on radical prostatectomy examination. One in three will be seen to have intermediate or occasionally high risk prostate cancer at radical prostatectomy.

One of the current diagnostic challenges is in distinguishing these two groups. If an imaging test were able to assist with this, it would be a very valuable test. Men with very low risk disease, if there was greater certainty attached to that diagnosis, could be discharged from further biopsy or follow up (Klotz, 2007).

Men diagnosed with low or very low risk prostate cancer are subjected to the psychological morbidity of having a 'cancer', with many undergoing radical therapy (surgery or radiotherapy) when their disease poses little risk of affecting their life expectancy (Thompson et al., 2004) (Klotz, 2007). Some will choose surveillance, in order to avoid the side effects of immediate radical treatment. However, this is still associated with anxiety (Latini et al., 2007) as well as the burden and cost of repeat biopsies every 2-3 years and 3 monthly clinic visits for PSA tests.

If an imaging tool could reliably rule out significant prostate cancer, and prevent diagnosis of low risk disease, this would represent a significant breakthrough. It may also potentially reduce the negative health impact attached to a cancer diagnosis for the patient and reduce the burden on health services by allowing these men to be discharged from routine follow-up.

Morbidity from the diagnostic process

As well as the diagnostic inaccuracy inherent in TRUS biopsy, there is also a significant risk of: - infection/sepsis; haematuria; haemospermia; pain/discomfort; dysuria, and urinary retention (de Jesus et al., 2006). There is also evidence to suggest that the rate of infection with multi-resistant organisms is increasing (Grummet et al., 2013, Chang et al., 2013).

If an imaging modality could be found that reliably allowed men at low risk of significant prostate cancer to avoid biopsy, these unpleasant and potentially life-threatening side effects could be avoided.

1.4.2 Prostate Cancer Significance

The issue of what is and what is not clinically important disease is also important to address. The observation from post mortem studies is that most men, were they to live long enough, will harbour foci of cancer within their prostate, with, on average 50% over the age of 50 years having foci of prostate cancer (Haas et al., 2008). Yet the observation that only 3% of men die of prostate cancer makes it evident that most men with prostate cancer die of other unrelated causes.

There have been numerous attempts to define the characteristics of 'indolent' disease from disease that might progress in a clinically significant manner and affect life expectancy. Whilst no absolute consensus exists, most experts agree that currently Gleason grade and tumour volume remain the key determinants of disease significance. Stamey et al, investigated tumour volume in defining significant cancer using a cysto-prostatectomy series and proposed that tumours less than 0.5 cc, were likely to be insignificant cancers (Stamey et al., 1993). Epstein et al, showed that a tumour volume of 0.2cc with a Gleason grade <7 are likely to be insignificant cancers based on analysis of radical prostatectomy specimens (Epstein and Potter, 2001).

Since then, many studies have used these tumour volumes, with 0.5 cc or 0.2 cc as thresholds for defining significant or insignificant disease. More recently, however, Wolters et al examined the data from the ERSPC cancer screening trial and suggested that in fact 1.3 cc index lesion and 2.5 cc total cancer volumes may more accurately reflect significant cancer thresholds (Wolters et al., 2011).

Using the more established Stamey and Epstein criteria computer simulation studies performed at University College London have shown show that a maximum cancer core length (MCCL) involvement of 6 mm or greater in any one location derived from Template Prostate Mapping biopsies (TPM), identified 95% of lesions that are 0.5 ml or more in volume. Involvement of any core by 4 mm or greater identified over 95% of lesions 0.2ml or more in volume. These definitions required further validation within prospective trials, and were used within projects outlined later in this thesis.

1.5 Imaging as a Diagnostic Test for Prostate Cancer

In other cancer care pathways imaging plays a large role in diagnosis by identifying patients at risk and specifying a target towards which biopsies are directed. In contrast, in the prostate cancer care pathway, imaging is mainly used at a late stage to identify spread of disease, if at all.

Currently, imaging of the prostate gland is performed to detect the presence of extra capsular extension, the involvement of nodal disease, or distant metastases. Thus, the role of imaging in diagnosing prostate cancer is very limited and diagnosis primarily relies on invasive biopsy procedures.

The prostate is a small organ which is histologically heterogeneous with malignancy, benign prostatic hypertrophy and inflammation, often all occurring at the same time. This histological heterogeneity makes radiological interpretation difficult.

However, as outlined above, with the rising incidence of prostate cancer there is an urgent need for a triage test that can identify those men who are unlikely to have clinically significant prostate cancer, and could therefore avoid invasive testing.

Imaging would be ideal as those with a negative test could be spared invasive biopsy procedures and any areas of suspicion at imaging could be targeted with a biopsy needle.

Currently there are two main imaging platforms demonstrating promise for the detection of cancer: - enhanced ultrasound techniques; and Magnetic Resonance Imaging (MRI).

1.6 Thesis Aims and Hypothesis

This thesis will examine the role of imaging modalities in the prostate cancer diagnostic pathway. It will focus primarily on the role of Prostate HistoScanning (PHS) – an enhanced ultrasound technique - and multi parametric Magnetic Resonance Imaging (mp-MRI).

The hypothesis of this thesis is: imaging has a role in improving prostate cancer detection and that by utilising imaging in the form of either multi-parametric MRI (mpMRI) or Prostate HistoScanning (PHS), men with a negative test may be spared further prostate biopsy, and those with an imaging lesion may be afforded more accurate disease detection and risk stratification.

2 Imaging in Prostate Cancer

2.1 Current Role of Imaging in Prostate Cancer

Currently in the UK, men identified at risk of prostate cancer undergo a routine trans-rectal biopsy guided by ultrasound. The ultrasound is used only to direct the biopsy to the prostate, not to identify lesions within the prostate.

According to UK NICE guidelines in 2008: 'further imaging is not routinely recommended for men in whom no radical treatment is intended. For men with high risk prostate cancer, optional pelvic imaging with CT or MRI may be performed and also Isotope bone scans may be undertaken' (National Institute for Health and Care Excellence, 2008).

However, new NICE guidance issued in January 2014 suggested that 'Magnetic resonance imaging for re-biopsy should be for men with a negative transrectal ultrasound 10–12 core biopsy to determine whether another biopsy is needed' (National Institute for Health and Care Excellence, 2014b).

This recommendation is strongly in keeping with the hypothesis of this thesis - that imaging may be a useful adjunct to the prostate cancer diagnostic pathway.

The issue remains however, one of debate amongst experts, with many suggesting more robust evidence is required.

There are many imaging modalities that are in use or under investigation to assess their role within the prostate cancer pathway. As mentioned previously, the main two contenders appear to be multi-parametric MRI and enhanced ultrasound techniques.

2.2 Review of Transrectal Ultrasound and Enhanced Ultrasound Imaging

Ultrasonography has many advantages as an imaging modality as it is relatively easy to use; it is portable and readily available to most urologists. It is low cost in comparison to other forms of imaging, and images are available in real time. Trans-rectal ultrasound (TRUS) was originally developed to assess rectal pathology. In 1963 Takahashi et al used TRUS for the evaluation of the prostate, but these images were of fairly poor quality and not medically diagnostic (Takahashi H, 1963). In 1974 Wantanabe et al produced the first images with clinical utility using a 3.5MHz transducer (Watanabe et al., 1974).

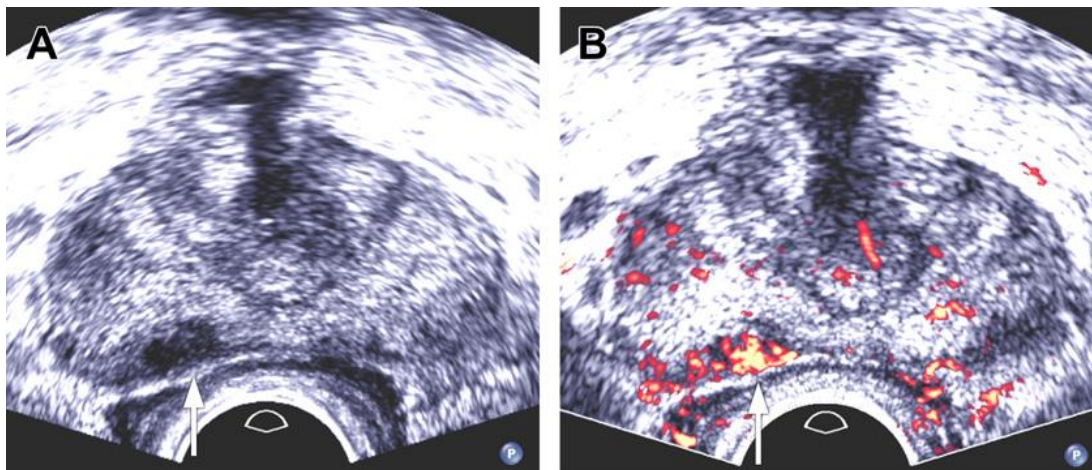
TRUS has since developed to become the primary imaging modality for structural assessment of the prostate and seminal vesicles. It is also used as the primary method for guiding needles into the prostate for diagnostic biopsy. Estimates of sensitivity and specificity of conventional Brightness mode (B-mode) TRUS imaging for detection of prostate cancer range from 44% to 90% from 30% to 74%, respectively (Aigner et al., 2010).

Many technologies have been developed to try to enhance the diagnostic utility of TRUS scanning.

2.2.1 Enhanced TRUS - Colour Flow Doppler/Power Doppler Imaging

Prostate cancer tends to have an increased vascularity in comparison to healthy prostate tissue, particularly the micro vessel density (Erbersdobler et al., 2010). Colour flow Doppler (CFD) aims to detect these differences in prostate tumour neo-vascularity. By identifying the flow of blood away from or towards the TRUS transducer and superimposing this blood flow on the B-mode ultrasound image as a colour (Figure 5) it was hoped that colour doppler would increase the diagnostic accuracy of TRUS.

Since its initial use in prostate imaging in the early 1990's a number of studies have assessed the added value of colour and power doppler, with varied results (Table 1). Power Doppler imaging (PDI) is a special form of colour doppler imaging. It is an amplitude based technique, that it is reported to be able to detect slower flow and be less angle dependent than Colour Doppler imaging (Frauscher et al., 2005) and is therefore generally considered to be better.

Figure 5. TRUS image A, with colour doppler B ⁴**Table 1. Colour and Power doppler imaging studies**

Modality	Study	Year	Number of patients	Sensitivity (%)	Specificity (%)	PPV (%)	NPV (%)
Colour	(Kelly et al., 1993)	1993	158	86.6	-	77	-
Colour/Power Doppler	(Cho et al., 1998)	1998	40	82.6	76.5	82.6	-
Power	(Sauvain et al., 2003)	2003	282	92.4	72	80.6	88.2
Colour/(Elastography)	(Nelson et al., 2007)	2007	137	29	80	18	88
Power	(Eisenberg et al., 2010)	2010	620	40	35	88	6

⁴ Reprinted from GHAI, S. & TOI, A. 2012. Role of transrectal ultrasonography in prostate cancer. *Radiol Clin North Am*, 50, 1061-73., with permission from Elsevier.

Figure 6. Power doppler⁵

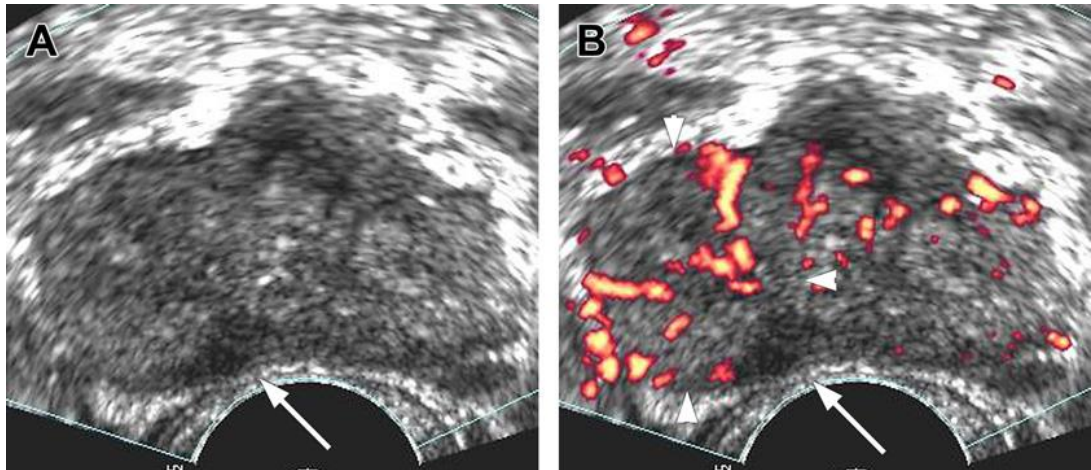


Figure 6 shows a power doppler image, in image A there is a small posterior hypoechoic cancer nodule (arrow). In image B, however power doppler shows that the small nodule is not vascular (arrow) even though it is cancer (Ghai and Toi, 2012).

Additional information from colour doppler and power doppler imaging has not yet been conclusively proven to add significant diagnostic value for prostate cancer. There are a wide range of results in the published literature, with most studies showing little or no improvement in cancer detection over grey scale TRUS. The variability of the results in the literature (Kelly et al., 1993, Cho et al., 1998, Sauvain et al., 2003, Nelson et al., 2007, Eisenberg et al., 2010) suggests that the use of colour and power doppler is heavily user and interpreter dependent.

2.2.2 Contrast Enhanced Doppler- Microbubble

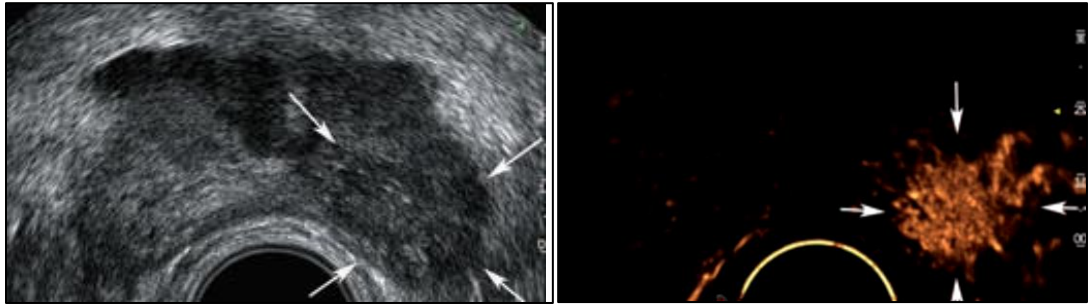
Contrast enhanced doppler (CED) imaging is a further enhancement added to standard B-mode TRUS to attempt improve to the diagnostic ability of TRUS. The most promising agent is Microbubble CED.

Contrast enhanced doppler ultrasound (CEUS) imaging utilises the neo-vascularity in prostate adenocarcinoma, the microbubble contrast agents being small enough to negotiate the microvasculature of the tumours and enable better visualisation of the tumours.

⁵ Reprinted from GHAI, S. & TOI, A. 2012. Role of transrectal ultrasonography in prostate cancer. *Radiol Clin North Am*, 50, 1061-73., with permission from Elsevier.

Figure 7 demonstrates a lesion seen and demonstrated by arrows at grey scale imaging (left) and CED (right).

Figure 7. *Grey scale and contrast enhanced image of prostate lesion⁶*



Contrast microbubbles are visible in the vasculature for several minutes after intravenous injection, and can be visualized with the use of grey scale harmonic and doppler imaging. One of the disadvantages of CEUS is the subjective interpretation by the investigator (Sano and Uemura, 2015).

Earlier versions of CEUS agents were degraded by the doppler imaging which uses fairly high force and therefore the agents were destroyed before they reached the microvasculature. Newer contrast agents (Dindyal and Kyriakides, 2011) and newer imaging methods specific for contrast enhanced imaging such as narrow band imaging, flash echo imaging and harmonic imaging have improved the technology (Trabulsi et al., 2010) with lower imaging powers leading to less microbubble destruction and improved imaging times.

Many investigators have evaluated the use of contrast enhanced doppler for the detection of prostate cancer. Halpern et al investigated the use of CEUS prior to TRUS and directed biopsies to abnormal areas on imaging followed by routine TRUS: 34% of their cohort (n=103/301) had prostate cancer. They found that targeted cores were twice as likely to be

⁶ Reprinted from Xie, S.W. et al; Contrast-enhanced ultrasonography with contrast-tuned imaging technology for the detection of prostate cancer: Comparison with conventional ultrasonography. *BJU Int.* 2012, 109, 1620–1626, with permission from John Wiley and Sons.

positive, odds ratio [OR] = 2.0, $P < 0.001$, and the ROC AUC for contrast enhanced imaging ranged from 0.60-0.65 (Halpern et al., 2005).

Xie et al investigated the use of CEUS vs grey scale and power doppler imaging in 150 men undergoing TRUS biopsies. They found no statistical difference in the number of patients diagnosed on grey scale imaging, power doppler or contrast enhanced, but a combination of the three detected more than grey scale alone with 48% of their cohort having cancer detected (Xie et al., 2012).

Performance characteristics of CEUS per biopsy site for this study are shown in Table 2: it is important to keep in mind that Xie et al looked only at peripheral zone (PZ) areas for biopsy for this study, because enhancement by the microbubbles in the TZ makes interpretation and differentiation between cancerous and non- cancerous areas of the TZ near impossible.

Seitz et al publish favourable sensitivity results for their series of CEUS prior to radical prostatectomy; however, their paper also states that only a 54.5% agreement on the prostate lobe containing the cancer was achieved when considering a per patient lobe analysis rather than whole gland detection i.e. CEUS was detecting cancer on the opposite side of the prostate to RP in nearly 50% of cases (Seitz et al., 2011). Table 2 shows a selection of performance characteristics in published literature for this technology.

Table 2. Contrast enhanced doppler

Study	Year	Number of patients	Sensitivity (%)	Specificity (%)	PPV (%)	NPV (%)	Reference test
(Halpern et al., 2005)	2002	40	40	79	-	-	TRUS biopsy
(Xie et al., 2012)	2012	150	73.1	87.3	66.4	90.4	TRUS biopsy, by site
(Seitz et al., 2011)	2009	35	71	50	91.7	18.2	RP, whole gland

2.2.3 Elastography

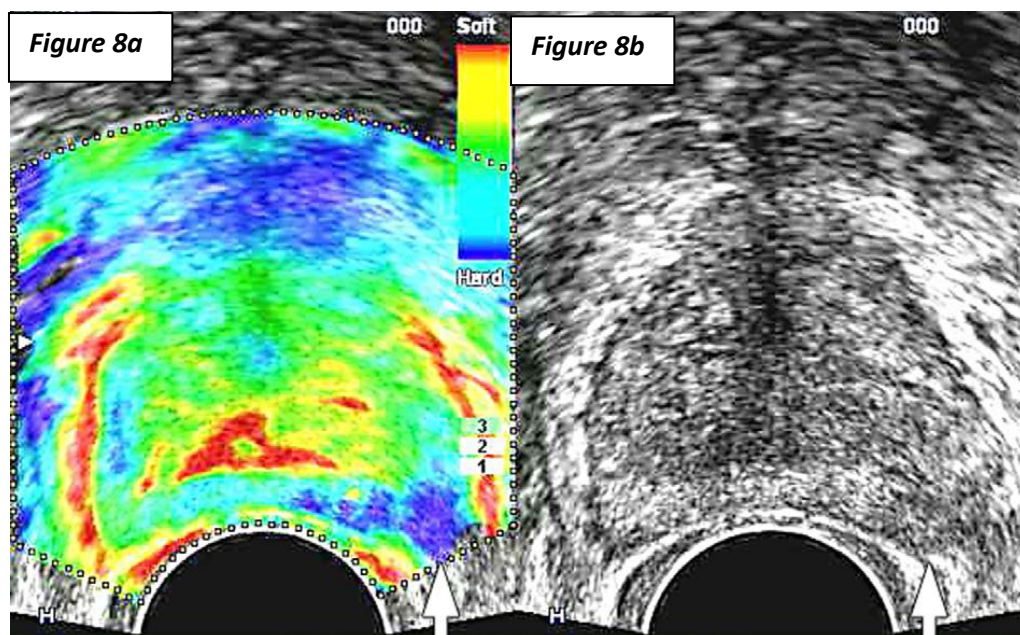
Elastography works on the principle that benign and malignant tissues have different stiffness, caused by the increased cellular density of prostatic adenocarcinoma. There are two types of elastography - static/strain elastography (SE) and shear wave elastography (SWE). They work by slightly different mechanisms, but both aim to predict the presence or absence of prostate cancer depending on the different tissue stiffness.

Static elastography requires the operator to submit pressure on the prostate to produce its effect, and examines the strain or deformation of tissue due to that force: it is a qualitative form of imaging.

Shear wave elastography (SWE) works by using acoustic radiation to produce a shear wave force across the prostate, and analysing the propagation speed of the shear wave, and is able to provide quantitative measure of stiffness.

Early studies on RTE were mainly with static RTE, with shear wave being developed more recently. Shear wave elastography (SWE) facilitates a more quantitative assessment of tissue elasticity during elastography; it measures this elasticity in Young's modulus (kPa). SWE is thought to overcome some of the limitations of quasistatic RTE and the errors caused by operator skill, lack of reproducibility and subjectivity.

Figure 8. Elastography⁷



⁷ Reprinted from GHAI, S. & TOI, A. 2012. Role of transrectal ultrasonography in prostate cancer. *Radiol Clin North Am*, 50, 1061-73., with permission from Elsevier.

In Figure 8a the elastography image shows a stiffer blue area (arrow) that is suspicious for cancer. The area is less obvious on the corresponding grey-scale image figure 8b (arrow).

Salomon et al studied the use of static RTE in 109 men with biopsy proven prostate cancer prior to radical prostatectomy (RP). Pre-operative elastography was performed and a report of suspicious areas made. 439 areas were deemed to be suspicious at RTE compared to 451 tumour foci at histology. Performance characteristics are in Table 3, sensitivity ranged from 72-84% and specificity from 67-84%. The range of sensitivity and specificities was produced by looking at the performance of RTE in different areas of the gland. RTE demonstrated better tumour correlation with lesions in the apical regions, and also showed better detection of higher grade tumours (Salomon et al., 2008).

Tsutsumi et al investigated a novel form of elastography called real time balloon inflation elastography (RBIE) to try to overcome some of the issues around unequal compression of tissues using standard RTE. They investigated the use of RBIE in 55 men undergoing RP, and once again divided the prostate into regions to assess the performance of RBIE in prostate cancer detection. They also aimed to assess if their novel balloon system could reduce artefact at RTE.

They identified that although the RBIE did lead to less slippage artefact; it produced further issues due to air in the balloon. Using the RBIE technique, 88% of the images obtained were available for analysis. Previous studies by the same authors with a manual compression RTE had a 32% artefact rate, thus the balloon reduced artefact by 20% (Tsutsumi et al., 2010).

Cancer detection characteristics were similar to those found by Salomon et al: however, the divisions of the prostate used by Tsutsumi were able to demonstrate acceptable performance for RTE in the anterior gland.

Brock et al investigated 353 men with increased PSA or suspicious DRE. The men were randomized to receive grey scale ultrasound (GSU) or static real time elastography (RTE). Systematic TRUS biopsies were taken and depending on the imaging the analyst predicted whether histology would be benign or malignant (Brock et al., 2012).

Overall cancer detection was 45.3% (n=160/353), with significantly higher detection in the RTE group versus grey scale ultrasound (11.7% p=0.027). Sensitivity for cancer detection using RTE differed from the apex to the base of the prostate, apex (60-76.9%) vs. base (34.2-45%).

The study also demonstrated that 8.1% of the sectors (n=87/1068) contained prostate cancer, that were not deemed suspicious on RTE. RTE had a false positive rate of 24.2%, with 258 areas showing features of malignancy on RTE without histological confirmation of disease. Performance characteristics for RTE are shown in table 3, and were significantly better than those for grey scale ultrasound.

Of note once again with the study by Brock et al, the transition zone was excluded from investigation. It was concluded by the authors that “RTE guided systematic biopsy improved prostate cancer detection compared to grey scale ultrasound guidance”, (Brock et al., 2012) but they also specified that as RTE sensitivity for prostate cancer detection was low systematic biopsies were still required.

Table 3. *Elastography performance characteristics*

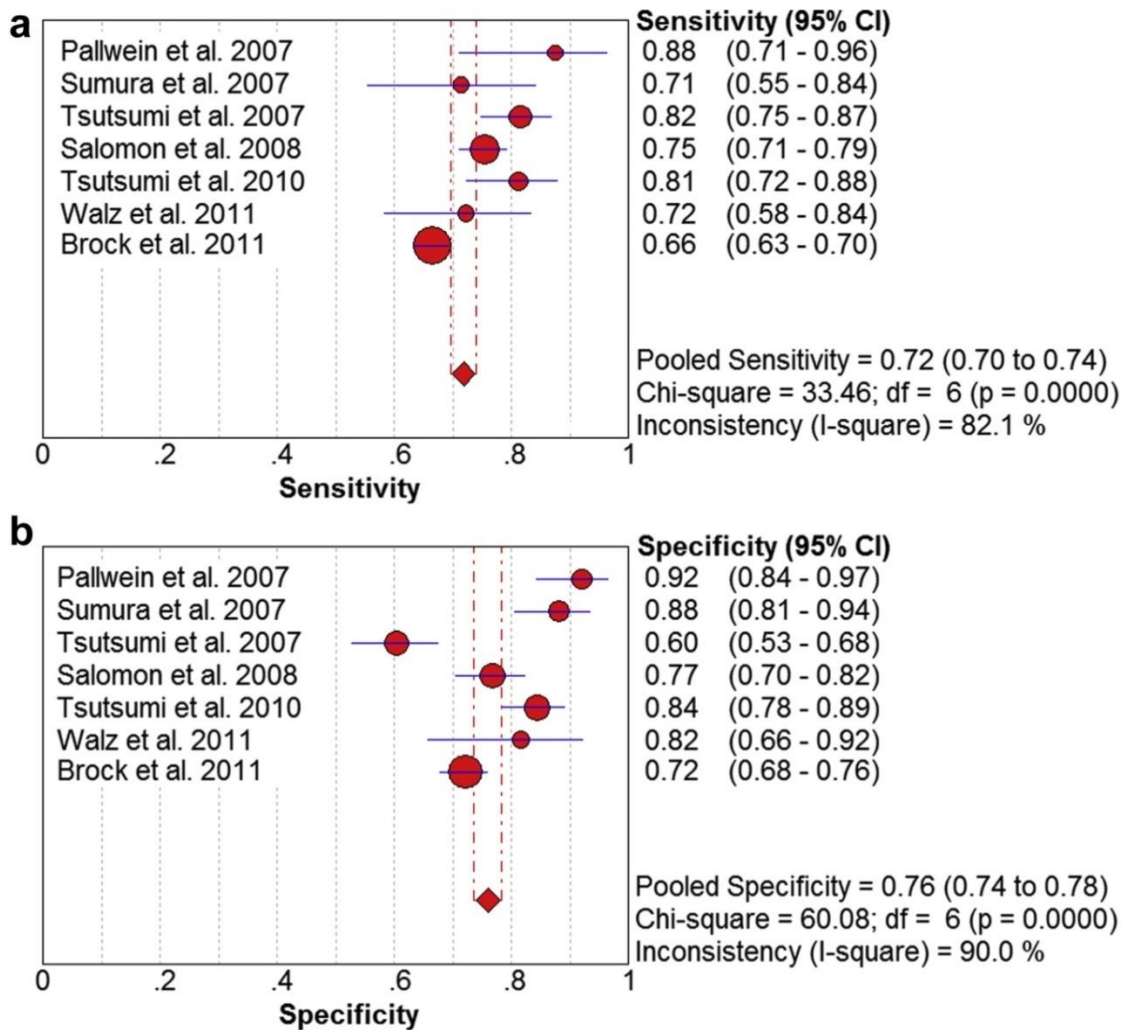
	Study	Year	Number of patients	Sensitivity (%)	Specificity (%)	PPV (%)	NPV (%)
RTE (colour doppler)	(Nelson et al., 2007)	2007	137	25	86	20	88
RTE vs. RP	(Salomon et al., 2008)	2008	109	75.4	76.6	87.8	59
RBIE vs. RP	(Tsutsumi et al., 2010)	2010	55	60-84	80-96	75-93	71-94
RTE vs. TRUS biopsy	(Brock et al., 2012)	2012	353	60.8	68.4	32.4	87.8
Meta- analysis RTE vs. RP	(Zhang et al., 2014)	2014	508	72	76		
SWE vs. TRUS biopsy	(Ahmad et al., 2013)	2013	50	90	88	93	83
SWE vs. TRUS	(Barr et al., 2012)	2012	53	96	96	69	100
SWE vs. RP	(Boehm et al., 2015)	2013	60 (28 in validation cohort)	81	69.1		

A meta-analysis performed on elastography by Zhang et al included 7 studies investigating RTE vs RP, and showed a pooled sensitivity of 72% (95% CI 70-74) and a specificity 76% (95% CI 74-78). Nine studies comparing RTE to TRUS biopsy were not included in the meta-analysis (Zhang et al., 2014).

Figure 9 demonstrates a Forest plot of sensitivity (a) and specificity (b) for real-time elastography in the diagnosis of prostate cancer, for the studies included in the meta-analysis.

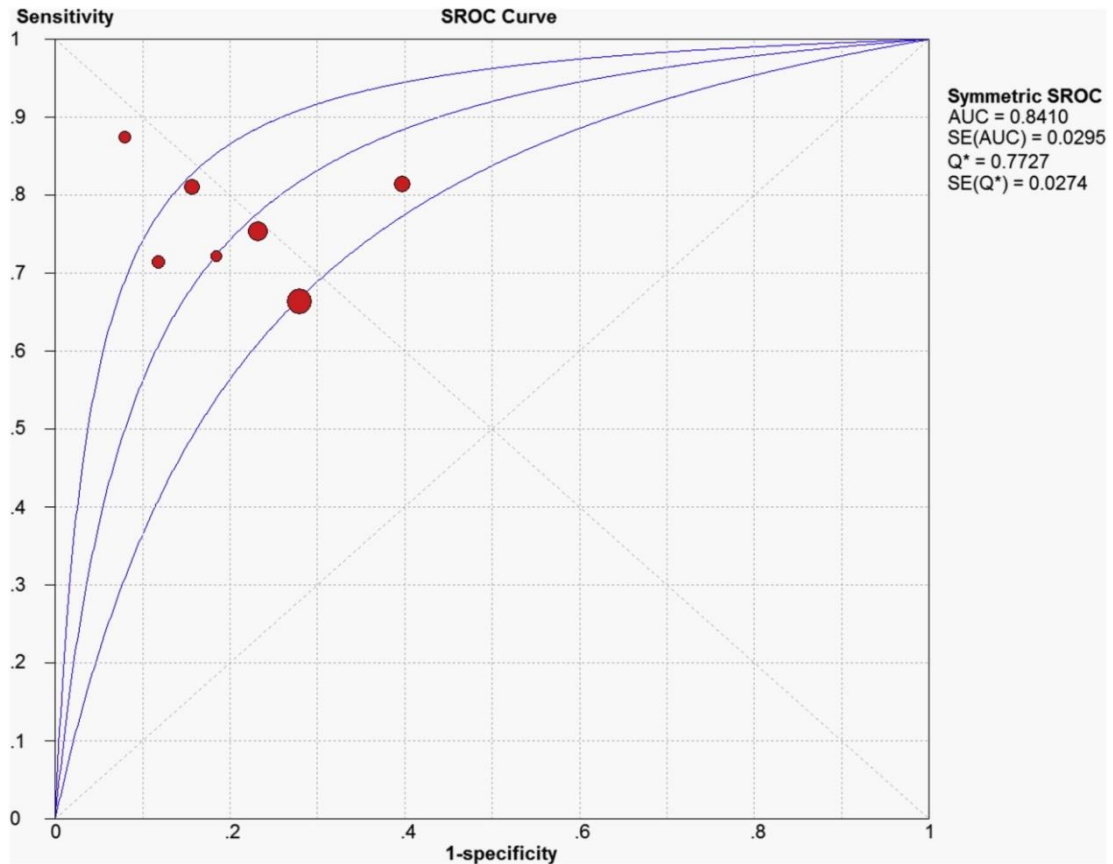
The receiver operator characteristic (ROC) curves for elastography for the articles included in the meta-analysis are shown below in Figure 10, with the AUC for elastography in this analysis being 84.1%. The meta analysis is limited by the fact that all men in all studies were scheduled for RP and thus all had cancer of significant gravitas to warrant radical treatment. Whether these favourable results would translate to a population of men without known cancer is unclear.

Figure 9. Forest plots of sensitivity (a) and specificity (b) for real-time elastography in the diagnosis of prostate cancer.⁸



⁸ Reprinted from ZHANG, B., MA, X., ZHAN, W., ZHU, F., LI, M., HUANG, J., LI, Y., XUE, L., LIU, L. & WEI, Y. 2014. Real-time elastography in the diagnosis of patients suspected of having prostate cancer: a meta-analysis. *Ultrasound Med Biol*, 40, 1400-7. With permission from Elsevier.

Figure 10. Summary receiver operating characteristic (SROC) curve for prostate cancer detection⁹



Data on shear wave elastography is more limited than for static/strain elastography; Ahmad et al examined SWE in 50 men suspected of prostate cancer, prior to 12 zone biopsy SWE being performed. Men had at least one biopsy from each of the 12 zones. Additional biopsies were obtained from areas of SWE suspicion (Ahmad et al., 2013).

The results were split into two groups men with PSA ≥ 4 but < 20 ug/L (n=39), and those with PSA ≥ 20 (n=11). In the PSA <20 group sensitivity 0.9 (95% CI 0.6-0.69) and specificity 0.88 (95%CI 0.82-0.92). In PSA ≥ 20 group these performance characteristics improved, sensitivity 0.93 (95%CI 0.86-0.97) and specificity 0.93 (95%CI 0.77-0.98) but it is worth considering that in this sub-group all 11 men had cancer.

⁹ Reprinted from ZHANG, B., MA, X., ZHAN, W., ZHU, F., LI, M., HUANG, J., LI, Y., XUE, L., LIU, L. & WEI, Y. 2014. Real-time elastography in the diagnosis of patients suspected of having prostate cancer: a meta-analysis. *Ultrasound Med Biol*, 40, 1400-7, with permission from Elsevier.

The study also contained a small number of men from a single centre, giving unreliable estimates of these performance characteristics as demonstrated by the wide confidence intervals. No cut off for stiffness was mentioned in the paper by Ahmed et al.

Despite these limitations, it showed that SWE may be a promising technique for prostate cancer detection. This study has also suggested that there may be a correlation between Young's modulus and Gleason grade- which, if this association can be proven in subsequent studies could prove very helpful in risk stratification. The Young's modulus is the measure of the stiffness of tissues that is produced by SWE.

Barr et al investigated SWE against sextant TRUS biopsy with a Young's modulus cut off of 37kPa, (Barr et al., 2012). They demonstrated 96.2% sensitivity and 96.2% specificity. They also noted that the Young's modulus was higher in areas of malignant tissue than in atypia or inflammation. It is important to note that out of 53 patients examined in the study only 11 patients had cancer (26 foci in 11 men); thus these results are based on a small sample size. Also a further limitation of SWE is highlighted by the authors as a shear wave pulse is known to only penetrate 3-4cm, and in large prostates may not be able to penetrate deep enough into tissues to scan the entire gland.

A further study on SWE by Boehm et al investigating SWE prior to RP in 60 men did not show any correlation between Young's modulus and Gleason grade, in contrast to the results of Ahmad et al. Once again the performance characteristics for SWE were promising with 80.9% sensitivity and 69.1% specificity (Boehm et al., 2015).

Although shear wave has removed the limitation from static RTE of non-uniform compression over the gland, elastography still has a number of limitations including:

- Lack of penetration into the anterior gland, and different performance characteristics in different areas of the prostate
- Steep learning curve for the performance and interpretation of elastography images
- False positives are prevalent, especially in areas of previous prostatitis or BPH nodules.
- Small number of studies investigating SWE

Also elastography suffers from the fundamental limitation in that not all prostate cancers have increased tissue stiffness. Furthermore, there are areas within the prostate which

harbour calcifications or fibrosis that can be much firmer and therefore detected as false positives on elastography.

Despite these limitations, the evidence available so far on elastography suggests that further investigations of this technology in larger cohorts of men - and in multi-centre trials - are warranted.

2.2.4 Artificial Neural Network Analysis/Computerised-TRUS

First devised in 1990, Artificial neural network analysis/Computerised TRUS (ANNA/C-TRUS) aimed to distinguish benign from malignant tissues using an artificial neural network. This network utilises static TRUS images that are transmitted to a static computer server by a secure web connection. The images are then analysed using the ANNA algorithms to highlight suspicious areas and data sent back to the referring clinician. Data sent back to the referring clinician indicates C-TRUS predicted presence or absence of prostate cancer and the Gleason grade.

In the first series of C-TRUS vs. Radical Prostatectomy (RP) step sectioned histopathology, the image analysis system yielded 90% sensitivity, and a 5% false positive ratio (Loch et al., 1990). The study was performed only in the peripheral zone of the prostate and this training set of 5 patients was the basis for further work with C-TRUS ANNA.

In a further study looked at ANNA vs. Radical prostatectomy (Loch et al., 1999), 61 patients had 289 whole mount slices, in which 553 matched pathological lesions were confirmed. Fifty three were used for further training and 500 for a blinded analysis.

This early study on the ANNA found that ANNA correctly classified 99% (378 lesions) as benign and incorrectly called 1% (n=3) malignant, out of the 381 pathology confirmed benign specimens. Of the 119 malignant samples – 94 (79%) were correctly classified as cancer, 25 (21%) falsely classified as benign. These figures correspond to 79% sensitivity and 99% specificity.

Grabski et al investigated the use of C-TRUS on a network capable module, thus allowing the patient and the C-TRUS analysis to occur in different locations, as up until this point the C-TRUS computer had been a static stand-alone piece of equipment (Grabski et al., 2011). The new system allowed TRUS images to be sent from an internet platform for analysis, the

C-TRUS analysis centre then analysed the images and returned a report to the urologist with suspicious areas transposed onto the TRUS image.

In this study, 1545 digital images were examined, and following C-TRUS analysis TRUS biopsies were obtained from suspicious areas in the prostate. Using the C-TRUS analysis to guide biopsy, 91 prostate malignancies were identified in this group of men whom on average had 8 (Range 0-54) prior negative biopsies.

More recently Strunk et al investigated a combination of C-TRUS and mpMRI in 20 men (Strunk et al., 2014). Each patient underwent a 3 Tesla MRI and TRUS imaging, which were sent for C-TRUS reporting. Based on the results of the C-TRUS and mpMRI patients underwent targeted biopsy.

C-TRUS found suspicious lesions in 20/20 men, the median number of lesions was 7 (range 4-8). 17/20 men showed lesions on MRI, with the median number of lesions being 1 (range 1-3). Nineteen out of 20 men underwent targeted biopsy, in only 11/19 biopsies (58%) was a prostate adenocarcinoma detected. However, it must be mentioned that the study is severely limited by the low number of patients involved and the lack of an adequate reference standard.

From information available to date on C-TRUS/ANNA, it is difficult to recommend its use in clinical practice as there is not enough data from well-designed, high number patient studies.

2.2.5 Prostate HistoScanning

A novel tissue characterisation technology – Prostate HistoScanning™ has shown some promise.

In its first clinical study comparing pre-operative HistoScanning™ with radical prostatectomy specimen histology, it was shown to detect all cancers above 0.5cc - and accurately matched the location of these significant cancers (Braeckman et al. 2008a; Braeckman et al. 2008b).

Studies published during the evolution of this thesis have shown less optimistic results for PHS in its ability to detect prostate cancer (Macek et al., 2014, Schiffmann et al., 2013, Javed et al., 2013).

HistoScanning is often compared to C-TRUS/ANNA in its use of algorithms to determine the presence or absence of prostate cancer; their technologies, however, are fundamentally different. Whilst C-TRUS analyses the 2D grey scale image produced by any ultrasound machine, prostate HistoScanning extracts the raw radiofrequency data of the ultrasound wave, prior to its processing and loss of information by the ultrasound machine. It is on the basis of the RF data for each voxel of a 3-dimensional TRUS scan that HistoScanning applies its tissue characterisation algorithms.

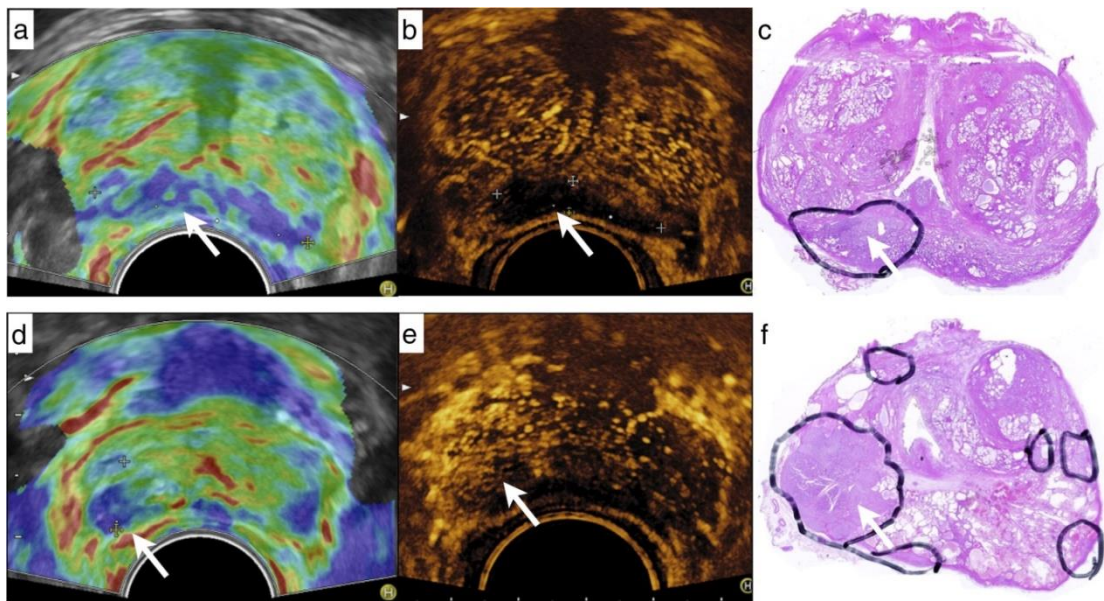
Chapter 3 explores the evolution and initial interrogation of HistoScanning technology in further detail. The main body of work for this thesis, the PICTURE Study, aimed to determine if HistoScanning has a role in prostate cancer detection and is discussed in depth in later chapters.

2.2.6 Multiparametric Ultrasound

There are several enhanced ultrasound modalities that have shown promising performance characteristics for the detection of prostate cancer lesions. To date there has been little work to assess if a combination of these modalities enhances these performance characteristics further.

Several groups have postulated that multi-parametric ultrasound (mpUS), may be possible, and several literature reviews have been published with this question in mind. They conclude that “By effectively combining these ultrasound techniques, all targeting different properties of malignant tissue, a valuable clinical tool with all the advantages of ultrasound could be constructed. The literature shows that combining ultrasound modalities in a crude fashion can already improve sensitivity by 13–59 %” (Postema et al., 2015a, Postema et al., 2015b).

The only study of multiparametric ultrasound, to date, has been performed by Brock et al who investigated the combination of contrast enhanced ultrasound and real time elastography. 100 patients with TRUS biopsy proven prostate cancer underwent an mpUS- following RTE suspicious target lesion were highlighted and assigned a prostate sector, then further evaluated using CEUS. These findings were correlated to final pathology following RP (Brock et al., 2013).

Figure 11. RTE images and corresponding CEUS and RP histology¹⁰

14 men were excluded as correlation between their imaging and pathology slides could not be performed accurately due to fixation artefacts or slide disruption. 1032 prostate sectors were examined from 86 men (12 per patient), 621 sectors contained prostate cancer. RTE identified cancer with overall sensitivity 49% and specificity 73.6%, and had a false positive rate in 30 out of 86 target lesions (34.9%). The addition of CEUS to RTE decreased the false positive rate to 6 out of 58 target lesions (10.3%).

The group found that “if the RTE positive target lesion showed a suspicious perfusion pattern, the likelihood of correctly detecting histopathological cancer was 89.7%” (Brock et al., 2013).

The results are promising for the ability of CEUS to reduce the false positive rate of RTE; however, the study has a major limitation in that the authors evaluated the detection of what they defined as target lesions only - not the whole prostate; these targeted lesions were defined by RTE and then further imaged using CEUS. The authors acknowledge the difficulty of visualising the whole gland in a short time using CEUS; thus, these limitations and inability to image the whole gland is a major barrier to using the technology reliably in routine clinical practice.

¹⁰ Reprinted from BROCK, M., EGGERT, T., PALISAAR, R. J., ROGHMANN, F., BRAUN, K., LOPPENBERG, B., SOMMERER, F., NOLDUS, J. & VON BODMAN, C. 2013. Multiparametric ultrasound of the prostate: adding contrast enhanced ultrasound to real-time elastography to detect histopathologically confirmed cancer. *J Urol*, 189, 93-8. with permission from Elsevier.

2.2.7 Ultrasound Summary

There are mixed findings in the literature about the accuracy of enhanced ultrasound techniques for the detection of prostate cancer. Whilst they are attractive in that they are more affordable and easier to use/interpret than costly MRI images, the use of ultrasound modalities for the detection of disease is hampered by a number of limitations.

Ultrasound is known to be a highly user dependent technique and the enhancements to ultrasound suffer from this same user variability. There is also poor penetration of ultrasound signal in to the transition zone of the prostate and this can affect the performance of the technologies.

Many of the studies for enhanced ultrasound modalities that are published in the literature are small series or contain methodological flaws such as selection bias (all men known to have cancer), verification bias (TRUS biopsy used as the verification test which is in itself not an accurate test), this reduces the confidence with which we can interpret the findings.

It is important that the ultrasound techniques be compared to MRI in large well designed studies, as is discussed later in this thesis.

There are, however, increasing arguments for combining the ultrasound modalities, as they each target different properties of malignant tissue. With a combination of ultrasound techniques, it is likely that more accurate prostate cancer detection and risk stratification could be performed than with one technology alone.

As such, further well designed studies of mpUS are recommended to further assess the usefulness of the technologies.

2.3 Review of Magnetic Resonance Imaging

MRI has been conventionally used in the prostate cancer pathway as a staging investigation to identify extra capsular disease due to its superior soft tissue delineation, but had been thought to be poor in characterising the disease within the prostate gland. The sensitivity of unenhanced MRI in the detection of prostate cancer varies from 37% - 96%, (Ahmed et al., 2009) but is accepted to be on average approximately 50%.

The variation is due to the criteria for a positive result and exclusion of incidental cancers as well as using various numbers of regions of interest and many studies excluding the transition zone.

The current practice of performing MRI after TRUS biopsy makes the interpretation even more difficult due to post biopsy haemorrhagic changes within the gland (Qayyum et al., 2004, Tamada et al., 2008b). These post biopsy artefacts can last over 3 months and can significantly affect diagnostic performance (White et al. 1995).

Magnetic resonance imaging can include a number of different sequences that exploit the different physical and anatomical properties of the tissues and of the movement of water molecules within the tissues. Combining these sequences together has been labelled a multi-parametric MRI (mpMRI).

MRI of the prostate can be performed at 1.5 Tesla; however, the development of new scanners with 3 Tesla magnets has seen an improvement in the signal-to-noise ratio, as has the use of pelvic array coils - this coupled with the mpMRI approach being adopted for MRI has led to an improvement in performance characteristics for the technology. (Turkbey et al., 2009, Turkbey et al., 2010, Aydin et al., 2012, Aydin et al., 2013b)

The anatomic sequences are T1 and T2 weighted imaging, the functional sequences include: dynamic contrast enhanced imaging (DCE); diffusion weighted imaging (DWI); apparent diffusion co-efficient maps (ADC Maps), and MR spectroscopic imaging (MRSI).

2.2.1 T2 Weighted Imaging

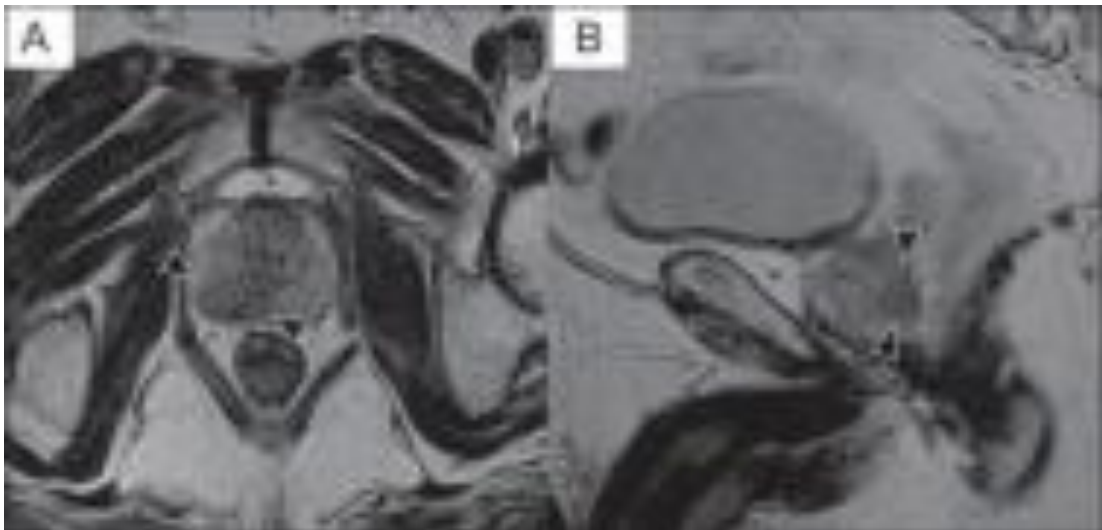
T2 weighted imaging provides the anatomic imaging, and is considered by many the mainstay of mpMRI. T2 imaging clearly outlines the zonal anatomy of the prostate- the prostatic capsule, peripheral zone and transition zone (Hricak et al., 1987).

Prostate cancer on T2 imaging is characterised by hypo-intense lesions in the peripheral zone (PZ) replacing the normal hyper-intense signal of the PZ, or the homogenous signal of the transition zone (TZ). The signal intensity (SI) is one of the key features on T2 imaging that helps reporting radiologists determine the presence or absence of prostate cancer on T2.

The presence of a hypo-intense lesion on T2 is considered highly sensitive for the presence of prostate cancer, however T2 weighted imaging alone suffers from poor specificity, due to post biopsy artefact, prostatitis, atrophy and post treatment changes (Bittencourt et al., 2014).

Some studies have shown a link between low signal intensity and the presence of higher gleason grades (Gleason 4-5) tumours (Wang et al., 2008).

Figure 12. T2 weighted image¹¹



The presence of prostate cancer in the central and transition zone can be harder to detect on T2 weighted imaging because of the heterogeneity of the region, and the changes caused by benign prostatic hypertrophy (BPH), that can also demonstrate low T2 signal. Studies have shown that it is possible to detect TZ tumours on T2, but acknowledge that it remains more challenging as the signal intensity characteristics of the TZ and cancers can overlap. Detection of disease in the TZ proved more reliable the bigger the TZ lesion (Akin et al., 2006, Barentsz et al., 2012b).

¹¹ Image kindly reproduced from BITTENCOURT, L. K., HAUSMANN, D., SABANEEFF, N., GASPARETTO, E. L. & BARENTSZ, J. O. 2014. Multiparametric magnetic resonance imaging of the prostate: current concepts. *Radiol Bras*, 47, 292-300. Accessed 20/6/15 <http://www.ncbi.nlm.nih.gov/pmc/articles/PMC4341390/#!po=2.27273>

Despite showing some utility for the detection of prostate cancer T2 weighted imaging alone lacks sensitivity due to problems in detection in the central zone (CZ) and specificity is affected by other processes within the prostate. This leads to a range of performance characteristic values in the literature for T2 weighted imaging shown in Table 4.

Table 4. *T2 weighted imaging performance characteristics*

Study	Number of patients	Zone studied	Sensitivity % (95% CI)	Specificity % (95% CI)
(Akin et al., 2006)	148 (46 control)	TZ	75 (67-82)	87 (74-95)
(Turkbey et al., 2010)	70	PZ/TZ	42 (36-47)	83 (81-86)
(Tan et al., 2012)	Meta-analysis	PZ/TZ	57-62	74-78

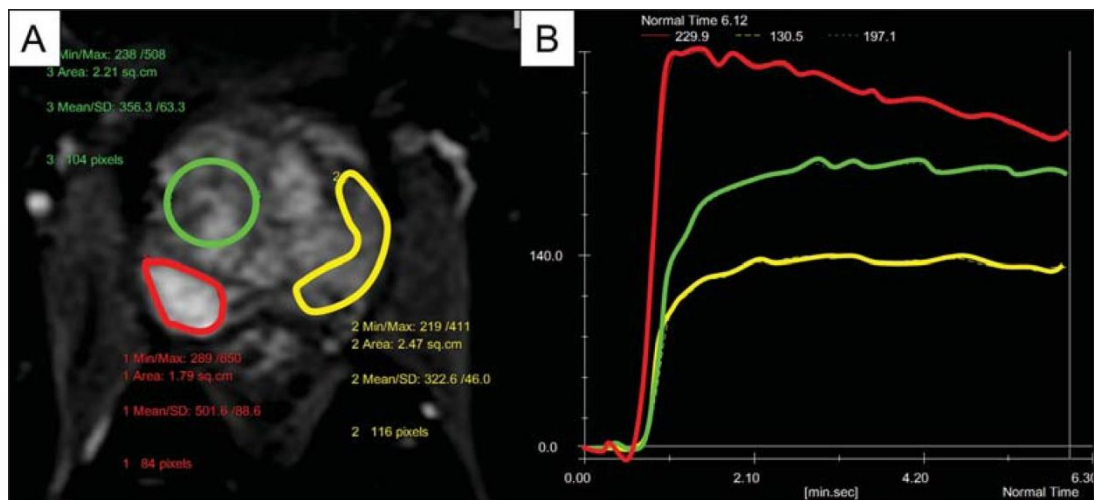
2.2.2 T1 Weighted and Dynamic Contrast Enhanced (DCE)

Pre-contrast T1 axial images are used in the mpMRI protocol prior to DCE images. A T1W image allows imaging of the gland to ensure that changes seen on DCE are not due to biopsy-related haemorrhage. Post biopsy haemorrhage on DCE can be mistaken for tumour. DCE sequences are based on the MRI T1 sequences that are acquired pre contrast injection and then sequentially throughout the exposure to contrast for several minutes.

DCE enables the calculation of parameters related to the microvascular properties of tissue angiogenesis (Bittencourt et al., 2014). The presence of increased neo-vascularity in prostate cancer leads to an intense and early enhancement on DCE sequences (wash in), (Kim et al., 2005) followed by a rapid wash out period, when intravenous contrast such as gadolinium is injected into the patient. The DCE images are then processed to provide either semi-quantitative or quantitative enhancement curves, and colour parametric maps to demonstrate wash-in rate, maximum intensity (k_{trans}, k_{ep} etc) and suspicious areas. The aim is to analyse the pharmacokinetic behaviour of the contrast agent on the T1 images over time (Futterer et al., 2006, Ocak et al., 2007, Tanaka et al., 1999).

Simple visual examination of DCE images has been shown to be successful and is used in many institutions (Girouin et al., 2007). The more quantitative approaches to DCE-MRI interpretation require specialist computer hardware and software, and can be quite time consuming.

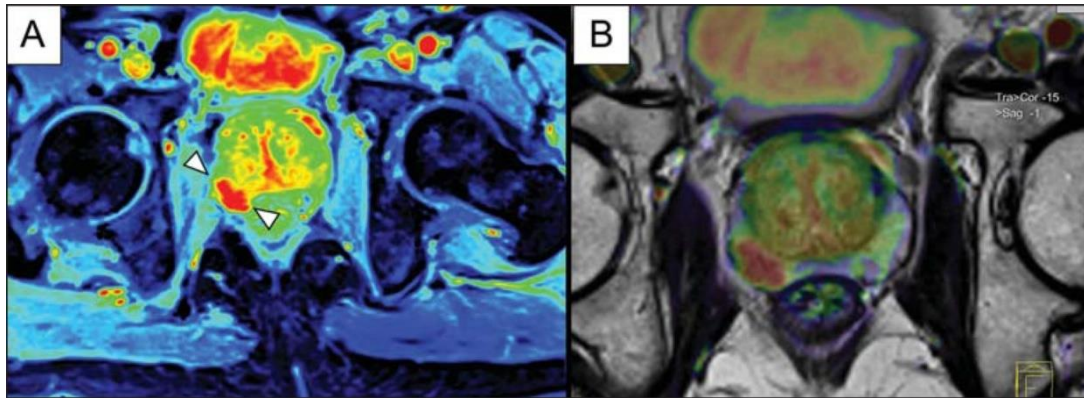
Figure 13. Dynamic contrast enhanced image signal intensity¹²



'Signal intensity versus time curve in a typical tumour lesion. The image **A** represents the early arterial phase of DCE evaluation, showing a focal area of early contrast enhancement in the peripheral zone at right (outlined by the red line). Normal appearing areas were also outlined in the contralateral peripheral zone (yellow) and internal gland (green). The resulting curves (**B**) show that the suspicious lesion (red curve) is characterized by a high and steep rise (washin), followed by a marked decrease (washout), with a significantly different behavior from the other curves'. (Bittencourt et al., 2014)

¹² Image kindly reproduced from BITTENCOURT, L. K., HAUSMANN, D., SABANEFF, N., GASPARETTO, E. L. & BARENTSZ, J. O. 2014. Multiparametric magnetic resonance imaging of the prostate: current concepts. *Radiol Bras*, 47, 292-300. Accessed 20/6/15

Figure 14. *Semi-quantitative post processing of DCE¹³*



'Semi-quantitative post-processing of DCE. Image A represents the parametric map generated from DCE evaluation of the same patient of Figure 13, corresponding to the area under the curve during the first minute (positive enhancement index – PEI). Note that on this map, the suspected area cited in Figure 13 is coded in red (arrowheads), standing out from the other portions of the prostatic parenchyma. On B, one observes a fusion between the DCE parametric map and the T2-weighted sequence in the axial plane, enabling better correlation of anatomic and functional findings' (Bittencourt et al., 2014).

In one study evaluating 24 men with raised PSA who underwent T2-weighted and DCE-MRI with 3-Tesla pelvic phased array coil before prostate biopsy compared to whole-mount radical prostatectomy step-sectioned histology (Villers et al. 2006). DCE MRI showed a sensitivity, specificity, positive predictive value and negative predictive value of 90%, 88%, 77% and 95%, respectively for cancer lesions above 0.5cc, and 77%, 91%, 86 % and 85% respectively for cancer lesions above 0.2cc.

Table 5 outlines a selection of performance characteristics for DCE as found in current literature.

A number of studies have evaluated the role of DCE-MRI, DW and MRSI in detecting prostate cancer either prior to prostate biopsy or radical prostatectomy. These studies have found that a combination of DCE and DWI imaging demonstrates the most promising sensitivity for anterior PZ and central zone tumours (Turkbey et al., 2011). Other studies have shown that DCE is more useful when used in combination with T2 weighted imaging than alone (Turkbey et al., 2010).

¹³ As above Accessed 20/6/15 <http://www.ncbi.nlm.nih.gov/pmc/articles/PMC4341390/#!po=2.27273>

Table 5. DCE imaging performance characteristics

Study	Number of patients	Zone studied	Sensitivity % (95% CI)	Specificity % (95% CI)	PPV % (95% CI)	NPV % (95% CI)
(Kim et al., 2005)	53	PZ/TZ	96	82	82	96
(Ocak et al., 2007)	50	PZ	73 (62-82)	88 (80-95)	75 (65-85)	75 (68-82)
(Turkbey et al., 2010)	70	PZ/TZ	18 (13-23)	96 (94-97)	-	-
(Turkbey et al., 2011)	45	PZ/TZ	38	98	86	87

There have been suggestions that the addition of DCE improves T2W imaging specificity: if lesions are seen on T2, they are more likely to be due to cancer than benign processes, but that DCE alone is unlikely to highlight new lesions that have not been detected at T2 (Ocak et al., 2007).

A meta-analysis of 24 articles investigating DCE (Tan et al., 2015) found that the AUC for DCE MRI alone and that for DCE and T2-weighted imaging was superior to that of T2-weighted imaging alone.

DCE also has the advantage that it can be performed quickly on most MRI scanners, unlike MRSI. DCE imaging however, due to its dynamic nature, can be severely affected by patient movement, and subsequent mis-registration of the image set (Aydin et al., 2013a, Verma et al., 2012).

There is also at present a lack of consensus in how DCE images should be read and interpreted; the previously mentioned meta-analysis (Tan et al., 2015) did find that simple visual analysis of DCE performed similarly to semi quantitative approaches.

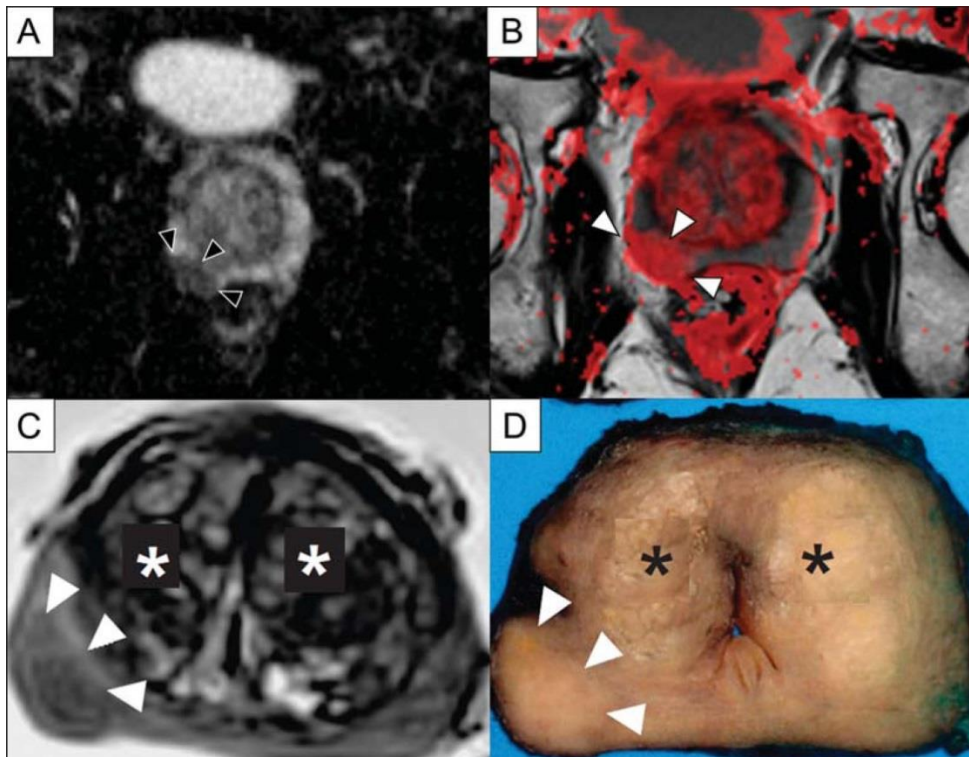
2.3.1 Diffusion Weighted Imaging (DWI)

Diffusion imaging studies the random movement of water molecules by “Brownian motion”. In prostate cancer tissues these movements are restricted by altered cellular density. (Koh and Collins, 2007) DWI imaging does not require contrast and takes approximately 5 minutes on the MRI scanner.

DWI images create sets depending on the “b-value” chosen. The b-value chosen for DWI relates to the time scale over which the DWI interrogates water movement. If more than two b-value images are acquired an Apparent Diffusion Co-efficient map (ADC map) can be made by combining the b-value sequences. Prostate cancer (PCa) is characterised by increased cell density and a higher nucleus/cytoplasm ratio as compared with the surrounding prostate tissue. This leads to impeded diffusion, with a marked reduction in the ADC values relative to the healthy prostate tissue. (Bonekamp et al., 2011)

DWI has been shown to be a valuable sequence for prostate cancer in a number of studies in recent years. (Anderson et al., 2000, Isebaert et al., 2013, Delongchamps et al., 2011)

Figure 15. *Diffusion weighted images and ADC map¹⁴*



¹⁴ Image kindly reproduced from BITTENCOURT, L. K., HAUSMANN, D., SABANEEFF, N., GASPARETTO, E. L. & BARENTSZ, J. O. 2014. Multiparametric magnetic resonance imaging of the prostate: current concepts. *Radiol Bras*, 47, 292-300. Accessed 20/6/15

'Detection of PCa with DWI. ADC map of the same patient in Figure 14 (A) showing a suspicious hypointense focal lesion in the right peripheral zone (arrowheads), determining restricted water diffusion, with ADC values around $750 \times 10^{-6} \text{ mm}^2/\text{s}$, while the contralateral peripheral zone exhibits ADC values in the range of $1,600 \times 10^{-6} \text{ mm}^2/\text{s}$. The fusion of information from DWI with T2-weighted images (B) shows that the lesion detected on ADC map, coded in red (arrowheads) has topographic correspondence with suspicious areas on T2-weighted image. The patient underwent radical prostatectomy, and the surgical specimen was sent for ex vivo MR examination (C), which showed a suspicious lesion (arrowhead) in the same region as of preoperative MR examination. The whole mount specimen at the same level and orientation of the MR images (D) also shows the tumor area (arrowhead) on the same location indicated by MR images. Asterisks on C and D represent areas with BPH'. (Bittencourt et al., 2014)

Two recent meta-analyses of DWI have shown that the performance of DWI is better than that of T2WI alone (Tan et al., 2012, Wu et al., 2012) (Table 6). However, the addition of T2-weighted images, DWI and DCE performed significantly better in some studies than T2W and DWI alone. (Delongchamps et al., 2011, Tamada et al., 2011, Chen et al., 2008)

High B value images provide better contrast, and there have been suggestions of benefit to ultra-high b values (b1000-2000) in the determination of benign from malignant disease with sensitivities ranging 0.71-0.88, and specificity 0.9-0.92 (Kim et al., 2010, Tamada et al., 2014).

Table 6. Diffusion weighted imaging

Study	Year	Number of patients	Sensitivity % (95% CI)	Specificity % (95% CI)
(Tan et al., 2012)	2012	5892 lesions	67-72	87-90
(Wu et al., 2012)	2012	627	76 (65-84)	82 (77-87)

There is also evidence to suggest DWI has a role in assessing prostate cancer aggressiveness. As cancers become more aggressive, they become more poorly differentiated and studies have suggested that this can be detected in changes in the DWI/ADC images, with lower ADC values more likely to represent higher grade disease (Itou et al., 2011, Tamada et al., 2008a, Verma et al., 2011, Woodfield et al., 2010). Within

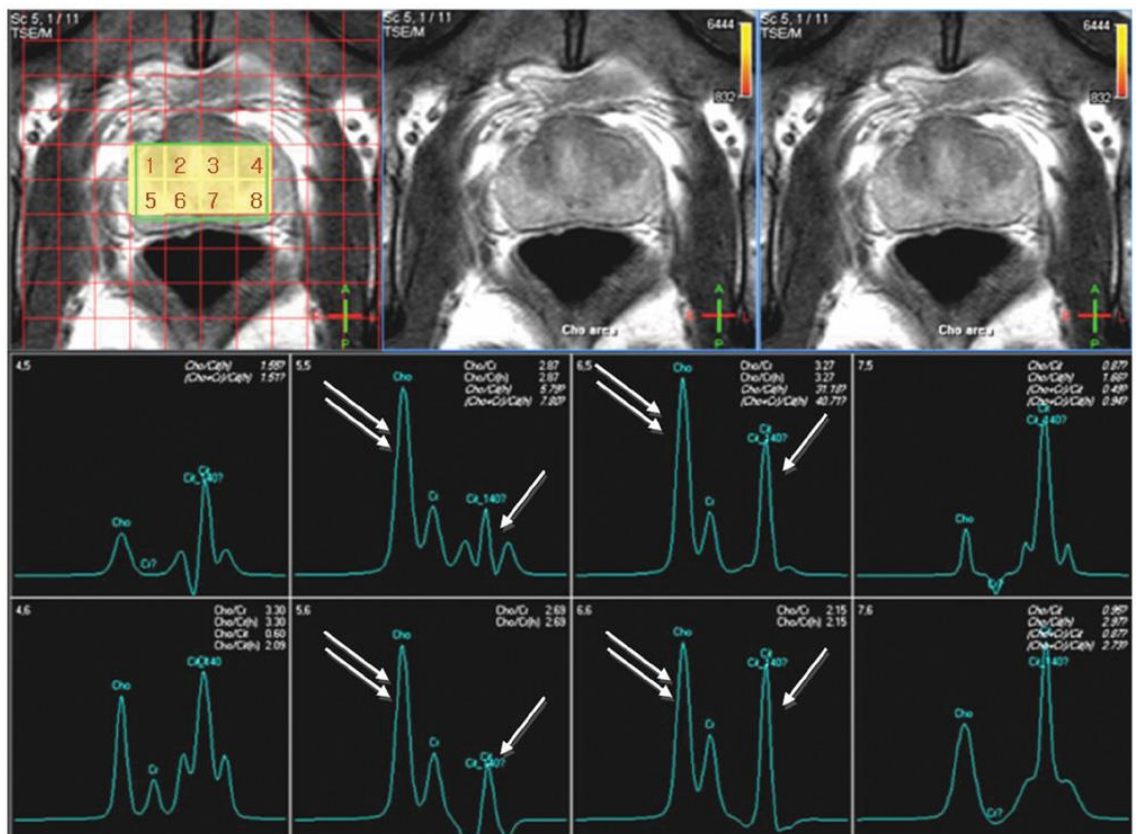
the transition zone however, BPH can sometimes also demonstrate restricted diffusion and low ADC values

2.2.3 MR Spectroscopy Imaging (MRSI)

MR spectroscopy is slightly different from the other MRI techniques: instead of the anatomy of the prostate, MRSI assess the metabolic changes in tissues induced by prostate cancer.

The theory behind MRSI imaging is that changes in the metabolites can be tracked over set regions of interest. The three main metabolites traced in MRSI imaging are citrate, choline and creatinine. Choline is of particular interest in prostate cancer as it has found to be elevated in the disease (Kurhanewicz et al., 2002).

Figure 16 reproduced from Kim et al, demonstrate images of 62-year-old man with prostate cancer. The prostate cancer is not clearly identified on T2-weighted imaging; the MR spectroscopy, however, shows increased choline and creatine (double arrows) over citrate (arrow) ratio in voxels 2, 3, 6 and 7, which were confirmed as prostate cancer (Kim et al., 2009).

Figure 16. MRSI images¹⁵

Results of the 2009 multi-institutional study investigating the performance characteristic of MRSI using an endo-rectal coil, demonstrated little benefit in performing MRSI- MRI imaging AUC 0.6 and combined MRI and MRSI AUC 0.58 for sextant localization of cancer vs. RP histology (Weinreb et al., 2009).

However, several single institutions have shown that the addition of MRSI to MRI improves detection (Scheidler et al., 1999, Futterer et al., 2006). Scheidler et al found the addition of MRSI to MRI reading significantly improved tumour localization (reader 1 AUC 0.8 from 0.73, and reader 2 0.77 from 0.68, both $P < 0.001$); the sensitivity and specificity found by this group for the combination of MRI and MRSI was 91% and 95%, respectively. Vilanova et al, found in a study of 54 men (Vilanova et al., 2009) that MRSI alone had a AUC= 87.2% vs. MRI alone AUC=85.1%. The best detection in the study was found when incorporating MRI, MRSI and free-to-total PSA ratio, AUC =97.5%. Table 7 outlines MRSI performance characteristics.

¹⁵ Kindly reproduced from KIM, J. K., JANG, Y. J. & CHO, G. 2009. Multidisciplinary functional MR imaging for prostate cancer. *Korean J Radiol*, 10, 535-51. Accessed 20/06/15

It is likely that the difference in methodologies of the studies, also the different level of expertise in different centres, is responsible for the less favourable findings for MRSI in the multi institutional study by Weinreb et al (Weinreb et al., 2009).

Table 7. MRSI performance characteristics

Study	Number of patients	Zone imaged	Sensitivity %	Specificity %	PPV %	NPV %	Reference test
(Scheidler et al., 1999)	53	PZ	63	75	83	51	RP
(Futterer et al., 2006)	34	PZ/TZ/CZ	77-80	84-87	64-68	91-93	RP
(Kaji et al., 1998)	42	PZ/TZ/CZ	88	66	-	-	Biopsy

However, although MRSI may be a useful addition to mpMRI, it has a number of weaknesses. Firstly, it is time-consuming on the MRI scanner. It provides a low signal-to-noise (SNR) resolution and no direct vision of peri-prostatic anatomy. There is also a high variability in concentrations of metabolites between patients observed, leading to difficulty in standardised reporting - and similar to several of the other MRI techniques, MRSI can be affected by post-biopsy haemorrhage, making interpretation of the metabolite ratios unreliable (Choi et al., 2007).

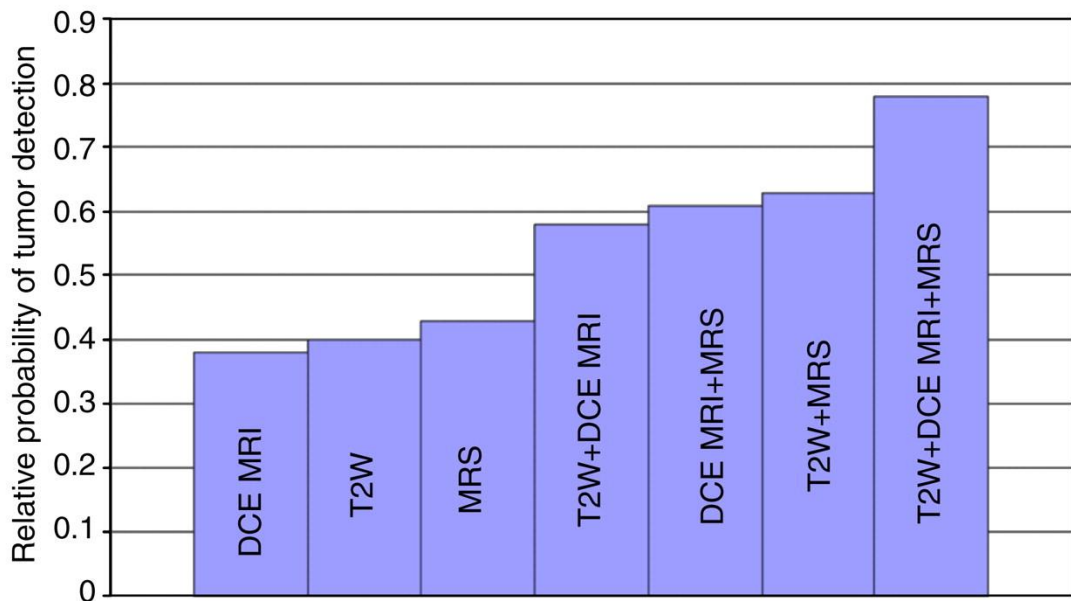
2.2.4 Multi-Parametric MRI Summary

Several studies have evaluated the additional sequences of dynamic gadolinium contrast enhanced T1; diffusion weighted imaging and magnetic resonance spectroscopy sequences. Evidence is accumulating that multi-parametric MRI, using a number of different sequences, might be useful in accurately localising clinically significant prostate cancer. Indeed, most studies as discussed in previous sections, found that the addition of a sequence to T2- weighted imaging improved performance characteristics.

It is becoming widely acknowledged that the addition of functional and anatomical sequences to mpMRI leads to higher performance characteristics.

Figure 17 shows the additive value of each sequence as shown by one study group. (Turkbey et al., 2010)

Figure 17. Predictive value of each MRI sequence¹⁶



Each MRI sequence has shown promise individually and in various combinations, but the literature has been limited by a number of methodological issues. These include: the use of an inaccurate reference test (TRUS biopsy); selection bias in using whole-mount histology as reference test (men with high risk, high volume disease are more likely to undergo radical prostatectomy); dividing the prostate into various regions of interest rather than evaluating data on a per patient basis (greater numbers of ROIs increases accuracy); studying only a portion of the gland (PZ or TZ) rather than the whole gland; small study numbers; retrospective analysis of data; and using only two or three MRI sequences rather than all four (Ahmed et al. 2007; Ahmed, Kirkham, Arya, Illing, Freeman, Allen, & Emberton 2009; Kurhanewicz et al. 2008).

Interestingly, in a study by Turkbey et al that examined the usefulness of T2W imaging, DCE and MRSI, two separate approaches to the analysis were taken - one a stringent analysis

¹⁶ Reprinted from TURKBEY, B., PINTO, P. A., MANI, H., BERNARDO, M., PANG, Y., MCKINNEY, Y. L., KHURANA, K., RAVIZZINI, G. C., ALBERT, P. S., MERINO, M. J. & CHOYKE, P. L. 2010. Prostate cancer: value of multiparametric MR imaging at 3 T for detection--histopathologic correlation. *Radiology*, 255, 89-99. With permission from Radiological Society of North America

that took no account of registration errors, and a nearest neighbour analysis that allowed for the lesion to be located in the adjacent sectors. The nearest neighbour analysis saw an improvement in performance characteristics from T2 sensitivities of 0.42 on stringent analysis to 0.73 (Turkbey et al., 2010). This highlights the importance of understanding methodology when assessing the various performance characteristics reported for these technologies, and demonstrates how a modification in method can result in vastly different characteristics.

A number of consensus meetings have been held to try to identify what are the minimum requirements and best practices to gain the best performance from mp-MRI (Kirkham et al., 2013, Dickinson et al., 2013, Barentsz et al., 2012a) and also to try and streamline methodologies for these studies so that they can be more easily compared.

One of the criticisms of mpMRI is the low reproducibility of interpretation; (Barentsz et al., 2012b) alongside the provision of guidelines and reporting scales for MRI to improve uniformity.

A further current active area of research in radiology (outside the parameters of this thesis) is the use of computer aided detection systems to aid radiology reporting and in-depth discussion (Lemaitre et al., 2015, Niaf et al., 2012, Litjens et al., 2014, Litjens et al., 2015, Wang et al., 2014).

2.4 Imaging Review Summary

Many of these emerging technologies show promise in small 'proof of concept' studies; however, there is a large variation in published literature due to differing methodologies. The techniques need to be validated in a prospective manner against a reference standard that is better than TRUS biopsy but does not rely on whole-mount histology.

This thesis will address the technologies of HistoScanning and mpMRI for their role in prostate cancer detection and characterisation to answer the question:

Can imaging be used as a biomarker to reliably rule out the presence of significant prostate cancer?

3 Prostate HistoScanning

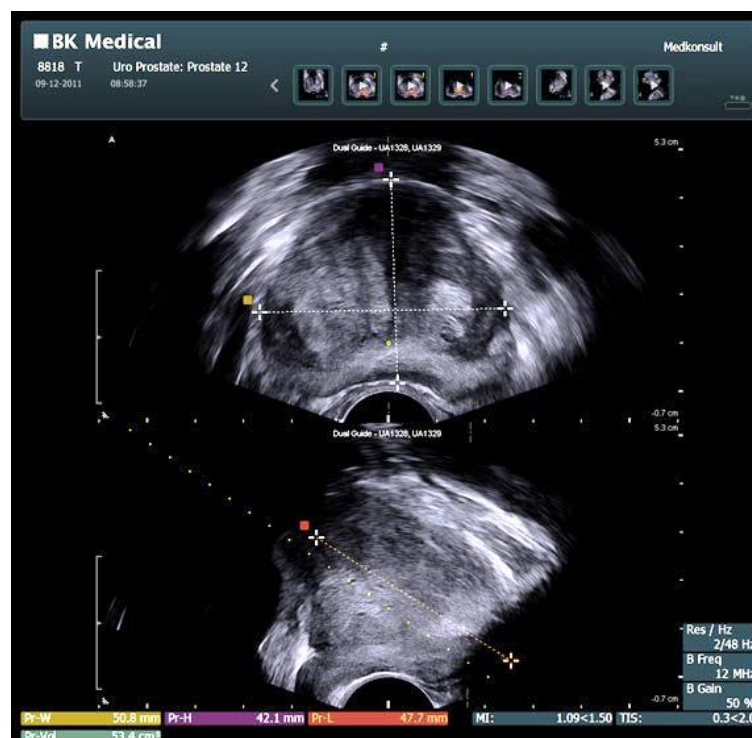
3.1 HistoScanning Background and Development

HistoScanning is an advanced ultrasound technology that was developed with the intention of aiding the discrimination between benign and malignant tissue in a number of organs. HistoScanning algorithms were initially developed for both ovarian tissue and prostate tissue (Vaes et al., 2011).

The HistoScanning technology uses the raw backscatter data from 3D ultrasound and via statistical processing aims to discriminate between benign and malignant tissue.

As ultrasound waves pass through tissue, the different acoustic impedance of the tissue (which depends on tissue properties such as cell density) reflects back the ultrasound wave differently, and as such these ultrasound waves can be processed and images can be formed. Brightness (B Mode) imaging (Figure 18) is the basic mode of ultrasound that is usually used, and images produced by this mode are two dimensional black and white images.

Figure 18. *B mode Ultrasound image of the prostate –transverse and sagittal view¹⁷*

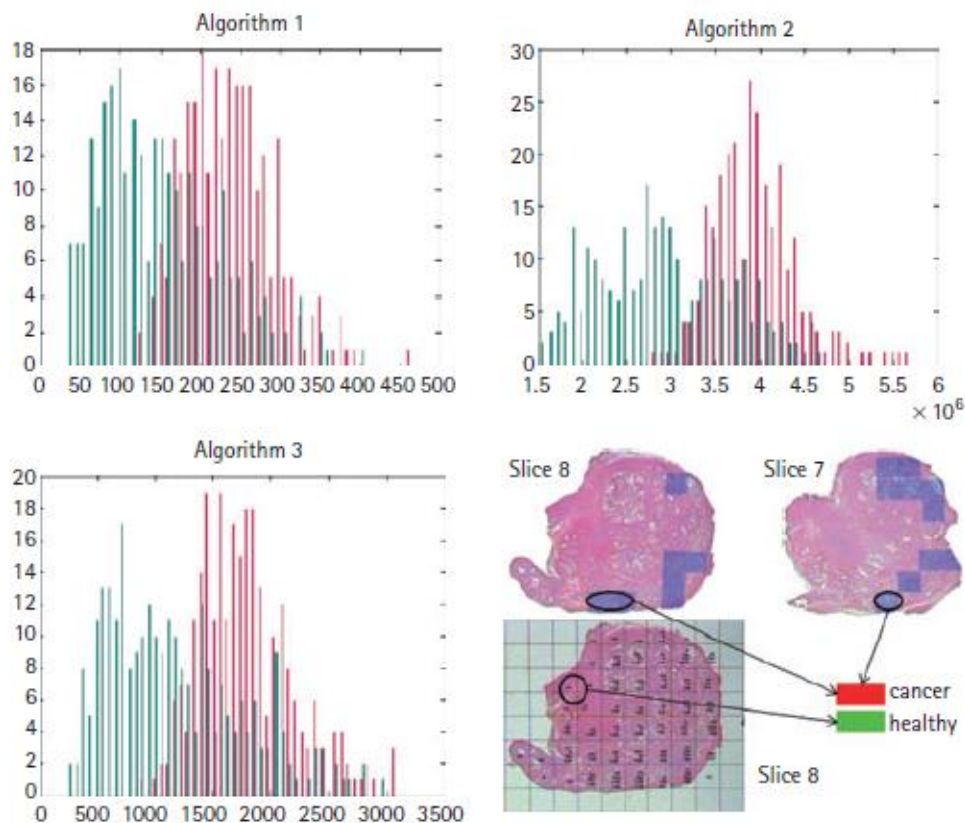


¹⁷ Image kindly reproduce with the permission of BK medical. (<http://bkultrasound.com/>)

HistoScanning technology utilises the raw ultrasound wave data, (often referred to as radio frequency (RF) backscatter data) which is a series of mathematical quantitative data. The raw data has not yet been processed to enable a grey-scale image to be determined from it. By processing the data through a number of mathematical algorithms the HistoScanning technology aims to discriminate between the properties of the tissue. HistoScanning algorithms were developed to allow them to be applied to discrete regions of interest (ROI) within the ultrasound data file - thus allowing the algorithms to be run, for example on the ROI that is the prostate.

Figure 19 shows the statistical separation of HistoScanning signals when applied to prostate tissue (Braeckman et al., 2008a).

Figure 19. HistoScanning algorithms¹⁸



¹⁸ Reprinted from, BRAECKMAN, J., AUTIER, P., SOVIANY, C., NIR, R., NIR, D., MICHELSEN, D., TREURNICHT, K., JARMULOWICZ, M., BLEIBERG, H., GOVINDARAJU, S. & EMBERTON, M. 2008b. The accuracy of transrectal ultrasonography supplemented with computer-aided ultrasonography for detecting small prostate cancers. *BJU Int*, 102, 1560-5. With permission from Wiley Publishing.

Braeckman et al describe how the histograms displayed in Figure 19 demonstrate the distribution of numerical patterns related to specific tissue characteristics captured by each algorithm. The comparison of benign and malignant areas in the prostate result in different distributions of numerical patterns, with distributions related to cancerous areas (in red) systematically shifted to the right (higher values) when compared to distributions related to the benign area (in green). Mathematical integration of the distributions provided by the three characterisation algorithms allow the definition of numerical patterns likely to be specific of non-malignant or of malignant prostatic tissues (Braeckman et al., 2008a).

3.2 Algorithm Development

The first trials of HistoScanning performed on the prostate were by Braeckman et al; these studies were required to enable the algorithms that had been developed to be further trained and tested on human prostate tissue. This study took place between September 2004 and February 2006 at UZ Brussels (Braeckman et al., 2008a, Braeckman et al., 2008b).

29 men scheduled for radical prostatectomy underwent a three-dimensional ultrasound with acquisition of the raw ultrasound data image prior to their radical prostatectomy.

The aim of the study was to allow proof-of-concept work to take place: - the algorithms required adaption to test their ability to discriminate between benign and malignant prostate tissue. The study also aimed to assess if HistoScanning was able to detect and locate malignant prostate tissue within the prostate.

The study was performed in two stages. The first development phase enabled further calibration and refinement of the algorithms by allowing the scientists at Advanced Medical Diagnostics access to the histopathology data. The second blinded stage was designed to allow testing of the algorithms with no prior knowledge of histopathology data.

In this initial study the HistoScanning algorithms were applied to processed two-dimensional matrices of the grey level data acquired and related to the three dimensional ROI. Each tissue area was = 0.08cm^3 , which equates to a volume of = 0.04mL .

The study recruited non-consecutively initially to allow for further development of the algorithms. The first 15 patients were analysed with a degree of un-blinding to allow

algorithm refinement and the final 14 patients were analysed with no knowledge of the pathology.

The first paper published on the study assessed 1) the maximum diameter of the index lesion, 2) the focality of lesions 3) the laterality i.e. unilateral or bilateral 4) the presence of extra prostatic extension (EPE) (Braeckman et al., 2008a).

Data were only statistically analysed for the 14 men in the blind phase of the study.

The results were favourable with a strong correlation in tumour volume diameter between HistoScanning and pathology $r= 0.95$, $P<0.001$. 100% concordance on the presence of multifocality and the laterality of lesions was also achieved. HistoScanning over-called the presence of EPE in this study on one case but correctly identified the presence of EPE in three other patients.

The initial results presented in this paper demonstrated an encouraging ability of HistoScanning to identify prostate cancer.

The study sample however, was very small - only 14 men, once the training cases were excluded.

The pathological processing in the study was also performed in a non-standard manner to allow for easier registration between the index and reference test.

Furthermore, although presenting promising results on the ability of prostate HistoScanning to correctly identify multifocal lesions/laterality, the study made no mention of its performance characteristics with relation to prostate cancer size.

Also, it was not made explicit: - how many tumours were correctly identified by Prostate HistoScanning and how many cancer foci were missed.

A second paper published on the same exploratory cohort went some way to addressing the above weaknesses (Braeckman et al., 2008b). The authors explored the same data set to identify the ability of prostate HistoScanning to identify lesions $\geq 0.5\text{mL}$ and to make a comparison between prostate HistoScanning lesions called $\geq 0.1\text{mL}$ and total cancer volumes, compared to the histopathology findings.

One of the fourteen blind phase patients in the study was excluded from this analysis

In the 13 patients assessed, 28 cancerous lesions $\geq 0.1\text{mL}$ were identified. HistoScanning correctly identified all 12 lesion $\geq 0.5\text{cc}$. It incorrectly classified 3 lesions as $\geq 0.5\text{cc}$ and on histology these lesions were 0.42, 0.46 and 0.47ml.

Performance characteristics for the detection of lesions $\geq 0.5\text{ml}$ were sensitivity 100% ($n=12/12$), specificity 81% ($n=13/16$), PPV 80% ($12/15$) and NPV 100% ($13/13$).

The study also demonstrated a strong correlation between the volumes of the lesions as estimated by HistoScanning and found at the reference test of radical prostatectomy histopathology with a Pearson's correlation co-efficient $r = 0.98$, $P < 0.001$.

These findings also provided some insight into how many cancers can be detected and missed using HistoScanning in this cohort.

However, there continue to be a number of limitations to this study. Firstly, the sample size of patients is very small- 29 overall and only 14 in the blinded assessment. Also, all the men are known to have cancer, a selection bias, which is a negative feature of the study. It could however be argued that to allow for validation of an innovative technology, the bias is a necessity at this stage of its development.

Also, the patients selected were all from the same institution and were selected in a non-consecutive manner.

The algorithm in these studies is also only applied to a pre-processed two dimensional pixel of the ultrasound image, rather than the raw radio-frequency (RF) data and in a three dimensional voxel. The reference test applied in this study was also unorthodox, in that the radical prostatectomy samples did not undergo standard apical to base step sectioning but an unusual sagittal step sectioning-something the authors thought may enhance correlation between the index and reference test.

However, despite its limitations, this preliminary work showed some promise for the application of prostate HistoScanning technology, suggesting that further studies would be useful.

3.3 PHS02 Study

3.3.1 Methodology of PHS02 Study

To further validate the technology of Prostate HistoScanning, a European multi-centre trial was designed. The study was ethics approved by local European ethics committees in Belgium, Germany, Czech Republic, Hungary and the UK. The ClinicalTrials.gov Identifier is NCT01191931. The study aims were to assess the ability of prostate HistoScanning to detect and localise prostate cancer.

The earlier studies on Prostate HistoScanning as discussed in section 3.2 showed accurate localisation of disease using two dimensional grey level data as the input. By using the raw unprocessed RF data it was thought that higher resolutions could be obtained. The PHS02 study was designed to adapt the tissue characterisation algorithms to this RF data and evaluate the use of Prostate HistoScanning using RF input against a rigorous reference test.

The research was designed in an open phase, to allow further refinement of the HistoScanning algorithms and a rigorously controlled blind phase for validation. Although not involved in the protocol development for the study, I was involved in the data collection, analysis and presentation of the PHS02 open phase. I had primary responsibility for the analysis of the blind phase scans, the data collection and analysis was performed with the aid of an independent statistician.

Men over 18 years with histologically proven prostate cancer scheduled to undergo radical prostatectomy and willing to undergo pre-operative transrectal ultrasound scanning were eligible for the study.

For eligibility purposes the prostate cancer must have been organ confined (T1-2, Nx or N0, Mx or M0) and patients must not have received any prior treatment for prostate cancer, including any hormonal therapy. They must also have been free from major calcifications at transrectal ultrasound scan.

Patients became in-eligible for analysis if they did not proceed to radical prostatectomy, or (for whatever reason) the ultrasound data was insufficient, or if the reference test was compromised in any way during prostatectomy, shipping or processing.

Table 8 outlines the exclusion criteria for the study.

Table 8. PHS02 exclusion criteria

	Criteria for exclusion
Screening Failures	Previous prostate surgery – i.e. Transurethral resection of prostate (TURP) Prior treatment for prostate cancer (including hormones) Gland unable to be captured on one ultrasound scan Prostate cancer not organ confined
Problems with the Index test	Ultrasound data insufficient for analysis Lack of raw backscatter ultrasound data acquired for entire prostate Presence of calcifications ≥ 5 mm diameter Fault in transfer of raw ultrasound data rendering it un-analysable
Problems with the Surgery	Surgery does not go ahead Incomplete prostate excised
Problems with the reference test	Prostate unable to be processed according to standard operating procedure (SOP) on reaching centralised laboratory Prostate incomplete or damaged on arrival at the pathology laboratory

3.3.2 The Index test- Prostate HistoScanning

All patients initially underwent 3D TRUS in two modes sagittal and transverse. The 3D TRUS was performed by a competent medical practitioner, experienced in TRUS and trained in Prostate HistoScanning. For scan quality control purposes a technician from AMD was present at the time of all 3D TRUS acquisition.

Following the initial phase the plane for ultrasound acquisition was defined and for the blinded verification phase of the study men underwent only sagittal acquisition, using a rotational motor.

After the acquisition of the 3D TRUS raw RF data, this data subsequently underwent HistoScanning analysis, which was performed by a competent reporter, blinded to clinical data, centrally at the offices of Advanced Medical Diagnostics.

In the open phase of the study the HistoScanning analysis was performed using two methods. The first used the embedded software in the HistoScanning technology to

automatically define lesion volumes, according to set criteria for contiguous positive voxels that is programmed into the software.

The second method used only in the open phase was a manual estimation of volume of lesions, using a planimetry method designed to replicate that carried out at histopathology, measuring the height x width x depth of a lesion x 0.52, to get the volume of an ellipse.

For the blind phase only the embedded software tool was used for estimating the volume of a lesion.

For the blinded verification stage of the study access to the results of the reference test were only made available to AMD following complete analysis of the Prostate HistoScanning image, and once it has been received and documented by the independent data monitoring committee.

3.3.3 The Reference Test – Radical Prostatectomy step sectioned Histopathology

The reference test of radical prostatectomy step sections, were carried out centrally at Bostwick Laboratories, London, UK. The centralisation of reporting allowed for standardised processing and reporting across the centres.

In the initial phase the plane for the step-sectioning was defined. Other studies investigating prostate HistoScanning had used a sagittal step sectioning approach to allow for correlation with the PHS image. However, during the initial open phase of this study a standard apical to base transverse step sectioned approach was decided upon.

Prior to sectioning the specimen was inked using two colours for left and right, to aid with orientation of the step sections. Sections were prepared at 3mm slices, and trimmed to full face. Measurements of any trimmings recorded to assist correlation with the index test.

Standard Haematoxylin and Eosin staining performed and slides cover slipped.

Each prostatic step section was measured using callipers at 5 point locations around the slice. This information along with the information on trimmings was to allow for accurate 3D reconstruction of the prostate to correlate with the Index Test.

Each step sectioned slice was further analysed by a 5 x 5 mm grid analysis, within the grid - the presence or absence of cancer, the predominant and secondary Gleason grade and the

percentage of the grid each grade of cancer occupies were defined. In addition, the presence or absence of high grade prostatic intraepithelial neoplasia (PIN) and percentage was noted. Inflammation, both chronic and acute, atrophy, and the background stroma were also commented upon.

Photographs of the gland were taken following inking and prior to sectioning (Figure 20). Each slice photographed and the tumour outlined upon the slice, producing a 3D tumour map (Figure 21). Each 5 x 5 mm grid analysis was documented and photographed (Figure 22).

Figure 20. *Photograph of gland*



Figure 21. 3D Tumour map

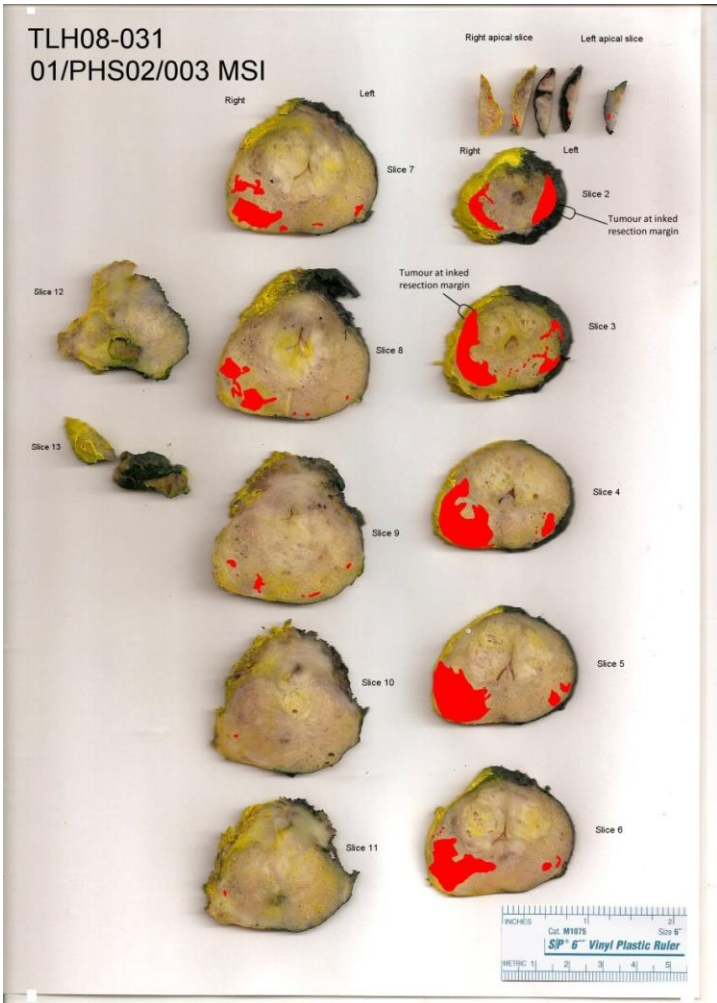
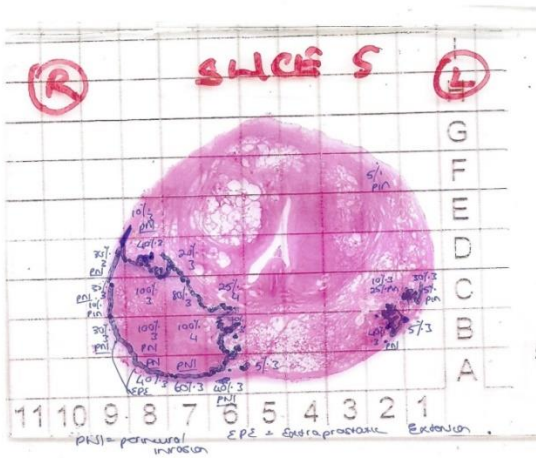


Figure 22. 5 x 5mm Histopathology grid analysis



The Histopathologist reported the gland volume (cc) and, tumour volume (cc); they also reported on the location of Prostate cancer lesions diagrammatically on a specific proforma, with the prostate divided into sextants.

3.3.4 Data Matching and Statistics

An independent data monitoring committee was established and was responsible for matching between the index and the reference test. In the blind phase of the study data pertaining to the reference test was not released until the database of HistoScanning results had been locked and circulated to ensure strict blinded comparison. At this point, Bostwick Laboratories released the Histopathology reports to the data monitoring committee for further processing and analysis.

Matching for lesions ≥ 0.5 cc and ≥ 0.2 cc was performed using 2 x 2 contingency tables, allowing accuracy to be determined.

3.4 Results of PHS02 Open Phase

3.4.1 Open Phase Analysis Plan

The following analyses were carried out in order to compare the index test with the reference test.

(i) Whole gland analysis: The total cancer volume as estimated by the prostate HistoScanning embedded software tool plus manual estimation of cancer volume versus the total cancer volume, as determined by the reference test.

(ii) Lesional analysis: The attribution of cancer foci at the volume thresholds of ≥ 0.5 cc and ≥ 0.2 cc at the whole gland level.

(iii) Sextant analysis: Analysis for cancer foci at ≥ 0.5 cc and ≥ 0.2 cc volume thresholds. Sextant data analysis was performed using standard 2 by 2 contingency tables for sensitivity and specificity analysis. Calculation of 95 % confidence intervals was done using the normal distribution approximation.

Sextants were formed by subdividing the prostate into six sectors, using the midline urethra as an anatomical landmark for right and left lobes. Each lobe was then further

subdivided in an equidistant manner into apex, mid and basal sextants, generating 6 sectors in all. A sextant was deemed positive at histology if cancer was present in $\geq 10\%$ of the surface pathology. This subdivision was performed in order to estimate the Negative Predictive Value (NPV) of HistoScanning, as although all prostates in this series contained cancer, not all sectors did.

3.4.2 Open Phase Results

The open phase results for this study were published in the BJUI in 2012, and this section pertains to the results of the study as published (Simmons et al., 2012). During the recruitment period for the open phase of the study, 51 patients were screened, 31 eligible patients from 6 European institutions were included in this phase of the study (Table 9).

Table 9. *Eligible patients according to recruiting centre*

Institute	City	No. Patients
Jules Bordet Institute	Brussels, Belgium	3
University Hospital Tuebingen	Tuebingen, Germany	3
Semmelweis University	Budapest, Hungary	6
UZ-Brussels	Brussels, Belgium	3
Princess Grace	London, UK	3
Olomouc University	Olomuc, Czeck Rep.	13
Total		31

Figure 23 demonstrates the open phase patient study flow.

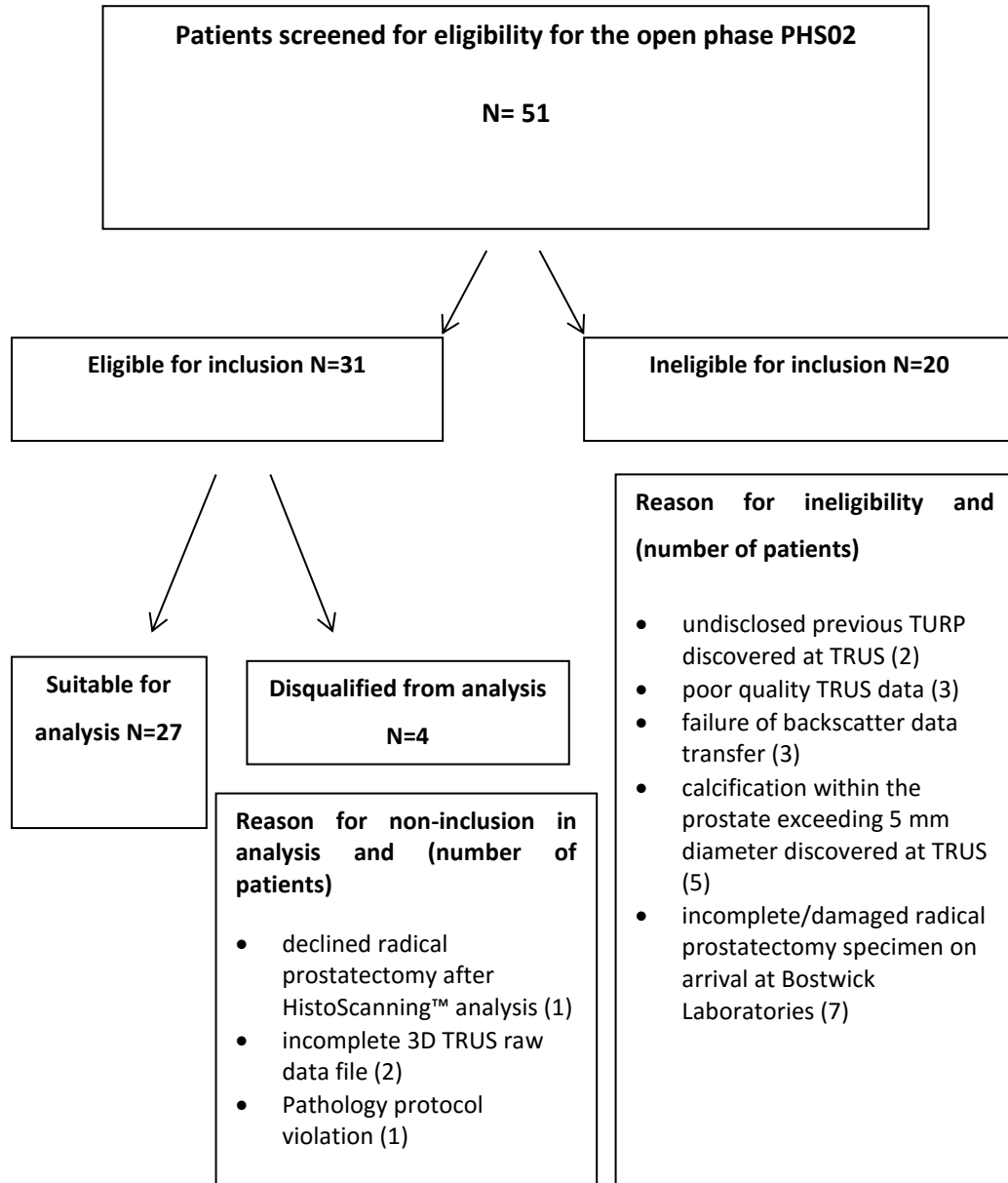


Figure 23. PHS02 open phase patient study flow

Twenty seven men remained eligible for final analysis; figure 23 shows the reasons for non-inclusion in the analysis. Mean age (range) was 63 (56-75) years, PSA level range was 2.6-26ng/ml

Table 10 outlines the patient demographic data and results of HistoScanning and Histopathology.

Table 10. PHS02 open phase data

Patient ID	PSA ng/ml	Gleason grade at TRUS biopsy	Gleason grade at Radical prostatectomy	Total cancer volume at Pathology (cc)	TCV using PHS embedded volume tool (cc)	TCV using manual PHS volume estimation (cc)	Index lesion volume at pathology (cc)	Index lesion volume using PHS (cc)
1	6.47	3 + 4	3 + 4	3.38	0.78	1.68	2.92	0.42
2	3.3	3 + 3	3 + 4	2.12	1.8	1.63	1.45	1.77
3	4.28	3 + 4	3 + 4	0.88	0.86	0.94	0.88	0.52
4	5.13	4 + 3	3 + 4	2.46	0.34	0.96	2.46	0.22
5	10.2	3 + 3	4 + 3	3.85	3.08	6.96	3.85	2.43
6	7.9	4 + 5	3 + 4	3.85	4.22	2.83	2.25	4.17
7	21	3 + 3	3 + 4	9.5	2.32	5.28	9.5	2.25
8	18.2	3 + 3	4 + 3	2.33	1.25	2.67	2.33	1.23
9	9.2	3 + 4	4 + 3	6.56	1.58	5.03	6.56	1.45
10	7.1	3 + 3	3 + 3	0.33	0.4	0.87	0.33	0.3
11	6	3 + 3	3 + 4	0.32	1.32	0.97	0.32	0.49
12	23.71	3 + 4	5 + 4	2.7	0	0	2.7	0
13	4.96	3 + 3	4 + 3	3.51	3.74	3.66	2.9	3.71
14	9	4 + 4	4 + 3	1.82	1.28	3.41	1.82	0.78
15	4.4	3 + 4	3 + 3	0.57	0.9	2.06	0.32	0.37
16	2.56	3 + 4	3 + 3	1.4	2.04	2.13	1.4	1.56
17	7.35	3 + 4	4 + 3	4	1.2	3.5	4	0.66
18	5.07	4 + 4	4 + 3	4.52	0.74	2.5	4.52	0.61
19	3.4	3 + 4	4 + 3	3.45	1.01	2.13	3.45	0.69
20	6.6	3 + 3	3 + 3	0.58	0.39	0.88	0.58	0.39
21	2.64	2 + 3	3 + 3	0.33	0.26	0.89	0.33	0.15
22	26.3	3	3 + 4	3.24	0.9	3.73	3.24	0.79
23	16.6	3 + 4	4 + 3	7.33	1.93	5.4	7.33	1.86
24	13.1	3 + 4	3 + 4	3.14	1.75	4.6	3.14	1.17
25	10.98	3 + 3	3 + 4	1.71	1.49	1.29	1.71	1.2
26	3.3	3 + 3	3 + 3	1.94	0.36	0.35	1.94	0.29
27	16.24	2 + 4	4 + 3	2.77	1.18	2.6	2.77	0.87

Key to shading
Considered negative at PHS as embedded tool detected lesion <0.2
Lesion ≥0.5 at pathology detected <0.5 at PHS

3.4.3 Whole Gland Analysis

The open phase of the study found a strong correlation between the total cancer volumes found using the HistoScanning manual estimation of volume and the total cancer volume at histopathology.

Prostate HistoScanning found total cancer volumes ranging from 0 to 4.22ml using the embedded software tool (Figure 24) and 0 to 6.96ml using the manual estimation planimetry method (Figure 25). Histopathology reporting of the lesions found at radical prostatectomy found total cancer volumes ranging from 0.32 – 9.5ml. The Pearson’s correlation coefficient r between the PHS volume estimation methods and histology was 0.72 and 0.41 for the manual estimation and the embedded software tool respectively.

Figure 24. Relationship of total cancer volume at HistoScanning (embedded software) and Histopathology

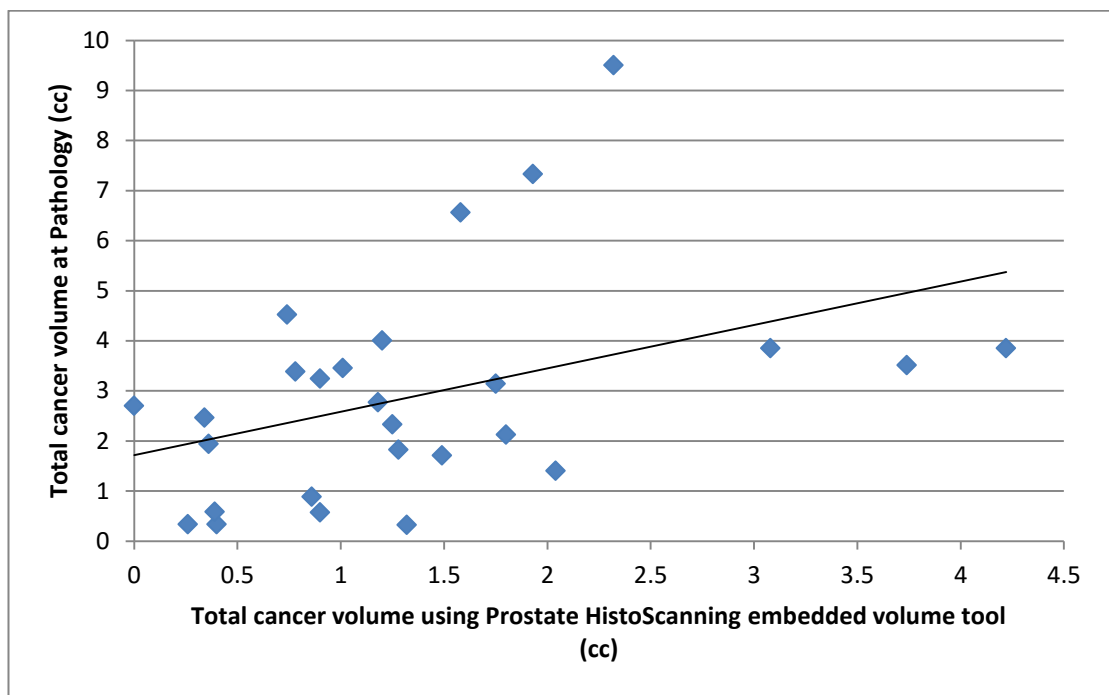
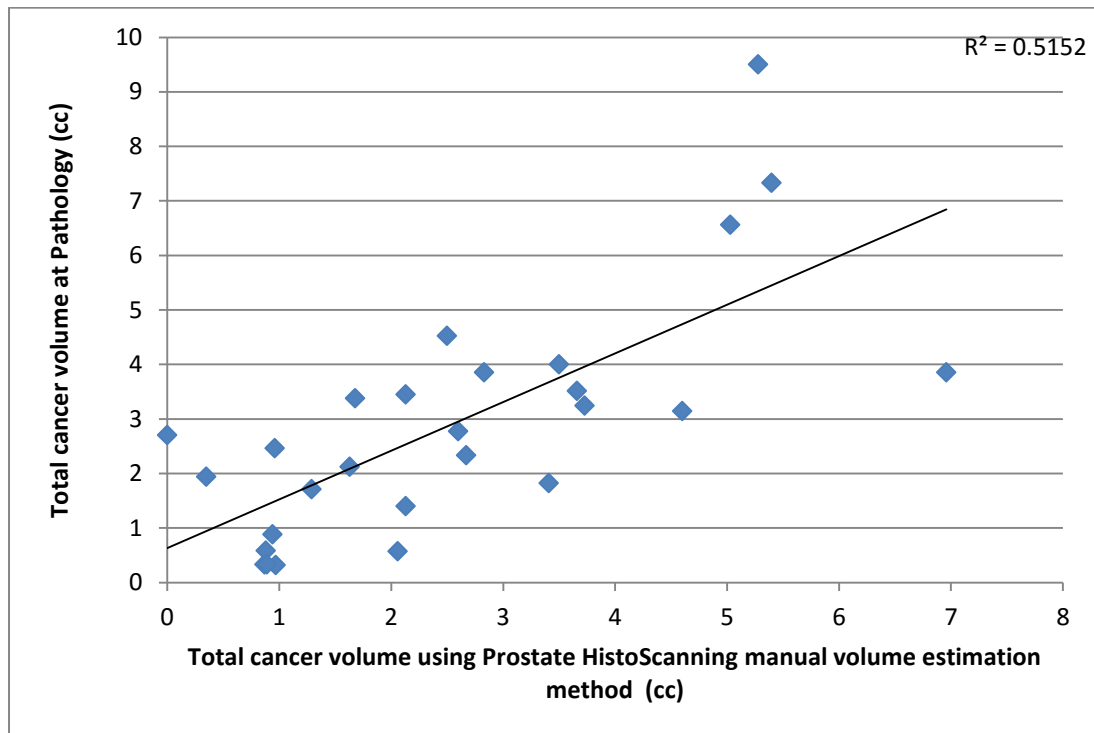


Figure 25. Relationship of total cancer volume at HistoScanning manual volume estimation method and Histopathology



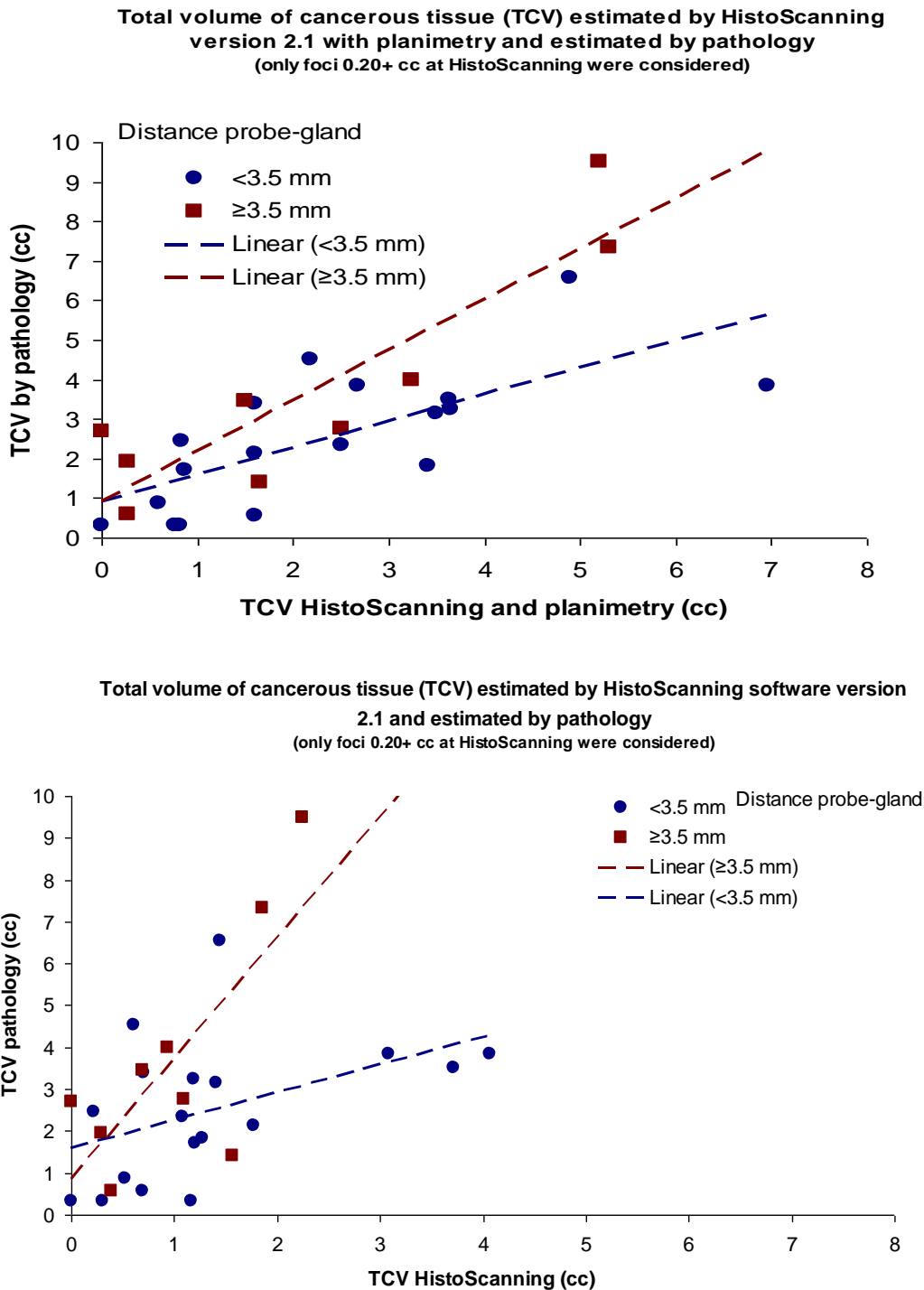
During the open phase of the study further analysis was performed to assess the variables that could have affected the correlation between volumes, specifically looking at the influence of the probe to gland (PG) distance.

In the 27 patients eligible for analysis, the distance (in mm) from probe to gland measured on the middle part of the gland ranged from 1.8 to 12.8 mm, with a median of 3.2 mm (mean 3.8 mm).

In 14 patients with index focus ≥ 0.5 cc at pathology and PG < 3.5 mm, there was only one false negative HistoScanning result. There were however 3 false negative results in the 9 patients with index focus ≥ 0.5 cc at pathology but PG ≥ 3.5 mm.

The two following graphs (Figure 26) show how the total cancer volume (TCV) is underestimated, mainly when the distance exceeds 3.5 mm. The manual planimetry method of lesion volume estimation yields the best relationship but a distance ≥ 3.5 mm still leads to substantial underestimation of volume.

Figure 26. Relationship of total cancer volume correlation with respect to probe gland difference



A regression model was fitted on plots displayed in two previous graphs with volume at pathology as dependent variable and including as independent variable the volume predicted from HistoScanning analysis and distance PG. Results of regression models applied are displayed in the Table 11.

Table 11. Multiple linear regression of volumes predicted by HistoScanning on volumes found at pathology

Table - Multiple linear regression of volume predicted by HistoScanning on volumes found at pathology

Model	Endpoint measured by pathology	Volume index focus*		Total cancer volume (TCV)*		Distance 3.5+ mm	Constant	R-square
		from PHS	from planimetry	from PHS	from planimetry			
(1)	Volume index focus	0.83	-	-	-	1.67	1.3	0.25
(2)	Volume index focus	-	0.90	-	-	1.56	0.2	0.65
(3)	Total cancer volume (TCV)	-	-	1.0	-	1.61	1.1	0.31
(4)	Total cancer volume (TCV)	-	-	-	0.90	1.36	0.4	0.63

For the three independent variables, data in Table are the β -coefficients

*Taking account only foci ≥ 0.2 cc

From the Table, we can derive that:

1/ When volumes estimated by HistoScanning embedded software are used, the underestimation of the index focus volume is of about 1.3 cc on average (the constant), that increases to $1.3+1.67 =$ about 3 cc when the PG distance exceeds 3.5 mm.

2/ When planimetry is used, there is a fairly good correlation between volumes when the PG distance is less than 3.5 mm: for instance, an index focus volume of, for instance 2 cc predicted by HistoScanning/planimetry would be exactly the same: that is $[(0.9*2) +0.2]$. When the PG distance exceeds 3.5 mm, volume is underestimated by about 1.6 cc. The same reasoning holds for total cancer volume (TCV).

Hence, the distance is a strong source of false negative result and of underestimation of volume, no matter the way the HistoScanning volumes are estimated.

3.4.4 Lesional Analysis

The reference test identified prostate cancer foci ≥ 0.5 cc in 23 out of 27 patients and prostate cancer foci of ≥ 0.20 cc in all 27 patients.

At the 0.5cc threshold prostate HistoScanning identified 21 of the 23 foci ≥ 0.5 cc using the manual planimetry volume estimation method (sensitivity 91%; 95% CI: 0.80-1.00), two tumours found at the reference test were not identified by HistoScanning.

19 of the 23 foci ≥ 0.5 cc were detected (sensitivity 83%; 95% CI: 0.67-0.98) using the Prostate HistoScanning embedded software.

At the 0.2 cc threshold, the Index test identified 25 of the 27 foci using both the embedded tool and manual method (sensitivity 91%; 95% CI: 0.83-1.00) (Simmons et al., 2012).

3.4.5 Sextant Analysis

The open phase analysis found that all 27 men included in the final analysis had lesions \geq 0.2 ml detected at RP histopathology, 23 men had lesions \geq 0.5 ml.

Overall 162 sextants for the 27 men were examined for the men with index lesions \geq 0.2 cc and 138 sextants for those with index lesion \geq 0.5 cc. (Table 12 and Table 13)

In the tables below the following is true for the definitions of true positive, true negative etc.:-

- True positive = Lesion present at histology, and predicted by HistoScanning
- True negative = Lesion not present at histology and not predicted by HistoScanning
- False positive = Lesion predicted by HistoScanning, but not present at histology
- False negative = Lesion not predicted by HistoScanning, but present at histology (i.e. missed lesion)

Table 12. Sextant analysis for all 27 men.

AREA	True Positive	True Negative	False Positive	False Negative	
1 (Right apex)	18	3	4	2	
4 (Left apex)	16	6	4	1	
2 (Right mid zone)	20	4	2	1	
5 (Left mid zone)	17	5	5	0	
3 (Right base)	10	12	0	5	
6 (Left base)	6	17	3	1	
Total No. of Sextants	87	47	18	10	162
% of all areas	54	29	11	6	

Table 13. Sextant analysis of the 23 men with index foci ≥ 0.5 cc at histopathology.

AREA	True Positive	True Negative	False Positive	False Negative	
1 (Right apex)	16	2	3	2	
4 (Left apex)	14	5	3	1	
2 (Right mid zone)	18	3	2	0	
5 (Left mid zone)	16	3	4	0	
3 (Right base)	9	9	0	5	
6 (Left base)	6	13	3	1	
Total No. of Sextants	79	35	15	9	138
% of all areas	57	25	11	7	

Using the embedded software tool sensitivity of 90% and specificity of 72% were achieved for localisation of ≥ 0.2 ml focus within a sextant, 90% sensitivity and 70% specificity for localisation of ≥ 0.5 ml. Table 14 demonstrates the sextant analysis performance characteristics at the two volume thresholds.

Table 14. Sextant analysis sensitivity/specificity results for HistoScanning™ at differing volume thresholds

Volume threshold for detection	≥ 0.20 cc	≥ 0.50 cc
Sensitivity	90%	90%
Specificity	72%	70%
Positive Predictive Value	83%	84%
Negative Predictive Value	82%	80%

3.5 Results of the Blind Phase of PHS02

The primary objective for the blind phase of the study was the same as that for the open phase, to assess the detection of prostate cancer on a whole gland basis using the accepted threshold for significance, ≥ 0.2 cc, ≥ 0.5 cc and ≥ 1.3 cc. The threshold of 1.3 cc was incorporated into the analysis for the blind phase because of the updated evidence from Wolters et al suggesting that lesions of this size may represent the boundary for when prostate cancer lesions become significant disease (Wolters et al., 2011).

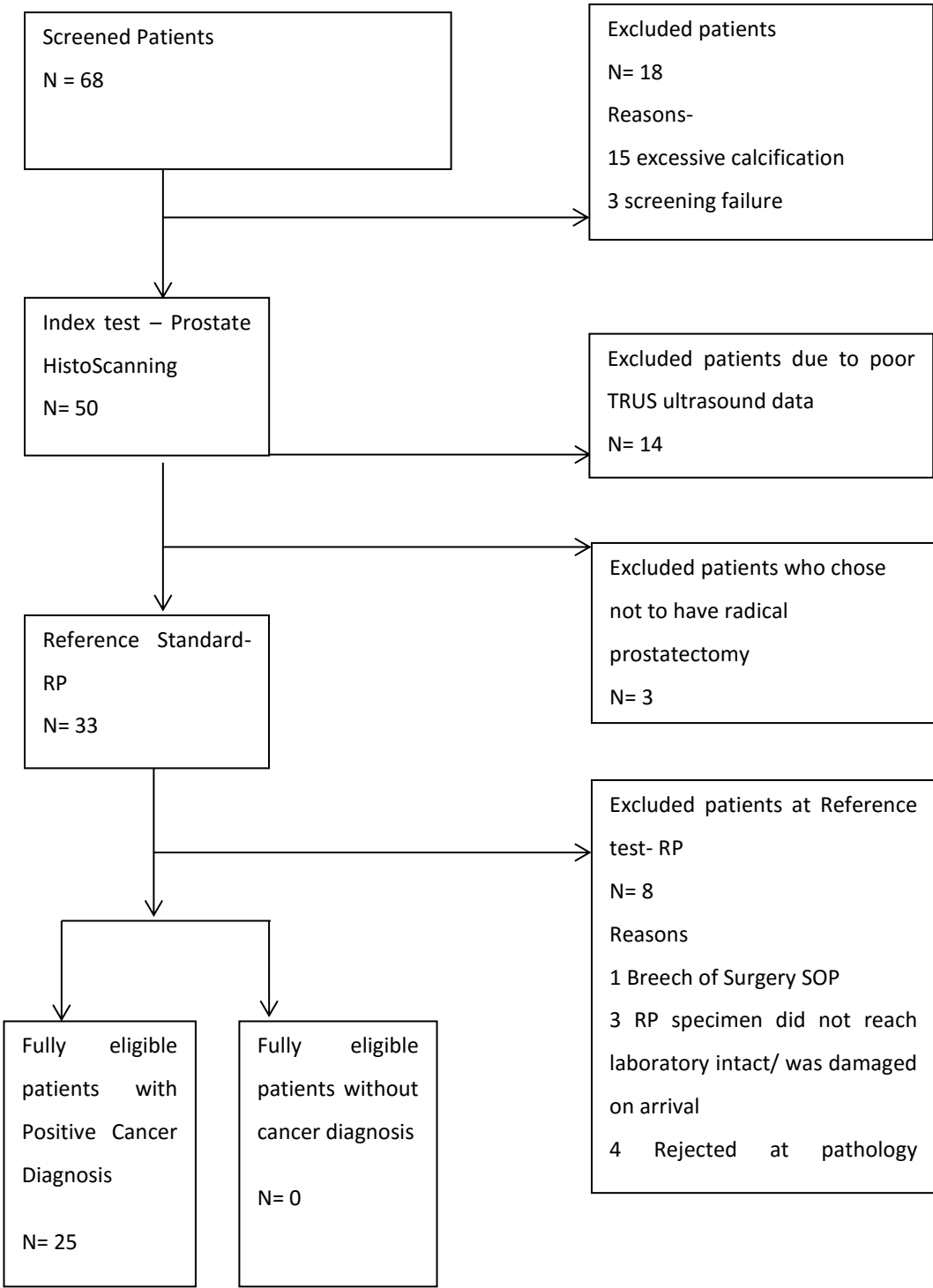
Primary lesion location matching analysis was performed for tumours ≥ 0.2 cc using the sextant containing the maximal volume of the lesion at RP and HistoScanning. A true match was called only when the sextant for PHS was in total agreement for the sextant containing the maximal volume of the tumour at RP.

Further analysis was performed to assess for the matching of lesions between prostate laterality (left and right side). This compensated for differences in segmentation between the index and reference test.

3.5.1 Recruitment

68 patients were screened for the blind phase of the study and 25 were found to remain eligible for analysis after application of the exclusion criteria at each stage in the study flow. Figure 27 demonstrates the patient flow.

Figure 27. Recruitment flow diagram for the blind verification phase of PHS-02 study



3.5.1 Results of Blind Phase

Median age and PSA were 66 years (interquartile range [IQR] 63-71) and 6.95 ng/ml (IQR 3.85- 7.75), respectively. All men were found to have cancer at RP - 14, 21 and 24 men had

index tumour volumes ≥ 1.3 cc, ≥ 0.5 cc and ≥ 0.2 cc, respectively. 21/25 men had primary or secondary pattern Gleason grade 4 at RP (Table 15).

Table 15. *Blind phase patient disease characteristics*

Patient ID	PSA (ng/mL)	Gleason grade at biopsy	Gleason grade at RP
1	24.0	4+5	4+5
2	6.5	3+3	3+4
3	11.0	4+3	3+4
4	8.8	3+3	3+4
5	5.4	4+3	3+4
6	7.9	3+4	3+4
7	15.4	3+5	4+5
8	11.0	3+4	3+4
9	3.1	3+3	3+4
10	5.2	4+3	3+4
11	3.5	3+3	3+4
12	6.9	3+3	3+4
13	19.9	3+3	4+5
14	4.0	3+3	3+4
15	4.9	3+3	3+4
16	8.8	3+3	3+4
17	4.4	3+4	3+4
18	11.1	4+4	4+5
19	4.5	3+3	3+4
20	7.3	3+4	3+3
21	7.0	3+3	3+3
22	12.9	3+3	3+3
23	9.8	3+4	3+4
24	5.8	3+4	3+3
25	5.9	4+3	3+4

Table 16 demonstrates the total cancer volumes and index lesion volumes detected by both HistoScanning and at RP histopathology.

Table 16. Total cancer volume and lesion volume at histopathology and HistoScanning

Patient ID.	No of lesions		Total cancer volume (cc)		Lesion volume at RP (cc)				Lesion volume at PHS (cc)			
	RP	PHS	RP	PHS	Index	2 nd	3 rd	Total	Index	2 nd	3 rd	Total
1	1	2	8.2	2.0	8.20	-	-	8.20	1.58	0.24	-	1.82
2	2	3	3.5	3.4	2.30	1.20	-	3.50	2.66	0.52	0.22	3.40
3	1	2	4.4	1.7	3.90	-	-	3.90	1.33	0.26	-	1.59
4	3	2	4.8	4.9	3.84	0.62	0.28	4.74	4.60	0.32	-	4.92
5	2	3	4.2	3.0	3.83	0.37	-	4.20	2.32	0.34	0.30	2.96
6	1	3	1.2	1.2	1.10	-	-	1.10	0.52	0.35	0.22	1.09
7	1	1	26.5	2.1	26.5	-	-	26.5	2.02	-	-	2.02
8	1	3	0.9	2.9	0.48	-	-	0.48	1.07	1.01	0.85	2.93
9	1	1	0.9	3.7	0.80	-	-	0.80	3.34	-	-	3.34
10	2	3	2.9	3.3	2.10	0.60	-	2.70	1.37	1.22	0.44	3.03
11	1	3	0.9	0.8	0.80	-	-	0.80	0.34	0.24	0.21	0.79
12	2	2	4.5	1.9	3.40	0.70	-	4.10	0.92	0.78	-	1.70
13	2	3	6.2	4.8	5.70	0.40	-	6.10	4.25	0.28	0.28	4.81
14	3	3	5.2	3.2	3.61	1.00	0.26	4.87	1.65	1.08	0.43	3.16
15	3	3	2.2	1.3	1.10	0.50	0.30	1.90	0.49	0.43	0.40	1.32
16	1	1	1.5	2.7	1.30	-	-	1.30	2.42	-	-	2.42
17	2	3	1.7	2.1	1.00	0.60	-	1.60	1.47	0.30	0.29	2.06
18	2	3	8.5	4.6	7.80	0.30	-	8.10	2.30	1.82	0.26	4.38
19	3	3	0.9	5.0	0.50	0.20	0.20	0.90	1.74	1.50	0.90	4.14
20	2	1	4.1	3.8	1.27	1.27	-	2.54	3.74	-	-	3.74
21	1	3	0.2	4.1	0.16	-	-	0.16	2.84	1.00	0.22	4.06
22	1	2	0.5	3.5	0.40	-	-	0.40	3.08	0.22	-	3.30
23	2	2	5.4	3.5	3.30	0.90	-	4.20	2.82	0.72	-	3.54
24	2	2	0.8	3.2	0.40	0.20	-	0.60	2.74	0.28	-	3.02
25	2	3	2.1	1.3	1.30	0.50	-	1.80	0.64	0.34	0.31	1.29

3.5.2 Total Cancer Volume Comparison

HistoScanning demonstrated total cancer volumes ranging from 0.8 cc to 5.0 cc, median 3.2 cc (IQR 2.37); index lesion volumes ranged from 0.34 cc to 4.6 cc, median 2.02 cc (IQR 1.33-2.82).

The total cancer volumes at RP ranged from 0.2 cc to 26.5 cc with a median volume of 2.9 cc. (IQR 0.9-4.8). The index lesion volume at pathology ranged from 0.16 cc to 26.5 cc with median volume of 1.3 cc (IQR 0.8-3.72).

By plotting the distribution of total cancer volumes on a box plot it can be seen that there is little difference between the two median volumes; there was no statistical difference in median cancer volumes between the two modalities (P=0.59). (Figure 28)

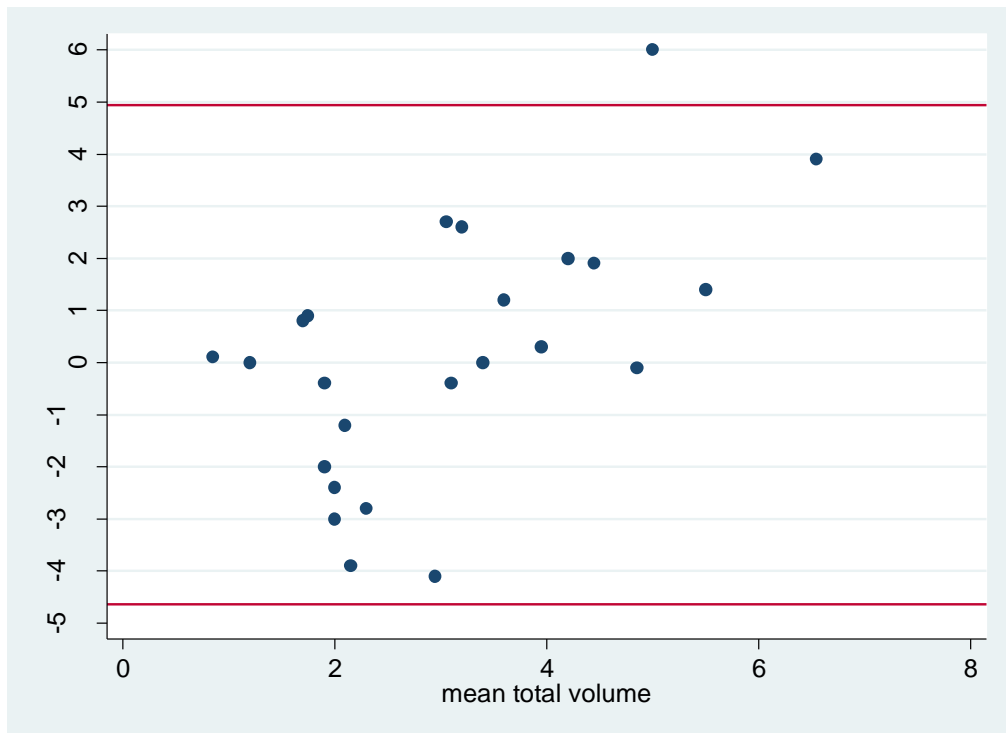
Figure 28. Box plot of total cancer volumes at Prostate HistoScanning and Radical Prostatectomy



A Bland-Altman correlation for the total cancer volumes as predicted by HistoScanning and found at RP histopathology demonstrated a poor correlation between the two volumes (Bland and Altman, 1986). (Figure 29) For those not familiar with Bland-Altman plots, the

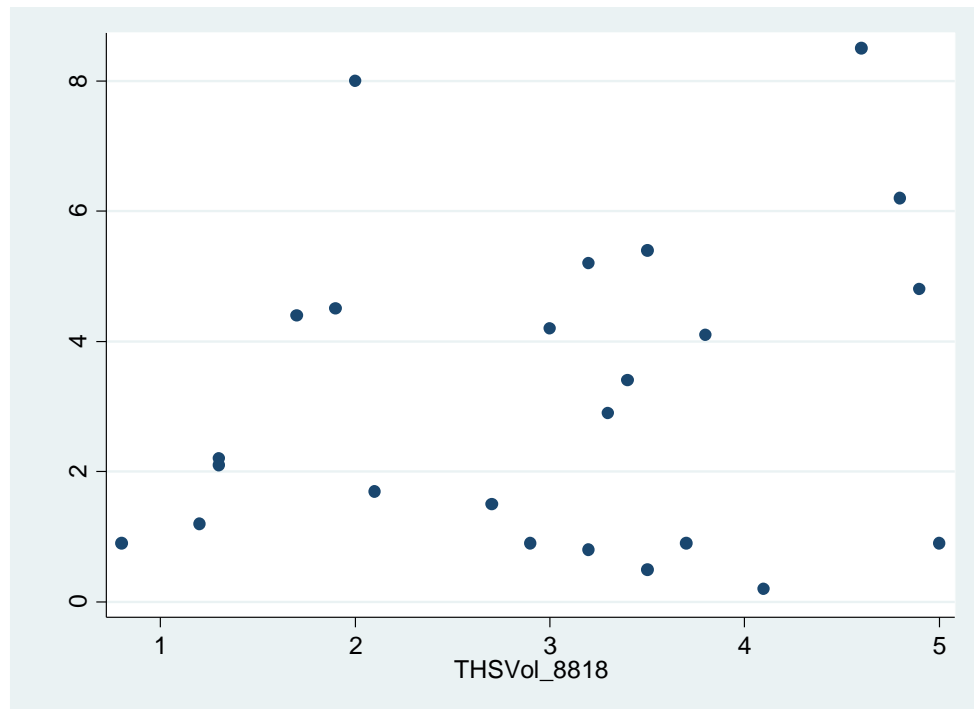
plot aims to demonstrate the agreement between two different measurements. The red bars show the limits of agreement. In figure 29 the limits of agreement are from +5 to -4.7, unfortunately it is clinically unacceptable to have such a variation in cancer volumes between the tests.

Figure 29. *Bland Altman plot indicating the agreement between RP and Prostate HistoScanning in assessing total cancer volume*



A scatter graph produce to show the correlation between the total cancer volumes at HistoScanning and those at RP histopathology (excluding patient 7 who is an outlier who skews the graph) also demonstrates that there is a poor correlation, the Pearson's correlation coefficient $R^2 = 0.04$. (Figure 30)

Figure 30. Scatter graph of correlation between HistoScanning total cancer volume (TCV) and RP TCV –blind phase



3.5.3 Whole Gland Analysis

When disease significance was defined as lesions ≥ 1.3 cc detected at RP histopathology, HistoScanning demonstrated sensitivity 88.2% (95% CI 63.6-98.5%) and PPV 71.4% (95% CI 47.8-88.7%).

Changing the disease significance level to ≥ 0.5 cc lesions on the reference test, HistoScanning demonstrated a sensitivity of 100% (CI 85.7-100%) and PPV 96% (CI 79.6-99.3%).

For detecting and ruling-out lesions ≥ 0.2 cc, HistoScanning demonstrated 100% sensitivity for detection of disease over this threshold. At these two thresholds no comment can be made on specificity as too few men tested negative at these disease thresholds (only one man had PHS cancer volume ≤ 0.5 cc and all had lesions ≥ 0.2 cc).

3.5.4 Sextant Analysis

For the sextant analysis in the blind phase, the method of 'bootstrapping' (Walsh and Reznikoff, 1990) was used to account for the non-independence of prostate sectors. Table 17 outlines the performance characteristics at each volume threshold.

Table 17. Sextant analysis for detection of 0.5cc and 0.2cc lesions using Boot Strapping correction as a result of non-independence of the sectors of analysis

	Sensitivity (CI) %	Specificity (CI) %	PPV (CI) %	NPV (CI) %
Volume Cut Off				
≥0.5cc	46 (33-60)	62 (53-72)	43 (30-55)	66 (56-76)
≥0.2cc	69 (59-79)	31 (21-42)	53 (44-63)	47 (32-62)

3.5.5 Lesional Analysis

Prostate HistoScanning detected 60 lesions ≥0.2cc. There were 43 tumours ≥0.2cc found on RP. One patient had an index lesion <0.2cc at radical prostatectomy histopathology.

For the primary method of lesional analysis of the 43 tumours ≥0.2cc detected at RP, 12 lesions were detected in the same sextant (28%), 28/43 (65%) of lesions did not possess an exact sextant match. Three (7%) lesions found at RP histopathology were not identified by HistoScanning.

Seventeen (30%) lesions were identified by HistoScanning that had no corresponding histological lesion at RP.

By considering each prostate lobe as the sector of analysis, 61% (27/43) of lesions were correctly identified on the correct side of the prostate by PHS.

A further, more subjective lesional analysis was performed in the blind phase analysis. In this analysis, two independent analysts assessed both the HistoScanning lesions and the RP histopathology lesions visually to decide if there was a location match. Once each analyst had visually assessed the location of lesions at the index and reference test and decided upon the location matching. Each case was then discussed, and a consensus agreement reached. When a consensus could not be reached a third independent urologist blinded to

the decisions of the consensus was asked to make a decision as to whether the lesion at prostate HistoScanning was confirmed on RP histopathology.

Of the sixty tumours detected by prostate HistoScanning, consensus was reached between the two analysts in 57 lesions (95%). The analysts were assessing whether the lesion at prostate HistoScanning had a corresponding matching lesion at RP ('a hit') or not ('a miss'). For the remaining three lesions where consensus could not be reached, a third independent analyst was asked to review the cases.

Overall, 37/60 lesions were deemed 'a hit' at histopathology (62%), 23/60 tumours (38%) were deemed 'a miss'. Of the index lesions at prostate HistoScanning, 68% were deemed a positive match for lesions seen at RP.

3.6 PHS02 Study Design Challenges

A number of challenges exist when trying to conduct an ideal study to verify a new diagnostic modality.

3.6.1 Target Patient Selection and the Ideal Reference Test

The patient population in this study were men undergoing Radical Prostatectomy. This allows for accurate verification of the Index Test against histopathology. It does however allow for an element of bias to be introduced into the study. By selecting men with known cancer we have introduced a positive selection bias as we are aware that all men have cancer. Additionally, men who have surgery for prostate cancer tend to have higher risk disease than those who do not choose surgery (Harlan et al., 2003).

By opting for a radical prostatectomy cohort we exclude a significant proportion of men who have other treatments for prostate cancer, such as: - radiotherapy; brachytherapy; hormones; cryotherapy and high intensity focused ultrasound - as well as those men opting to have active surveillance. Such groups will have differing tumour burdens when compared with those undergoing radical prostatectomy.

An ideal study of a diagnostic modality would apply the test to all men on whom it would eventually be applicable: namely, all men at risk of prostate cancer. However, in order to do such an ideal study, a number of men would need to be unnecessarily subjected to a

harmful reference test - radical prostatectomy. In a population of men who are all 'at risk' of prostate cancer and do not have confirmed disease this would be unethical.

An alternative strategy would be to select a less invasive reference test; however, most other reference tests would not allow for such exact matching with the index test.

Other possible reference standards considered were: - TRUS biopsy; Cysto-Prostatectomy and Transperineal Template mapping biopsy.

TRUS Biopsy is at present the standard of care for men deemed to be at increased risk of prostate cancer. There are several important problems with TRUS biopsy and reasons why TRUS guided biopsy would serve as a poor reference test:

TRUS guided biopsies have a false negative rate of up to 30% (Merrick et al., 2007). TRUS systematically under samples the anterior, the midline and the apical parts of the prostate.

The deployment of the biopsy needle is tangential (neither sagittal nor transverse), so it is difficult to attribute any sample to any particular location within the prostate. This would prove difficult for matching with the index test.

TRUS biopsies are unrepresentative of the true disease burden or grade of the cancer in more than one third of cases, and are therefore a poor indicator of prognostic factors such as Gleason grade and cancer burden. (Mazzucchelli et al., 2009, Crawford et al., 2005)

Studies investigating the incidental prevalence of prostate carcinoma in cysto-prostatectomy series vary widely in their results, ranging from 3-50% harbouring prostate cancer (Autorino et al., 2009). In contrast to the radical prostatectomy series who have higher risk disease characteristics than the background population, patients undergoing cysto-prostatectomy have been shown to have low risk disease in around 80% of the cases with incidental prostate carcinoma identified (Mazzucchelli et al., 2009). This along with the significant morbidity of cysto-prostatectomy means it is not an ideal reference test.

The reference test that closely meets the required specification for our defined population is transperineal template prostate mapping biopsies at 5mm intervals; however, 3D correlation with the Index Test using this strategy is challenging.

Transperineal template mapping biopsy (TPM) has shown a sensitivity of 95% and negative predictive value of 95% for clinically significant cancers of volume >0.5cc and 76% sensitivity for all cancers (Crawford et al., 2005, Lecornet et al., 2012, Hu et al., 2012a,

Ahmed et al., 2011). It also has the advantage over TRUS biopsy that it is able to assess the anterior part of the prostate and to be able to attribute each biopsy core to a particular coordinate.

However, although transperineal template mapping biopsy would be an attractive reference test as it could be applied to a wider population of men, the 3D matching of biopsy cores with ultrasound imaging would prove very difficult, and thus in the PHS02 study Radical Prostatectomy was chosen as the reference standard.

In addition, for the purpose of validating the prostate HistoScanning technology, as PHS02 aimed to do, whole mount radical prostatectomy specimens are the current gold standard reference test.

3.6.2 Problems with the Reference Test

Radical prostatectomy operations are performed worldwide and different surgeons operate in subtly different ways. Clearly, it was necessary for this study to standardise the reference test as much as possible. Therefore, all surgeons were required to work to a strict standard operating procedure (SOP): only prostates that had been successfully removed as a complete whole gland specimen were sent for processing.

Despite the rigorous controls in place, problems still arose with regard to collection and transportation of the removed glands, rendering some of them unsuitable for further analysis.

Processing was centralised to minimise inter-reporter variability and followed a rigorous SOP, as stated previously. Processing was performed according to the stanford protocol 3mm slices, there is however the possibility in this slicing that small tumours could be missed when preparing the slices and trimming to full face.

3.6.3 Problems with the Index test

The aim of the study was to verify the ability of HistoScanning to detect and localise prostate cancer.

For the verification of this technology it was vital that optimal images were included in this study. Ultrasound is a notoriously user dependent technology and as such a strict SOP for collection of the study images was implemented. Technicians from AMD were present with each operator at the time of PHS screening to advise on technique to obtain optimum scans.

However, a number of scans were ineligible for further analysis as they revealed large amounts of calcification on the gland: ultrasound signal does not easily transmit through calcified areas of the prostate, and although Prostate HistoScanning is able to make a prediction of the presence or absence of cancer in areas behind calcification it is likely to be an unreliable predication. Thus, for the purposes of this verification study, men with large calcifications were excluded. Also, scans which failed to capture the entire gland were also excluded, as the whole gland is required for correlation with the reference test.

3.6.4 Problems with Matching between the Index and Reference Test

For all studies comparing new diagnostic modalities to a reference test one of the major challenges is how to correlate the two tests to obtain accurate information on the performance of the technology. Matching between the index test and the reference test was indeed one of the major challenges within the study.

Histopathological specimen to image correlation is adversely affected by a number of processes including surgical distortion and tissue shrinkage during fixation.

By rigorously controlled SOP's at both the index test (prostate HistoScanning) and the reference test (RP Surgery and histopathological processing) the effects of any distortion to produce a matched cohort were limited.

However, as a prostate gland undergoes processing, its morphology changes; the prostate ex-vivo and processed in formaldehyde is a different shape to the prostate in- vivo. To mitigate the effects of this, localisation of lesions was done using a division of the prostate into sextant areas. Both the reporting Histopathologist and the Prostate HistoScanning reporter provided reports on the volume of cancer within each sextant of the prostate. Images were matched by independent analysts.

3.6.5 Defining Prostate Cancer Significance/Determining Volume Thresholds

It is established that not all prostate cancer is significant and there is a need to be able to better 'risk stratify' patients, but criteria for disease significance vary widely between studies. Ideally a diagnostic test would have the ability to detect significant cancer whilst not identifying too many insignificant cancers, and thus reducing the over-treatment burden.

It is possible to argue that the prostate HistoScanning signal should be correlated with all cancer detected. However, in the knowledge that not all prostate cancer is significant, and given that prostate HistoScanning is not able yet to differentiate between cancers of different grades, a volume cut off was required.

Stamey et al established a volume threshold for disease significance at ≥ 0.5 cc and this definition has been widely used since (Stamey et al., 1993). However as previously mentioned, it has recently been reported by Wolters et al after studying the ERSPC data that for those with low grade, low risk disease, index tumour volumes of up to 1.3 cc and total tumour volumes of 2.5cc may still constitute low risk disease (Wolters et al., 2011).

Despite this recent study showing that tumours may be insignificant at more than twice the volume suggested by Stamey et al, PHS02 opted to use the well-established volume criteria of 0.5cc for disease significance for the purpose of primary analysis.

3.7 Discussion of PHS02

The PHS02 study both open and blind phases has several limitations, most of which have been discussed in the study design challenges section. The data from the two phases demonstrates reasonable performance characteristics for the technology, although the blind phase data shows reduced performance characteristics compared with the open phase.

The rigorously controlled nature of the blind phase may have had some degree of negative impact on the performance characteristics. To date, there are very few if any truly 100% blinded comparisons between imaging and histopathology in the literature, and although the performance characteristics found at the blind phase of PHS02 may at first glance appear inferior to other imaging modalities and other studies, the impact of a truly blinded comparison must not be underestimated: the biases of retrospective and un-blinded

analysis on the performance characteristics of other test modalities - and indeed even in the open phase of the PHS02 study - must be recognised. These biases are likely to lead to an inflation of the performance characteristics.

The PHS02 study showed a high degree of accuracy for the detection of prostate cancer lesions on a patient/whole gland level with sensitivity for detection of ≥ 0.5 cc volumes of 100%.

A limitation to the work is the volume of disease demonstrated by each man in the study: all men had cancer that was suitable for radical prostatectomy, and the primary analysis was performed on a whole gland level. As such, the very high sensitivities demonstrated by both the open and blind phases may account merely for the detection of false positive signal. Indeed, in the blind phase of the study using the sextant analysis showed a significant reduction in the performance characteristics.

However, when interpreting the data from the PHS02 study it is important to remember that as HistoScanning cannot as yet quantify Gleason grade, lesion significance is based on lesion size criteria as established by current literature (Stamey et al., 1993, Epstein and Potter, 2001, Wolters et al., 2011).

Data from both the open and blind phase of the study suggests that the prediction of volume by HistoScanning may be unreliable. The open phase data suggesting that depending on the quality of the scan lesion sizes may be under- or over- estimated.

The blind phase data suggests from the analysis of the Bland-Altman that there is very little true correlation between the size of lesion detected at HistoScanning and that detected by RP histopathology. This therefore may have a great impact on the performance characteristic analysis of HistoScanning; which is based on lesion size criteria compared to RP histopathology.

PHS02 study results demonstrate that the technology may have potential for use in the prostate cancer pathway, but due to a number of limitations within the study such as the patient group, the reference test and the significance criteria, further studies on the technology are warranted. Further studies are also needed to assess the reliability of the test.

3.8 HistoScanning Reliability Work

For a diagnostic test to be valid it requires not only good performance characteristics in terms of sensitivity/specificity, positive and negative predictive value, it also needs to be reliable and reproducible, not only in terms of the technique but also in the reporting of the images produced by HistoScanning.

A number of pilot experiments on the reliability of HistoScanning have been performed and the results are described in the following section.

3.8.1 Intra-operator Pilot Data

To examine the reproducibility of HistoScanning output when applied by different operators a small study was conducted.

3.8.1.1 Method

Ten men with low risk prostate cancer on TRUS guided biopsies, undergoing HistoScanning analysis in our institution as part of the PICTURE study and covered by the ethics of this trial, were approached for inclusion in the pilot. All men underwent a standard HistoScanning acquisition performed by a trained operator (Operator 1)- with 3 years' experience at PHS, in the same session a second operator (Operator 2)- with 1 year experience at PHS who was blinded to the previous scan performed a HistoScanning acquisition, using the same equipment and independent of the primary operator.

Both scans were reported by a single reporter to minimise reporter variability. An analysis of HistoScanning images for Prostate Volume and Prostate HistoScanning signal was performed for both acquisitions. HistoScanning analysis is as previously discussed in this thesis a semi-automated process the reporter is required to define apex, base, left and right borders of the prostate. Delineation of the prostate outline, division into sextants, and analysis of ultrasound signal for presence or absence of cancer is automated.

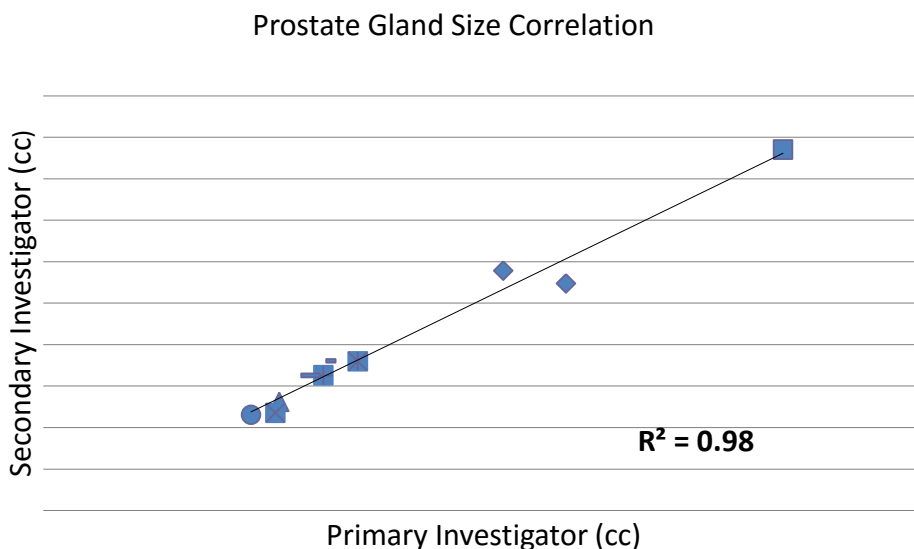
Linear regression was used to calculate the correlation in both gland and cancer volume generated by each acquisition. Cohen's kappa statistic was performed to estimate the agreement for presence or absence of a focus $\geq 0.5\text{cc}$ in any one sextant. Kappa values ranges indicate a range of agreement, <0 indicates no agreement, $0-0.20$ slight, $0.21-0.40$ fair, $0.41-0.60$ moderate, $0.61-0.80$ substantial, and $0.81-1$ almost perfect agreement

3.8.1.2 Results

60 sextants from 10 patients were analysed. Operators agreed on the presence or absence of a lesion $\geq 0.5\text{cc}$ within a sextant in 75% of sextants ($n=45$). Cohen’s kappa co-efficient was 0.57 (95% CI: 0.30-0.72).

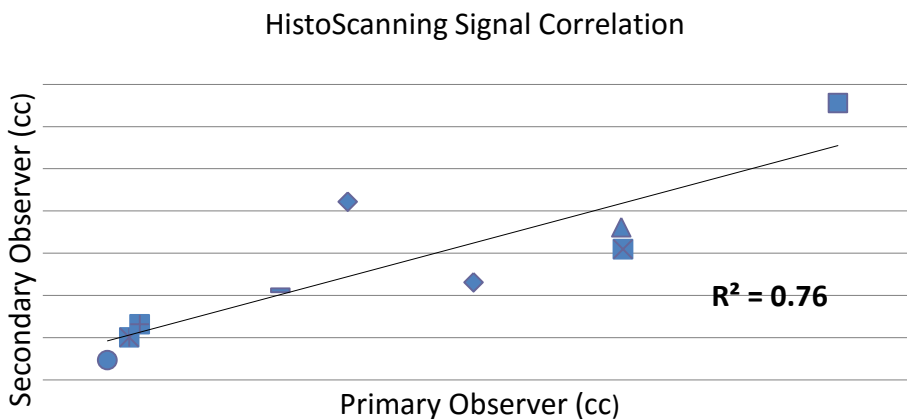
Linear regression for prostate volume between the two acquisitions exhibited strong correlation ($R^2 = 0.98$). (Figure 31)

Figure 31. Graph demonstrating Prostate gland size correlation



For tumour volume, linear regression was also good ($R^2 = 0.76$) (Figure 32). Further analysis of the data revealed that scans deemed to be of poor quality by the reporter, showed a reduced correlation in HistoScanning lesion volume than those of good quality.

Figure 32. Graph demonstrating HistoScanning signal correlation



3.8.1.3 Conclusion:

There are clearly limitations to this work. A very small sample size of men was examined, due to the pilot nature of the work, and the need for two intimate examinations in a short time frame. Operators also had slightly differing levels of experience. There was also no histological gold standard to which to compare the HistoScanning lesions.

However, in this first reliability study of its type for Prostate HistoScanning, the outputs from HistoScanning analysis were stable between two operator-acquired images. The strength of association was greater for prostate volume than it was for tumour volume. Reliability in the latter was sensitive to the quality of the images obtained.

3.8.2 Inter-observer Reporting Work

Another aspect of test reliability is that the outcome when reported by different reporters should be stable and with minimal inter-observer variation.

3.8.2.1 Patients and Methods

Patients managed by active surveillance, who had undergone HistoScanning more than once, as part of the Rotterdam arm of the Prostate cancer Research International: Active Surveillance (PRIAS) study, Dutch Trial Register with ID NTR1718, were eligible for this pilot study. Two independent observers with 2 years' experience each in the interpretation of PHS scans processed and analysed the HistoScanning outputs for each acquisition.

Observers first contoured the prostate gland, and then HistoScanning automatically defined the sextants and probable cancer volumes (unrefined). The observer then deselected volumes deemed unlikely to represent prostate cancer and recalculated volumes (refined).

Agreement between the two observers for estimation of total cancer volume in prostates of the 12 patients was estimated by least square linear regression. The kappa statistic was used to estimate the inter-observer agreement for presence of a focus ≥ 0.5 cc in any one sextant. Kappa values range from -1 (total disagreement) to +1 (perfect agreement), and zero corresponds to no agreement.

3.8.2.2 Results

198 sextants generated by 33 scans from twelve patients were analysed independently by two observers. Both observers found a refined focus $\geq 0.5\text{cc}$ in 40 sextants and no such focus in 138 sextants (Table 18). Hence, both observers agreed on the presence or absence of focus in 90% of sextants, achieving a kappa statistic of 0.81 for unrefined and 0.73 for unrefined focus volumes.

Table 18. Inter-observer variability

		Observer 2		Total
		Focus yes	Focus no	
Observer 1	Focus yes	40	11	51
	Focus no	9	138	147
Total		49	149	198

The least square regression for unrefined and refined volumes was 0.83 (Figure 33) and 0.94 (Figure 34) respectively.

Figure 33. Least squared regression for unrefined HistoScanning volumes

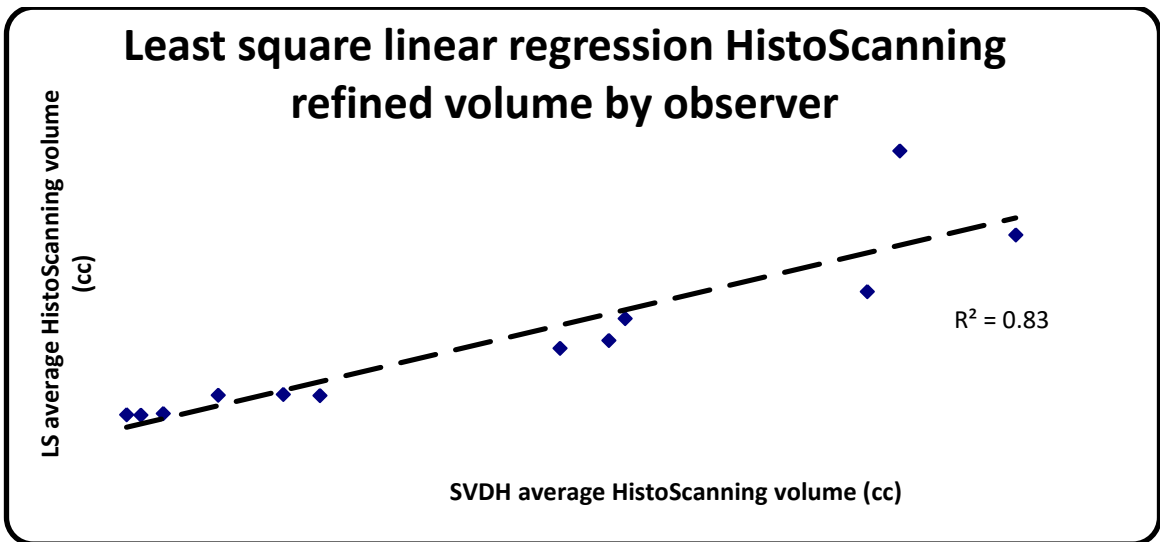
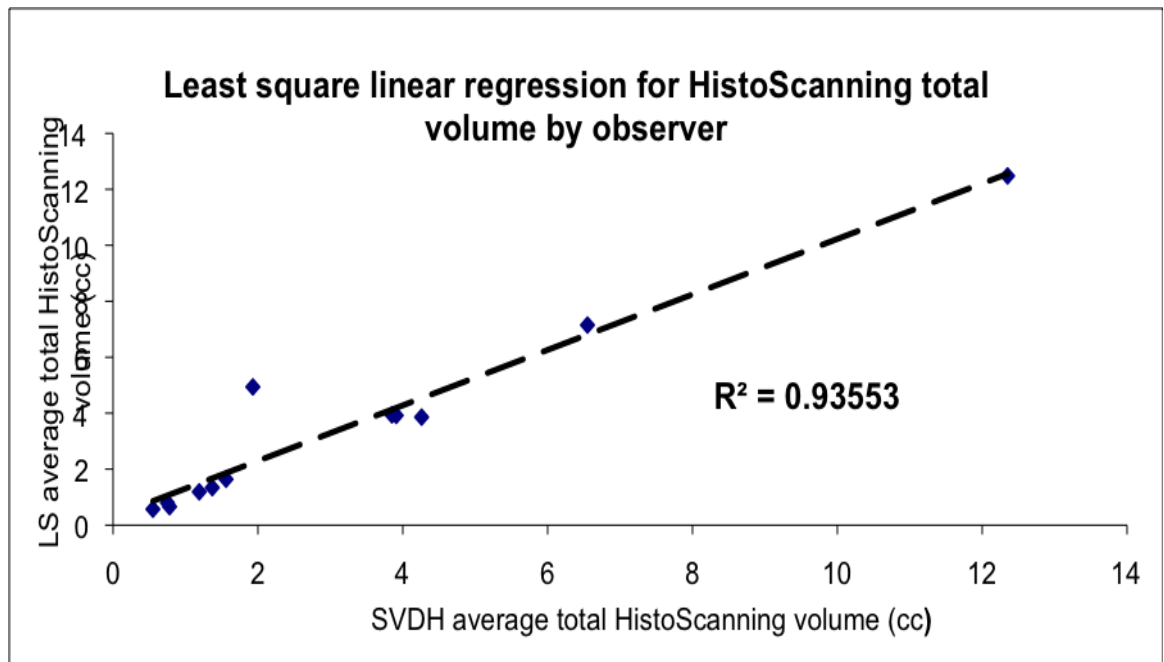


Figure 34. Least squared regression for refined HistoScanning volumes



The first obvious limitation to this work is once again the small numbers of patients involved in the study and secondly the lack of a histopathological confirmation of the HistoScanning signals.

However, despite its limitations this pilot study demonstrated that Inter-observer agreement is high when two trained observers progress through the HistoScanning™ workflow to determine prostate cancer volume and presence of focus within a sextant.

3.8.3 Pilot Study Prostate HistoScanning Gleason Grade Discrimination

The HistoScanning technology at present is not able to discriminate grade of disease. Lesion significance is therefore based on sized criteria alone, as outlined in the PHS02 study results some inaccuracies between the volumes found at prostate HistoScanning and those found at RP histopathology exist, which may impact on the accuracy of the test.

A pilot experiment was carried out to assess the ability of Prostate HistoScanning to determine Gleason grade, as if the test were able not only to predict the presence of prostate cancer but also to estimate grade: it would then prove a very useful tool in the diagnostic pathway.

The basis of the prostate HistoScanning technology is that it uses mathematical algorithms to predict whether an ultrasound radiofrequency (RF) backscatter signal has been reflected from normal prostate tissue or prostate cancer tissue.

The hypothesis of this pilot experiment was that if prostate HistoScanning were able to differentiate between benign and malignant tissue, it could differentiate between low grade (Gleason 3) disease and high grade cancer (Gleason 4 or above).

3.8.3.1 Methods:

Three men scheduled for radical prostatectomy, as part of the ethics approved PHS02 study, were included in this pilot study. Standardised 3mm whole mount histopathology was performed. Reporting was segmented into 5mm by 5mm grids. Within each grid, if cancer was present, the dominant Gleason grade was quantified as a percent of the total (the reference test).

Preoperative prostate HistoScanning was performed (the index test). Prostate HistoScanning was then used to interrogate volumes of tissue for the presence or absence of prostate cancer in units of 0.05 mm^3 and each data point registered to its 5 x 5mm histological grid (Figure 35).

3.8.3.2 Results

14 grids with prostate cancer were analysed (Table 19). Of these, 6 had a Gleason grade 4 or more at histology. The relative risk of grids with predominant Gleason grade 4/5 being labelled as such compared to grids that contained predominant Gleason grade 3 is 3.2 (95% CI: 3.0-3.3), Chi-square p value<0.0001.

Table 19. Histological vs HistoScanning attribution of Gleason grade (GIG)

Source: Patient No (overall Gleason score)	No. of cells Analysed	Predominant Gleason grade in analysed cells at Histology	% of data points with Gleason grade attributed by PHS (number of data points analysed)	
			% ≤ Gleason grade 3	% ≥ Gleason grade 4
1 (4+3)	4	3	83 (1373)	17 (285)
2 (3+4)	4	3	77 (3817)	23 (1121)
1 (4+3)	3	4	24 (173)	76 (551)
3 (4+3(+5))	3	5	33 (1657)	67 (3303)

The distribution of HistoScanning™ scores generated when applying the newly developed tool to the RoI's of different Gleason grades shows a predominant left shift for lower Gleason grade and a right shift for higher Gleason grades. The higher Gleason grades also demonstrate a narrower distribution relative to the lower Gleason grades. (Figure 36)

Figure 36. *Graph of Prostate HistoScanning Gleason tool frequency analysis*



3.8.3.3 Limitations

Although a large number of data points were analysed per patient, the sample population itself was small.

In addition, although registration of Prostate HistoScanning to histopathology grids was performed as accurately as possible using measurements of trimmings and lengths taken at histopathology, there remained a risk of mis-registration between the index and the reference test.

3.8.3.4 Conclusions

This preliminary proof of concept data demonstrated that interrogation of raw radiofrequency ultrasound spectra by Prostate HistoScanning™ may be able to discriminate between prostate cancers of different histological grade.

The ability to accurately attribute tumour grade using this non-invasive technique may allow for more accurate prostate biopsy and treatment planning.

4 Prostate Imaging Compared to Transperineal Ultrasound guided biopsy for significant prostate cancer Risk Evaluation (PICTURE)

4.1 PICTURE Study Design and Objectives

The PICTURE study is a single centre STARD compliant (Bossuyt et al., 2003) prospective diagnostic trial that conforms to level one evidence, that was carried out at University College London Hospitals (UCLH). The trial assesses the diagnostic performance of mp-MRI and Prostate HistoScanning against the reference test of Transperineal template mapping biopsies.

The primary objective of the PICTURE study is to assess the negative predictive value of both imaging modalities to allow us to answer the question “could imaging allow men to avoid further unnecessary prostate biopsy?”

4.1.1 Study Objectives

The primary objective of the study is to assess the negative predictive value of multi-parametric MRI and prostate HistoScanning in ruling out **clinically significant** prostate cancer.

Main secondary objectives are:

- To evaluate the proportion of men correctly identified by multi-parametric MRI and prostate HistoScanning to have **no prostate cancer** as determined by specificity and negative predictive value (NPV)
- To evaluate the proportion of men correctly identified by multi-parametric MRI and prostate HistoScanning to have **clinically significant prostate** cancer as determined by sensitivity and positive predictive values (PPV)
- To assess whether the use of MRI to US registration targeted biopsies alone is comparable to the use of i) systematic biopsies and ii) cognitive targeted biopsies in stratifying patients into prostate cancer risk groups.

- To assess the test – retest reproducibility of prostate HistoScanning

Further PICTURE outcomes which are not the key focus of the work within this thesis include:

- To evaluate the ability of urinary Engrailed 2 (EN2) to predict the presence of prostate cancer and to determine its ability to predict clinically significant disease.
- To evaluate the ability of seminal citrate and zinc levels as determined by FScan to predict the presence of prostate cancer and to determine its ability to predict clinically significant disease.
- To evaluate the diagnostic validity of multi-parametric MRI and prostate HistoScanning when various regions of interest are used to assess accuracy in detection of prostate cancer at different thresholds for clinical significance.
- To evaluate the ability of Tissue Type Imaging (TTI) to predict the presence of prostate cancer
- To evaluate using validated questionnaire's (IPSS, IPSS QoL and IIEF-15) the impact of transperineal Template prostate mapping biopsy on Urinary and sexual function.

4.1.2 Trial Design

The PICTURE study followed a prospective cohort design; all men will undergo both Index tests (mp-MRI and PHS) and transperineal template mapping biopsies. Men remained blinded to the results of the Index tests prior to the reference test to prevent attrition bias, as if aware of a negative index test result men may choose not to undergo the reference test.

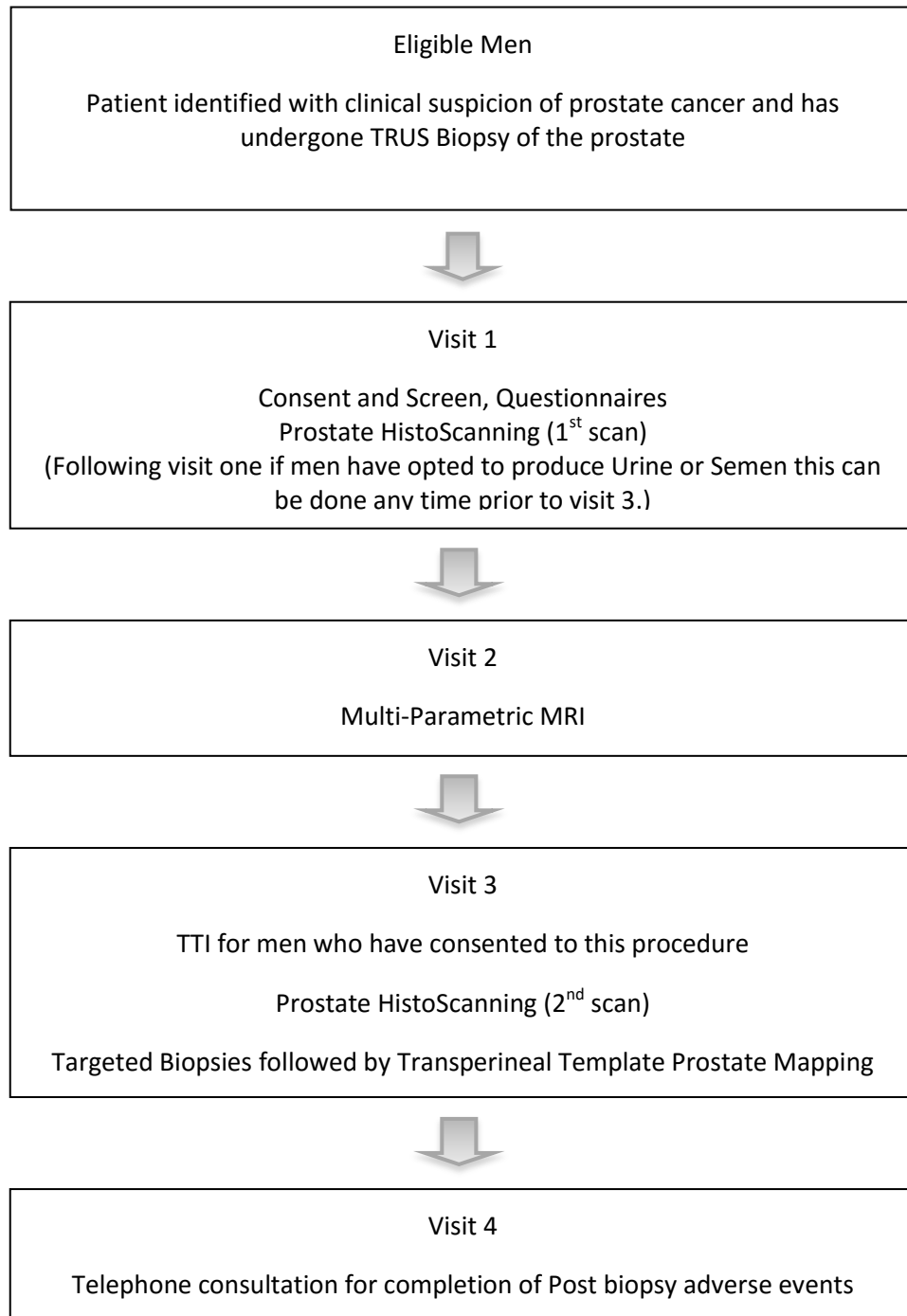
Both of the index tests were reported blind to the results of each other and prior to the reference test of Transperineal template mapping biopsies.

The use of TPM as a reference test allows for a unique opportunity to validate not only imaging as a biomarker but also other biomarkers that may be advantageous in the prostate cancer pathway. PICTURE therefore included optional additional tests that men may choose to undertake including ultrasound-based Tissue Type Imaging (TTI) (Feleppa et al., 2011, Feleppa et al., 2004, Feleppa, 2008), urine and semen biomarkers (urinary Engrailed 2 - EN2 (Morgan et al., 2011, Pandha et al., 2012) and seminal citrate and zinc

levels as determined by FScan (Costello and Franklin, 2009) to be performed pre-biopsy and the reports or assays derived blinded to the TPM result.

Figure 37 demonstrates the PICTURE trial study flow.

Figure 37. *PICTURE trial study flow*



The study was partially funded by a grant from Advanced Medical Diagnostics, it also received supportive funding from the University of Durham (Fscan) and University of Surrey (EN2).

4.1.3 Inclusion/Exclusion criteria

4.1.3.1 Inclusion criteria

- Men who have undergone prior trans-rectal biopsies.
- Men undergoing further evaluation of their prostate and who are suitable for characterisation using transperineal template prostate mapping biopsy.

4.1.3.2 Exclusion criteria

- Previous history of prostate cancer treatment
- Men unable to have MRI scan, or in whom artefact would reduce quality of MRI.
- Men unable to have general or regional anaesthesia
- Men unable to give informed consent

4.1.3.3 Withdrawal Criteria

- Men who are unfit or choose to not undergo prostate mapping biopsies after undergoing either or both index test.
- Men in whom either of the index tests are inadequate for analysis due to artefact or image acquisition problems.
- Men in whom the reference test is inadequate for analysis due to lack of complete gland sampling or inadequate sampling density.

4.1.4 Ethics and Registration

Ethical approval for the study was granted by London City Road and Hampstead National Research Ethics Committee REC reference 11/LO/1657 and the trial is registered with ClinicalTrials.gov identifier NCT01492270

4.2 Rationale and Methodological Discussion

4.2.1 Choice of Patient Population

As discussed in section 3.6, it is vital for a diagnostic study to evaluate a cohort of patients in whom the diagnostic test would eventually be applied. An important cohort of men in whom prostate cancer imaging may prove beneficial is the group of men who have undergone an initial TRUS biopsy for the suspicion of prostate cancer but in whom concern remains regarding the negative or positive status to which they have been assigned.

PICTURE recruited men from this cohort. The first group of men eligible for PICTURE are those with an elevated or rising PSA despite a negative TRUS biopsy. The second group includes those men with low/intermediate disease on TRUS biopsy for which concern remains that the burden of their disease is under represented by TRUS biopsy. In the diagnostic pathway at University College London Hospitals (UCLH) both of these groups would normally be offered transperineal template mapping biopsies as a further diagnostic test.

By selecting the men from this cohort both those with known prostate cancer and men without were included. This population is representative of the population in whom imaging for prostate cancer may prove beneficial in the future. The heterogeneity of the study population adds to the external validity of the trial.

This population of men were selected, rather than the pre-biopsy cohort, as with the financial constraints of the NHS system it is likely for imaging to be adopted primarily at this point in the pathway. Indeed, during the evolution of this thesis NICE guidelines have changed to suggest the use of mp-MRI following initial TRUS biopsy and rising PSA. (National Institute for Health and Care Excellence, 2014b).

Also a further study investigating the use of mp-MRI in the pre-biopsy cohort is underway at UCLH; the PROMIS study will investigate the utility of mp-MRI prior to biopsy and also the financial impact of the introduction of mp-MRI on the NHS system, and is expected to report in early 2016.

4.2.2 Choice of Reference Test

The reference test for the PICTURE study was carefully considered to enable the interrogation of both of the imaging modalities, without introducing significant bias.

The reference standards available for the study included Radical Prostatectomy step sectioned histopathology, cystoprostatectomy, TRUS biopsy and transperineal template mapping prostate biopsy (TPM).

The use of radical prostatectomy step-sectioned histopathology, although providing excellent histological verification, introduces significant selection bias to any study, as to proceed to radical prostatectomy all men undergoing this procedure will have cancer. Also those men choosing radical prostatectomy tend to have significant disease burdens, than in other treatment groups.

Cystoprostatectomy series as a reference standard also introduces selection bias but not to the same degree as RP specimens- as within the cohorts men may or may not have prostate cancer: burdens of disease in this population tend to be less than in the population as a whole (Trpkov et al., 2010).

TRUS biopsy does not fulfil the characteristics of a good reference standard for validation of these technologies as TRUS is inaccurate in sampling the whole gland, and is known to systematically under-sample the anterior gland (Ayres et al., 2012, Bott et al., 2002).

The reference test that most closely meets the requirements for the study was Transperineal template mapping biopsy.

Transperineal template mapping prostate biopsy, can be applied to all men at risk both those with known prostate cancer and those without. It has also shown a sensitivity of 95% for clinically significant cancer ≥ 0.5 cc and 76% sensitivity for the detection of any prostate cancer (Crawford et al., 2013, Ahmed et al., 2011, Crawford et al., 2005). TPM also allows for accurate assessment of all areas of the prostate, including the anterior portion of the prostate, and enables biopsies to be accurately assigned to specific areas of the prostate.

The side-effect profile of trans-perineal template mapping biopsy is not dissimilar to that of TRUS biopsy, which makes it a tolerable procedure. There are two main differences to the side effect profile: - firstly the post procedural sepsis rate is much lower with TPM biopsy than TRUS biopsy as the needle is not required to traverse the rectal mucosa in TPM (<1%

vs. 4%); secondly, the post-procedural urinary retention rate is higher with TPM than with TRUS, with 5-10% of men suffering self-limiting urinary retention vs. 1% with TRUS. (Merrick et al., 2007).

Although TPM provides a gold standard reference test for our chosen study population, it carries some potential disadvantages for both the individual and the institution. The potential disadvantages for the individual include the need for a general or regional anaesthetic, and the risk of over-detection of insignificant prostate cancer - although the very accurate nature of the diagnosis of low risk disease is likely to increase both patient and physician confidence to carry out active surveillance (Barzell et al., 2012).

TPM also requires additional healthcare resources when compared to TRUS biopsy, such as general or regional anaesthesia and an increased pathology burden of processing and reporting up to 80 biopsy specimens as opposed to 8-12 with TRUS.

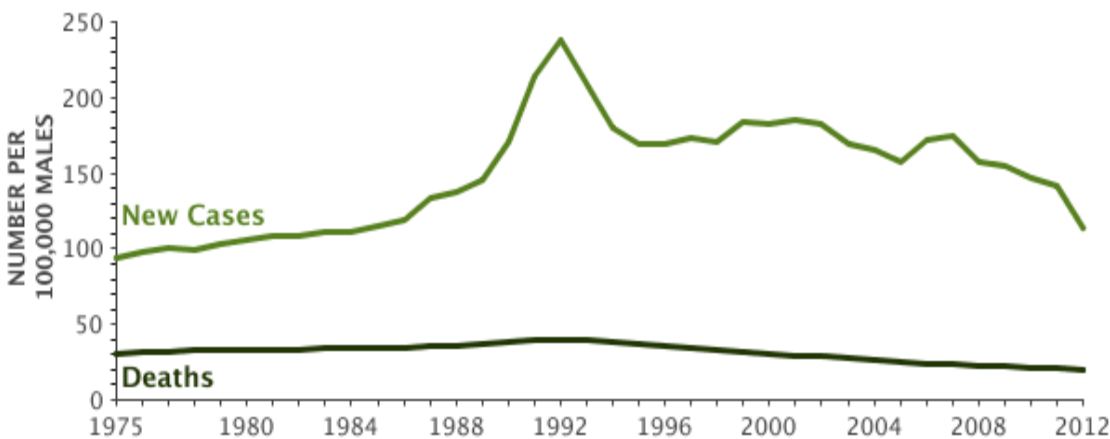
Despite these additional burdens, because of the accuracy with which disease risk stratification can be performed by TPM (Gleason grading, tumour burden and location), and the acceptable side effect profile, it was selected as the most valid reference test.

4.2.3 Definitions of Clinically Significant Disease

Another important consideration when designing the PICTURE study was the definition of clinically significant disease. Much debate exists amongst experts about the nature of prostate cancer disease progression and what constitutes clinically important disease (Berman and Epstein, 2014, Ahmed et al., 2012).

It has been demonstrated in the USA with the introduction of PSA screening that many more cancers are detected using a PSA screening approach. The below graph shows a peak in incidence of prostate cancer at the time of introduction of PSA screening in the US, around 1992 (Figure 38). This increased detection of cancer did little however to alter the mortality rate from cancer.

Figure 38. SEER 9 Incidence & U.S. Mortality 1975-2012, All Races, Males. Rates are Age-Adjusted¹⁹



Year	1975	1980	1985	1990	1995	1999	2003	2007
5-Year Relative Survival	66.0%	70.2%	74.9%	88.4%	95.7%	99.2%	99.1%	99.7%

These figures suggest that not all prostate cancers are likely to cause mortality and therefore it follows that not all cancers are clinically significant.

Many studies have tried to define what constitutes clinically significant disease and as discussed in section 3.6.5 the most widely used definitions for disease significance are based on those by Stamey et al, who established a volume threshold for disease significance at $\geq 0.5\text{cc}$ and Epstein et al, who set a threshold of $\geq 0.2\text{ cc}$ (Stamey et al., 1993, Epstein et al., 1994).

From the European Randomised Study of Screening for Prostate Cancer (ERSPC) data , of men with low grade, low volume disease Wolters et al summated that an index tumour volume of up to 1.3 cc and total tumour volume of 2.5cc may still constitute low risk disease (Wolters et al., 2011).

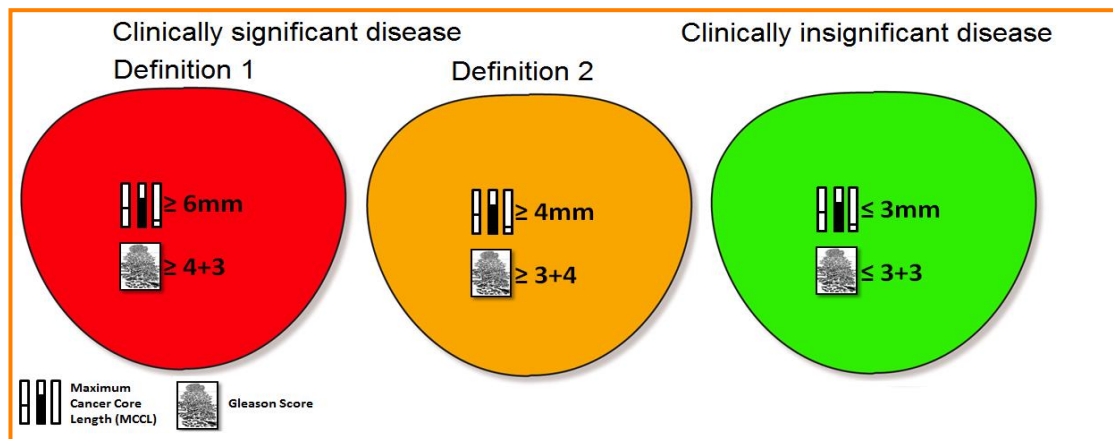
¹⁹ Kindly reproduced with permission form SEER Cancer Statistics Factsheets: Prostate Cancer. National Cancer Institute. Bethesda, MD, <http://seer.cancer.gov/statfacts/html/prost.html>, accessed 20/06/2015

Ahmed et al defined the characteristics of clinically significant disease using TPM biopsy, by the use of TPM computer simulations on reconstructed RP whole mount specimens (Ahmed et al., 2011).

Two main definitions of clinically significant disease were defined from this study, and these (Figure 39) are the definitions for significance selected for use in the PICTURE study.

The primary definition for clinically significant disease, and that used for the study power calculation, will be definition one primary Gleason pattern ≥ 4 OR Maximum cancer core length (MCCL) ≥ 6 mm.

Figure 39. UCL definitions of clinically significant disease



4.3 Index Tests

All men in the study underwent both index tests of mp-MRI and prostate HistoScanning.

4.3.1 Multiparametric-MRI

Each sequence of an mp-MRI has different properties that, when assessed by a radiologist can assist in the decision whether an abnormal area represents cancer or not.

Within the PICTURE study several sequences were obtained, these include:-

1) a T2 weighted sequence, which allows for accurate anatomical imaging of the prostate and surrounding tissues.

2) diffusion weighted imaging (DWI), which evaluates the interstitial free water and permeability - cancers tend to have greater cell density and demonstrate restricted diffusion signal. DWI images include various B value sequences, extended B value images (B1400 at 1.5T and B2000 at 3T) and enable the production of Apparent Diffusion Coefficient (ADC) maps.

3) dynamic contrast enhanced images (DCE). These images are acquired by injecting gadolinium contrast agent, whilst imaging the prostate every few seconds to evaluate the temporal contrast properties of tissue in order to derive information on vascularity. The aim of DCE is to detect prostate cancers by exploiting the angiogenic nature of cancers and their increased vascularity.

Full sequence information can be found in appendix 10.4.

Due to the nature of the study, mp-MRI's were performed primarily at 3 Tesla; however, for men for whom a 3T scan was not possible, a 1.5T scan was performed.

The mp-MRI images in PICTURE were reported blinded to other imaging information, but the radiologist was aware of the patient's clinical information - including prior TRUS biopsy result and PSA value: - this pragmatic inclusion is to reflect what would occur in daily clinical practice.

The radiologist reported the MRI according to a strict SOP on a proforma, with a single radiologist reporting all scans within the study. Planned re-reporting of a selection of scans was performed to assess reliability. Figure 40 demonstrates the mp-MRI reporting form.

Figure 40. PICTURE mp-MRI reporting form



PICTURE
MP-MRI Reporting Form
Version 1.0 December 2011

University College London Hospitals 
NHS Foundation Trust

Page 1 of 1

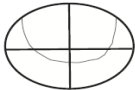
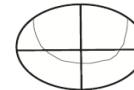
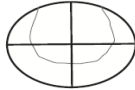
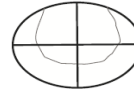
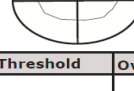
Patient's Initials: Date of Birth: Trial Number:

Hospital Number: Scan Date:

1. SIZE OF PROSTATE

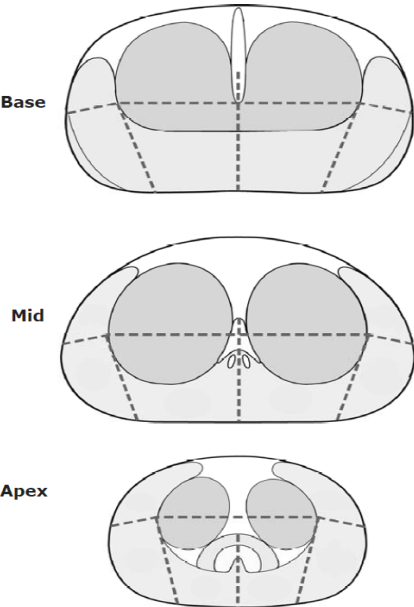
Transverse: • cm Anterior-Posterior: • cm Cranio-Caudal: • cm Volume: cm³

2. SECTOR (Please report strictly in order on the diagram below, please put a value 1-5 (MRI Score[†]) in each Region of Interest)
P = Posterior 1.7cm (Measured from posterior capsule)

	T2	T2 + DW	T2 + DW + DCE
Base	A 	A 	A 
	P 	P 	P 
Mid	A 	A 	A 
	P 	P 	P 
Apex	A 	A 	A 
	P 	P 	P 

Risk category	Disease Threshold	Overall MRI Score [†] (1-5)
Any cancer	Any Disease	
Definition Two	≥ 0.2cc and/or ≥ 3+4	
Definition One	≥ 0.5cc and/or ≥ 4+3	

3a. INDIVIDUAL LESIONS (Please draw and number measurable lesions on diagram below)



3b. INDIVIDUAL LESIONS
(Using the lesions drawn in 3a please score each lesion on the table below)

Lesion No.	T2	D	C	All	Likely co-ordinates** (z most likely)	Curve 1=Slow rise 2=Flat 3=Early peak	ADC	Zone	Max diameter	Volume	Distance from posterior capsule	Estimated Gleason Grade	Estimated Cancer Significance
	MRI Score [†] (1-5)					1-3	Value	PZ/TZ/both	mm	cc	mm	e.g. 3+4	Not sign/Def 1/Def 2
1													
2													
3													
4													
5													
6													

** x,y grid coordinate + apex (a) or base (b) e.g. b2.5a, C2.5a, g1.5b (lower case underlined for 'c').

4. STAGING

	Vesicles involved?	Extra-capsular?	Sphincter (T4)?	Rectum (T4)?	Nodes?
MRI Score [†] (1-5)					
If score >2, Left or Right?					

If score for nodes > 2, max short axis nodal diameter? (mm)

† MRI Score
1=Highly likely benign
2=Likely benign
3=Equivocal
4=Likely malignant
5=Highly likely malignant

Signature:

Author Name:

Report Date:

The radiologist used the Likert scale for mp-MRI reporting that has been agreed in a number of consensus papers (Dickinson et al., 2013, Barentsz et al., 2013, Barentsz et al., 2012a). The Likert scale assesses radiologists' confidence levels in the presence of prostate cancer on the MRI with:-

- Score 1 = Clinically significant disease is highly unlikely to be present,
- Score 2 = Clinically significant cancer is unlikely to be present,
- Score 3 = Clinically significant cancer is equivocal,
- Score 4 = Clinically significant cancer is likely to be present and
- Score 5 = Clinically significant cancer is highly likely to be present

This score was used to sequentially score 12 sectors of the prostate (left and right anterior and posterior zones at apex, mid and base). Mp-MRI's were reported sequentially starting with the T2 alone; then the DWI images, followed by DCE images and finally an overall impression given on the likelihood of disease and clinically significant disease. The incremental read of the mp-MRI will enable incremental quantification of each sequence and the assessment of the need for each sequence in the mp-MRI.

Each lesion identified was scored and measured and depicted diagrammatically. The radiologist also gave a subjective judgement as to the Gleason grade for each lesion, and provided likely co-ordinates for hitting the most significant lesion at TPM.

4.3.2 Prostate HistoScanning

Prostate HistoScanning was performed using the BK ultrasound probes 8818 and 8848, attached to the specialist prostate HistoScanning equipment. Men underwent two sessions of HistoScanning to allow for assessment of reproducibility.

Reporting of PHS was carried out using the commercially available software version 2.3, which has a semi-automated tool for reporting.

The clinician reporting the PHS scans was blinded to the results of the other imaging but once again was aware of the patient's clinical parameters, including previous TRUS results and PSA. Reporting of PHS is a semi-automated process. The software requires that the analyst defines the apex and base points in the sagittal plane of the prostate and the most lateral left and right points on a mid-gland transverse slice of the image: this enables automated segmentation of the prostate into the 12 zones.

The prostate HistoScanning analysis algorithms are applied to the selected prostate volume, and suspicious areas that are felt to contain prostate cancer are depicted by a red overlay on the grey scale ultrasound image. The PHS automated software automatically

assigns the three largest lesions with the prostate area. The clinician reporting the scan will not be able to refine the signal deemed positive by the software so as to reduce reporter variability. The clinician reporting the scan assigned likely TPM biopsy co-ordinates to the three largest PHS lesions to enable targeted biopsy.

Disease significance on PHS was defined by size criteria only, not using a scale, as there is as yet no way to assess grade on PHS.

Figure 41. HistoScanning Reporting form



PICTURE
HistoScanning Reporting Form
Version 1.0 December 2011

University College London Hospitals 
NHS Foundation Trust

Page 1 of 1

Patient's Initials:

Scan Date:

Date of Birth:

Trial Number:

1. SIZE OF PROSTATE

Transverse: • cm Anterior-Posterior: • cm Cranio-Caudal: • cm Volume: cm³

2. REPORTERS RATING OF SCAN QUALITY

1 Perfect Scan 2 High quality 3 Average Scan 4 Poor quality 5 Very Poor Quality

3a. INDIVIDUAL LESIONS (please mark individual lesions on diagram 3a)

	Volume (cc)	Location
Total		
Lesion 1		
Lesion 2		
Lesion 3		

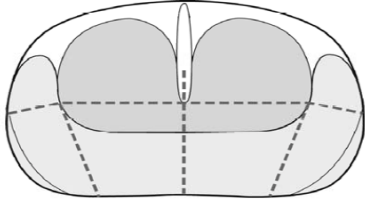
4. STAGING

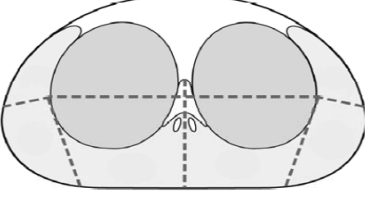
	Vesicles involved?	Extra-capsular?	Sphincter (T4)?	Rectum (T4)?
PHS Score [†] (1-5)				
If score >2, Left or Right?				

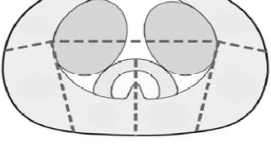
[†] PHS Score

1=Highly likely benign
2=Likely benign
3=Equivocal
4=Likely malignant
5=Highly likely malignant

3a. INDIVIDUAL LESIONS (Please draw and number measurable lesions on diagram below)

Base 

Mid 

Apex 

Calcification: Absent Minimal Moderate Significant Unspecified

Signature:

Author Name:

Report Date:

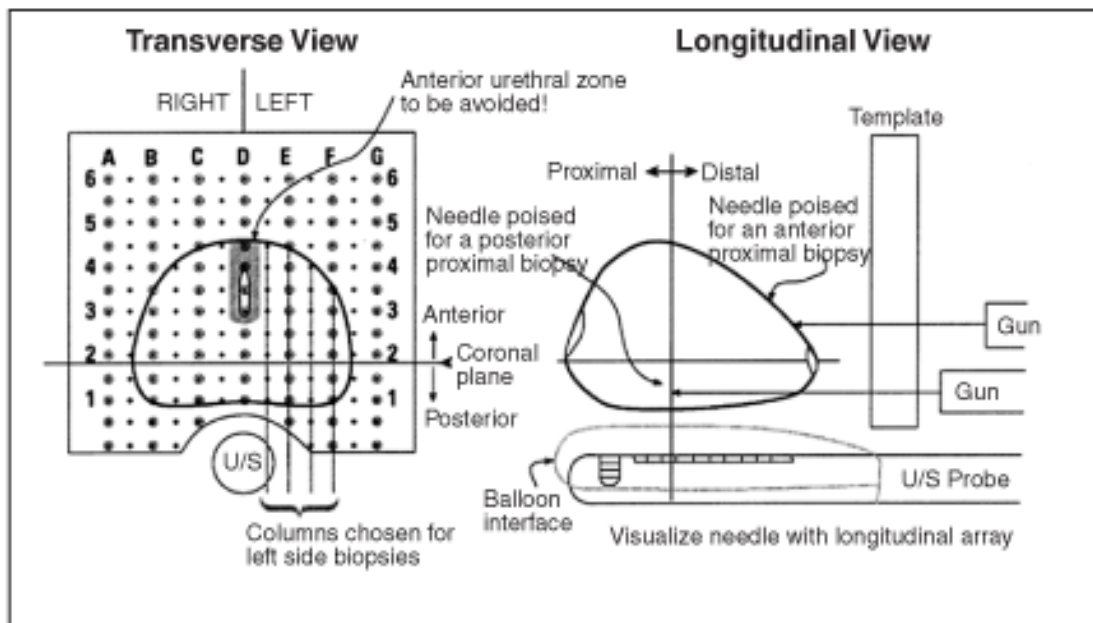
Please attach Computer generated report

4.4 The Reference Test- Transperineal Template Mapping Biopsy

Men underwent transperineal template mapping biopsies of as the reference standard.

TPM is performed under general or regional anaesthetic. Men were placed in the lithotomy position and the perineum cleaned with chlorhexidine 2% prep solution. They were also all given Gentamycin antibiotic prophylaxis.

Figure 42. Transperineal template biopsy set up²⁰

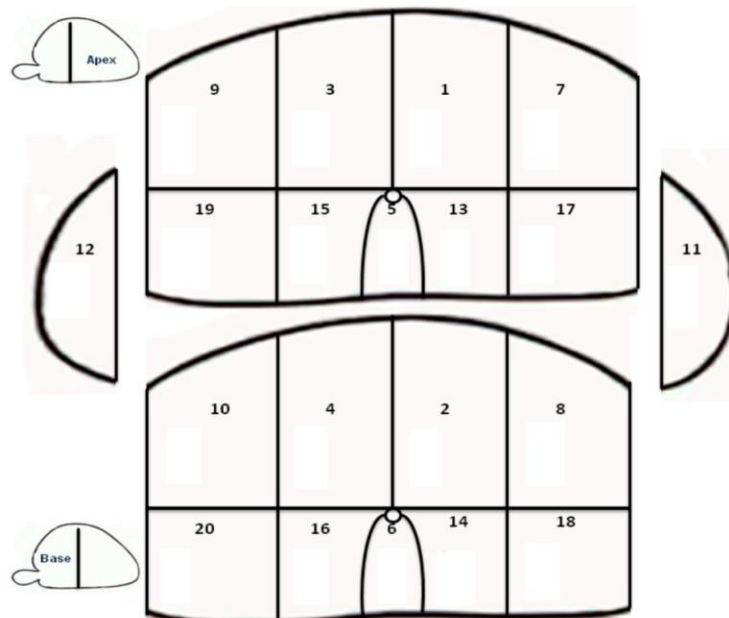


The TPM was then performed to a standard operating procedure; this involved taking samples of the prostate using a bard 16ch biopsy needle via the perineum at 5mm spacing with a brachytherapy grid placed on the perineum as a guide.

Biopsies were taken within 20 modified Barzell zones that covered the entirety of the prostate; they were first taken from the apical segments and then the basal sectors.

Figure 43 demonstrates the modified Barzell Zones in which TPM is performed at UCLH.

²⁰ Kindly reprinted from Barzell WE, Whitmore WF III: How to perform transperineal saturation prostate biopsy. Urology Times. Available www.urologytimes.com/urologytimes/article/articleDetail.jsp?id=56612.

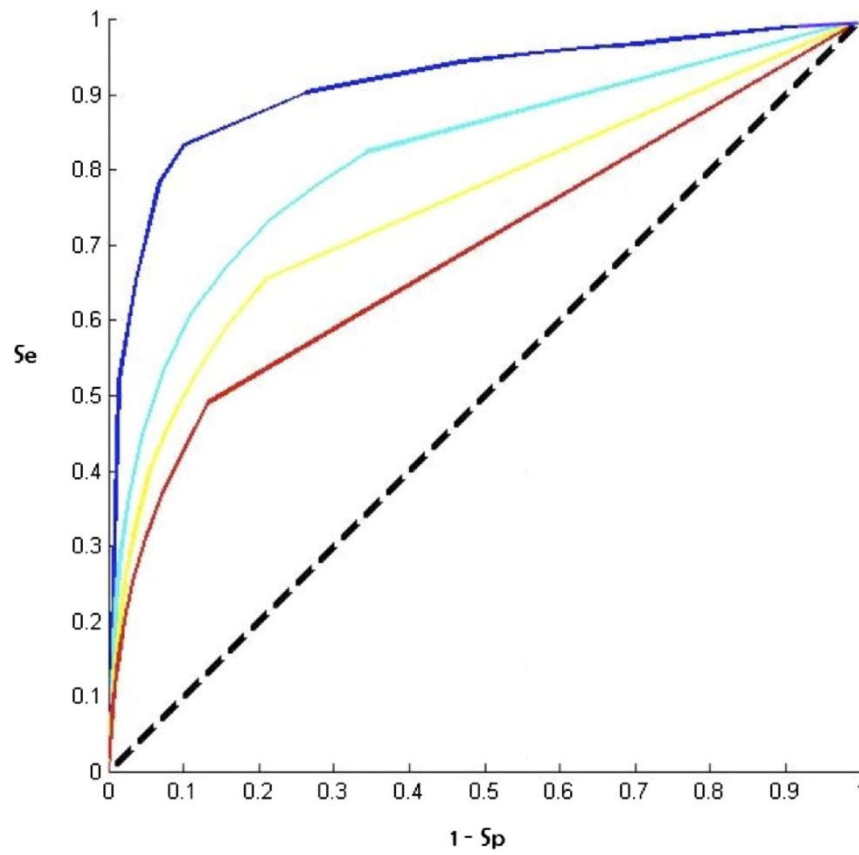
Figure 43. Modified Barzell Zones**Modified Barzell Zones**

1 Left Parasagittal Anterior Apex	11 Left Lateral
2 Left Parasagittal Anterior Base	12 Right Lateral
3 Right Parasagittal Anterior Apex	13 Left Parasagittal Posterior Apex
4 Right Parasagittal Anterior Base	14 Left Parasagittal Posterior Base
5 Midline Apex	15 Right Parasagittal Posterior Apex
6 Midline Base	16 Right Parasagittal Posterior Base
7 Left Medial Anterior Apex	17 Left Medial Posterior Apex
8 Left Medial Anterior Base	18 Left Medial Posterior Base
9 Right Medial Anterior Apex	19 Right Medial Posterior Apex
10 Right Medial Anterior Base	20 Right Medial Posterior Base

4.4.1 Template Mapping Biopsy Sampling Density

Template mapping biopsies were chosen as the reference test for PICTURE for their high detection rate for clinically significant disease. A study by Le Cornet et al, that undertook a computer simulation of biopsy strategies in the reconstructed prostates of men that had undergone cystoprostatectomy found that TPM when performed at 5mm spacing had a ROC AUC of 0.91 for the detection of clinically significant disease as defined by Definition one (Gleason score 7 or greater, and/or lesion volume 0.5 ml) (Lecornet et al., 2012).

Figure 44 shows the ROC curves for a variety of biopsy strategies. The study aimed to test TPM (dark blue curve, AUC 0.91) against TRUS (all other curves). The ROC shown below also demonstrates the ROC curves for optimised TRUS with anterior directed cores (light blue, AUC 0.82), standard TRUS biopsy with a random localisation error of 10mm (yellow curve, AUC 0.75), and standard TRUS with a 15mm random localisation error (red AUC 0.69).

Figure 44. ROC curves for TPM and TRUS biopsy strategies²¹

During the evolution of the PICTURE study the burden of 5mm sampling on patients was felt to be too high. Initially, a number of men suffer from adverse side effects such as gross haematuria and urine retention. The high burden of taking a full 5mm TPM; in terms of theatre time, histological processing time and cost, also factored into the decision making.

Due to this, computer simulation was utilised to explore the accuracy of various transperineal sampling strategies for the detection of prostate cancer. The aim was to determine a strategy that might give accurate cancer detection rates but minimise sampling burden, minimise morbidity for patients and allow a reduction in biopsy cost and pathology processing time.

Different patient populations carry different disease burdens, and often the way in which a test is interpreted is influenced by the population in which it was examined. It is well known that radical prostatectomy series incorporate a large degree of work up bias as all men have tested positive for cancer on a previous biopsy strategy and have chosen to

²¹ Reprinted from LECORNET, E., AHMED, H. U., HU, Y., MOORE, C. M., NEVOUX, P., BARRATT, D., HAWKES, D., VILLERS, A. & EMBERTON, M. 2012. The accuracy of different biopsy strategies for the detection of clinically important prostate cancer: a computer simulation. *J Urol*, 188, 974-80. With permission from Elsevier

undergo radical surgery. Therefore, they will more likely have larger disease burdens than men in the population as a whole.

The group most closely matching the background population are those who have their prostates removed in a cystoprostatectomy for bladder cancer. As they have not previously been diagnosed with prostate cancer this group can act as a good representation for the male population.

The aim of this computer simulation study was to assess how the use of different transperineal biopsy strategies altered disease detection characteristics. Alongside investigating how different sampling strategies altered disease detection, an aim was to examine how the use of a different patient population altered the performance characteristics of a test.

It was therefore decided to simulate the use of several different biopsy strategies in order to assess their performance characteristics for the detection of significant cancer. For this simulation the definition of significant cancer was defined as Definition 1 cancer (volume \geq 0.5cc and/or Gleason \geq 7). Modelling was also performed for Definition 2 disease (Volume \geq 0.2cc, or Gleason \geq 7).

The cystoprostatectomy models came from a series of 346 men identified from 1983 to 1997 at the Department of Urology, Stanford University School of Medicine who underwent radical cystoprostatectomy for invasive bladder cancer. They were deemed to be free of clinically apparent prostate cancer before surgery. Prostate cancer was found in 104 of 338 patients (31%).

Due to the large volume prostate cancer occupying most of the gland 8 patients were excluded from analysis, leaving 96 evaluable specimens. Table 20 shows the demographic data for this group. The same series were used in a previous biopsy simulation by our group assessing varying biopsy strategies.(Lecornet et al., 2012)

Table 20. Demographic data for Cystoprostatectomy series for 96 men

	No. Samples/Total No. (%)
Gleason score:	
No grade 4	88 (84)
Grade 4	8 (8)
Grade 4 or 5, or undifferentiated	4 (4)
T stage:	
T2a	50 (48)
T2b	3 (3)
T2c	45 (43)
T3a	2 (2)
Site (215):	
Anterior	79 (37)
Posterior	136 (63)
Vol (ml):	
Less than 0.2	170 (79)
0.2 or Greater	45 (21)
0.5 or Greater	21 (10)
Clinical significance definition (215):	
1	25 (12)
2	47 (22)
Definition 1 cohort (ng/ml PSA):	23/96 (24)
Less than 4 or unknown	15/76 (20)
4 or Greater	8/20 (40)
Definition 2 cohort:	36/96 (38)
Less than 4 or unknown	27/76 (36)
4 or Greater	9/20 (45)

The radical prostatectomy series, constituted 107 consecutive radical prostatectomies performed between 1999-2001. All underwent 3mm step sectioning according to the Stanford protocol. This cohort has also been used in a study investigating prostate cancer risk inflation as a consequence of targeting. (Robertson et al., 2014) Table 21 outlines demographics for this group.

Table 21. Demographic data for Radical Prostatectomy series

Characteristic	Value Median (mean, SD, range)
Age, years	62 (61.1, 6.4, 44–74)
PSA concentration, ng/ml	8.5 (9.7, 5.9, 0.8–36.2)
Gleason score, % (n)	
<=6	57 (61)
7	35 (37)
>=8	8 (9)
Pathologic stage, % (n)	
pT2a	7.5 (8)
pT2b	2 (2)
pT2c	49.5 (53)
pT3a	33.6 (36)
pT3b	5.6 (6)
pT4	2 (2)
Risk groups, NCCN classification, % (n)	
Low	5.6 (6)
Intermediate	47.7 (51)
High	46.7 (50)
Prostate volume, ml, median (range)	50.2 (26.8–127.7)
No. of lesions	
Anterior	415
Posterior	250
Full cohort	
>= 0.2 ml	149
>= 0.5 ml	97
Low to intermediate risk	
>= 0.2 ml	68
>= 0.5 ml	43
Lesions per prostate, median (range)	5 (1–21)
Lesion volumes, ml, median (mean, SD, range)	
All (n = 665)	0.031 (0.374, 1.110, 0.001–13.242)
Index (n = 107)	1.215 (1.895, 2.176, 0.015–13.242)
Non index (n = 558)	0.019 (0.082, 0.343, 0.001–1.842)
NCCN = National Comprehensive Cancer Network; PSA = prostate-specific antigen; SD = standard deviation.	

Both of the cohorts' specimens had been processed according to the Stanford Protocol: - inked, fixed and sectioned as 3mm whole mount specimens, with contours of their cancer foci outlined. Each then underwent computerised reconstruction, with slides being digitally scanned and reconstructed. 3-D geometric modelling software designed at UCL was used to ensure accurate alignment and registration of each slice.

For the computer simulations a standard 15mm core length was used for all biopsies. 500 simulations of each strategy were performed, on each prostate.

More in depth explanations of how the simulations were performed can be found in the following papers Hu et al, a biopsy simulation study to assess the accuracy of several transrectal ultrasonography (TRUS)-biopsy strategies compared with template prostate mapping biopsies in patients who have undergone radical prostatectomy and Ahmed et al, Characterizing clinically significant prostate cancer using template prostate mapping biopsy (Hu et al., 2012a, Ahmed et al., 2011).

In order to assess and compare the diagnosis methods without considering the choice of the cut-off value, Receiver operating characteristic (ROC) curves were used with the sensitivity/specificity/PPV/NPV versus a range of sensible cut-off values plotted. ROC curves, are graphs that illustrates the performance of test. They are created by plotting the true positive rate (TPR) against the false positive rate (FPR) at various sensitivity and specificity settings. The sensitivity and specificity graphs at varying Maximum cancer core length (MCCL) in millimetres (mm) were performed to allow the decision of what the cut-off value for MCCL should be, MCCL was measured in mm. The cut-off needed to be determined to have a desired balance between sensitivity and specificity, therefore being a complete 'diagnostic test'.

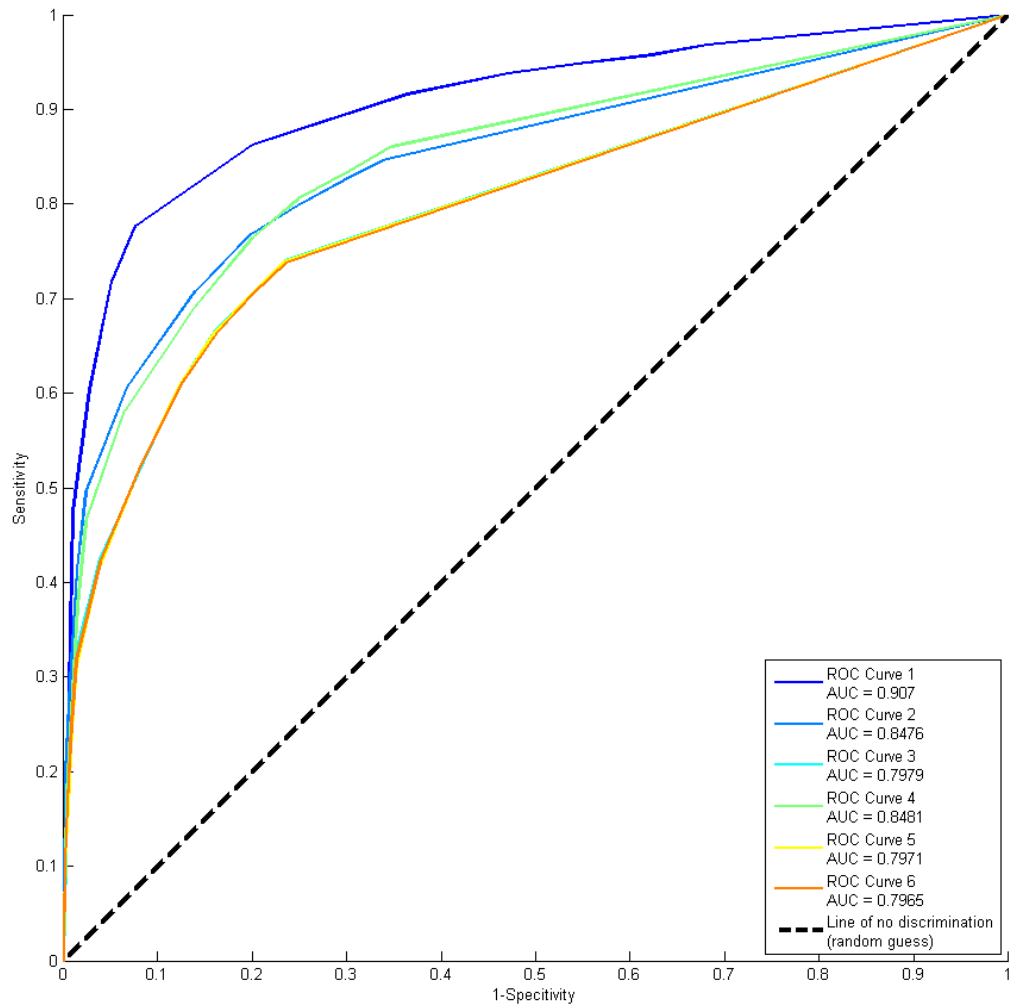
4.4.2 Cystoprostatectomy Series Simulation

The following simulations were carried out for both definitions of disease significance:

1. 5mm template (normal) – curve 1 peacock blue
2. 10mm template – curve 2 blue
3. 'random 1 biopsy per barzell sector' – curve 3 turquoise blue
4. 'random 2 biopsies per Barzell sector' – curve 4 green
5. 'random 1 per sector in glands $\leq 30\text{cc}$ and random 2 biopsies per sector in gland $>30\text{cc}$ ' – curve 5 yellow
6. 'random 1 per sector in gland $\leq 40\text{cc}$ and random 2 biopsies per sector in glands $>40\text{cc}$ '- curve 6 orange

4.4.2.1 Definition one disease:

Figure 45. ROC curve for Biopsy strategies for TPM in Cystoprostatectomy series (definition one disease)



Key:

1. 5mm template (normal) – curve 1 peacock blue
2. 10mm template – curve 2 blue
3. 'random 1 biopsy per barzell sector' – curve 3 turquoise blue
4. 'random 2 biopsies per Barzell sector' – curve 4 green
5. 'random 1 per sector in glands \leq 30cc and random 2 biopsies per sector in gland $>$ 30cc' – curve 5 yellow
6. 'random 1 per sector in gland \leq 40cc and random 2 biopsies per sector in glands $>$ 40cc' - curve 6 orange

Figure 46. Sensitivity curves for Biopsy strategies for TPM in Cystoprostatectomy series (definition one disease)

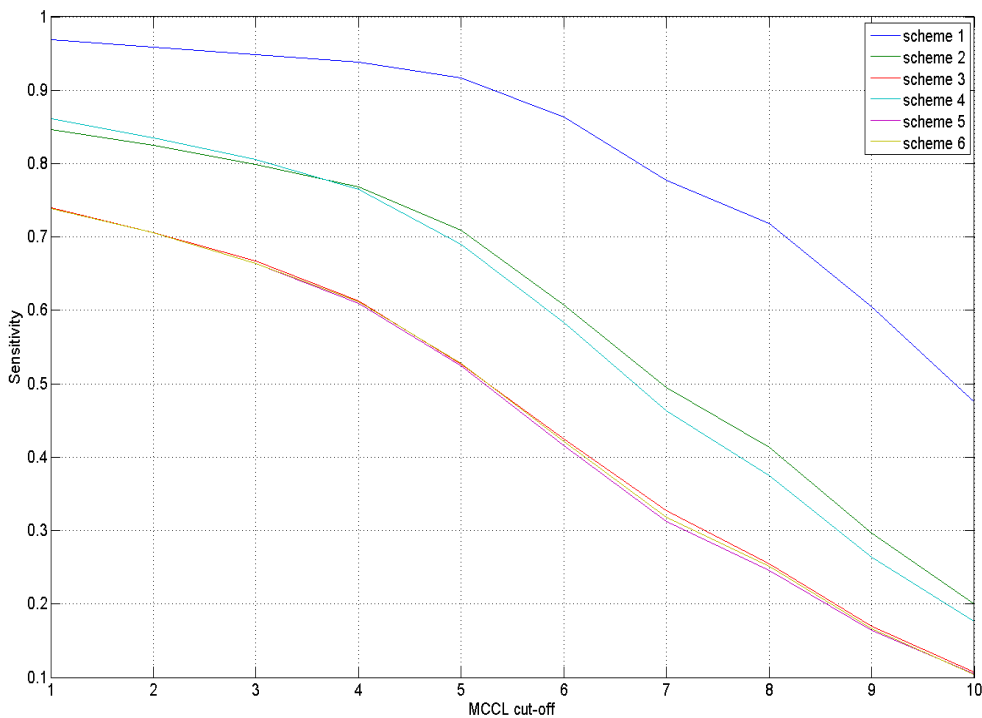
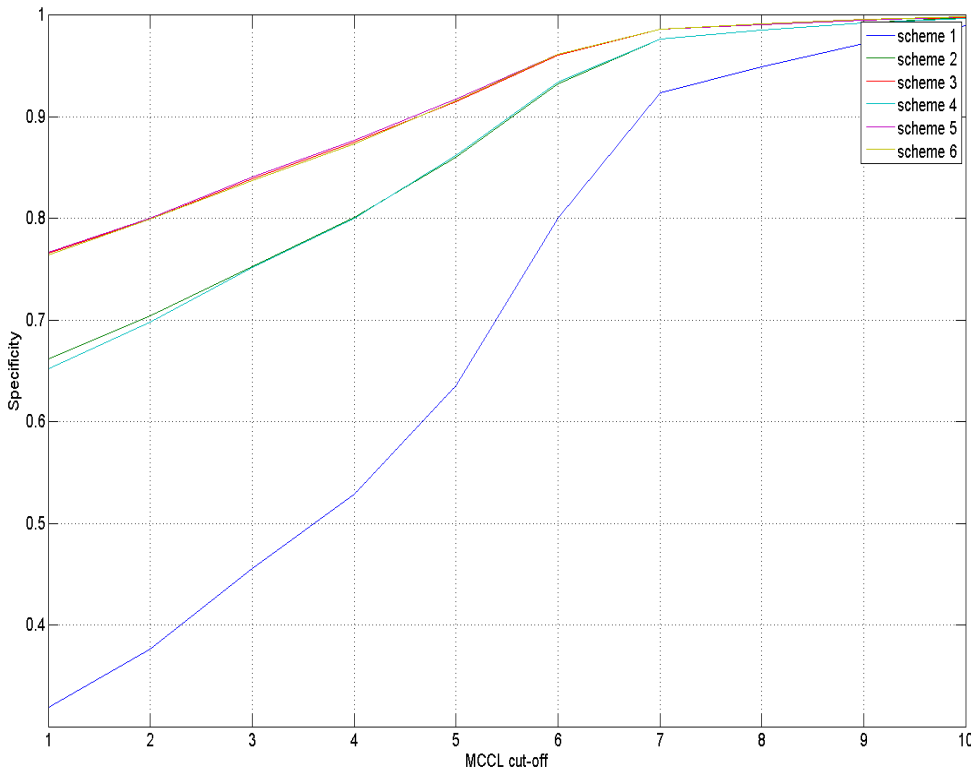


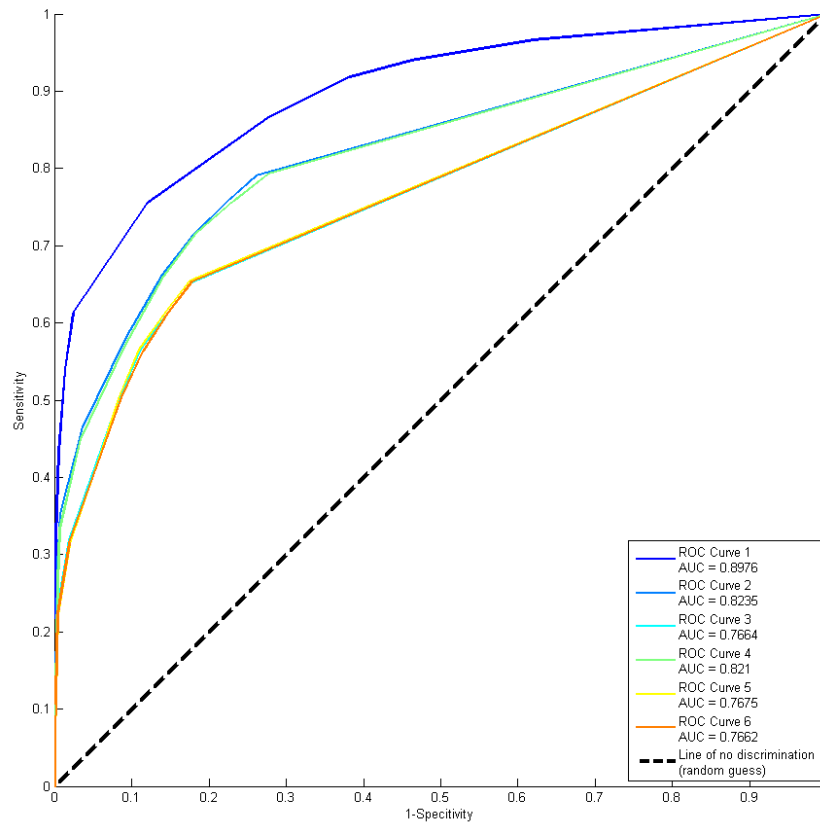
Figure 47. Specificity Curve for Biopsy strategies for TPM in Cystoprostatectomy series (definition one disease)



From this modelling in the cystoprostatectomy series it would appear that adopting a 2 core per Barzell zone (or a 10mm) sampling strategy would not significantly negatively impact on detection rates. Causing only a minimal reduction in detection rates from 0.907 to 0.8481 or 0.8476 respectively, which is at worst a 0.0594 reduction in the ROC AUC.

4.4.2.2 Definition 2 disease:

Figure 48. ROC curve for Biopsy strategies for TPM in Cystoprostatectomy series (definition two disease)



Key:

1. 5mm template (normal) – curve 1 peacock blue
2. 10mm template – curve 2 blue
3. ‘random 1 biopsy per barzell sector’ – curve 3 turquoise blue
4. ‘random 2 biopsies per Barzell sector’ – curve 4 green
5. ‘random 1 per sector in glands $\leq 30\text{cc}$ and random 2 biopsies per sector in gland $> 30\text{cc}$ ’ – curve 5 yellow
6. ‘random 1 per sector in gland $\leq 40\text{cc}$ and random 2 biopsies per sector in glands $> 40\text{cc}$ ’ - curve 6 orange

Figure 49. Sensitivity curves for Biopsy strategies for TPM in Cystoprostatectomy series (definition two disease)

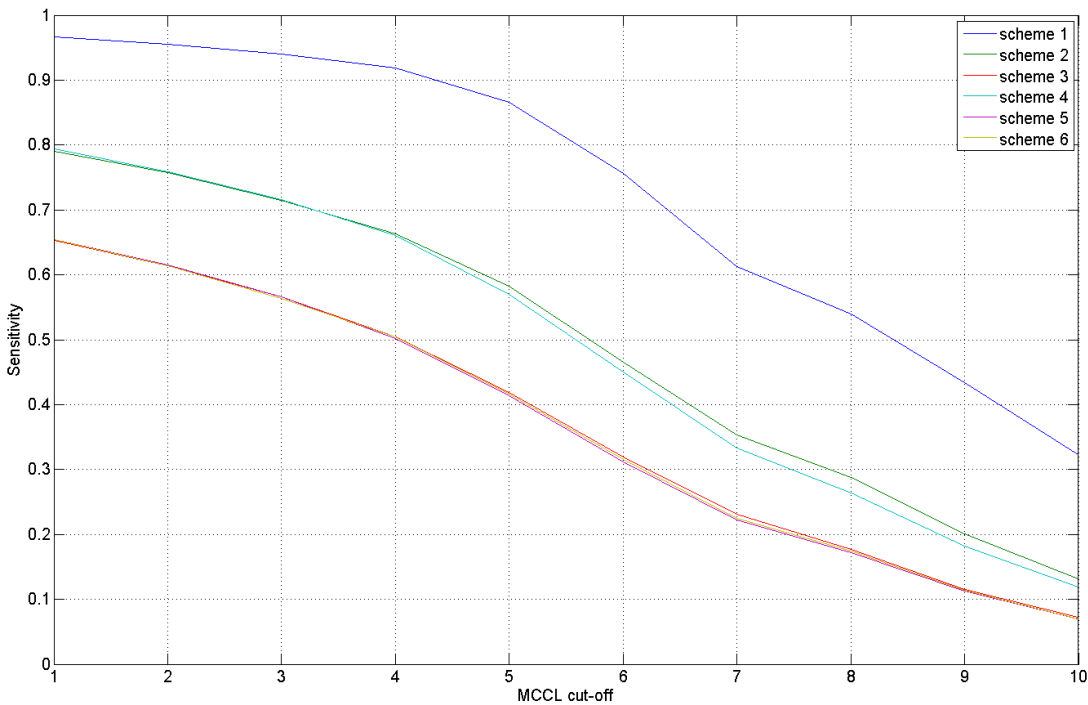
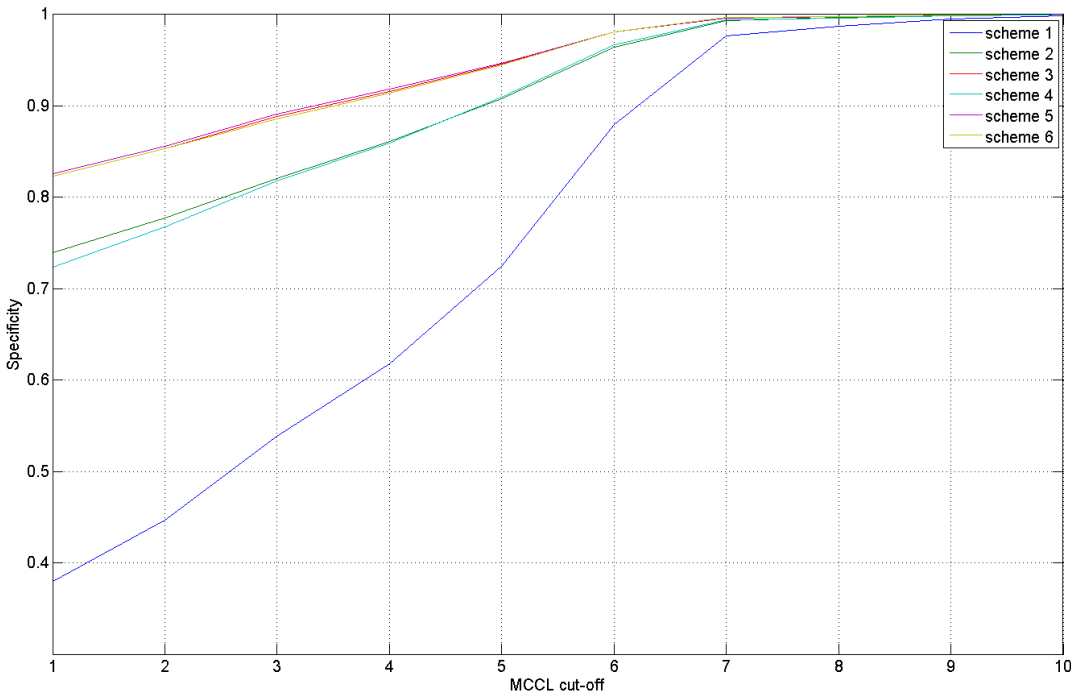


Figure 50. Specificity Curve for Biopsy strategies for TPM in Cystoprostatectomy series (definition two disease)

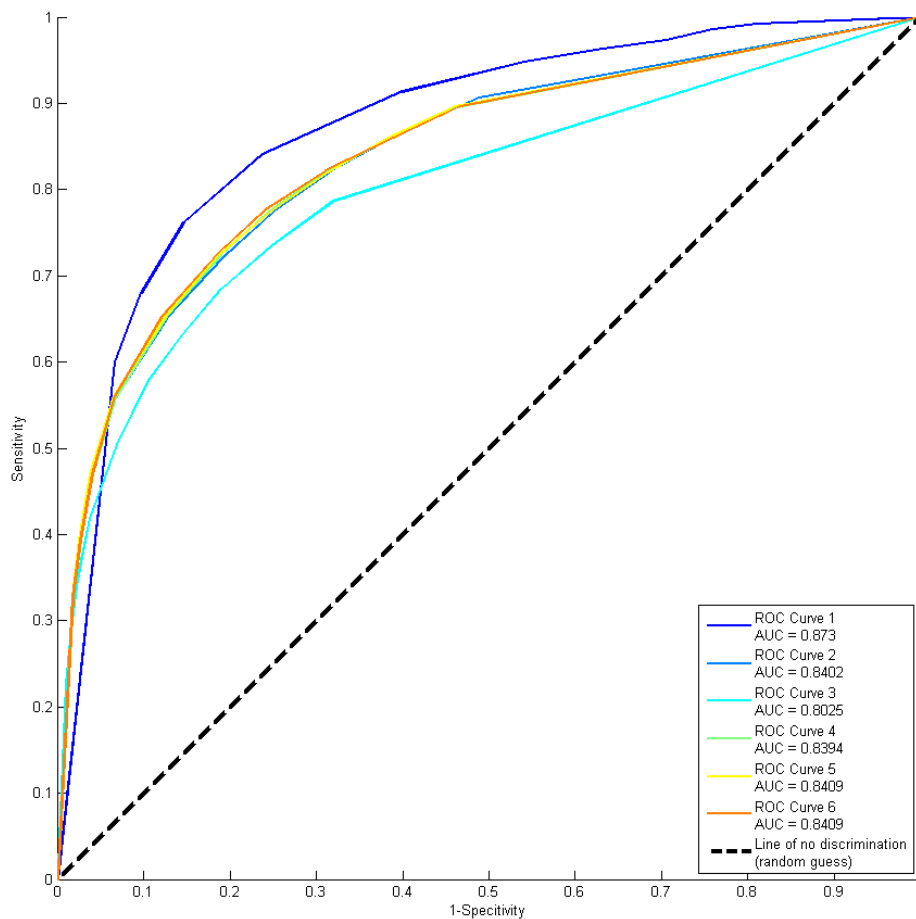


Again the above graphs (Figure 45, Figure 46, Figure 47) demonstrate that a reduction in sampling density to 10mm spacing (or two cores per Barzell zone will only decrease the area under the ROC curve for Definition 2 disease from 5mm Sampling AUC = 0.8976 to 10mm Sampling AUC = 0.8235 or Random 2 cores per sector AUC = 0.821, again a minimal reduction.

4.4.3 Radical Prostatectomy series:

4.4.3.1 Definition one disease

Figure 51. ROC curve for Biopsy strategies for TPM in Radical Prostatectomy series (definition one disease)



Key:

1. 5mm template (normal) – curve 1 peacock blue
2. 10mm template – curve 2 blue
3. ‘random 1 biopsy per barzell sector’ – curve 3 turquoise blue
4. ‘random 2 biopsies per Barzell sector’ – curve 4 green
5. ‘random 1 per sector in glands \leq 30cc and random 2 biopsies per sector in gland $>$ 30cc’ – curve 5 yellow
6. ‘random 1 per sector in gland \leq 40cc and random 2 biopsies per sector in glands $>$ 40cc’- curve 6 orange

Figure 52. Sensitivity curves for biopsy strategies for TPM in Radical prostatectomy series (definition one disease)

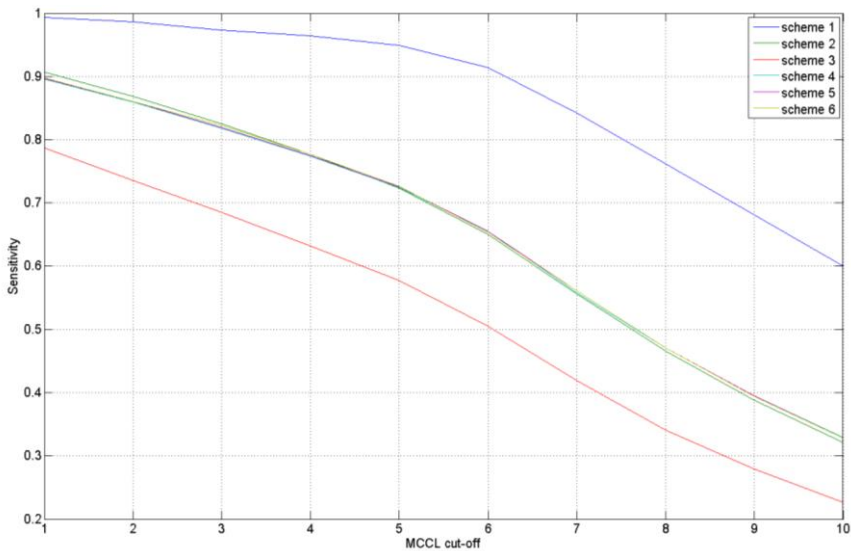
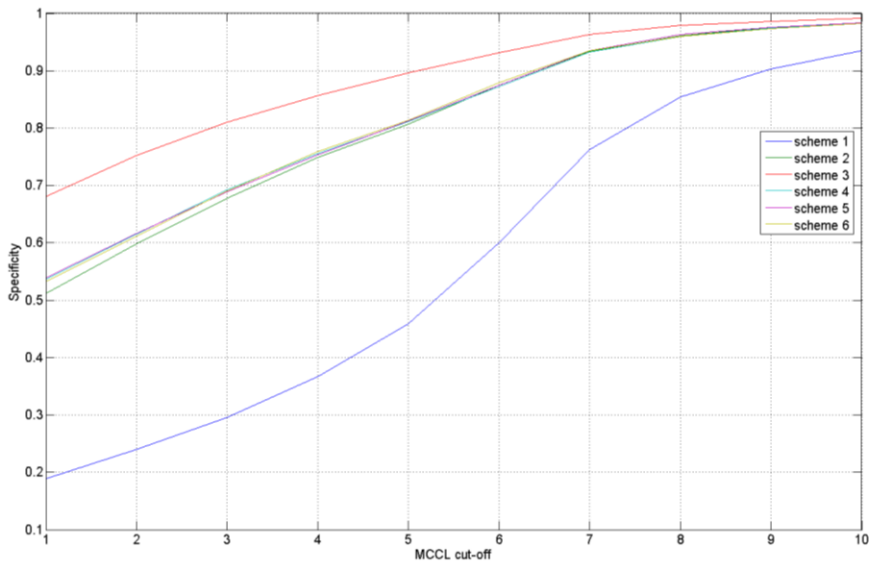


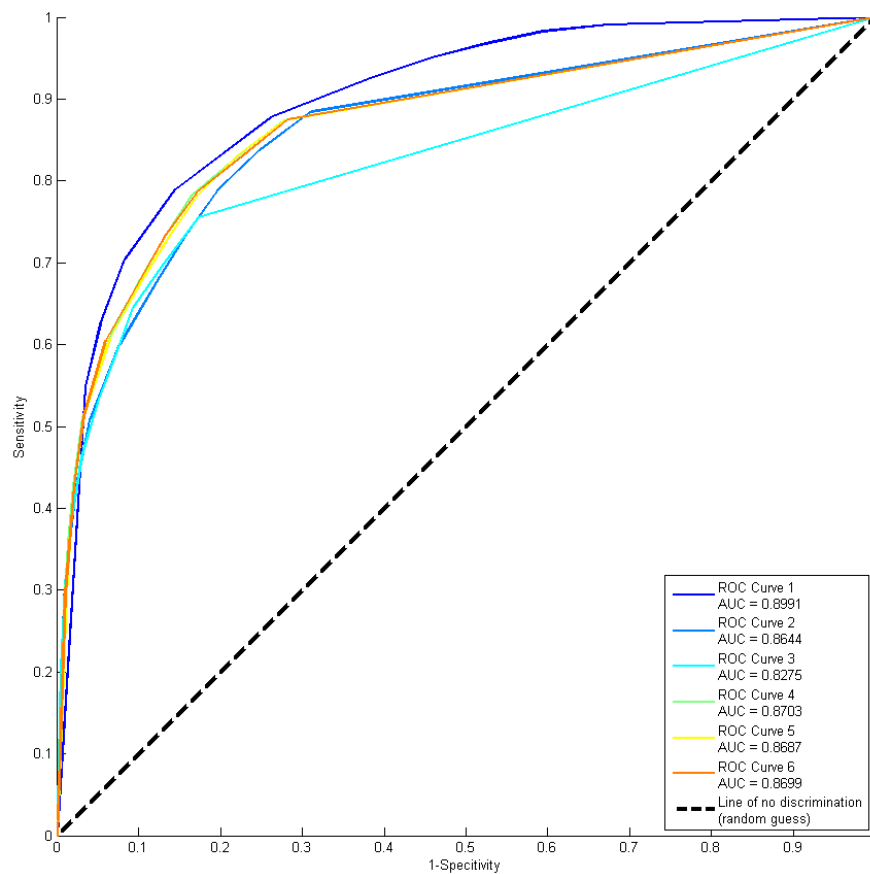
Figure 53. Specificity curves for biopsy strategies for TPM in Radical prostatectomy series (definition one disease)



From this modelling in the radical prostatectomy series it would appear that adopting a 2 core per Barzell zone (or a 10mm) sampling strategy would not significantly negatively impact on detection rates. Causing a minimal reduction in detection rates from 0.873 to 0.839 or 0.840 respectively, on the ROC AUC.

4.4.3.2 Definition two disease

Figure 54. ROC curve for Biopsy strategies for TPM in Radical Prostatectomy series (definition two disease)



Key:

1. 5mm template (normal) – curve 1 peacock blue
2. 10mm template – curve 2 blue
3. 'random 1 biopsy per barzell sector' – curve 3 turquoise blue
4. 'random 2 biopsies per Barzell sector' – curve 4 green
5. 'random 1 per sector in glands \leq 30cc and random 2 biopsies per sector in gland $>$ 30cc' – curve 5 yellow
6. 'random 1 per sector in gland \leq 40cc and random 2 biopsies per sector in glands $>$ 40cc'- curve 6 orange

Figure 55. Sensitivity curves for biopsy strategies for TPM in Radical prostatectomy series (definition two disease)

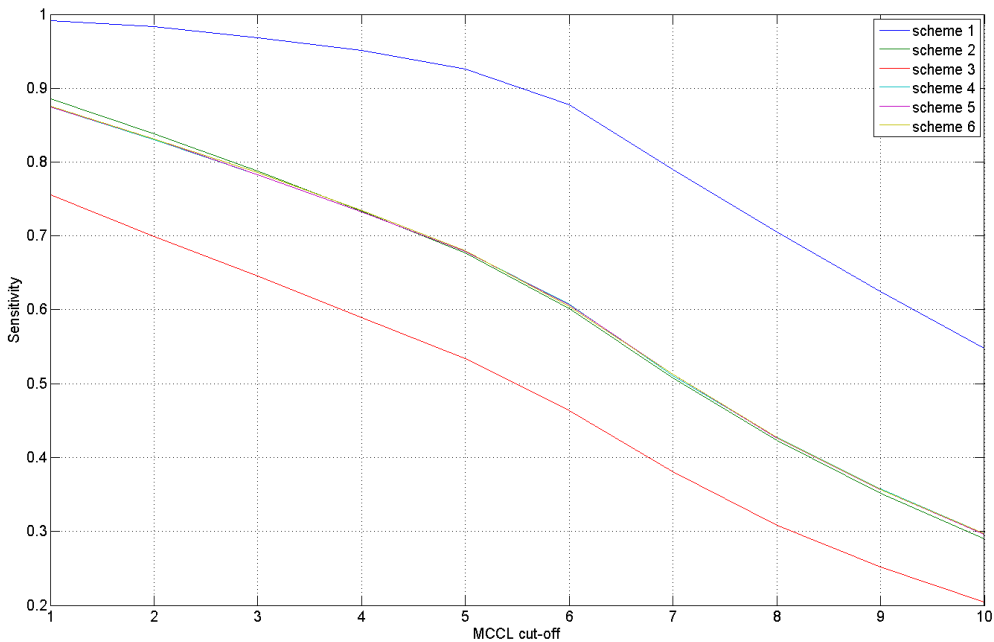
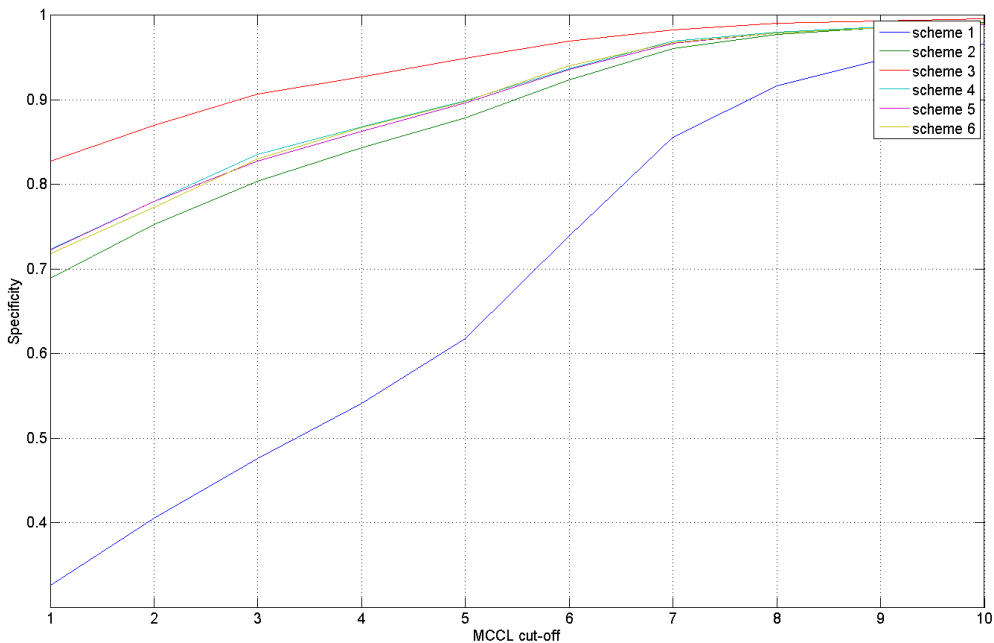


Figure 56. Specificity curves for biopsy strategies for TPM in Radical prostatectomy series (definition two disease)



Once again, altering the strategy from full 5mm sampling to 10mm sampling did not show a significant reduction in the ROC AUC.

Some further work was performed looking at the 'hit rate' for significant lesions by each strategy. Table 22 demonstrates the detection rate of significant lesions when the different strategies are applied. 5mm sampling has over 99% detection for significant lesions in both cohort, which reduces slightly to an approximately 89% detection rate when sampling density is reduced to 10mm or 2 cores per Barzell zone.

Table 22. *Detection rates of significant disease for different biopsy strategies*

	Cystoprostatectomy data		Radical	Prostatectomy
	Number of cases having significant lesions	Detection rate (excluding insignificant cases)	data	data
Standard template	19	0.9988	77	0.9968
10mm template	19	0.8996	77	0.8862
Barzell-1	19	0.7596	77	0.7466
Barzell-2	19	0.8945	77	0.8730

In summary, the investigation into altering the biopsy density of TPM showed that a reduced sampling density from 5mm sampling to 10mm sampling did not significantly alter the ROC AUC in either cohort. There was however a reduction from near perfect detection of significant lesions (detection rate =0.99), with 5mm sampling to a roughly 90% detection rate with 10mm sampling. This was deemed to be an acceptable reduction in detection for the predicted benefits in terms of morbidity and cost reduction provided by the change, and thus it was instituted into the study after the initial 130 men.

4.5 Targeted Biopsies

Prior to the standard TPM, in men with lesions detected on imaging targeted biopsies was taken. Three sets of targeted biopsies were obtained. MRI-USS registration biopsies, cognitively registered MRI targeted biopsies and cognitively registered PHS guided biopsies.

For PHS targets the biggest lesion seen on imaging was targeted, given the co-ordinates stated on the PHS report and the clinician's review of the PHS imaging the area. The lesion was then targeted using cognitive registration; in other words the clinician targets the lesion using spatial awareness of the location of the lesion within the gland without any image fusion technology.

The primary MRI lesion that was identified with an MRI score of ≥ 3 was targeted using two techniques. The method of cognitive registration using the information given by the reporting radiologist was used as the primary method of registration. The second method of targeting was performed using MRI/US registration. MRI/US registration is a computerised process to assist with targeting lesions seen on mp-MRI - the system in PICTURE is a deformable system that allows for distortion of the gland by the biopsy probe at the time of biopsy (Hu et al., 2009, Hu et al., 2012a, Hu et al., 2011) (Hu et al., 2009).

Registration requires that the prostate outline and the lesion on MRI are contoured on specially designed software. Following the delineation of the gland and lesion a biomechanical mesh model of each man's prostate and lesion is developed. At the time of biopsy, a 3D ultrasound volume was acquired and then 5-10 points on several images from the ultrasound volume were selected to allow the MRI model and ultrasound image to be fused/registered together. The registration system then automatically computed the most likely co-ordinates to obtain a maximum cancer core length through the prostate cancer lesion.

Each type of targeting involved 2 targeted biopsies unless they overlapped in which case this was made clear. Following the targeted biopsy sampling, men had 5mm or 10mm sampling performed within a 20 modified Barzell zone layout.

4.5.1 Rationale for Targeted biopsy

Within the PICTURE Study, men underwent targeted sampling to areas on imaging that were deemed suspicious for disease, as well as the reference standard biopsy of TPM. The

rationale behind targeted sampling is that if imaging can accurately predict the presence of disease, it must be able to answer the question as to whether we can accurately sample that disease to correctly risk stratify patients.

Current literature suggests that an MRI guided image biopsy technique is able to accurately sample prostate cancer lesions and that these are highly representative of the true tumour grade found at radical prostatectomy in around 88% of cases (Hambrock et al., 2012).

Additionally, if men can be correctly attributed their risk status by a more limited biopsy protocol with fewer cores, this may enable the procedure to be performed similarly to TRUS biopsy under local anaesthetic. A reduction in the number of cores taken compared to current best diagnosis of template mapping biopsy, may also allow a reduction in the time the procedure takes, a reduced morbidity to the procedure. It is likely that by taking less cores men will suffer less pain and lower risk of infections. Biopsy processing time and cost at the histopathology laboratories would also be reduced by adopting a targeted approach.

At PICTURE Study inception, no PHS biopsy advanced targeting strategy existed, so PHS lesions were targeted using 'cognitive registration' biopsies i.e. the performing clinician used their awareness of prostate anatomy and spatial awareness to target the biopsy needle towards the area of greatest PHS signal.

Of note, since the design of the PICTURE study, a biopsy guidance system for PHS 'True Targeting' was developed and released: evidence from clinical trials of this targeting technology is awaited.

For MRI imaging there exist a number of methods for targeting lesions detected on the MRI image. Alongside the described 'cognitive MRI targeted biopsy' technique there exists a number of different platforms that allow ultrasound/MRI registration or image fusion, and also MRI in bore targeted biopsy techniques have been explored.

Image fusion is the process of combining multiple images from various sources into a single representative image. It requires image registration, which is a process of mapping equivalent points from the different imaging studies so that they correspond. Standard ultrasound (US) is not as good as MRI in differentiating between normal prostate and tumour; however ultrasound is the imaging modality used to guide most biopsy strategies.

Image fusion/registration using computer software is being developed with the aim of super-imposing an MRI image of a tumour taken prior to biopsy onto a real time US image so that the tumour focus can be more accurately targeted during the biopsy procedure.

A challenge that presents itself when performing image registration for prostate biopsies is 'deformation' - the change in shape that occurs to the prostate when an ultrasound probe is introduced into the rectum - and also when biopsies are taken due to swelling. (Hu et al., 2012b)

To address the issue of deformation a novel "model-to-image" registration method has been developed that allows automatic registration of the deformable prostate model surface to the TRUS images (Hu et al., 2012b, Hu et al., 2009).

Currently, this registration method does not account for the deformation from gland swelling, only probe distortion. However work is in progress to assess and compensate for the swelling caused by prostate biopsy and incorporate this into the registration (Hu et al., 2011).

MRI in-bore targeted biopsies have been investigated by other groups and have found detection rates of approximately 40-50% (Hoeks et al., 2012, Overduin et al., 2013). However, there are significant cost and resource implications to these biopsies: they require a large amount of time within the MRI scanner, and a number of different MRI safe materials.

The biopsy guidance scheme that is most likely to become widely adopted if found to be viable is one in which pre-biopsy imaging is performed and then fused with the ultrasound image at the time of biopsy.

A deformable registration system will likely be the most accurate as it will be able to allow for changes in shape of the prostate when a probe is introduced at the time of biopsy. Within the PICTURE Study a novel prototype device of deformable MRI/US registration system designed by colleagues at the Centre for Medical Imaging and Computing, UCL (Smart Target) was used to target biopsies at the time of TPM.

One group looked also at the use of MRI fusion systems vs. cognitive biopsies, using a similar methodology to that in the PICTURE Study. They found no significant improvement of MRI targeting by the use of fusion technology over that of MRI 'cognitive targeting'.(Puech et al., 2013)

The objectives for the addition of targeted biopsy sampling in the PICTURE Study were to:- assess if PHS targeted biopsy were comparable the use of systematic biopsies stratifying patients into prostate cancer risk groups; if MRI 'cognitive' targeted biopsies were comparable the use of systematic biopsies in stratifying patients into prostate cancer risk groups and whether the use of MRI to US registration targeted biopsies alone was comparable the use of systematic biopsies and cognitive targeted biopsies in stratifying patients into prostate cancer risk groups.

4.6 PICTURE Additional Procedures

The PICTURE Study provides a unique opportunity to validate a number of other procedures against a high quality reference standard in a population of men who do not all have known disease.

As such a urine and seminal biomarker were selected for inclusion in the study.

4.6.1 Urine Engrailed 2 (EN2)

Engrailed-2 is a protein that has been found to be present in the first pass urine. Preliminary work has shown EN2 to be expressed in prostate cancer cell lines and prostate cancer cells but not by normal prostate epithelial tissue.

Initial studies have shown that an ELISA based EN2 assay can detect EN2 in urine with sensitivity 66% and specificity of 88.2%- when the cut off for a positive assay is set at 42.5ng/mL. (Morgan et al., 2011)

EN2 was also found to be easily detectable in a small sample of urine, without the need for digital rectal examination, which may enable it to be used as a useful diagnostic or screening test.

First pass urine samples were collected from men and analysed for EN2, in order to assess the ability of this assay for the detection of prostate cancer, and its ability to differentiate between clinically significant and non-clinically significant disease.

4.6.2 Seminal Fluid Analysis for Citrate and Zinc (FScan)

Another interesting metabolic relationship investigated and explored for its potential role in prostate cancer detection is the change in citrate and zinc levels in prostatic fluid. In contrast to the normal prostatic fluid which contains very high concentrations of citrate and zinc, in the presence of prostate adenocarcinoma the levels of citrate dramatically reduce, demonstrating a 70-90% reduction in level.

The reduction in citrate and zinc levels is due to metabolic transformation in malignant cells that results in their inability to accumulate zinc. In the absence of high zinc levels malconitase activity is no longer inhibited and citrate can be oxidised by the Krebs cycle (Medarova et al., 2014, Costello and Franklin, 2009).

Moreover, malignant cells are proliferating cells that require citrate for cell growth and proliferation. These processes occur early in malignant transformation of prostate epithelial cells and as such may allow disease detection at early stages.

Prostatic fluid typically constitutes between 30 and 50% of seminal fluid and is the only fluid component with citrate levels greater than about 5mM. Citrate levels in healthy men average 94 (\pm 32) mM in prostatic fluid and 33 (\pm 8) mM in seminal fluid (Kavanagh, 1985). As previously stated, as malignant cells proliferate within the prostate citrate levels fall in prostatic fluid, and thus in seminal fluid.

Parker et al have developed and patented - a rapid (< 3minute) method for measuring microlitre samples of citrate in prostatic and seminal fluid samples, this is called FScan (Pal et al., 2011).

The FScan method is based on the emission intensity ratio of two bands in the luminescence spectrum of a europium complex that binds citrate selectively in the presence of competing ions such as lactate, phosphate and carbonate. This seminal fluid assay was incorporated in PICTURE as an optional test for the patients. The aim was to analyse the relationship between the assay and its ability to rule out prostate cancer as determined by negative predictive value.

Also, in men who test positive for prostate cancer using FScan, can the assay provide an indication of clinical disease significance?

4.7 PICTURE Study Size Calculation

Consecutive prospective recruitment of patients from a clinically relevant population with masked test results will minimise bias ensured that the results from this study have clinical applicability.

Patients who fulfilled the eligibility criteria were selected so that the study sample has a disease prevalence that was representative of the population of interest. This is particularly important as predictive values depend on the disease prevalence in the population. Both patients and assessors were blinded to the test results until both index tests were completed and reported.

The biopsy tests were carried out once MRI and HistoScanning™ reporting was completed and results of the tests were disclosed simultaneously to each patient, in order to prevent attrition bias.

Sample size calculations were undertaken for both definitions of clinically significant disease- definition 1 (red disease) and definition 2 (amber disease).

Unpublished data from UCLH shows a disease prevalence of 38% definition 1 (red) disease and 65% clinically significant (definition 1 and 2, red and amber disease) in men undergoing transperineal template prostate mapping biopsy following an initial trans-rectal biopsy.

4.7.1 Sample Size Calculation

The sample size calculation was performed for the primary objective of calculation of the negative predictive value of the imaging modalities, using a precision based estimate.

For definition 1 disease the prevalence within our population was 38%. Targeting a NPV of 90% for definition one disease, for a 95% confidence interval with a confidence width 10% the number of patients needed with a negative test was 139.

Assuming the performance characteristics of mp-MRI and PHS equated to sensitivity and specificity of 70% - a sample size of 254 patients would allow for 139 patients with a negative test. Allowing a 10% drop out rate from the study it was aimed to recruit 280 patients.

Table 23. Numbers for precision based estimates with 95% Confidence level with varying confidence widths

	width of interval			
	0.1	0.15	0.2	0.3
0.7	323	144	81	36
0.75	289	129	73	33
0.8	246	110	62	28
0.85	196	88	49	22
0.9	139	62	35	16

To allow us to tailor the sample size to the disease prevalence we have used the following formula to provide the factor which must be applied to the precision based estimate.

$$\text{NPV factor} = ((1 - \text{Sensitivity}) * \text{Disease prevalence}) + ((\text{Specificity}) * (1 - \text{disease prevalence}))$$

The following tables (Table 24 and Table 25) demonstrates what happens to the sample size if the performance characteristics of the test alter. Numbers shaded light green are those that our chosen sample size (highlighted yellow) will cover.

For definition one disease- this has a prevalence of 38% in our population:

Table 24. Sample size calculation- calculated for 95% CI around NPV- assuming sensitivity and specificity of 70%

Factor=0.548	width of interval			
	0.1	0.15	0.2	0.3
0.7	589.4160584	262.7737226	147.810219	65.69343066
0.75	527.3722628	235.4014599	133.2116788	60.2189781
0.8	448.9051095	200.729927	113.1386861	51.09489051
0.85	357.6642336	160.5839416	89.41605839	40.1459854
0.9	253.649635	113.1386861	63.86861314	29.19708029

Table 25. Sample size calculation- Calculated for 95% CI around NPV- assuming sensitivity and specificity of 80%

Factor=0.572	width of interval			
	0.1	0.15	0.2	0.3
0.7	564.6853147	251.7482517	141.6083916	62.93706294
0.75	505.2447552	225.5244755	127.6223776	57.69230769
0.8	430.0699301	192.3076923	108.3916084	48.95104895
0.85	342.6573427	153.8461538	85.66433566	38.46153846
0.9	243.006993	108.3916084	61.18881119	27.97202797

For definition two disease, which has a prevalence of 65% in our population, tables Table 26 and Table 27 outline the numbers of test subjects required.

Table 26. Sample size calculation-calculated for 95% CI around NPV- assuming sensitivity and specificity of 70%

	width of interval			
	0.1	0.15	0.2	0.3
0.7	734.0909091	327.2727273	184.0909091	81.81818182
0.75	656.8181818	293.1818182	165.9090909	75
0.8	559.0909091	250	140.9090909	63.63636364
0.85	445.4545455	200	111.3636364	50
0.9	315.9090909	140.9090909	79.54545455	36.36363636

Table 27. Sample size calculation -Calculated for 95% CI around NPV- assuming sensitivity and specificity of 80%

	width of interval			
	0.1	0.15	0.2	0.3
0.7	787.804878	351.2195122	197.5609756	87.80487805
0.75	704.8780488	314.6341463	178.0487805	80.48780488
0.8	600	268.2926829	151.2195122	68.29268293
0.85	478.0487805	214.6341463	119.5121951	53.65853659
0.9	339.0243902	151.2195122	85.36585366	39.02439024

4.8 Statistical Analysis

Baseline demographic data of all men was assessed, for a number of factors, including: - age; PSA; gland size, and pre-study TRUS risk category.

Clinical validity was evaluated on a whole-gland basis using each patient as the unit of assessment. Sensitivity, specificity, positive and negative predictive values were calculated for all eligible men with binomial 95% confidence intervals.

4.8.1 Analysis of Multi-parametric MRI and Prostate Mapping Biopsy Results

For MRI primary analysis calculations used both an MRI-score of 3 or greater and MRI score 4 or greater as a positive test and histological definition 1 as the target condition on the reference TPM biopsy.

Results are presented in a 2 by 2 tables (Table 28) and estimates presented together with 95% confidence intervals (CI).

Table 28. 2 by 2 tables to demonstrate accuracy of MRI with respect to TPM

		MRI		
		+ve	-ve	Total
TPM	+ve	a	b	a+b
	-ve	c	d	c+d

Specificity = $d / (c+d)$ where, d = number of men testing negative on MRI and negative for clinically significant cancer on TPM, c = number of men testing positive on MRI who have clinically insignificant cancer on TPM.

Negative Predictive Value (NPV) = $d / (b+d)$ where, d = number of men testing negative on MRI and negative for clinically significant cancer on TPM, b= number of men testing negative on MRI who have clinically significant cancer on TPM.

Sensitivity = $a / (a+b)$ where, a = number of men testing positive on MRI and positive for clinically significant on TPM, b = number of men testing negative for MRI who have clinically significant cancer on TPM.

Positive Predictive Value (PPV) = $a / (a+c)$ where, a = number of men testing positive on MRI and positive for clinically significant on TPM, c = number of men testing positive on MRI who have clinically insignificant cancer on TPM.

4.8.2 Varying the Definitions of Clinical Significance at TPM

2 by 2 tables were constructed for MRI comparison to TPM at patient level for:

Definition 1 disease

Definition 2 disease

All cancer

4.8.3 MRI Targeted Biopsy Analysis

Targeted biopsies were analysed as both separate targeting strategies and pooled targeted sampling using both methods to assess validity. The detection rate of cancer and the proportion of clinically significant disease detected or missed by targeting were assessed. Overall accuracy was assessed using receiver operating characteristic curves.

Additionally, these performance characteristics were assessed when the MRI score threshold was changed from 4 to 3. Each targeted biopsy strategy was also evaluated separately, and as pooled targeted approach.

4.8.4 Secondary Analysis

Inter-observer variability was assessed using kappa agreement. STATA version 3.0 software was used with any tests of significance using $p=0.05$ as the threshold for statistical significance.

Further analysis of targeted cores was performed to assess whether targeted sampling errors were a result of inaccurate localisation by MRI (Out of field miss) or were due to a likely mis-registration/Targeting error (In-field errors). For this analysis each individual case was assessed to establish the zone in which the targeted biopsy was aimed at, compared with the zone in which the maximal Gleason grade/UCL risk score at TPM was obtained.

4.9 Analysis of Prostate HistoScanning™ and Transperineal Template

Prostate Mapping Biopsy Results

The visit one HistoScanning report was used for the main analysis and the second HistoScanning examination results were used only for test reproducibility analysis.

Results were presented in a 2 by 2 tables (as shown below Table 29) and estimates presented together with 95% confidence intervals (CI).

Table 29. 2 by 2 tables to demonstrate accuracy of HistoScanning with respect to TPM

		PHS		
		+ve	-ve	Total
TPM	+ve	a	b	a+b
	-ve	c	d	c+d

Specificity = $d / (c+d)$ where, d = number of men testing negative on HistoScanning™ and negative for clinically significant cancer on TPM, c = number of men testing positive on HistoScanning™ who have clinically insignificant cancer on TPM.

Negative Predictive Value (NPV) = $d / (b+d)$ where, d = number of men testing negative on HistoScanning™ and negative for clinically significant cancer on TPM, b= number of men testing negative on HistoScanning™ who have clinically significant cancer on TPM.

Sensitivity = $a / (a+b)$ where, a = number of men testing positive on HistoScanning™ and positive for clinically significant on TPM, b = number of men testing negative for HistoScanning™ who have clinically significant cancer on TPM.

Positive Predictive Value (PPV) = $a / (a+c)$ where, a = number of men testing positive on HistoScanning™ and positive for clinically significant on TPM, c = number of men testing positive on HistoScanning™ who have clinically insignificant cancer on TPM.

4.9.1 Varying the Definitions of Clinical Significance at TPM

2 by 2 tables were constructed for HistoScanning™ comparison to TPM at patient level for Definition 1 disease, Definition 2 disease and all cancer.

4.9.2 PHS Targeted Biopsy Analysis

The ability of PHS to accurately locate cancer using targeted biopsy was assessed. The detection rate of cancer and the proportion of clinically significant disease detected or

disease missed by targeting was assessed. Overall accuracy was assessed using receiver operating characteristic curves.

4.9.3 HistoScanning Test Re-Test Reproducibility

The test retest reproducibility of HistoScanning was assessed using kappa analysis for the strength of agreement between the two scans and paired test (McNemar) to measure variability between the two HistoScanning reports.

This was done for both the variability between the 8818 and 8848 at the consent visit

In addition, the 8818 T0 at consent and the 8818 T2 performed at the time on template biopsy, and also the 8848 probe performed at the two time points T0 and 8848 T2 were compared.

4.9.4 Biomarker Analysis

For both the urine biomarker EN2 and the seminal marker (FScan), performance was assessed by calculation of the AUROC for the technology.

5 PICTURE Results

The PICTURE study aimed to assess the use of imaging to accurately detect and localise prostate cancer. The primary outcome results include the whole gland analysis of both of the index imaging tests, (mp-MRI and Prostate HistoScanning) for their ability to accurately rule out significant prostate cancer. An important secondary analysis is the ability of each imaging modality to give an accurate location for targeted sampling of the gland.

Therefore, this chapter is structured to first address the overall demographic data, and then to address each modality in turn for its primary outcome result sensitivity and NPV, and to also address its ability to accurately guide targeting.

Further secondary outcomes are discussed in a second results chapter (Chapter 6).

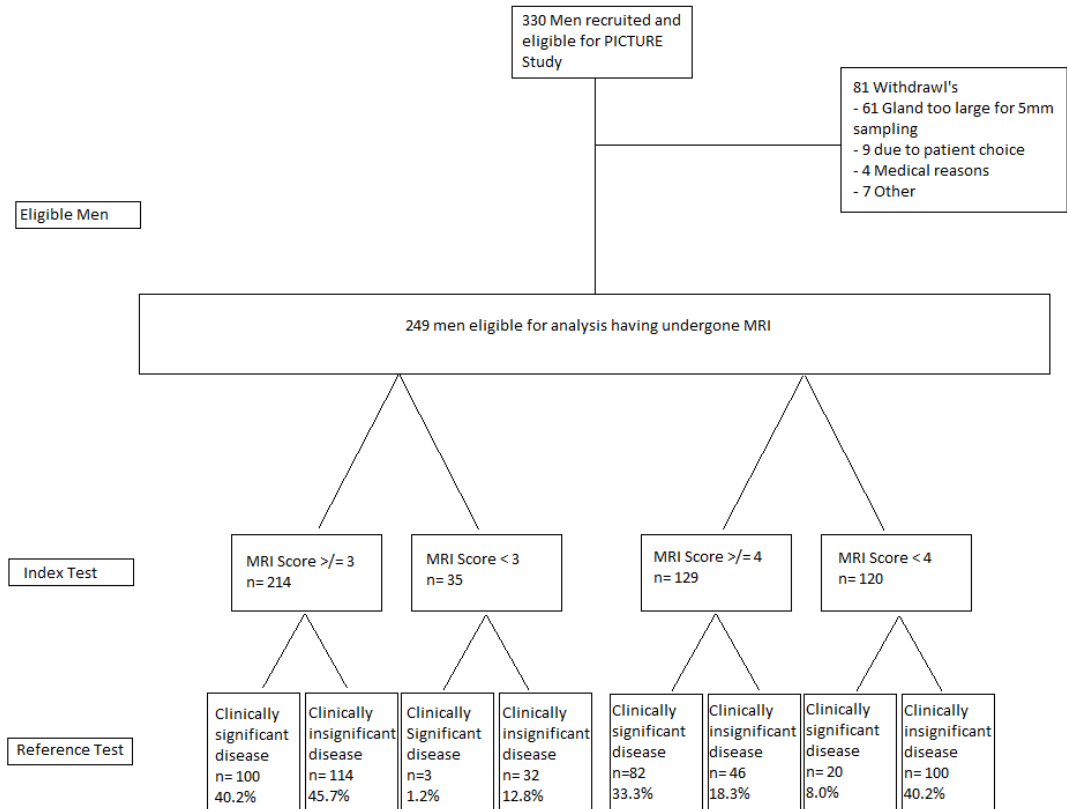
5.1 Recruitment

Picture recruited at University College Hospitals London, consecutively from 11th January 2012 and completed recruitment on 29th January 2014. Figure 57 demonstrates the PICTURE recruitment STARD flow diagram.

Overall, 330 men were recruited to the study. A number of men were withdrawn leaving 249 for final study analysis.

The reasons for withdrawal included: - 61 men who had a gland sizes too large to allow adequate sampling density, 9 men who were withdrawn at their own request, 4 men were withdrawn for medical reasons and 7 men withdrew for other reasons.

Figure 57. PICTURE recruitment STARD flow diagram.



5.2 Baseline Demographic Data

Three-hundred and thirty men were enrolled with mean (SD) age of 63 (7) years. Median (IQR) PSA at consent was 7.4 (5.3-10.7) ng/ml. Median (IQR) number of previous biopsies was 1 (1-2), with men having had from 1 to 5 prior prostate biopsies (Table 30). Pre-study TRUS biopsy Gleason grade data is shown in Table 31.

81 men withdrew leaving 249 for primary analysis. Men eligible for analysis had mean (SD) age 62(7) years, median (IQR) PSA 6.8 (4.98-9.50) ng/ml and median (IQR) number of previous biopsies 1 (1-2) and mean (SD) gland size 37ml (15.5).

Median (IQR) number of days between mp-MRI and biopsy was 78 (43-107).

Table 30. PICTURE Patient demographics

	All men n=330	Men eligible for analysis n=249
Characteristic	Median (IQR)	Median (mean, SD, range)
Age, years	63 (42-83)	62 (62.0, 7.16, 42-83)
PSA concentration at consent, ng/ml	7.4 (0.7-58.05)	6.8 (7.81, 4.26, 0.7-30.3)
	Mean (SD)	Mean (SD)
Number of previous biopsies	1.49, (0.79)	1.41 (0.69)
Number of previous negative biopsies	0.69 (0.96)	0.51 (0.79)
Number of previous positive biopsies	0.79 (0.65)	0.87 (0.62)
MRI Prostate volume, cc	46.48 (26.53)	39.1 (15.5)

Table 31. Study entry TRUS biopsy Gleason grading

Gleason score on pre-study TRUS biopsy	All men n=330 Number of men (%)	Men eligible for analysis n=249 Number of men (%)
Missing info	22 (6.7)	12 (4.8)
Benign	101 (30.6)	64 (25.7)
3+3	147 (44.6)	121 (48.6)
3+4	55 (16.7)	48 (19.3)
4+3	5 (1.5)	4 (1.61)
Total	330	249

5.3 Template Mapping Biopsy (TPM) Results

Following template biopsy 40 men (16%) were found to be benign, 41% of men (n=103) had Definition one disease detected at TPM. A mean of 48.7 (SD 12.3, range 15-86) cores were taken per man at TPM. Maximum cancer core length detected was 15mm.

Disease characteristics on the reference test, TPM biopsy, are shown in Table 32.

Table 32. Template biopsy disease distribution for eligible men n=249

	Mean (SD)	
Total number of cores	48.69 (12.3)	
Number of cancer cores	6.88 (5.95)	
MCCL (mm)	4.65 (3.59)	
Gleason Risk group n (%)	Number	%
Benign	40	16.1
3+3	66	26.5
3+4 or 4+3	139	55.8
>/= 4+4	3	1.2
(3+5)	1	0.4
UCL Risk group	Number of men	%
Benign	40	16.1
Insignificant (G3+3 or MCCL</=3mm)	41	16.5
Intermediate (Definition 2= G3+4 or MCCL>4mm)	168	67.5
High (Definition 1= G4+3 or MCCL>6mm)	103	41.4

5.4 Whole Gland MRI Results

5.4.1 Report Demographics

57% of men (n=142) were considered highly unlikely or unlikely to have significant prostate cancer, 16% (n=39) of men were equivocal and 27% (n=68) were felt likely or highly likely to have clinically significant disease according to the MRI consensus agreed scoring system used in PICTURE (Dickinson et al., 2011)

50 men did not have a lesion on MRI. Of those with a lesion average size of index lesion was 11.7mm (SD 6.7). (Table 33)

Of the lesions reported the majority 50.6% (n=126) were thought to contain Gleason 3+4 disease.

Table 33. *MRI characteristics*

Overall MRI score for UCL definition 1 disease	<i>n=</i>	<i>%</i>
1-2 <i>highly unlikely/unlikely</i>	142	57
3 <i>equivocal</i>	39	16
4-5 <i>likely/highly likely</i>	68	27
MRI lesion details		
0	50	20
1	198	79.5
2	74	29.7
3	14	5.6
Index lesion estimated Gleason grade		
Benign	7	2.8
3+3	43	17.3
3+4	126	50.6
4+3	22	8.8
4+4	1	0.4
Any pattern 5	0	0
	<i>Mean</i>	<i>SD</i>
Index lesions size (mm)	11.7	6.7

5.4.2 Primary Outcome 1

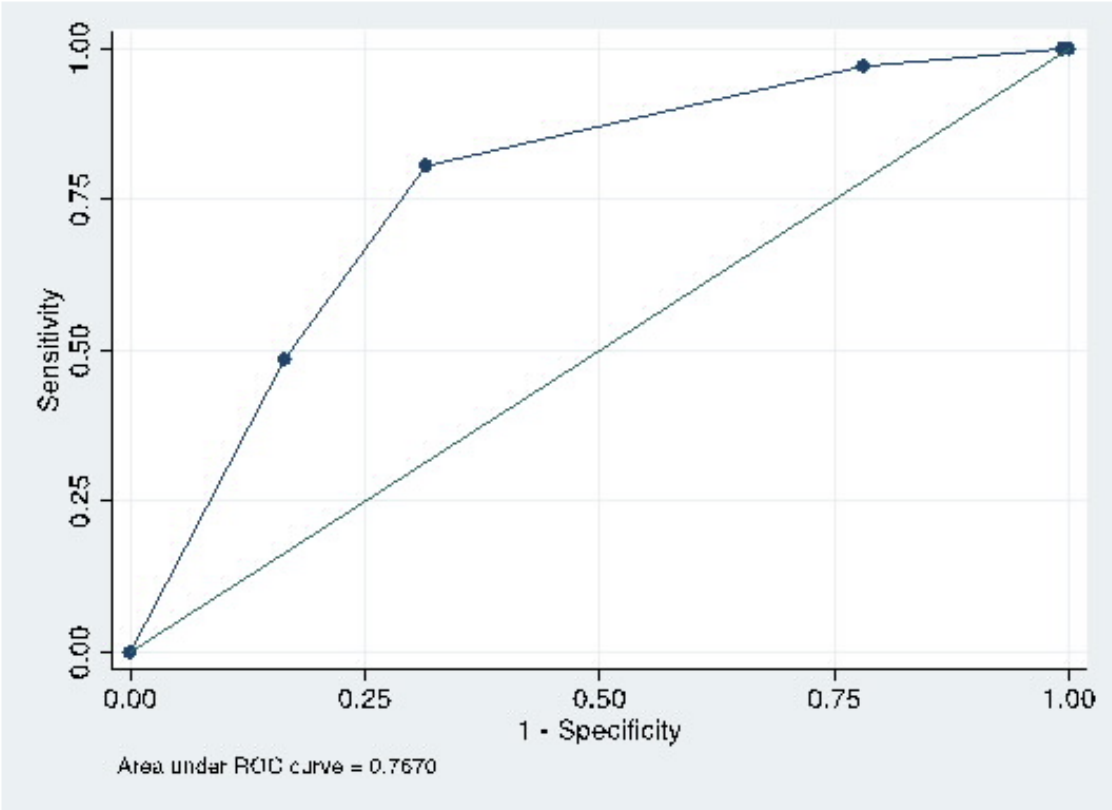
First, using mpMRI score ≥ 4 as a positive test, mpMRI demonstrated sensitivity of 80.6% (95% CI 71.6-87.7) and specificity 68.5% (95% CI 60.3-75.9), NPV 83.3% (95% CI 75.4-89.5) and PPV 64.3% (95% CI 55.4-72.6), for the detection of clinically significant disease. Area under ROC curves was 0.76 (95% CI 0.69-0.80). (Figure 58)

Secondly, incorporating mpMRI score ≥ 3 (equivocal) as a positive test sensitivity was 97.1% (95% CI 92-99), specificity 21.9% (95% CI 15.5-29.5), NPV 91.4% (95% CI 76.9-98.1) and PPV 46.7% (95% CI 35.2-47.8). (Table 34)

Table 34. *mpMRI performance characteristics for Definition 1 disease*

	Sensitivity % (95% CI)	Specificity % (95% CI)	PPV % (95% CI)	NPV % (95% CI)	Positive likelihood ratio (95% CI)	Negative likelihood ratio (95% CI)
mpMRI Score ≥ 4	80.6 (71.6-87.7)	68.5 (60.3-75.9)	64.3 (55.4-72.6)	83.3 (75.4- 89.5)	2.56 (1.98-3.31)	0.28 (0.19- 0.43).
mpMRI Score ≥ 3	97.09 (92-99)	21.92 (15.5-29.5)	46.73 (35.2-47.8)	91.4 (76.9- 98.1)		

Figure 58. ROC curve analysis for mpMRI detection of disease



5.5 MRI Targeting Results

The analysis of the MRI targeting results has been divided to first analyse each targeting strategy according to all men targeted for MRI score 3 or above. This has been done for each modality ‘Cognitive MRI’ targeting, ‘MRI/US registration’ targeting and pooled results of both modalities, for Definition one disease. These results are outlined in sections 5.5.1 to 5.5.4.

Results have then been explored for altering the target group to only include those men targeted for lesions scoring 4 or above on MRI and therefore deemed ‘likely’ or ‘highly likely’ to be malignant on the mp-MRI likert scoring scale, once again results are given for Definition one disease. These results are outlined in sections 5.5.5 onwards.

5.5.1 MRI ‘Cognitive’ Targeted Results - MRI Score ≥3

In the 199 men who underwent MRI cognitive targeted biopsy, sensitivity was 47.9% (95% CI 37.9-58.4), specificity 88.3% (95% CI 80.5-93.8), NPV 64.5% (95% CI 56.0-72.4) and PPV 79.3% (66.6-88.8), for the detection of UCL definition 1 disease, when using MRI score ≥ 3 as the cut off (Table 35).

MRI cognitive targeted biopsies identified 14/58 (21%) men as clinically significant who had been incorrectly classified as insignificant or benign at TPM biopsy. Cognitive MRI biopsies incorrectly classified 50 men (52%) as benign or insignificant when they were found to have significant disease on TPM. (Table 35)

Table 35. MRI Cognitive vs TPM biopsies by UCL risk criteria

		Template Mapping biopsies				Total
		Benign	Insignificant	Definition 2	Definition 1	
MRI cognitive targeted biopsies	No MRI target	22	12	9	7	50
	Benign	15	22	24	12	73
	Insignificant	0	3	11	12	26
	Definition 2	0	3	13	26	42
	Definition 1	3	1	8	46	58
Total		40	41	65	103	249

Key to shading
No MRI target
Significant disease missed by TPM
Significant disease missed by targeting

5.5.2 MRI/US Registration Targeted Results - MRI Score ≥ 3

In the 169 (30 cases had technical failure of the software) who had MRI/US fusion targeted biopsies sensitivity was 51.8% (95% CI 40.6-62.9), specificity 88.4% (95% CI 79.7-94.3), NPV 65.5% (95% CI 56.1-74.1) and PPV 81.8% (95% CI 68.0-90.6), when using MRI score ≥ 3 as the cut off (Table 36).

MRI/US fusion targeted biopsies identified 10/53 (18.8%) men as clinically significant who had been incorrectly classified as insignificant or benign at TPM biopsy. Fusion targeted biopsies incorrectly classified 40 men (38.8%) as benign or insignificant when they were found to have significant disease on TPM.

Table 36. MRI/US registration targeted biopsy

		Template biopsies				
		Benign	Insignificant	Definition 2	Definition 1	
MRI/US registration targeted biopsies	No MRI/US target	25	16	19	20	80
	Benign	13	21	16	11	61
	Insignificant	0	2	8	10	20
	Definition 2	0	1	15	19	35
	Definition 1	2	1	7	43	53
		40	41	65	103	249
Key to shading						
No MRI target						
Significant disease missed by TPM						
Significant disease missed by targeting						

5.5.3 Pooled MRI Targeted Results - MRI Score ≥ 3

Using the pooled MRI targeted data for 200 men having targeted biopsies for an MRI score ≥ 3 ; there was 78% direct agreement in cancer classification between targeted biopsy and TPM, with targeting and TPM agreeing on the presence or absence of disease in 156 men. Demographic data for these men is shown in Table 37.

18/81 (22%) men with clinically significant disease were found to be incorrectly risk stratified by TPM; 3 of these had been classified as benign at TPM. Pooled MRI targeting failed to identify 34/103 (33%) of men with clinically significant disease identified by TPM. (Table 38)

Table 37. MRI pooled targeted biopsy demographics n=200

	Mean (SD)	
Total number of cores	4.26 (2.37)	
Number of cancer cores	1.87 (1.03)	
Gleason Risk group n (%)		
	Number	%
Benign	56	28.0
3+3	38	19.0
3+4	83	41.5
4+3	18	9.0
>/= 4+4	5	2.5

Table 38. Pooled MRI Targeted results

		Template Mapping biopsies				
		Benign	Insignificant	Definition 2	Definition 1	
MRI targeted biopsies	No MRI target	22	12	9	6	49
	Benign	15	19	15	7	56
	Insignificant	0	4	10	8	22
	Definition 2	0	4	18	19	41
	Definition 1	3	2	13	63	81
		40	41	65	103	249
Key to shading						
No MRI target						
Significant disease missed by TPM						
Significant disease missed by targeting						

Further analysis of pooled MRI targeted data was performed to identify the source of error- MRI miscalls vs. target registration error. This analysis demonstrated that in the 55 men who underwent MRI targeted sampling that did not yield a cancer diagnosis; 15 (30%) of these had no cancer on the reference test of TPM. They were therefore correctly classified by the targeted sampling.

Analysis of MRI scores for these men revealed that 10/15 men (66.6%) were felt to be unlikely and highly unlikely of having significant disease (MRI score 1 and 2), and 4/15 men (26.6%) were rated equivocal (MRI score 3). Only one man (6%) was incorrectly rated as likely to have significant disease (MRI score 4)

Of the 40 men who had cancers detected at TPM and therefore were incorrectly classified by MRI targeting as benign, only 5 of these men (12.5%) had clinically significant disease according to UCL definition 1 criteria.

22 out of 40 (55%) were in-field targeting errors (i.e. target localisation errors/mis-registration) and thus the MRI localisation of disease was correct. 21 out of 22 (96%) were targeted to the correct quadrant in which the reference test detected the maximal cancer burden. One patient had disease in the quadrant targeted but maximal cancer burden in a different area.

18 of those for whom MRI targeting was benign (45%) were out of field errors and thus represent mis-localisation by MRI. 9 of these were called on the incorrect hemi-prostate. 9 were targeted to the correct hemi-prostate but were directed to the incorrect quadrant (anterior/posterior).

5.5.4 Summary MRI Targeting Results - MRI Score ≥ 3

MRI-targeted biopsies had a detection rate of 78.6% (95% CI 69.9-82.1) for clinically significant cancer when lesions scoring 3 or greater on mpMRI were considered.

Two analyses were carried out: one including all the men who had not undergone targeted biopsy and assuming them to be benign; the other including only those men targeted.

When assessing the performance characteristics for MRI targeted biopsy in the cohort (including those not targeted) sensitivity was 61.2% (95%CI 51.1-70.6), specificity 87.7 (95%CI 81.2-92.5), NPV 76.2 (95%CI 69.0-82.4) and PPV 77.8 (95%CI 69.0-82.4). (Table 39)

By excluding those men without a target on MRI and assessing only those who had a targeted biopsy, an increase in sensitivity was seen, but a decrease in specificity and NPV.

Table 39. MRI Targeted performance characteristics for detection of UCL Definition 1 disease for MRI score ≥ 3 . (Including men not targeted and assuming non targeted are benign)

	Sensitivity % (95% CI)	Specificity % (95% CI)	PPV % (95% CI)	NPV % (95% CI)	AUC (95% CI)
MRI Cognitive	44.7 (34.9-54.8)	91.8 (86.1-95.7)	79.3 (66.6-88.8)	70.2 (63.1-76.5)	0.68 (0.63-0.74)
MRI/US fusion	41.7 (32.1-51.9)	93.2 (87.8-96.7)	81.1 (68.0-90.6)	69.4 (62.4-75.8)	0.67 (0.62-0.78)
MRI Targeted Pooled results	61.2 (51.1-70.6)	87.7 (81.2-92.5)	77.8 (67.2-86.3)	76.2 (69.0-82.4)	0.74 (0.69-0.80)

Table 40. MRI Targeted performance characteristics for detection of UCL Definition 1 disease, excluding non-targeted men, for MRI score ≥ 3

	Sensitivity % (95% CI)	Specificity % (95% CI)	PPV % (95% CI)	NPV % (95% CI)	AUC (95% CI)
MRI Cognitive	47.9 (37.6-58.4)	88.3 (80.5-93.8)	79.3 (66.6-88.8)	64.5 (56.0-72.4)	0.68 (0.62-0.74)
MRI/US fusion	51.8 (40.6-62.9)	88.4 (79.7-94.3)	81.1 (68.0-90.6)	65.5 (56.1-74.1)	0.70 (0.64-0.76)
MRI Targeted Pooled results	64.9 (54.6-74.4)	82.5 (73.8-89.3)	77.8 (67.2-86.3)	71.4 (62.4-79.3)	0.74 (0.68-0.80)

5.5.5 MRI Cognitive Targeted Results - MRI Score ≥ 4

When the target condition for biopsy was changed to exclude those men deemed equivocal on MRI (MRI score= 3), and to only include those men with lesions ‘likely’ (MRI score 4) or ‘highly likely’ (MRI score 5) to involve significant disease, there were 137 men who underwent MRI cognitive targeting.

For the 137 men who underwent MRI cognitive targeted to MRI lesions ≥ 4 biopsy, sensitivity was 51.8% (95% CI 40.7-62.7), specificity 80.8% (95% CI 67.5-90.4), NPV 50.6% (95% CI 39.4-61.8) and PPV 81.5% (95% CI 68.6-90.7, for the detection of UCL definition 1 disease. (Table 44)

MRI cognitive targeted biopsies identified 10/54 (19%) men as clinically significant who had been incorrectly classified as insignificant or benign at TPM biopsy. Cognitive MRI biopsies incorrectly classified 41 men (29%) as benign or insignificant when they were found to have significant disease on TPM. (Table 41)

Table 41. MRI Cognitive (MRI score ≥ 4) vs TPM biopsies by UCL risk criteria

		Template Mapping biopsies				
		Benign	Insignificant	Definition 2	Definition 1	
MRI cognitive targeted biopsies	Benign	3	6	13	8	30
	Insignificant	0	1	8	9	18
	Definition 2	0	3	8	24	35
	Definition 1	3	1	6	44	54
	Totals	6	11	35	85	137
Key to shading						
Significant disease missed by TPM						
Significant disease missed by targeting						

5.5.6 MRI/US Registration Targeted Results - MRI Score ≥ 4

In the 137 men who had MRI/US fusion targeted biopsies for MRI lesions ≥ 4, biopsy sensitivity was 56.0% (95% CI 44.1-67.5), specificity 83.3% (95% CI 68.6-93.0) , NPV 51.5% (95%CI 39.0-63.8), and PPV 85.7 (95% CI 72.8-94.1) (Table 44).

MRI/US fusion targeted biopsies identified 7/49 (14.2%) men as clinically significant who had been incorrectly classified as insignificant or benign at TPM biopsy. Fusion targeted biopsies incorrectly classified 33 men (38.8%) as benign or insignificant when they were found to have significant disease on TPM.

Table 42. MRI/US registration targeted biopsy- MRI score ≥ 4

		Template biopsies				Total
		Benign	Insignificant	Definition 2	Definition 1	
MRI/US registration targeted biopsies	No MRI/US target	2	2	6	10	20
	Benign	2	7	9	7	25
	Insignificant	0	1	5	9	15
	Definition 2	0	0	11	17	28
	Definition 1	2	1	4	42	49
	Total	6	11	35	85	137
Key to shading						
No MRI/US target						
Significant disease missed by TPM						
Significant disease missed by targeting						

5.5.7 Pooled MRI Targeted Results - MRI Score ≥ 4

Using the pooled MRI targeted data for the 137 men having targeted biopsies for an MRI score ≥ 4 , there was 57% direct agreement in cancer classification between targeted biopsy and TPM, with targeting and TPM agreeing on the presence or absence of disease in 77/137 men.

14/74 (18.9%) men with clinically significant disease were found to be incorrectly risk stratified by TPM. Three of these had been classified as benign at TPM. Pooled MRI targeting failed to identify 25/85 (29%) of men with clinically significant disease identified by TPM. (Table 43)

Table 43. Pooled MRI Targeted results- MRI score ≥ 4

		Template Mapping biopsies				Total
		Benign	Insignificant	Definition 2	Definition 1	
MRI targeted biopsies	Benign	3	5	7	2	17
	Insignificant	0	1	6	6	13
	Definition 2	0	3	13	17	33
	Definition 1	3	2	9	60	74
	Total	6	11	35	85	137

Key to shading	
Significant disease missed by TPM	
Significant disease missed by targeting	

5.5.8 Summary MRI Targeting Results MRI score ≥ 4

Table 44 demonstrates the MRI targeted biopsy characteristics for those men targeted for an MRI lesion \geq MRI score 4.

Table 44. MRI Targeted performance characteristics for detection of UCL Definition 1 disease excluding non-targeted men, for MRI score ≥ 4

	Sensitivity % (95% CI)	Specificity % (95% CI)	PPV % (95% CI)	NPV % (95% CI)	AUC (95% CI)
MRI Cognitive	51.8 (40.7-62.7)	80.8 (67.5-90.4)	81.5 (68.6-90.7)	50.6 (39.4-61.8)	0.66 (0.46-0.74)
MRI/US fusion	56.0 (44.1-67.5)	83.3 (68.6-93.0)	85.7 (72.8-94.1)	51.5 (39.0-63.8)	0.70 (0.62-0.78)
MRI Targeted	70.6 (59.7-80.0)	73.1 (59.0-84.4)	81.1 (70.3-89.3)	60.3 (47.2-72.4)	0.72 (0.64-0.80)

5.5.9 Altering the MRI Threshold for Biopsy

Table 45 has been included to allow easy comparison between the performance characteristics of the two thresholds for MRI targeted biopsy.

As anticipated sensitivity for the detection of clinically significant disease is increase with increasing MRI reporter confidence on the likelihood of disease (i.e. higher MRI likert scale scores). The increase in sensitivity is possible without a gross impact on other performance characteristics, and with similar percentages of men undergoing incorrect classification as benign by targeted biopsy in comparison to TPM (29% for MRI target ≥ 4 vs. 33% for MRI target ≥ 3).

Table 45. Comparison of performance characteristics between targeting for MRI lesion ≥ 3 and MRI lesion ≥ 4

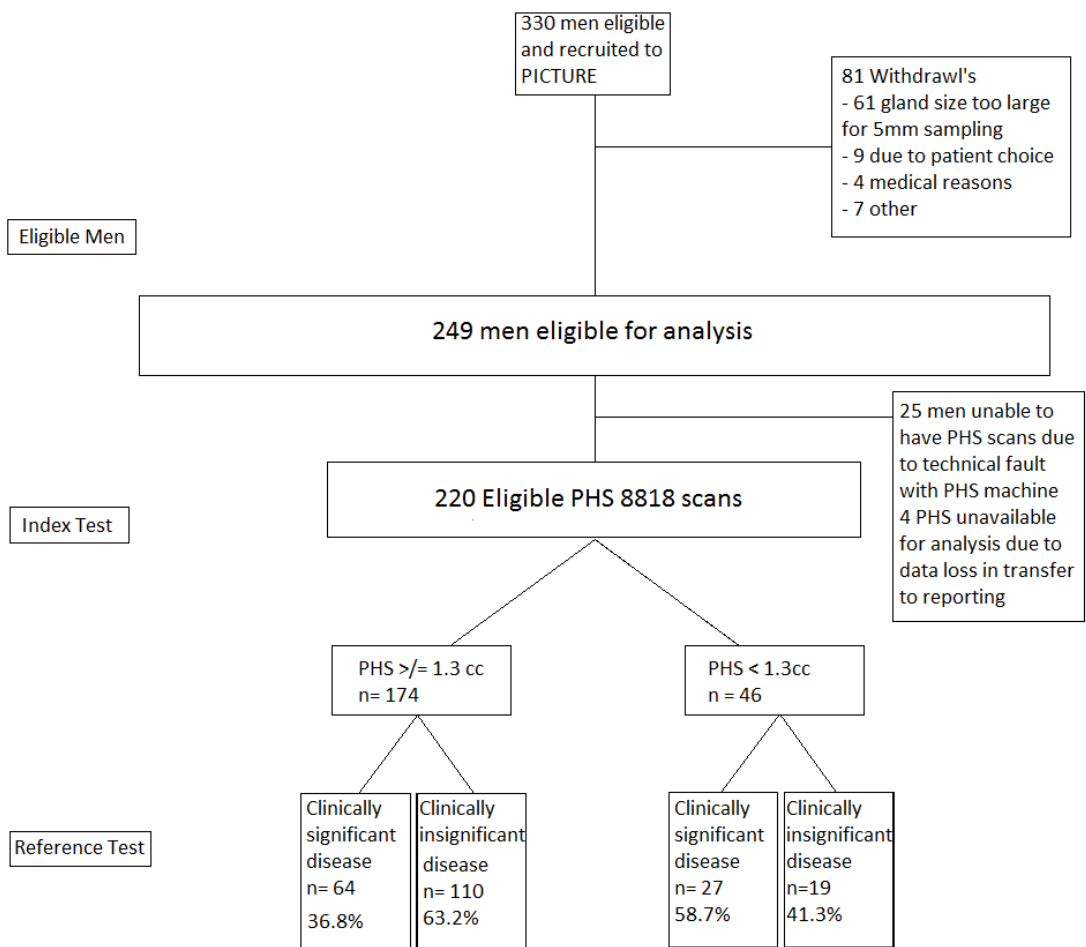
	Sensitivity (95% CI)	Specificity (95% CI)	PPV (95% CI)	NPV (95% CI)	AUC (95% CI)
MRI Cognitive MRI score ≥ 3	47.9 (37.6-58.4)	88.3 (80.5-93.8)	79.3 (66.6-88.8)	64.5 (56.0-72.4)	0.68 (0.62-0.74)
MRI Cognitive MRI score ≥ 4	51.8 (40.7-62.7)	80.8 (67.5-90.4)	81.5 (68.6-90.7)	50.6 (39.4-61.8)	0.66 (0.46-0.74)
MRI/US fusion MRI Score ≥ 3	51.8 (40.6-62.9)	88.4 (79.7-94.3)	81.1 (68.0-90.6)	65.5 (56.1-74.1)	0.70 (0.64-0.76)
MRI/US fusion MRI score ≥ 4	56.0 (44.1-67.5)	83.3 (68.6-93.0)	85.7 (72.8-94.1)	51.5 (39.0-63.8)	0.70 (0.62-0.78)
MRI Targeted Pooled results MRI score ≥ 3	64.9 (54.6-74.4)	82.5 (73.8-89.3)	77.8 (67.2-86.3)	71.4 (62.4-79.3)	0.74 (0.68-0.80)
MRI Targeted Pooled results MRI score ≥ 4	70.6 (59.7-80.0)	73.1 (59.0-84.4)	81.1 (70.3-89.3)	60.3 (47.2-72.4)	0.72 (0.64-0.80)

5.6 Whole Gland Prostate HistoScanning Results

5.6.1 Report Demographics

Due to a combination of hardware technical failure and loss of PHS data prior to analysis 29 men who remained in the study did not have PHS scans available for analysis: Figure 59 outlines the patient flow for PHS patients in the PICTURE study.

Figure 59. PICTURE Prostate HistoScanning flow diagram



The reference test (TPM) found cancer meeting the target definition for significance in 41.8% of men (n=92), further disease characteristics at TPM are shown in Table 46.

Prostate HistoScanning cancer volumes were on average 3.4cc (SD 2.27), with the primary most significant lesion volumes averaging 2.7cc (SD 2.3). PHS found 174 men to have cancer volumes greater than 1.3cc.

Table 46. Template biopsy disease distribution for all study eligible men n=249, and men eligible for PHS analysis n=220

	Mean (SD)			
Total number of cores	48.69 (12.3)			
Number of cancer cores	6.88 (5.95)			
MCCL (mm)	4.65 (3.59)			
	All study eligible men N=249		For men in PHS analysis n=220	
Gleason Risk group n (%)	Number	%	Number	%
Benign	40	16.1	28	12.7
3+3	66	26.5	63	28.6
3+4 or 4+3	139	55.8	125	56.8
>/= 4+4	3	1.2	3	1.4
(3+5)	1	0.4	0	0
UCL Risk group	Number	%	Number	%
	of men		of men	
Benign	40	16.1	28	12.7
Insignificant (G3+3 or MCCL</= 3mm)	41	16.5	38	17.3
Intermediate (Definition 2= G3+4 or MCCL> 4mm)	168	67.5	165	75.0
High (Definition 1= G4+3 or MCCL> 6mm)	103	41.4	92	41.8

5.6.2 Primary Outcome 1

Prostate HistoScanning showed 70.3% (95% CI 59.8-79.5) sensitivity for the detection of cancer volumes ≥ 1.3 cc. Specificity, positive predictive and negative predictive values were 14.7% (95% CI 9.1-22.0), 36.8% (95% CI 29.6-44.4) and 41.3% (95%CI 27.0-56.8) respectively.

When the target condition was changed to ≥ 0.5 cc cancer volumes sensitivity was 93.4% (95% CI 86.2-97.5) and specificity dropped to 0.8% (95% CI 0.00-4.2). (Table 47)

Table 47. PHS Performance Characteristics for Definition 1 Disease

	Sensitivity % (95% CI)	Specificity % (95% CI)	PPV % (95% CI)	NPV % (95% CI)	AUC (95% CI)
PHS lesion ≥1.3cc	70.3 (59.8-79.5)	14.7 (9.1-22.0)	36.8 (29.6-44.4)	41.3 (27.0-56.8)	0.43 (0.37-0.48)
PHS lesion ≥0.5cc	93.4 (86.2-97.5)	0.8 (0.0-4.2)	39.9 (33.3-46.8)	14.3 (0.4-57.9)	0.47 (0.44-0.50)

5.7 Prostate HistoScanning Targeting Results

213 of 220 men had PHS lesions targeted. Sensitivity was 13.6% (95%CI 7.3-22.6), specificity 97.6% (95%CI 93.1-99.5), NPV 61.6% (95%CI 54.5-68.4) and PPV 80% (95%CI 51.9-95.7). (Table 48)

Of the 213 men targeted with PHS targeted biopsy, 23% showed direct correlation with the TPM biopsy result (Table 49). 76 men (36%) were incorrectly classified as benign or insignificant at Definition 1 threshold when they actually harboured Definition 1 significance disease at TPM. Three men (1.4%) were found to have significant disease at PHS biopsies that were incorrectly classified as insignificant at TPM.

Table 48. PHS Targeted performance characteristics for detection of UCL Definition 1 disease (excluding non-targeted men)

	Sensitivity % (95% CI)	Specificity % (95% CI)	PPV % (95% CI)	NPV % (95% CI)	AUC (95% CI)
PHS target	13.6 (7.3-22.6)	97.6 (93.1-99.5)	80 (51.9-95.7)	61.6 (54.5-68.4)	0.55 (0.51-0.59)

Table 49. PHS Targeted results for definition one disease

		Template Mapping biopsies				Totals
		Benign	Insignificant	Definition 2	Definition 1	
PHS targeted biopsies	Benign	26	32	44	58	160
	Insignificant	0	4	8	9	21
	Definition 2	0	0	8	9	17
	Definition 1	1	0	2	12	15
Totals		27	36	62	88	213
Significant disease missed by TPM						
Significant disease missed by targeting						

5.8 Discussion of Prostate HistoScanning Results

The Prostate HistoScanning results from the PICTURE study have shown that PHS has a poor ability to discriminate benign from malignant tissue. The AUC for PHS is worse than chance.

Although PHS seems to portray high acceptable sensitivity for disease detection, when assessing the whole gland performance characteristics this sensitivity can be seen to rise as the lesion size decreases from 1.3cc to 0.5cc: this is likely to be the effect of the false positive HistoScanning signal that plagues the modality.

The targeting results show that 75% of lesions targeted by PHS are found to be benign, with 62% of these being incorrectly assigned to the benign group. Also, by adopting a PHS targeted biopsy strategy, 36% of men with Definition 1 clinically significant disease would be incorrectly classified.

Only 23% of men (n=50/213) had direct correlation between their disease status at TPM and PHS targeted biopsy.

6 Secondary PICTURE Results

6.1 MRI Inter-Reporter Reproducibility Results

As previously stated, for a test to be useful as a valid diagnostic test, it requires not only adequate performance characteristics for the detection of disease but also must be reproducible when interpreted by different analysts.

To assess the inter-reporter reproducibility of mpMRI, a selection of 50 mpMRI's within the PICTURE Study were re-reported by a second radiologist. The reporter was blinded to previous reports and TPM histopathology but had necessary clinical details available, namely pre-study PSA and biopsy result.

Tables were constructed to assess agreement between the reporting radiologist, for any cancer, definition 2 disease, and definition 1 disease. Percentage agreement and Kappa values were calculated for each agreement.

Kappa values allow for a measure of agreement - measuring direct agreement/disagreement. Weighted kappa values try to account for the difference in levels of disagreement; namely, an MRI score of 3 to 4 is less of a disagreement, than an MRI score of 1 to 5, weighted kappa values allow for this.

Kappa agreements can be interpreted as follows (Altman, 1991):

Table 50. Kappa Values

Value of K	Strength of agreement
<0.2	Poor
0.21-0.40	Fair
0.41-0.60	Moderate
0.61-0.80	Good
0.81-1.00	Very good

Table 51. MRI Comparison for Any Disease

		MRI Reporter 2				Total
		MRI Score 2	MRI Score 3	MRI Score 4	MRI Score 5	
MRI reporter 1	MRI Score 2	0	0	0	0	0
	MRI Score 3	1	15	4	1	21
	MRI Score 4	0	1	7	0	8
	MRI Score 5	0	3	6	12	21
Totals		1	19	17	13	50
Key						
Direct MRI score agreement						

For any disease the two MRI reporters demonstrated a direct agreement in 34/50 MRI's, equating to a direct agreement of 68% (Table 51). Kappa values for this agreement = 0.53, with standard error= 0.09, demonstrating moderate agreement.

Using weighted kappa, agreement increases to 90%. With kappa values of 0.59, standard error was 0.11.

Table 52. MRI comparison for Definition 2 Disease

		MRI Reporter 2				Total
		MRI Score 2	MRI Score 3	MRI Score 4	MRI Score 5	
MRI reporter 1	MRI Score 2	2	4	1	1	8
	MRI Score 3	1	15	3	0	19
	MRI Score 4	0	4	4	3	11
	MRI Score 5	1	0	3	8	12
Totals		4	23	11	12	50
Key						
Direct MRI score agreement						

Assessing the agreement when radiologists were asked to score for the likelihood of definition 2 disease cancer (Table 52), agreement worsened slightly to 58% (n=29/50), with

Kappa values = 0.41, standard error = 0.08 (moderate agreement). Weighted agreement = 87%, K=0.52, standard error=0.10 (moderate agreement).

Table 53. MRI reporter comparison for Definition 1 Disease

		MRI Reporter 2					Total
		MRI Score 1	MRI Score 2	MRI Score 3	MRI Score 4	MRI Score 5	
MRI reporter 1	MRI Score 1	3	1	4	0	1	9
	MRI Score 2	0	13	8	1	0	22
	MRI Score 3	0	1	3	0	1	5
	MRI Score 4	0	0	3	3	0	6
	MRI Score 5	0	0	1	2	5	8
	Totals	3	15	19	6	7	50
Key							
Direct MRI score agreement							

For definition 1 disease agreement on MRI score between the two reporters was 54% (n= 27/50), K= 0.41, standard error= 0.067 (moderate agreement). Weighted agreement was 83.5%, K=0.53, standard error=0.089 (moderate agreement) (Table 53).

When comparing MRI scores for each reported to histology on TPM, there were minimal differences between each reporter in terms of AUROC analyses (Table 54).

Table 54. AUROC curve analysis for each reporter

	Reporter 1 ROC (95%CI)	Reporter 2 ROC (95%CI)
Any Cancer	0.61 (0.42-0.79)	0.60 (0.37-0.82)
Definition 2	0.76 (0.63-0.89)	0.75 (0.61-0.89)
Definition 1	0.72 (0.58-0.86)	0.70 (0.56-0.84)

6.1.1 Discussion of Multiparametric MRI Reliability Results

The mpMRI inter-reporter reliability analyses showed an acceptable level of agreement between two independent radiologists when scoring MRI using consensus agreed MRI 'likert' scale reporting. Kappa values for all definitions of disease significance demonstrate moderate agreement.

Also, there was little variation in AUROC curves for disease detection (sensitivity and specificity) between each observer for all definitions of significance.

6.2 Prostate HistoScanning Reproducibility Results

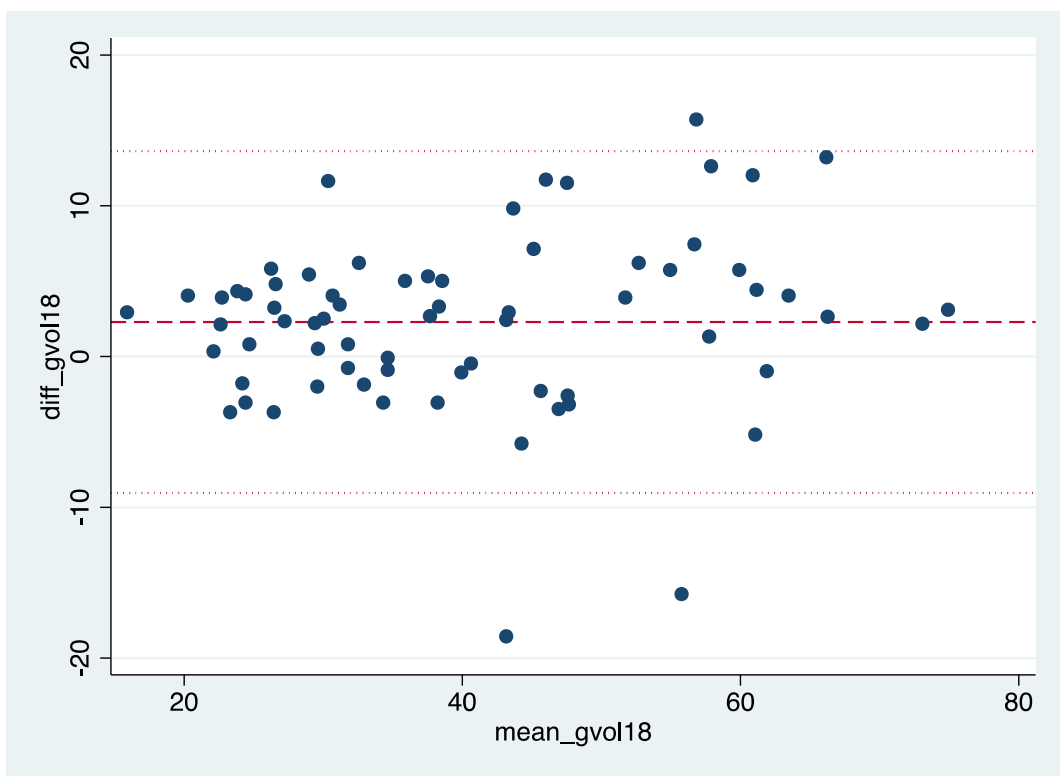
6.2.1 Test re-test Reliability - 8818 to 8818 Comparison

70 men had both 8818 scans at consent and prior to TPM. Mean gland volumes at consent were 39.43cc (SD 1.73); prior to TPM, mean gland volumes were 41.7cc (SD 1.82).

$t = 3.28$, $\Pr(T < t) = 0.9992$ $\Pr(|T| > |t|) = 0.0016$ $\Pr(T > t) = 0.0008$

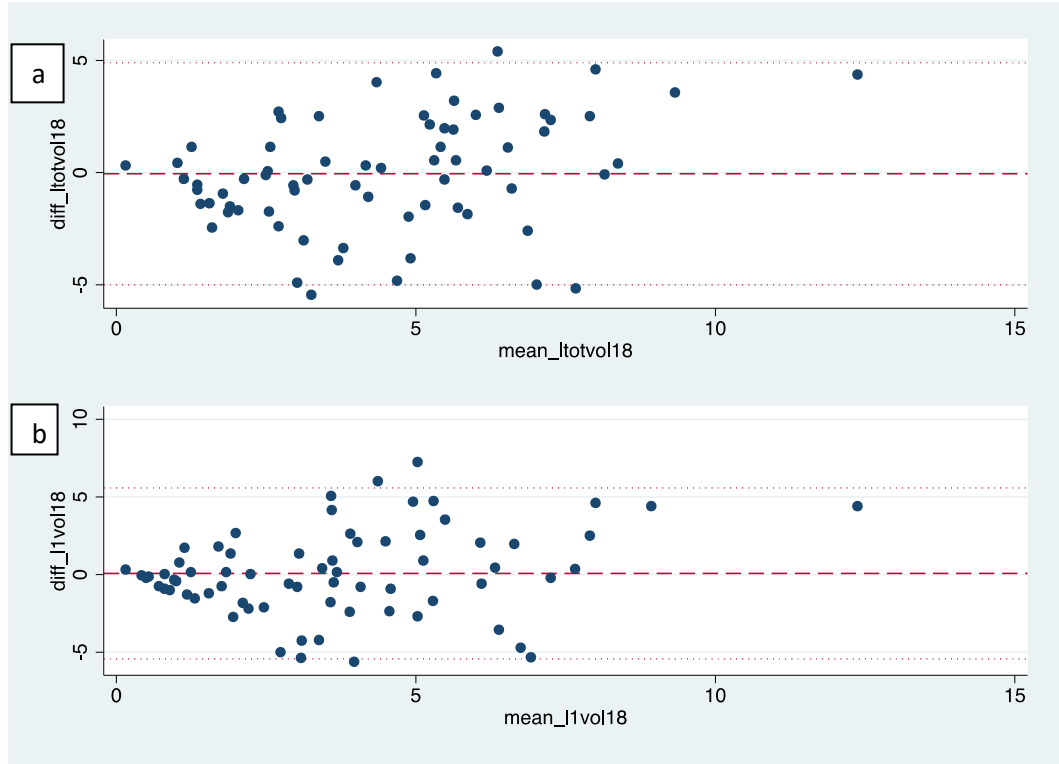
Figure 60 shows a Bland Altman plot showing limits of agreement for gland volume, for gland volume on probe 8818 the average difference between the 2 time points was 2.3 and the lower and upper limits of agreement were -9.0 and 13.6.

Figure 60. *Bland Altman plot of 8818 gland volume at consent and prior to TPM*



Predicted cancer volume agreement (Figure 61a) between the two scans showed a mean difference -0.5cc, with lower and upper limits of agreement of -4.99 and 4.89 respectively. Index lesion volumes showed a mean difference 0.07cc lower and upper limits of agreement of -5.42 to 5.57 respectively (Figure 61b).

Figure 61. Bland Altman plot of 8818 total predicted cancer (totvol) volume and lesion (l1vol) volume at consent and prior to TPM



6.2.2 8818 vs. 8848 Probe Comparison

201 men had both 8818 and 8848 scan at baseline. Paired t test of prostate volume showed $t=0.0748$, $\Pr(T < t) = 0.5298$, $\Pr(|T| > |t|) = 0.9405$, $\Pr(T > t) = 0.4702$.

Average difference between gland volumes was 0.02cc with lower and upper limits of agreement of -8.38 and 8.43 respectively (Figure 62).

Cancer volumes demonstrated a mean difference -2.07cc, with lower and upper limits of agreement of -8.90-4.76 (Figure 63a). Lesion volumes showed an average difference -2.18cc, with lower and upper limits of agreement of -9.40 to 5.04 (Figure 63b).

Figure 62. Comparing probes 8818 & 8848 at baseline- Gland Volume

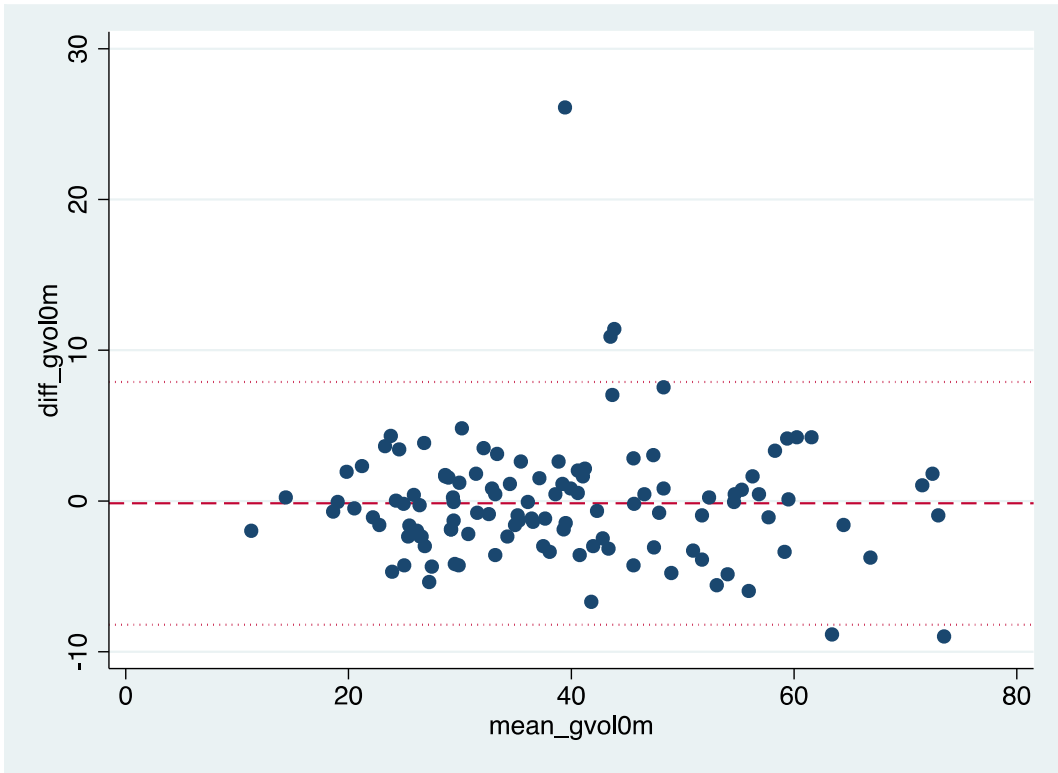
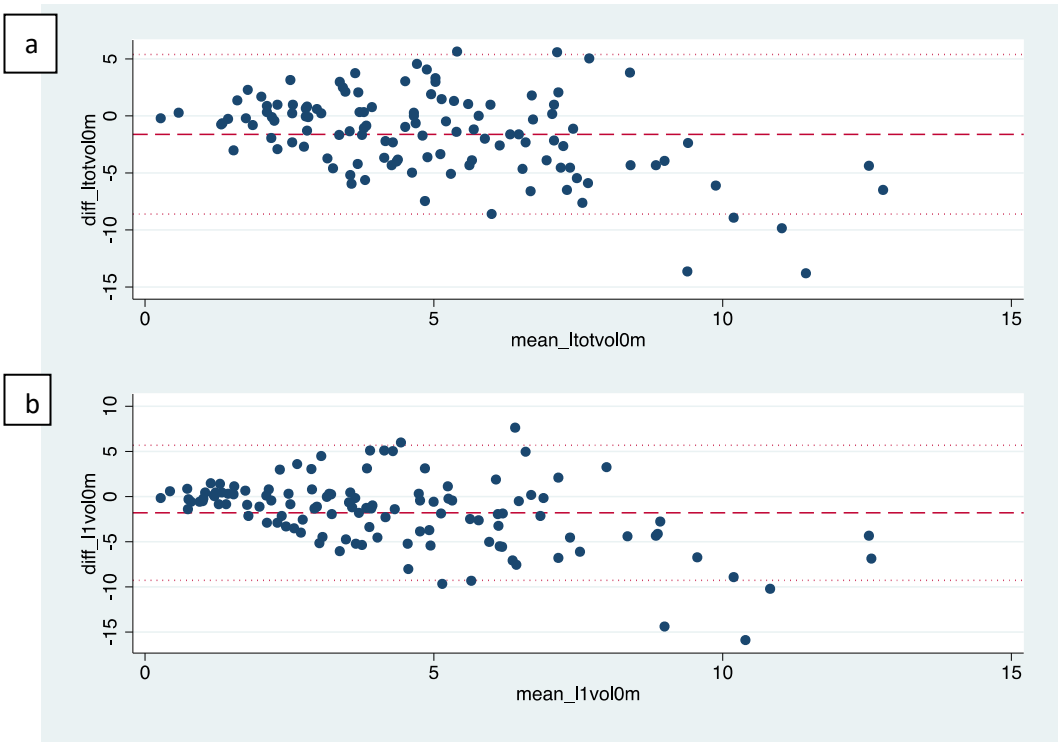


Figure 63. Comparing probes 8818 & 8848 at baseline-

a) Total cancer volume (totvol0m), b) Index lesion volume (l1vol0m)



6.2.3 Discussion of HistoScanning Reliability Results

In summary, the PHS reliability work in PICTURE showed that the results of PHS, both in terms of gland size and lesion volume, were not stable between two time points using the same probe. In fact, gland volume varied by as much as -9.0 and 13.6cc.

For a test to be reliable it needs to demonstrate not only high performance characteristics for the detection of disease but also it needs to be reliable when applied sequentially across time points.

The high variability in both the volume of the prostate gland and the volume of prostate lesions seen using prostate HistoScanning in this cohort deem the test almost unusable. For example, if Prostate HistoScanning were to be employed in an active surveillance cohort, there would be no way of detecting if the growth in lesion size seen was true growth, or if it was simply as a result of the unreliability of the test over several time points.

The 8848 side fire probe was, included in the PICTURE Study and used at the time of consent to scan each patient's prostate. As part of the secondary analysis for the PICTURE study the volumes of the gland and lesion at 8818 scan and 8848 scan both performed at the same time period were assessed; once again, the Bland Altman plots for the comparison between these two tests showed a large degree of difference, suggesting that the PHS software is not stable across different ultrasound probes.

When comparing between the two different ultrasound probes (8818 and 8848) it is worth considering that the developers of HistoScanning deemed the PHS algorithm for the 8848 Prostate HistoScanning probe incomplete at the time of the PICTURE Study, and this may have impacted on its' abilities.

6.3 Biomarker Analysis

6.3.1 Engrailed 2 Urine Biomarker

The urine biomarker in the PICTURE Study was Engrailed 2 (EN2). Participation in the biomarker analysis aspect of the study was optional. Overall 64 men participated in EN2 analysis. Mean EN2 values 14.4 (SD 7.07), Median 12 (IQR 9.3-18.05).

Table 55, Figure 64 and Figure 65 displays the AUROC for EN2 for the detection of both definition one and definition 2 disease, respectively.

Unfortunately no reliable pattern of EN2 value was found to predict disease. Previous studies had found that a cut off value of 42.5ng/mL had sensitivity and specificity of 66% and 88%, our work did not support these findings (Table 56).

Table 55. Engrailed 2, Citrate and Zinc Performance AUROC analysis

Marker	Definition 1 cancer		Definition 2 cancer	
	AUROC (95% CI)	N (%) with cancer	AUROC (95% CI)	N (%) with cancer
EN2 n=64	0.62 (0.48, 0.76)	30 (47%)	0.68 (0.54, 0.81)	41 (64%)
Citrate n=77	0.51 (0.37, 0.64)	34 (44%)	0.42 (0.29, 0.56)	55 (71%)
Zinc n=77	0.52 (0.39, 0.66)	34 (44%)	0.46 (0.32, 0.60)	55 (71%)

Figure 64. EN2 vs. Definition one cancer

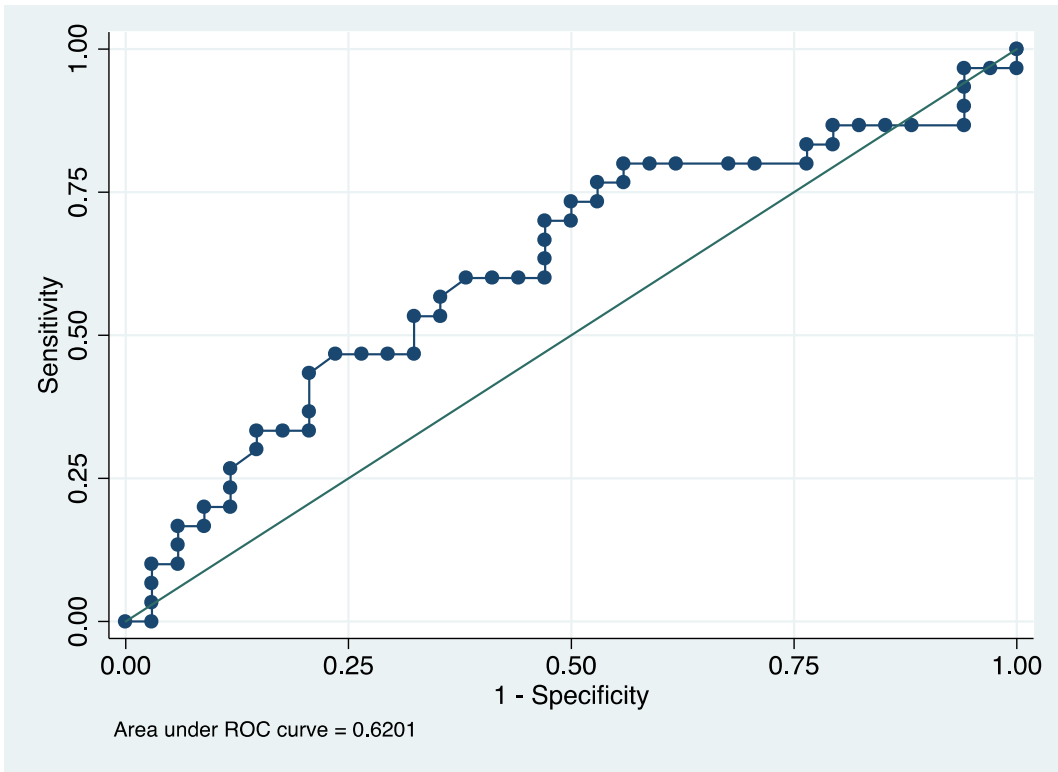


Figure 65. EN2 vs. Definition two cancer

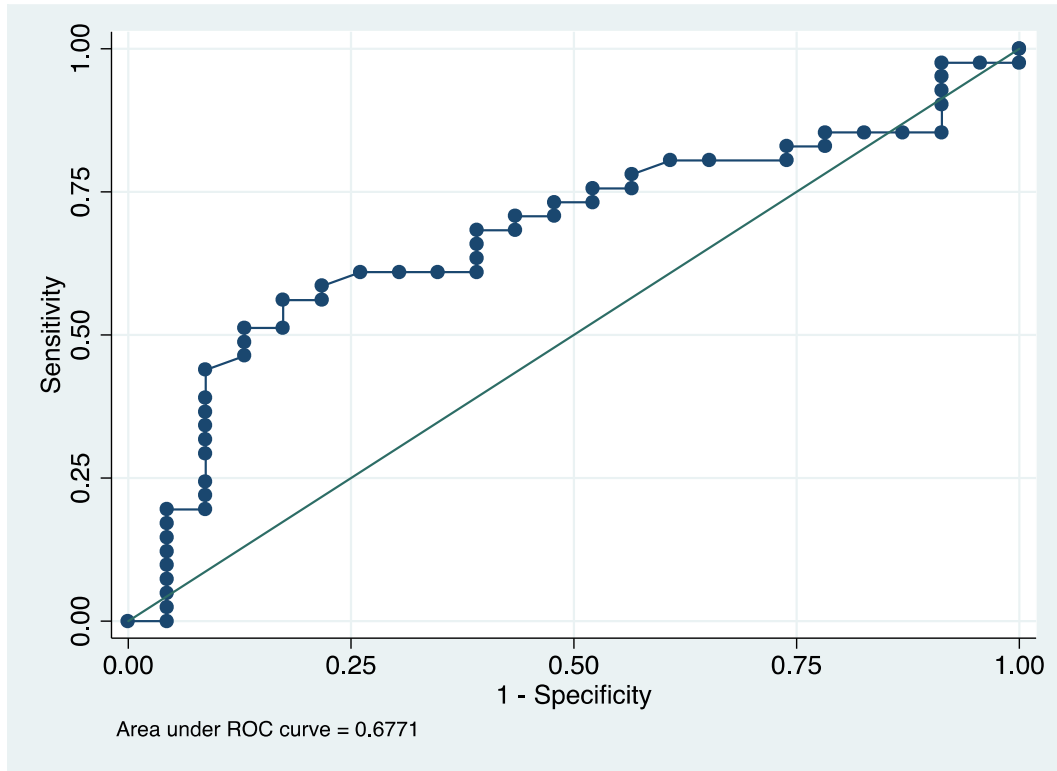


Table 56. EN2, Citrate and Zinc levels at varying disease thresholds

	Stats	EN2	Citrate	Zinc
Definition one cancer				
Benign	Mean	13.31	37.13	2.14
	(SD)	(6.9)	(30.37)	(2.16)
Definition one cancer	Mean	15.73	32.11	1.99
	(SD)	(7.06)	(20.05)	(1.76)
Definition two cancer				
Benign	Mean	15.74	36.51	2.24
	(SD)	(6.86)	(28.11)	(2.13)
Definition two cancer	Mean	14.44	34.91	2.08
	(SD)	(7.07)	(26.28)	(1.98)
Scores by Gleason grade				
Gleason <7	Mean	13.3	31.26	1.68
	(SD)	(7.35)	(19.78)	(1.38)
Gleason ≥7	Mean	15.34	37.38	2.34
	(SD)	(6.80)	(29.83)	(2.27)

6.3.2 FScan

Unfortunately, poor results for the FScan citrate and zinc assay were also found in our patient population, with the AUROC curve for both definition one and definition two cancer being around 50% (Table 55). Our results did not support the earlier findings that a lower citrate and zinc level was predictive of prostate cancer, nor was any correlation seen with cancer grade.

7 PICTURE Discussion

7.1 PICTURE Study Limitations

Prior to the summation and discussion of the PICTURE Study results, it is important to highlight some important limitations of the study that have direct implications for the application of the study's findings in the prostate cancer pathway.

1. The main limitation is that the PICTURE Study investigated men in whom a prior TRUS biopsy had already been performed but diagnostic uncertainty remained.

Although the investigation of imaging at this time point in the prostate cancer pathway captures a large group of men for whom imaging may be useful, it does not fully address the issue of prostate cancer detection in all men at risk. By this time point in the pathway a subset of men will have already gone on to treatment or been classified (correctly or incorrectly) as benign by their first prostate biopsy.

There are, however, many stages at which imaging may be a useful triage test in the prostate cancer pathway. For the cohort of men for whom a first TRUS biopsy has delivered uncertainty of diagnosis, the addition of mpMRI imaging to the pathway is attractive, and the results of the work within this study suggest it would be a useful addition.

2. The single centre nature of the PICTURE Study is also a limitation to the applicability of our findings. Whilst it is encouraging that within an expert centre high performance characteristics for the detection of clinically significant disease were demonstrated, one of the major criticisms of mpMRI to date is that results are not easily replicated outside of expert centres.

Further limitations of the PICTURE Study relates to the various methodological flaws.

3. All men in the study had been through the process of TRUS guided biopsy of the prostate prior to enrolment. It is acknowledged that prior prostate biopsy can cause alteration of the MRI images for a considerable amount of time post biopsy- with some literature suggesting that biopsy artefact can last up to one year (Qayyum et al., 2004, Tamada et al., 2008b, White et al., 1995).

Within the PICTURE Study no formal time limit was set on the time between MRI and biopsy; however; due to the work flow in the study, men had normally had 3-6 months from the time of their biopsy before enrolment. There may still, however, from the prior biopsies have been some element of image degradation that may have affected the performance characteristics demonstrated.

4. The PICTURE Study mpMRI's were performed predominantly on the 3 tesla MRI scanner at University College London Hospitals, where the 3T scanner was installed shortly prior to the commencement of the study.

The first 50 - 100 cases recruited to the PICTURE Study were a part of the familiarisation process and learning curve for this scanner. It is widely held that MRI magnets require slight 'tweaks' to their programming to ensure the best image acquisition; also scans performed at different field strengths and on different magnets may appear slightly different and as such the radiologist is required to 'learn' the interpretation of these mpMRI images. The familiarisation process for the new scanner may have impacted on the PICTURE results.

5. A further limitation to the work of this study relates to the targeting system used for the MRI/US fusion biopsies. The hardware and software used within the study were part of an early prototype device for the technology that had been designed at UCL. Its use within the PICTURE Study was to enable further refinement of the technology and start the validation process. It is important to consider this when assessing the MRI/US targeted results.
6. Another factor that may have impacted on the interpretation of the targeted results is the fact that targeted sampling was limited to only the largest lesion on PHS and the most suspicious lesion on mpMRI reporting: not all lesions seen were targeted. Targeted sampling was limited as well to the 2-3 cores per targeting methodology, per lesion; this low number of cores is likely to be unrepresentative of what would be required in everyday practice.
7. The PICTURE study did not include any cost effectiveness modelling. In today's economic climate this is a major flaw, as the addition of any new diagnostic test to a pathway needs to be evaluated not only for its value but also for its economic impact. A recent meta-analysis by Willis et al (Willis et al, 2015) has looked at the paucity of

data in this area, finding only 5 studies that relate to the cost impact of mpMRI on the prostate cancer pathway.

7.2 Summary of PICTURE Study Results

Prostate HistoScanning demonstrated poor ability in the discrimination of benign from malignant tissue. The AUC seen in the PICTURE Study for PHS is worse than chance (AUC=0.43). Although demonstrating 70.3% (95% CI 59.8-79.5) sensitivity for the detection of cancer volumes $\geq 1.3\text{cc}$, specificity was only 14.7% (95% CI 9.1-22.0).

PHS targeted biopsies demonstrated only a 23% disease concordance with transperineal template mapping biopsies, thus only 1 in 5 men were correctly classified by this technique.

Also, poor reproducibility of PHS for the detection of lesion size between two time periods was demonstrated.

Conversely, mpMRI has shown promising disease detection characteristics, with mpMRI demonstrating 80.6% (95% CI 71.6-87.7) sensitivity and 68.5% (95% CI 60.3-75.9) specificity, for the detection of clinically significant disease. The area under ROC curves for mpMRI was 0.76 (95% CI 0.69-0.80).

Whilst these results are very encouraging, being far better than the diagnostic performance characteristics for the current tests available for prostate cancer. In terms of diagnostic tests more globally mpMRI has not shown excellent specificity, and one should consider that although mpMRI may be at present our best diagnostic hope, Urologists should continue to strive for improvements in the diagnostic accuracy of the test.

MRI-targeted biopsies had a detection rate of 78.6% (95% CI 69.9-82.1) for clinically significant cancer when lesions scoring 3 or greater on mpMRI were considered.

Further analysis of the pooled MRI targeting data demonstrated that the majority of targeting errors seen in the PICTURE Study (55%) were classified as in-field targeting errors (i.e. correctly called on mpMRI however incorrectly localised/targeted at the time of sampling).

The mpMRI inter-reporter reliability analyses showed little variation in AUROC curve analysis for the two reporters in a subset of PICTURE Study mpMRI's. For all definitions of

disease significance kappa values indicating moderate agreement between two independent radiologists when scoring mpMRI using consensus agreed MRI 'likert' scale reporting, was found.

7.3 PICTURE Study Conclusions

The PICTURE Study results demonstrate that mpMRI may be a useful imaging tool in the prostate cancer diagnostic pathway, and that mpMRI targeted biopsy is a technique that allows accurate risk stratification with fewer biopsy cores. The further analysis of the targeted data within PICTURE demonstrating predominantly in-field targeting errors suggests that mpMRI targeted biopsy strategies may be even more accurate once further refinement is carried out to the technique of MRI/US guidance.

Results for prostate HistoScanning have demonstrated that PHS is not a useful tool in the detection of prostate cancer, and the PICTURE Study results do not support further adoption of this technique.

8 Critical Analysis of Work and Thesis Discussion

8.1 Main Limitations

The main limitations of the studies within this body of work have been discussed in the previous chapters regarding the limitations of the PHS02 and PICTURE studies.

With regards to the PHS02 study, a limitation that has not previously been addressed is the commercially sponsored nature of the study and the possible bias that this may have introduced.

PHS02 was a company funded study developed to validate the technology, although the study was run in an objective and methodologically sound manner. With input from independent monitors and rigorous blinding within the blind phase, there is a possibility that influence of the developers on patient selection criteria could have led to biased results.

The very strict patient selection criteria imposed in the study by the company does not reflect the nature of everyday prostate cancer detection and therefore limits the applicability of the results of the study to current practices in prostate cancer diagnosis.

A key limitation to the applicability of the findings of the PICTURE study to current prostate cancer pathways pertains to the single centre nature of the study. Whilst the results of the PICTURE Study for the use of mpMRI are sufficiently promising as to suggest that widespread adoption of the technique of mpMRI, and that of mpMRI targeted biopsy, it is vital that the results are replicated in large multi-centre trials.

8.2 Novel Contributions

This research has examined the role of prostate cancer detection using innovative imaging namely, Prostate HistoScanning and Multiparametric magnetic resonance imaging. Through the evolution of the studies that have formulated this thesis, some of the many challenges that face the adoption of a new technique in the prostate cancer pathway have been highlighted.

The findings of this thesis can be summarised as follows:-

➤ **Prostate HistoScanning has no role in prostate cancer detection**

Prostate HistoScanning was a new and promising technology at the start of this research. Through the experiments performed using the prostate HistoScanning technology for prostate cancer detection - firstly in validation studies against radical prostatectomy and latterly in verification testing against template mapping biopsy, a less biased reference test - a disappointing failure of the technology to accurately identify disease has been seen.

Throughout the time given to this research the results for the technology became less and less reliable: with the PICTURE Study revealing that prostate HistoScanning was no more use in predicting prostate cancer than chance. The poor results for PHS from the PICTURE Study have also been replicated by other independent research groups (Javed et al., 2013, Schiffmann et al., 2014b, Schiffmann et al., 2015, Schiffmann et al., 2014a).

Whilst disappointing that a technology could show such promise only to be found to be unreliable the tale of prostate HistoScanning is informative to the rapidly changing face of medicine, biomarkers and medical devices. It has highlighted the importance of thorough and rigorous clinical testing of biomarkers and medical devices prior to the implementation of their use on a wider clinical scale.

➤ **Multiparametric MRI is a useful tool for men in whom diagnostic uncertainty remains following primary biopsy**

This thesis in part aimed to assess the role of mpMRI for men in whom diagnostic uncertainty remained regarding their prostate cancer risk stratification. The PICTURE Study results demonstrated that for this group of men mpMRI is a useful tool to enable further risk stratification.

The PICTURE Study showed that men with a negative MRI have a low likelihood of harbouring significant prostate cancer (NPV 83.3%), and that mpMRI demonstrated has a high sensitivity for the detection of clinically significant disease - 80.6%.

These promising performance characteristics for mpMRI have proven the thesis' hypothesis that imaging in the prostate cancer pathway can be a useful tool, and that it may afford

men (who have undergone previous biopsy) – a better more accurate risk stratification without immediate further biopsy.

Multi-parametric MRI has demonstrated that for men who have a negative mpMRI, further biopsy could be safely avoided; additionally, for those with an mpMRI lesion the results of PICTURE suggest that a targeted biopsy approach may enable accurate risk stratification with far fewer biopsy cores than template mapping prostate biopsy.

The findings of this thesis are in keeping with the recommendations made by prominent advisory bodies for urology during the evolution of this study: namely, that imaging should be used for men in whom diagnostic uncertainty remains (National Institute for Health and Care Excellence, 2014b, Heidenreich et al., 2014).

➤ **Multiparametric MRI targeted biopsy provides accurate risk stratification, with fewer cores than TPM biopsy**

Alongside the usefulness of mpMRI in sparing men with a negative test the morbidity associated with repeat prostate biopsy, the work evaluating the role of targeted biopsy has shown the mpMRI targeted biopsies can detect most cancers found at template mapping biopsy with far fewer biopsy cores, and thus greater sampling efficiency.

This targeted approach could in the future lead to a diagnostic pathway that places a smaller burden in terms of morbidity on the patient (fewer cores are likely to lead to less infection, pain and other side effects).

Image directed targeted biopsy would allow for faster, more efficient biopsies to be performed - most likely under local anaesthetic - and the reduction in cores will mean a lesser burden not only on the patient but also on histopathology processing times and costs.

There were, as discussed in the previous chapter, a number of limitations to the targeted biopsy work within the PICTURE Study, which may have negatively affected the performance characteristics of targeting and led to the ultimate conclusion that as yet systematic biopsy cannot be disregarded. With further development of MRI/US registration technologies, it is likely that this technology will become the most preferred method for prostate cancer detection globally.

It is important to remember that all biopsy strategies will miss some disease, as shown in chapter 4.4, when modelling biopsy techniques, even the most stringent 5m template biopsy strategy did not detect all disease. Financially it is unsustainable within the NHS to focus on a transperineal template mapping biopsy techniques as they have such a high burden - in terms of operating time (requires general anaesthetic and theatre time), histological processing time and side effect profile.

Therefore, it is important that researchers do not strive for the 'perfect' test, but instead that techniques are adopted that allow a high degree of accuracy, in a manner that is both feasible economically and logistically. Multiparametric-MRI targeted biopsy strategies have shown great potential in being able to offer this, with the results of the PICTURE Study demonstrating detection rates almost in keeping with full 5mm TPM, with on average 4.2 biopsy cores rather than the average 48 cores taken at TPM.

8.3 Impact and Future Directions

The impact of the results of this thesis has already been evidenced by the change in practice at University College Hospitals London. There has been an adoption of the practice of a local anaesthetic 'cognitive' targeted transperineal targeted biopsy following mpMRI for men at risk of prostate cancer.

This research has however highlighted several areas for further work and development of the technology of mpMRI and also MRI guided targeted biopsy.

Firstly, it is vital that a large multi-centre trial is performed to assess the use of mpMRI in men prior to biopsy. Such a study should not only assess the performance characteristics of the test but should assess the cost implications for the adoption of MRI at this early stage in the pathway.

Such a study is already underway in the UK and publication of the results is anticipated in early 2016 (El-Shater Bosaily et al., 2015).

For mpMRI to remain a viable option for prostate cancer diagnosis it will need to continue to demonstrate the high performance characteristics found in the PICTURE study for mpMRI in men who have not undergone previous TRUS biopsy.

The multi-centre nature of such a study should allay any concern regarding the inability of lower volume, less specialist centres to be able to reproduce the mpMRI imaging results of more specialist centres. The economic modelling of the study is also vital in the current economic climate.

Another area for further research that has been highlighted by this study is the need for continued development of the novel MRI/US platform for the use in targeting areas seen on mpMRI.

The results from the PICTURE Study did not demonstrate a great improvement in detection by the use of MRI/US fusion over 'cognitive targeting'; this may however be due to the prototype device used in the study, or the expertise of those performing the 'cognitive' biopsy.

With further investigation and refinement of MRI/US fusion technology however, it seems likely that it might prove to be useful and become a widely adopted technique amongst urologists.

There currently is a number of MRI/US biopsy platforms on the market (ARTEMIS/ Eigen fusion etc.) none, however, has the ability to deform to a prostate as that developed at University College London and used within PICTURE.

A study that targets all lesions seen at MRI (and not just the primary as taken in PICTURE), using a more developed prototype of the UCL Smart Target system, is required. Currently this study is underway at UCL/UCLH as part of a Wellcome study grant.

It would also seem prudent to examine the use of mpMRI targeted biopsy vs. the gold standard systematic TRUS biopsy.

Several other areas, for further research and development were identified in the evolution of this research.

Many of the studies investigating imaging in prostate cancer divide the prostate into multiple sectors to obtain the results. Further work is required to assess the effect of such a methodology on the performance characteristics of a test.

The added value of each of the mpMRI sequences for the detection of disease also needs to be assessed. As discussed when reviewing the MRI literature in chapter two, several groups have looked at a couple of the sequences of mpMRI. By assessing the additive value

of each of the sequences included in an mpMRI by assessing sequential reporting it can be determined if each sequence is required in the mpMRI pathway. If, for example, DCE imaging was found to have little additive diagnostic value, it may be able to be avoided in mpMRI; thus, reducing the time taken to perform mpMRI and the cost in doing so - also the need not to require intravenous contrast is attractive.

A further element of study that is required is the development of a computer aided diagnosis (CAD) mpMRI reporting system. It is felt that by adding CAD to mpMRI reporting improved reporter accuracy and reduced inter-reported variability may be enabled. Such a technique may be able to rapidly decrease the learning curve of radiologists and enable easier widespread adoption of mpMRI for prostate cancer detection. Work is underway at UCL/UCLH to try and develop such a system.

8.4 Summary

Prostate cancer remains a large problem facing today's society. A large number of men will be labelled with the disease and suffer the morbidity and concern that the diagnosis and its investigations entails. Currently, there exists no consensus amongst experts on the use of imaging in the prostate cancer diagnostic pathway, however momentum is gathering in the support for this paradigm shift and the adoption of an imaging biomarker. This momentum is evidenced by statements from NICE guidance suggesting the use of mpMRI for men with previous negative TRUS biopsy (National Institute for Health and Care Excellence, 2014b).

The history of prostate cancer diagnosis draws many parallels to that of breast cancer diagnosis; however, the urological community seem some decades behind their breast surgical colleagues. Blind random sampling of breast tissue without imaging has not been performed since the introduction of the use of mammograms in the late 1980's.

It has been argued that breast cancer screening with mammography and ultrasound altered the landscape of breast cancer diagnosis for the better; however, at the time of its inception, and still, there remain supporters both for and against its introduction (Otto and Blecher, 2014, Fuller et al., 2015).

Similarly now, within the urological community there are supporters both for and against imaging in the diagnostic pathway. It is generally agreed upon by experts that not all prostate cancers require treatment (Wilt, 2012), indeed, it may be better for men with low

volume, low risk disease if they are never diagnosed and attributed a prostate cancer diagnosis. It has also been acknowledged that there is a lack of clear risk stratification for men - with many men undergoing either immediate upgrading or downgrading of disease on subsequent biopsies or at the time of their treatment.

The body of evidence for the use of imaging in the prostate cancer pathway, especially mpMRI is growing. However, there remains a scepticism surrounding its widespread adoption, in part because of the criticism that mpMRI not only misses low volume low grade disease but also because it is difficult to reproduce high quality mpMRI images and reports in every centre.

Although, the work in this thesis does not overcome all of the barriers to adoption that imaging for prostate cancer faces. It could be argued that the results of the PICTURE Study are sufficiently promising as to warrant much more widespread adoption of mpMRI and mpMRI targeted biopsy.

To the criticism that mpMRI does not detect all disease, it appears that it is not important to detect the very low volume, low risk disease that MRI is likely to miss: in fact, these men may be better off without a diagnosis of prostate cancer.

With regards to the difficulty of performing these technique outside of specialist prostate centres, it seems that with the correct training and motivation radiologists can improve their proficiency in reading an mpMRI scan (Gaziev et al., 2014, Latchamsetty et al., 2007), and therefore this should not be allowed to become a barrier to a test that may ultimately help men globally.

Finally, a word of caution with regards to the uptake of new technologies. During this research, a number of novel forms of prostate cancer diagnosis were presented – it is after all, a politically and financially attractive area of work for many entrepreneurs: this thesis, however, has demonstrated that rigorous testing of all biomarkers (imaging and biological) is required before widespread adoption.

Urologists must ensure that there is high quality level 1 evidence available for these technologies before they become of general use; allowing devices or biomarkers to become part of our routine practice prior to this rigorous testing could have harmful implications economically and medically for a large number of men.

9 Bibliography

- AHMAD, S., CAO, R., VARGHESE, T., BIDAUT, L. & NABI, G. 2013. Transrectal quantitative shear wave elastography in the detection and characterisation of prostate cancer. *Surg Endosc*, 27, 3280-7.
- AHMED, H. U., ARYA, M., FREEMAN, A. & EMBERTON, M. 2012. Do low-grade and low-volume prostate cancers bear the hallmarks of malignancy? *Lancet Oncol*, 13, e509-17.
- AHMED, H. U., HU, Y., CARTER, T., ARUMAINAYAGAM, N., LECORNET, E., FREEMAN, A., HAWKES, D., BARRATT, D. C. & EMBERTON, M. 2011. Characterizing clinically significant prostate cancer using template prostate mapping biopsy. *J Urol*, 186, 458-64.
- AHMED, H. U., KIRKHAM, A., ARYA, M., ILLING, R., FREEMAN, A., ALLEN, C. & EMBERTON, M. 2009. Is it time to consider a role for MRI before prostate biopsy? *Nat Rev Clin Oncol*, 6, 197-206.
- AIGNER, F., MITTERBERGER, M., REHDER, P., PALLWEIN, L., JUNKER, D., HORNINGER, W. & FRAUSCHER, F. 2010. Status of transrectal ultrasound imaging of the prostate. *J Endourol*, 24, 685-91.
- AKIN, O., SALA, E., MOSKOWITZ, C. S., KUROIWA, K., ISHILL, N. M., PUCAR, D., SCARDINO, P. T. & HRICAK, H. 2006. Transition zone prostate cancers: features, detection, localization, and staging at endorectal MR imaging. *Radiology*, 239, 784-92.
- ALTMAN, D. G. 1991. *Practical statistics for Medical research*, Chapman and Hall.
- ANDERSON, A. W., XIE, J., PIZZONIA, J., BRONEN, R. A., SPENCER, D. D. & GORE, J. C. 2000. Effects of cell volume fraction changes on apparent diffusion in human cells. *Magn Reson Imaging*, 18, 689-95.
- AUTORINO, R., DI LORENZO, G., DAMIANO, R., GIANNARINI, G., DE SIO, M., CHENG, L. & MONTIRONI, R. 2009. Pathology of the prostate in radical cystectomy specimens: a critical review. *Surg Oncol*, 18, 73-84.
- AYDIN, H., HEKIMOGLU, B. & TATAR, I. G. 2013a. Limitations, disabilities, and pitfalls of dynamic contrast-enhanced MRI as a diagnostic modality in prostate cancer. *AJR Am J Roentgenol*, 200, W326.
- AYDIN, H., HEKIMOGLU, B. & KIZILGOZ, V. 2013b. A brief review of the combined use of T2-weighted MRI and diffusion-weighted imaging for prostate cancer diagnosis. *AJR Am J Roentgenol*, 200, W219.
- AYDIN, H., KIZILGOZ, V., TATAR, I. G., DAMAR, C., UGAN, A. R., PAKER, I. & HEKIMOGLU, B. 2012. Detection of prostate cancer with magnetic resonance imaging: optimization of T1-weighted, T2-weighted, dynamic-enhanced T1-weighted, diffusion-weighted imaging apparent diffusion coefficient mapping sequences and MR spectroscopy, correlated with biopsy and histopathological findings. *J Comput Assist Tomogr*, 36, 30-45.
- AYRES, B. E., MONTGOMERY, B. S., BARBER, N. J., PEREIRA, N., LANGLEY, S. E., DENHAM, P. & BOTT, S. R. 2012. The role of transperineal template prostate biopsies in restaging men with prostate cancer managed by active surveillance. *BJU Int*, 109, 1170-6.

- BANGMA, C. H., ROEMELING, S. & SCHRODER, F. H. 2007. Overdiagnosis and overtreatment of early detected prostate cancer. *World J Urol*, 25, 3-9.
- BARENTSZ, J., VILLERS, A. & SCHOUTEN, M. 2013. ESUR prostate MR guidelines. Author reply. *Eur Radiol*, 23, 2322-3.
- BARENTSZ, J. O., RICHENBERG, J., CLEMENTS, R., CHOYKE, P., VERMA, S., VILLEIRS, G., ROUVIERE, O., LOGAGER, V. & FUTTERER, J. J. 2012a. ESUR prostate MR guidelines 2012. *Eur Radiol*, 22, 746-57.
- BARENTSZ, J. O., RICHENBERG, J., CLEMENTS, R., CHOYKE, P., VERMA, S., VILLEIRS, G., ROUVIERE, O., LOGAGER, V., FUTTERER, J. J. & EUROPEAN SOCIETY OF UROGENITAL, R. 2012b. ESUR prostate MR guidelines 2012. *Eur Radiol*, 22, 746-57.
- BARR, R. G., MEMO, R. & SCHAUB, C. R. 2012. Shear wave ultrasound elastography of the prostate: initial results. *Ultrasound Q*, 28, 13-20.
- BARZELL, W. E., MELAMED, M. R., CATHCART, P., MOORE, C. M., AHMED, H. U. & EMBERTON, M. 2012. Identifying candidates for active surveillance: an evaluation of the repeat biopsy strategy for men with favorable risk prostate cancer. *J Urol*, 188, 762-7.
- BERMAN, D. M. & EPSTEIN, J. I. 2014. When is Prostate Cancer Really Cancer? *Urol Clin North Am*, 41, 339-346.
- BILL-AXELSON, A., HOLMBERG, L., RUUTU, M., HAGGMAN, M., ANDERSSON, S. O., BRATELL, S., SPANGBERG, A., BUSCH, C., NORDLING, S., GARMO, H., PALMGREN, J., ADAMI, H. O., NORLEN, B. J. & JOHANSSON, J. E. 2005. Radical prostatectomy versus watchful waiting in early prostate cancer. *N Engl J Med*, 352, 1977-84.
- BITTENCOURT, L. K., HAUSMANN, D., SABANEEFF, N., GASPARETTO, E. L. & BARENTSZ, J. O. 2014. Multiparametric magnetic resonance imaging of the prostate: current concepts. *Radiol Bras*, 47, 292-300.
- BLAND, J. M. & ALTMAN, D. G. 1986. Statistical methods for assessing agreement between two methods of clinical measurement. *Lancet*, 1, 307-10.
- BOEHM, K., SALOMON, G., BEYER, B., SCHIFFMANN, J., SIMONIS, K., GRAEFEN, M. & BUDAEUS, L. 2015. Shear wave elastography for localization of prostate cancer lesions and assessment of elasticity thresholds: implications for targeted biopsies and active surveillance protocols. *J Urol*, 193, 794-800.
- BONEKAMP, D., JACOBS, M. A., EL-KHOULI, R., STOIANOVICI, D. & MACURA, K. J. 2011. Advancements in MR imaging of the prostate: from diagnosis to interventions. *Radiographics*, 31, 677-703.
- BOSSUYT, P. M., REITSMA, J. B., BRUNS, D. E., GATSONIS, C. A., GLASZIOU, P. P., IRWIG, L. M., LIJMER, J. G., MOHER, D., RENNIE, D. & DE VET, H. C. 2003. Towards complete and accurate reporting of studies of diagnostic accuracy: the STARD initiative. *Clin Biochem*, 36, 2-7.
- BOTT, S. R., YOUNG, M. P., KELLETT, M. J. & PARKINSON, M. C. 2002. Anterior prostate cancer: is it more difficult to diagnose? *BJU Int*, 89, 886-9.
- BRAECKMAN, J., AUTIER, P., GARBAR, C., MARICHAL, M. P., SOVIANY, C., NIR, R., NIR, D., MICHELSEN, D., BLEIBERG, H., EGEVAD, L. & EMBERTON, M. 2008a. Computer-aided ultrasonography (HistoScanning): a novel technology for locating and characterizing prostate cancer. *BJU Int*, 101, 293-8.

- BRAECKMAN, J., AUTIER, P., SOVIANY, C., NIR, R., NIR, D., MICHELSEN, D., TREURNICHT, K., JARMULOWICZ, M., BLEIBERG, H., GOVINDARAJU, S. & EMBERTON, M. 2008b. The accuracy of transrectal ultrasonography supplemented with computer-aided ultrasonography for detecting small prostate cancers. *BJU Int*, 102, 1560-5.
- BROCK, M., EGGERT, T., PALISAAR, R. J., ROGHMANN, F., BRAUN, K., LOPPENBERG, B., SOMMERER, F., NOLDUS, J. & VON BODMAN, C. 2013. Multiparametric ultrasound of the prostate: adding contrast enhanced ultrasound to real-time elastography to detect histopathologically confirmed cancer. *J Urol*, 189, 93-8.
- BROCK, M., VON BODMAN, C., PALISAAR, R. J., LOPPENBERG, B., SOMMERER, F., DEIX, T., NOLDUS, J. & EGGERT, T. 2012. The impact of real-time elastography guiding a systematic prostate biopsy to improve cancer detection rate: a prospective study of 353 patients. *J Urol*, 187, 2039-43.
- CANCER RESEARCH UK. 2011. <http://www.cancerresearchuk.org/>. Available: <http://www.cancerresearchuk.org/cancer-info/cancerstats/incidence/commoncancers/#Twenty> [Accessed 19/04/2014 2014].
- CANCER RESEARCH UK 2014. CancerStats.
- CHANG, D. T., CHALLACOMBE, B. & LAWRENTSCHUK, N. 2013. Transperineal biopsy of the prostate--is this the future? *Nat Rev Urol*, 10, 690-702.
- CHEN, M., DANG, H. D., WANG, J. Y., ZHOU, C., LI, S. Y., WANG, W. C., ZHAO, W. F., YANG, Z. H., ZHONG, C. Y. & LI, G. Z. 2008. Prostate cancer detection: comparison of T2-weighted imaging, diffusion-weighted imaging, proton magnetic resonance spectroscopic imaging, and the three techniques combined. *Acta Radiol*, 49, 602-10.
- CHO, J. Y., KIM, S. H. & LEE, S. E. 1998. Diffuse prostatic lesions: role of color Doppler and power Doppler ultrasonography. *J Ultrasound Med*, 17, 283-7.
- CHOI, Y. J., KIM, J. K., KIM, N., KIM, K. W., CHOI, E. K. & CHO, K. S. 2007. Functional MR imaging of prostate cancer. *Radiographics*, 27, 63-75; discussion 75-7.
- COOPERBERG, M. R., MOUL, J. W. & CARROLL, P. R. 2005. The changing face of prostate cancer. *J Clin Oncol*, 23, 8146-51.
- COSTELLO, L. C. & FRANKLIN, R. B. 2009. Prostatic fluid electrolyte composition for the screening of prostate cancer: a potential solution to a major problem. *Prostate Cancer Prostatic Dis*, 12, 17-24.
- CRAWFORD, E. D., ROVE, K. O., BARQAWI, A. B., MARONI, P. D., WERAHERA, P. N., BAER, C. A., KOUL, H. K., ROVE, C. A., LUCIA, M. S. & LA ROSA, F. G. 2013. Clinical-pathologic correlation between transperineal mapping biopsies of the prostate and three-dimensional reconstruction of prostatectomy specimens. *Prostate*, 73, 778-87.
- CRAWFORD, E. D., WILSON, S. S., TORKKO, K. C., HIRANO, D., STEWART, J. S., BRAMMELL, C., WILSON, R. S., KAWATA, N., SULLIVAN, H., LUCIA, M. S. & WERAHERA, P. N. 2005. Clinical staging of prostate cancer: a computer-simulated study of transperineal prostate biopsy. *BJU Int*, 96, 999-1004.
- CROSS, T. & MCPHAIL, S. 2008.

- DE JESUS, C. M., CORREA, L. A. & PADOVANI, C. R. 2006. Complications and risk factors in transrectal ultrasound-guided prostate biopsies. *Sao Paulo Med J*, 124, 198-202.
- DELONGCHAMPS, N. B., ROUANNE, M., FLAM, T., BEUVON, F., LIBERATORE, M., ZERBIB, M. & CORNUD, F. 2011. Multiparametric magnetic resonance imaging for the detection and localization of prostate cancer: combination of T2-weighted, dynamic contrast-enhanced and diffusion-weighted imaging. *BJU Int*, 107, 1411-8.
- DICKINSON, L., AHMED, H. U., ALLEN, C., BARENTSZ, J. O., CAREY, B., FUTTERER, J. J., HEIJMINK, S. W., HOSKIN, P., KIRKHAM, A. P., PADHANI, A. R., PERSAD, R., PUECH, P., PUNWANI, S., SOHAIB, A., TOMBAL, B., VILLERS, A. & EMBERTON, M. 2013. Scoring systems used for the interpretation and reporting of multiparametric MRI for prostate cancer detection, localization, and characterization: could standardization lead to improved utilization of imaging within the diagnostic pathway? *J Magn Reson Imaging*, 37, 48-58.
- DICKINSON, L., AHMED, H. U., ALLEN, C., BARENTSZ, J. O., CAREY, B., FUTTERER, J. J., HEIJMINK, S. W., HOSKIN, P. J., KIRKHAM, A., PADHANI, A. R., PERSAD, R., PUECH, P., PUNWANI, S., SOHAIB, A. S., TOMBAL, B., VILLERS, A., VAN DER MEULEN, J. & EMBERTON, M. 2011. Magnetic resonance imaging for the detection, localisation, and characterisation of prostate cancer: recommendations from a European consensus meeting. *Eur Urol*, 59, 477-94.
- DINDYAL, S. & KYRIAKIDES, C. 2011. Ultrasound microbubble contrast and current clinical applications. *Recent Pat Cardiovasc Drug Discov*, 6, 27-41.
- EISENBERG, M. L., COWAN, J. E., CARROLL, P. R. & SHINOHARA, K. 2010. The adjunctive use of power Doppler imaging in the preoperative assessment of prostate cancer. *BJU Int*, 105, 1237-41.
- EL-SHATER BOSAILY, A., PARKER, C., BROWN, L. C., GABE, R., HINDLEY, R. G., KAPLAN, R., EMBERTON, M., AHMED, H. U. & GROUP, P. 2015. PROMIS - Prostate MR imaging study: A paired validating cohort study evaluating the role of multi-parametric MRI in men with clinical suspicion of prostate cancer. *Contemp Clin Trials*, 42, 26-40.
- EPSTEIN, J. I. & POTTER, S. R. 2001. The pathological interpretation and significance of prostate needle biopsy findings: implications and current controversies. *J Urol*, 166, 402-10.
- EPSTEIN, J. I., WALSH, P. C., CARMICHAEL, M. & BRENDLER, C. B. 1994. Pathologic and clinical findings to predict tumor extent of nonpalpable (stage T1c) prostate cancer. *JAMA*, 271, 368-74.
- ERBERSDOBLER, A., ISBARN, H., DIX, K., STEINER, I., SCHLOMM, T., MIRLACHER, M., SAUTER, G. & HAESE, A. 2010. Prognostic value of microvessel density in prostate cancer: a tissue microarray study. *World J Urol*, 28, 687-92.
- FELEPPA, E. J. 2008. Ultrasonic tissue-type imaging of the prostate: implications for biopsy and treatment guidance. *Cancer Biomark*, 4, 201-12.
- FELEPPA, E. J., MAMOU, J., PORTER, C. R. & MACHI, J. 2011. Quantitative ultrasound in cancer imaging. *Semin Oncol*, 38, 136-50.
- FELEPPA, E. J., PORTER, C. R., KETTERLING, J., LEE, P., DASGUPTA, S., URBAN, S. & KALISZ, A. 2004. Recent developments in tissue-type imaging (TTI) for

- planning and monitoring treatment of prostate cancer. *Ultrason Imaging*, 26, 163-72.
- FRAUSCHER, F., GRADL, J. & PALLWEIN, L. 2005. Prostate ultrasound--for urologists only? *Cancer Imaging*, 5 Spec No A, S76-82.
- FULLER, M. S., LEE, C. I. & ELMORE, J. G. 2015. Breast cancer screening: an evidence-based update. *Med Clin North Am*, 99, 451-68.
- FUTTERER, J. J., HEIJMINK, S. W., SCHEENEN, T. W., VELTMAN, J., HUISMAN, H. J., VOS, P., HULSBERGEN-VAN DE KAA, C. A., WITJES, J. A., KRABBE, P. F., HEERSCHAP, A. & BARENTSZ, J. O. 2006. Prostate cancer localization with dynamic contrast-enhanced MR imaging and proton MR spectroscopic imaging. *Radiology*, 241, 449-58.
- GAZIEV, G., WADHWA, K., BARRETT, T., KOO, B. C., GALLAGHER, F. A., SERRAO, E., FREY, J., SEIDENADER, J., CARMONA, L., WARREN, A., GNANAPRAGASAM, V., DOBLE, A. & KASTNER, C. 2014. Defining the learning curve for multiparametric magnetic resonance imaging (MRI) of the prostate using MRI-transrectal ultrasonography (TRUS) fusion-guided transperineal prostate biopsies as a validation tool. *BJU Int*.
- GHAJ, S. & TOI, A. 2012. Role of transrectal ultrasonography in prostate cancer. *Radiol Clin North Am*, 50, 1061-73.
- GIROUIN, N., MEGE-LECHEVALLIER, F., TONINA SENES, A., BISSERY, A., RABILLOUD, M., MARECHAL, J. M., COLOMBEL, M., LYONNET, D. & ROUVIERE, O. 2007. Prostate dynamic contrast-enhanced MRI with simple visual diagnostic criteria: is it reasonable? *Eur Radiol*, 17, 1498-509.
- GRABSKI, B., BAEURLE, L., LOCH, A., WEFER, B., PAUL, U. & LOCH, T. 2011. Computerized transrectal ultrasound of the prostate in a multicenter setup (C-TRUS-MS): detection of cancer after multiple negative systematic random and in primary biopsies. *World J Urol*, 29, 573-9.
- GRUMMET, J. P., WEERAKOON, M., HUANG, S., LAWRENTSCHUK, N., FRYDENBERG, M., MOON, D. A., O'REILLY, M. & MURPHY, D. 2013. Sepsis and 'superbugs': should we favour the transperineal over the transrectal approach for prostate biopsy? *BJU Int*.
- HAAS, G. P., DELONGCHAMPS, N., BRAWLEY, O. W., WANG, C. Y. & DE LA ROZA, G. 2008. The worldwide epidemiology of prostate cancer: perspectives from autopsy studies. *Can J Urol*, 15, 3866-71.
- HALPERN, E. J., RAMEY, J. R., STRUP, S. E., FRAUSCHER, F., MCCUE, P. & GOMELLA, L. G. 2005. Detection of prostate carcinoma with contrast-enhanced sonography using intermittent harmonic imaging. *Cancer*, 104, 2373-83.
- HAMBROCK, T., HOEKS, C., HULSBERGEN-VAN DE KAA, C., SCHEENEN, T., FUTTERER, J., BOUWENSE, S., VAN OORT, I., SCHRODER, F., HUISMAN, H. & BARENTSZ, J. 2012. Prospective assessment of prostate cancer aggressiveness using 3-T diffusion-weighted magnetic resonance imaging-guided biopsies versus a systematic 10-core transrectal ultrasound prostate biopsy cohort. *Eur Urol*, 61, 177-84.
- HARLAN, S. R., COOPERBERG, M. R., ELKIN, E., LUBECK, D. P., MENG, M., MEHTA, S. S. & CARROLL, P. R. 2003. Time trends and characteristics of men choosing watchful waiting for initial treatment of localized prostate cancer: results from CaPSURE. *J Urol*, 170, 1804-7.

- HEIDENREICH, A., BASTIAN, P. J., BELLMUNT, J., BOLLA, M., JONIAU, S., VAN DER KWAST, T., MASON, M., MATVEEV, V., WIEGEL, T., ZATTONI, F., MOTTET, N. & EUROPEAN ASSOCIATION OF, U. 2014. EAU guidelines on prostate cancer. part 1: screening, diagnosis, and local treatment with curative intent-update 2013. *Eur Urol*, 65, 124-37.
- HRICAK, H., DOOMS, G. C., MCNEAL, J. E., MARK, A. S., MAROTTI, M., AVALLONE, A., PELZER, M., PROCTOR, E. C. & TANAGHO, E. A. 1987. MR imaging of the prostate gland: normal anatomy. *AJR Am J Roentgenol*, 148, 51-8.
- HU, Y., AHMED, H. U., ALLEN, C., PENDSE, D., SAHU, M., EMBERTON, M., HAWKES, D. & BARRATT, D. 2009. MR to ultrasound image registration for guiding prostate biopsy and interventions. *Med Image Comput Comput Assist Interv*, 12, 787-94.
- HU, Y., AHMED, H. U., CARTER, T., ARUMAINAYAGAM, N., LECORNET, E., BARZELL, W., FREEMAN, A., NEVOUX, P., HAWKES, D. J., VILLERS, A., EMBERTON, M. & BARRATT, D. C. 2012a. A biopsy simulation study to assess the accuracy of several transrectal ultrasonography (TRUS)-biopsy strategies compared with template prostate mapping biopsies in patients who have undergone radical prostatectomy. *BJU Int*, 110, 812-20.
- HU, Y., AHMED, H. U., TAYLOR, Z., ALLEN, C., EMBERTON, M., HAWKES, D. & BARRATT, D. 2012b. MR to ultrasound registration for image-guided prostate interventions. *Med Image Anal*, 16, 687-703.
- HU, Y., CARTER, T. J., AHMED, H. U., EMBERTON, M., ALLEN, C., HAWKES, D. J. & BARRATT, D. C. 2011. Modelling prostate motion for data fusion during image-guided interventions. *IEEE Trans Med Imaging*, 30, 1887-900.
- ISEBAERT, S., VAN DEN BERGH, L., HAUSTERMANS, K., JONIAU, S., LERUT, E., DE WEVER, L., DE KEYZER, F., BUDIHARTO, T., SLAGMOLEN, P., VAN POPPEL, H. & OYEN, R. 2013. Multiparametric MRI for prostate cancer localization in correlation to whole-mount histopathology. *J Magn Reson Imaging*, 37, 1392-401.
- ITOU, Y., NAKANISHI, K., NARUMI, Y., NISHIZAWA, Y. & TSUKUMA, H. 2011. Clinical utility of apparent diffusion coefficient (ADC) values in patients with prostate cancer: can ADC values contribute to assess the aggressiveness of prostate cancer? *J Magn Reson Imaging*, 33, 167-72.
- JAVED, S., CHADWICK, E., EDWARDS, A. A., BEVERIDGE, S., LAING, R., BOTT, S., EDEN, C. & LANGLEY, S. 2013. Does HistoScanning play a role in detecting prostate cancer in routine clinical practice? Results from three independent studies. *BJU Int*.
- KAJI, Y., KURHANEWICZ, J., HRICAK, H., SOKOLOV, D. L., HUANG, L. R., NELSON, S. J. & VIGNERON, D. B. 1998. Localizing prostate cancer in the presence of postbiopsy changes on MR images: role of proton MR spectroscopic imaging. *Radiology*, 206, 785-90.
- KAVANAGH, J. P. 1985. Sodium, potassium, calcium, magnesium, zinc, citrate and chloride content of human prostatic and seminal fluid. *J Reprod Fertil*, 75, 35-41.
- KELLY, I. M., LEES, W. R. & RICKARDS, D. 1993. Prostate cancer and the role of color Doppler US. *Radiology*, 189, 153-6.

- KIM, C. K., PARK, B. K. & KIM, B. 2010. High-b-value diffusion-weighted imaging at 3 T to detect prostate cancer: comparisons between b values of 1,000 and 2,000 s/mm². *AJR Am J Roentgenol*, 194, W33-7.
- KIM, J. K., HONG, S. S., CHOI, Y. J., PARK, S. H., AHN, H., KIM, C. S. & CHO, K. S. 2005. Wash-in rate on the basis of dynamic contrast-enhanced MRI: usefulness for prostate cancer detection and localization. *J Magn Reson Imaging*, 22, 639-46.
- KIM, J. K., JANG, Y. J. & CHO, G. 2009. Multidisciplinary functional MR imaging for prostate cancer. *Korean J Radiol*, 10, 535-51.
- KIRKHAM, A. P., HASLAM, P., KEANIE, J. Y., MCCAFFERTY, I., PADHANI, A. R., PUNWANI, S., RICHENBERG, J., ROTTENBERG, G., SOHAIB, A., THOMPSON, P., TURNBULL, L. W., KURBAN, L., SAHDEV, A., CLEMENTS, R., CAREY, B. M. & ALLEN, C. 2013. Prostate MRI: who, when, and how? Report from a UK consensus meeting. *Clin Radiol*, 68, 1016-23.
- KLOTZ, L. 2007. Active surveillance for favorable risk prostate cancer: rationale, risks, and results. *Urol Oncol*, 25, 505-9.
- KOH, D. M. & COLLINS, D. J. 2007. Diffusion-weighted MRI in the body: applications and challenges in oncology. *AJR Am J Roentgenol*, 188, 1622-35.
- KURHANEWICZ, J., SWANSON, M. G., NELSON, S. J. & VIGNERON, D. B. 2002. Combined magnetic resonance imaging and spectroscopic imaging approach to molecular imaging of prostate cancer. *J Magn Reson Imaging*, 16, 451-63.
- LATCHAMSETTY, K. C., BORDEN, L. S., JR., PORTER, C. R., LACRAMPE, M., VAUGHAN, M., LIN, E., CONTI, N., WRIGHT, J. L. & CORMAN, J. M. 2007. Experience improves staging accuracy of endorectal magnetic resonance imaging in prostate cancer: what is the learning curve? *Can J Urol*, 14, 3429-34.
- LATINI, D. M., HART, S. L., KNIGHT, S. J., COWAN, J. E., ROSS, P. L., DUCHANE, J. & CARROLL, P. R. 2007. The relationship between anxiety and time to treatment for patients with prostate cancer on surveillance. *J Urol*, 178, 826-31; discussion 831-2.
- LECORNET, E., AHMED, H. U., HU, Y., MOORE, C. M., NEVOUX, P., BARRATT, D., HAWKES, D., VILLERS, A. & EMBERTON, M. 2012. The accuracy of different biopsy strategies for the detection of clinically important prostate cancer: a computer simulation. *J Urol*, 188, 974-80.
- LEMAITRE, G., MARTI, R., FREIXENET, J., VILANOVA, J. C., WALKER, P. M. & MERIAUDEAU, F. 2015. Computer-Aided Detection and diagnosis for prostate cancer based on mono and multi-parametric MRI: a review. *Comput Biol Med*, 60, 8-31.
- LITJENS, G., DEBATS, O., BARENTSZ, J., KARSSEMEIJER, N. & HUISMAN, H. 2014. Computer-aided detection of prostate cancer in MRI. *IEEE Trans Med Imaging*, 33, 1083-92.
- LITJENS, G. J., BARENTSZ, J. O., KARSSEMEIJER, N. & HUISMAN, H. J. 2015. Clinical evaluation of a computer-aided diagnosis system for determining cancer aggressiveness in prostate MRI. *Eur Radiol*.
- LOCH, T., GETTYS, T., COCHRAN, J. S., FULGHAM, P. F. & BERTERMANN, H. 1990. Computer-aided image analysis in transrectal ultrasound of the prostate. *World Journal of Urology*, 8, 150-153.

- LOCH, T., LEUSCHNER, I., GENBERG, C., WEICHERT-JACOBSEN, K., KÜPPERS, F., YFANTIS, E., EVANS, M., TSAREV, V. & STÖCKLE, M. 1999. Artificial neural network analysis (ANNA) of prostatic transrectal ultrasound. *The Prostate*, 39, 198-204.
- MACEK, P., BARRET, E., SANCHEZ-SALAS, R., GALIANO, M., ROZET, F., AHALLAL, Y., GAYA, J. M., DURANT, M., MASCLE, L., GIEDELMAN, C., LUNELLI, L., VALIDIRE, P., NESVADBA, M. & CATHELINÉAU, X. 2014. Prostate histoscanning in clinically localized biopsy proven prostate cancer: an accuracy study. *J Endourol*, 28, 371-6.
- MAZZUCHELLI, R., BARBISAN, F., SCARPELLI, M., LOPEZ-BELTRAN, A., VAN DER KWAST, T. H., CHENG, L. & MONTIRONI, R. 2009. Is incidentally detected prostate cancer in patients undergoing radical cystoprostatectomy clinically significant? *Am J Clin Pathol*, 131, 279-83.
- MCNEAL, J. E. 1981. Normal and pathologic anatomy of prostate. *Urology*, 17, 11-6.
- MEDAROVA, Z., GHOSH, S. K., VANGEL, M., DRAKE, R. & MOORE, A. 2014. Risk stratification of prostate cancer patients based on EPS-urine zinc content. *Am J Cancer Res*, 4, 385-93.
- MERRICK, G. S., GUTMAN, S., ANDREINI, H., TAUBENSLAG, W., LINDERT, D. L., CURTIS, R., ADAMOVIČH, E., ANDERSON, R., ALLEN, Z., BUTLER, W. & WALLNER, K. 2007. Prostate cancer distribution in patients diagnosed by transperineal template-guided saturation biopsy. *Eur Urol*, 52, 715-23.
- MORGAN, R., BOXALL, A., BHATT, A., BAILEY, M., HINDLEY, R., LANGLEY, S., WHITAKER, H. C., NEAL, D. E., ISMAIL, M., WHITAKER, H., ANNELS, N., MICHAEL, A. & PANDHA, H. 2011. Engrailed-2 (EN2): a tumor specific urinary biomarker for the early diagnosis of prostate cancer. *Clin Cancer Res*, 17, 1090-8.
- NATIONAL INSTITUTE FOR HEALTH AND CARE EXCELLENCE. 2008. *Prostate Cancer: Diagnosis and Treatment* [Online]. Available: <https://www.nice.org.uk/guidance/cg58/resources/guidance-prostate-cancer-diagnosis-and-treatment-pdf> [Accessed 04/05/2013 2013].
- NATIONAL INSTITUTE FOR HEALTH AND CARE EXCELLENCE. 2014a. Available: <http://www.nice.org.uk/nicemedia/live/14348/66232/66232.pdf> [Accessed 27/02/2014 2014].
- NATIONAL INSTITUTE FOR HEALTH AND CARE EXCELLENCE. 2014b. *Prostate cancer: diagnosis and treatment* [Online]. Available: <http://publications.nice.org.uk/prostate-cancer-diagnosis-and-treatment-cg175/recommendations>) [Accessed 25/05/2015 2015].
- NELSON, E. D., SLOTOROFF, C. B., GOMELLA, L. G. & HALPERN, E. J. 2007. Targeted biopsy of the prostate: the impact of color Doppler imaging and elastography on prostate cancer detection and Gleason score. *Urology*, 70, 1136-40.
- NIAF, E., ROUVIERE, O., MEGE-LECHEVALLIER, F., BRATAN, F. & LARTIZIEN, C. 2012. Computer-aided diagnosis of prostate cancer in the peripheral zone using multiparametric MRI. *Phys Med Biol*, 57, 3833-51.
- OCAK, I., BERNARDO, M., METZGER, G., BARRETT, T., PINTO, P., ALBERT, P. S. & CHOYKE, P. L. 2007. Dynamic contrast-enhanced MRI of prostate cancer at 3 T: a study of pharmacokinetic parameters. *AJR Am J Roentgenol*, 189, 849.

- OFFICE FOR NATIONAL STATISTICS. 2010. *Cancer Statistics Registrations, England (Series MB1), No. 41, 2010* [Online]. Available: http://www.ons.gov.uk/ons/dcp171778_267154.pdf [Accessed 21/04/2013 2013].
- OTTO, P. M. & BLECHER, C. B. 2014. Controversies surrounding screening mammography. *Mo Med*, 111, 439-43.
- PAL, R., BEEBY, A. & PARKER, D. 2011. Analysis of citrate in low-volume seminal fluid samples using a time-gated measurement of europium luminescence. *J Pharm Biomed Anal*, 56, 352-8.
- PANDHA, H., SORENSEN, K. D., ORNTOFT, T. F., LANGLEY, S., HOYER, S., BORRE, M. & MORGAN, R. 2012. Urinary engrailed-2 (EN2) levels predict tumour volume in men undergoing radical prostatectomy for prostate cancer. *BJU Int*, 110, E287-92.
- POSTEMA, A., IDZENGA, T., MISCHI, M., FRINKING, P., DE LA ROSETTE, J. & WIJKSTRA, H. 2015a. Ultrasound modalities and quantification: developments of multiparametric ultrasonography, a new modality to detect, localize and target prostatic tumors. *Curr Opin Urol*, 25, 191-7.
- POSTEMA, A., MISCHI, M., DE LA ROSETTE, J. & WIJKSTRA, H. 2015b. Multiparametric ultrasound in the detection of prostate cancer: a systematic review. *World J Urol*.
- PUECH, P., ROUVIERE, O., RENARD-PENNA, R., VILLERS, A., DEVOS, P., COLOMBEL, M., BITKER, M. O., LEROY, X., MEGE-LECHEVALLIER, F., COMPERAT, E., OUZZANE, A. & LEMAITRE, L. 2013. Prostate cancer diagnosis: multiparametric MR-targeted biopsy with cognitive and transrectal US-MR fusion guidance versus systematic biopsy--prospective multicenter study. *Radiology*, 268, 461-9.
- QAYYUM, A., COAKLEY, F. V., LU, Y., OLPIN, J. D., WU, L., YEH, B. M., CARROLL, P. R. & KURHANEWICZ, J. 2004. Organ-confined prostate cancer: effect of prior transrectal biopsy on endorectal MRI and MR spectroscopic imaging. *AJR Am J Roentgenol*, 183, 1079-83.
- ROBERTSON, N. L., HU, Y., AHMED, H. U., FREEMAN, A., BARRATT, D. & EMBERTON, M. 2014. Prostate cancer risk inflation as a consequence of image-targeted biopsy of the prostate: a computer simulation study. *Eur Urol*, 65, 628-34.
- SALOMON, G., KOLLERMAN, J., THEDERAN, I., CHUN, F. K., BUDAUS, L., SCHLOMM, T., ISBARN, H., HEINZER, H., HULAND, H. & GRAEFEN, M. 2008. Evaluation of prostate cancer detection with ultrasound real-time elastography: a comparison with step section pathological analysis after radical prostatectomy. *Eur Urol*, 54, 1354-62.
- SANO, F. & UEMURA, H. 2015. The utility and limitations of contrast-enhanced ultrasound for the diagnosis and treatment of prostate cancer. *Sensors (Basel)*, 15, 4947-57.
- SAUVAIN, J. L., PALASCAK, P., BOURSCHEID, D., CHABI, C., ATASSI, A., BREMON, J. M. & PALASCAK, R. 2003. Value of power doppler and 3D vascular sonography as a method for diagnosis and staging of prostate cancer. *Eur Urol*, 44, 21-30; discussion 30-1.
- SCHEIDLER, J., HRICAK, H., VIGNERON, D. B., YU, K. K., SOKOLOV, D. L., HUANG, L. R., ZALOUDEK, C. J., NELSON, S. J., CARROLL, P. R. & KURHANEWICZ, J. 1999.

- Prostate cancer: localization with three-dimensional proton MR spectroscopic imaging--clinicopathologic study. *Radiology*, 213, 473-80.
- SCHIFFMANN, J., FISCHER, J., TENNSTEDT, P., BEYER, B., BOHM, K., MICHL, U., GRAEFEN, M. & SALOMON, G. 2013. Comparison of prostate cancer volume measured by HistoScanning and final histopathological results. *World J Urol*.
- SCHIFFMANN, J., FISCHER, J., TENNSTEDT, P., BEYER, B., BOHM, K., MICHL, U., GRAEFEN, M. & SALOMON, G. 2014a. Comparison of prostate cancer volume measured by HistoScanning and final histopathological results. *World J Urol*, 32, 939-44.
- SCHIFFMANN, J., MANKA, L., BOEHM, K., LEYH-BANNURAH, S. R., KARAKIEWICZ, P. I., GRAEFEN, M., HAMMERER, P. & SALOMON, G. 2015. Controversial evidence for the use of HistoScanning in the detection of prostate cancer. *World J Urol*.
- SCHIFFMANN, J., TENNSTEDT, P., FISCHER, J., TIAN, Z., BEYER, B., BOEHM, K., SUN, M., GANDAGLIA, G., MICHL, U., GRAEFEN, M. & SALOMON, G. 2014b. Does HistoScanning predict positive results in prostate biopsy? A retrospective analysis of 1,188 sextants of the prostate. *World J Urol*, 32, 925-30.
- SEITZ, M., GRATZKE, C., SCHLENKER, B., BUCHNER, A., KARL, A., ROOSEN, A., SINGER, B. B., BASTIAN, P. J., ERGUN, S., STIEF, C. G., REICH, O. & TILKI, D. 2011. Contrast-enhanced transrectal ultrasound (CE-TRUS) with cadence-contrast pulse sequence (CPS) technology for the identification of prostate cancer. *Urol Oncol*, 29, 295-301.
- SIEGEL, R., WARD, E., BRAWLEY, O. & JEMAL, A. 2011. Cancer statistics, 2011: the impact of eliminating socioeconomic and racial disparities on premature cancer deaths. *CA Cancer J Clin*, 61, 212-36.
- SIMMONS, L. A., AHMED, H. U., MOORE, C. M., PUNWANI, S., FREEMAN, A., HU, Y., BARRATT, D., CHARMAN, S. C., VAN DER MEULEN, J. & EMBERTON, M. 2014. The PICTURE study -- prostate imaging (multi-parametric MRI and Prostate HistoScanning) compared to transperineal ultrasound guided biopsy for significant prostate cancer risk evaluation. *Contemp Clin Trials*, 37, 69-83.
- SIMMONS, L. A., AUTIER, P., ZAT'URA, F., BRAECKMAN, J., PELTIER, A., ROMIC, I., STENZL, A., TREURNICHT, K., WALKER, T., NIR, D., MOORE, C. M. & EMBERTON, M. 2012. Detection, localisation and characterisation of prostate cancer by prostate HistoScanning(). *BJU Int*, 110, 28-35.
- SINGH, H., CANTO, E. I., SHARIAT, S. F., KADMON, D., MILES, B. J., WHEELER, T. M. & SLAWIN, K. M. 2004. Predictors of prostate cancer after initial negative systematic 12 core biopsy. *J Urol*, 171, 1850-4.
- STAMEY, T. A., FREIHA, F. S., MCNEAL, J. E., REDWINE, E. A., WHITTEMORE, A. S. & SCHMID, H. P. 1993. Localized prostate cancer. Relationship of tumor volume to clinical significance for treatment of prostate cancer. *Cancer*, 71, 933-8.
- STRUNK, T., DECKER, G., WILLINEK, W., MUELLER, S. C. & ROGENHOFER, S. 2014. Combination of C-TRUS with multiparametric MRI: potential for improving detection of prostate cancer. *World J Urol*, 32, 335-9.
- TAKAHASHI H, O. T. 1963. The ultrasonic diagnosis in the field of urology. *Proc Jpn Soc Ultrasonics Med.*, 3:7.

- TAMADA, T., KANOMATA, N., SONE, T., JO, Y., MIYAJI, Y., HIGASHI, H., YAMAMOTO, A. & ITO, K. 2014. High b value (2,000 s/mm²) diffusion-weighted magnetic resonance imaging in prostate cancer at 3 Tesla: comparison with 1,000 s/mm² for tumor conspicuity and discrimination of aggressiveness. *PLoS One*, 9, e96619.
- TAMADA, T., SONE, T., HIGASHI, H., JO, Y., YAMAMOTO, A., KANKI, A. & ITO, K. 2011. Prostate cancer detection in patients with total serum prostate-specific antigen levels of 4-10 ng/mL: diagnostic efficacy of diffusion-weighted imaging, dynamic contrast-enhanced MRI, and T2-weighted imaging. *AJR Am J Roentgenol*, 197, 664-70.
- TAMADA, T., SONE, T., JO, Y., TOSHIMITSU, S., YAMASHITA, T., YAMAMOTO, A., TANIMOTO, D. & ITO, K. 2008a. Apparent diffusion coefficient values in peripheral and transition zones of the prostate: comparison between normal and malignant prostatic tissues and correlation with histologic grade. *J Magn Reson Imaging*, 28, 720-6.
- TAMADA, T., SONE, T., JO, Y., YAMAMOTO, A., YAMASHITA, T., EGASHIRA, N., IMAI, S. & FUKUNAGA, M. 2008b. Prostate cancer: relationships between postbiopsy hemorrhage and tumor detectability at MR diagnosis. *Radiology*, 248, 531-9.
- TAN, C. H., HOBBS, B. P., WEI, W. & KUNDRA, V. 2015. Dynamic contrast-enhanced MRI for the detection of prostate cancer: meta-analysis. *AJR Am J Roentgenol*, 204, W439-48.
- TAN, C. H., WEI, W., JOHNSON, V. & KUNDRA, V. 2012. Diffusion-weighted MRI in the detection of prostate cancer: meta-analysis. *AJR Am J Roentgenol*, 199, 822-9.
- TANAKA, N., SAMMA, S., JOKO, M., AKIYAMA, T., TAKEWA, M., KITANO, S. & OKAJIMA, E. 1999. Diagnostic usefulness of endorectal magnetic resonance imaging with dynamic contrast-enhancement in patients with localized prostate cancer: mapping studies with biopsy specimens. *Int J Urol*, 6, 593-9.
- THOMPSON, I. M., PAULER, D. K., GOODMAN, P. J., TANGEN, C. M., LUCIA, M. S., PARNES, H. L., MINASIAN, L. M., FORD, L. G., LIPPMAN, S. M., CRAWFORD, E. D., CROWLEY, J. J. & COLTMAN, C. A., JR. 2004. Prevalence of prostate cancer among men with a prostate-specific antigen level < or =4.0 ng per milliliter. *N Engl J Med*, 350, 2239-46.
- THOMPSON, I. M., TANGEN, C. M. & KRISTAL, A. R. 2008. Prostate-specific antigen: a misused and maligned prostate cancer biomarker. *J Natl Cancer Inst*, 100, 1487-8.
- TRABULSI, E. J., SACKETT, D., GOMELLA, L. G. & HALPERN, E. J. 2010. Enhanced transrectal ultrasound modalities in the diagnosis of prostate cancer. *Urology*, 76, 1025-33.
- TRPKOV, K., YILMAZ, A., BISMAR, T. A. & MONTIRONI, R. 2010. 'Insignificant' prostate cancer on prostatectomy and cystoprostatectomy: variation on a theme 'low-volume/low-grade' prostate cancer? *BJU Int*, 106, 304-15.
- TSUTSUMI, M., MIYAGAWA, T., MATSUMURA, T., ENDO, T., KANDORI, S., SHIMOKAMA, T. & ISHIKAWA, S. 2010. Real-time balloon inflation elastography for prostate cancer detection and initial evaluation of clinicopathologic analysis. *AJR Am J Roentgenol*, 194, W471-6.

- TURKBAY, B., ALBERT, P. S., KURDZIEL, K. & CHOYKE, P. L. 2009. Imaging localized prostate cancer: current approaches and new developments. *AJR Am J Roentgenol*, 192, 1471-80.
- TURKBAY, B., MANI, H., SHAH, V., RASTINEHAD, A. R., BERNARDO, M., POHIDA, T., PANG, Y., DAAR, D., BENJAMIN, C., MCKINNEY, Y. L., TRIVEDI, H., CHUA, C., BRATSLAVSKY, G., SHIH, J. H., LINEHAN, W. M., MERINO, M. J., CHOYKE, P. L. & PINTO, P. A. 2011. Multiparametric 3T prostate magnetic resonance imaging to detect cancer: histopathological correlation using prostatectomy specimens processed in customized magnetic resonance imaging based molds. *J Urol*, 186, 1818-24.
- TURKBAY, B., PINTO, P. A., MANI, H., BERNARDO, M., PANG, Y., MCKINNEY, Y. L., KHURANA, K., RAVIZZINI, G. C., ALBERT, P. S., MERINO, M. J. & CHOYKE, P. L. 2010. Prostate cancer: value of multiparametric MR imaging at 3 T for detection--histopathologic correlation. *Radiology*, 255, 89-99.
- VAES, E., MANCHANDA, R., NIR, R., NIR, D., BLEIBERG, H., AUTIER, P., MENON, U. & ROBERT, A. 2011. Mathematical models to discriminate between benign and malignant adnexal masses: potential diagnostic improvement using ovarian HistoScanning. *Int J Gynecol Cancer*, 21, 35-43.
- VERMA, S., RAJESH, A., MORALES, H., LEMEN, L., BILLS, G., DELWORTH, M., GAITONDE, K., YING, J., SAMARTUNGA, R. & LAMBA, M. 2011. Assessment of aggressiveness of prostate cancer: correlation of apparent diffusion coefficient with histologic grade after radical prostatectomy. *AJR Am J Roentgenol*, 196, 374-81.
- VERMA, S., TURKBAY, B., MURADYAN, N., RAJESH, A., CORNUD, F., HAIDER, M. A., CHOYKE, P. L. & HARISINGHANI, M. 2012. Overview of dynamic contrast-enhanced MRI in prostate cancer diagnosis and management. *AJR Am J Roentgenol*, 198, 1277-88.
- VILANOVA, J. C., COMET, J., BARCELO-VIDAL, C., BARCELO, J., LOPEZ-BONET, E., MAROTO, A., ARZOZ, M., MORENO, A. & AREAL, J. 2009. Peripheral zone prostate cancer in patients with elevated PSA levels and low free-to-total PSA ratio: detection with MR imaging and MR spectroscopy. *Radiology*, 253, 135-43.
- WALSH, J. F. & REZNIKOFF, M. 1990. Bootstrapping: a tool for clinical research. *J Clin Psychol*, 46, 928-30.
- WANG, L., MAZAHARI, Y., ZHANG, J., ISHILL, N. M., KUROIWA, K. & HRICAK, H. 2008. Assessment of biologic aggressiveness of prostate cancer: correlation of MR signal intensity with Gleason grade after radical prostatectomy. *Radiology*, 246, 168-76.
- WANG, S., BURTT, K., TURKBAY, B., CHOYKE, P. & SUMMERS, R. M. 2014. Computer aided-diagnosis of prostate cancer on multiparametric MRI: a technical review of current research. *Biomed Res Int*, 2014, 789561.
- WATANABE, H., IGARI, D., TANAHASI, Y., HARADA, K. & SAITO, M. 1974. Development and application of new equipment for transrectal ultrasonography. *J Clin Ultrasound*, 2, 91-8.
- WEINREB, J. C., BLUME, J. D., COAKLEY, F. V., WHEELER, T. M., CORMACK, J. B., SOTTO, C. K., CHO, H., KAWASHIMA, A., TEMPANY-AFDHAL, C. M., MACURA, K. J., ROSEN, M., GERST, S. R. & KURHANEWICZ, J. 2009. Prostate cancer:

- sextant localization at MR imaging and MR spectroscopic imaging before prostatectomy--results of ACRIN prospective multi-institutional clinicopathologic study. *Radiology*, 251, 122-33.
- WHITE, S., HRICAK, H., FORSTNER, R., KURHANEWICZ, J., VIGNERON, D. B., ZALOUDEK, C. J., WEISS, J. M., NARAYAN, P. & CARROLL, P. R. 1995. Prostate cancer: effect of postbiopsy hemorrhage on interpretation of MR images. *Radiology*, 195, 385-90.
- WILLIS, SR., VAN DER MEULEN, J., VALERIO, M., MINERS, A., AHMED, HU., EMBERTON, M. 2015. A review of economic evaluations of diagnostic strategies using imaging in men at risk of prostate cancer. *Curr Opin Uro*. Nov;25(6):483-9.
- WILT, T. J. 2012. Implications of the prostate intervention versus observation trial (PIVOT). *Asian J Androl*, 14, 815.
- WILT, T. J., BRAWER, M. K., JONES, K. M., BARRY, M. J., ARONSON, W. J., FOX, S., GINGRICH, J. R., WEI, J. T., GILHOOLY, P., GROB, B. M., NSOULI, I., IYER, P., CARTAGENA, R., SNIDER, G., ROHRBORN, C., SHARIFI, R., BLANK, W., PANDYA, P., ANDRIOLE, G. L., CULKIN, D. & WHEELER, T. 2012. Radical prostatectomy versus observation for localized prostate cancer. *N Engl J Med*, 367, 203-13.
- WOLTERS, T., ROOBOL, M. J., VAN LEEUWEN, P. J., VAN DEN BERGH, R. C., HOEDEMAEKER, R. F., VAN LEENDERS, G. J., SCHRODER, F. H. & VAN DER KWAST, T. H. 2011. A critical analysis of the tumor volume threshold for clinically insignificant prostate cancer using a data set of a randomized screening trial. *J Urol*, 185, 121-5.
- WOODFIELD, C. A., TUNG, G. A., GRAND, D. J., PEZZULLO, J. A., MACHAN, J. T. & RENZULLI, J. F., 2ND 2010. Diffusion-weighted MRI of peripheral zone prostate cancer: comparison of tumor apparent diffusion coefficient with Gleason score and percentage of tumor on core biopsy. *AJR Am J Roentgenol*, 194, W316-22.
- WU, L. M., XU, J. R., YE, Y. Q., LU, Q. & HU, J. N. 2012. The clinical value of diffusion-weighted imaging in combination with T2-weighted imaging in diagnosing prostate carcinoma: a systematic review and meta-analysis. *AJR Am J Roentgenol*, 199, 103-10.
- XIE, S. W., LI, H. L., DU, J., XIA, J. G., GUO, Y. F., XIN, M. & LI, F. H. 2012. Contrast-enhanced ultrasonography with contrast-tuned imaging technology for the detection of prostate cancer: comparison with conventional ultrasonography. *BJU Int*, 109, 1620-6.
- ZHANG, B., MA, X., ZHAN, W., ZHU, F., LI, M., HUANG, J., LI, Y., XUE, L., LIU, L. & WEI, Y. 2014. Real-time elastography in the diagnosis of patients suspected of having prostate cancer: a meta-analysis. *Ultrasound Med Biol*, 40, 1400-7.